Specialisation for fast locomotion: performance, cost and risk

Thesis submitted in accordance with the requirements of the University of Liverpool for the degree of Doctor in Philosophy by Carol Ann Hercock

September 2010

Abstract

The racing Greyhound presents us with an opportunity to study the characteristics of a successful athlete and the costs and risks such specialisation entails. This thesis investigates the nature of the injuries suffered by racing Greyhounds and how adaptation of the musculoskeletal system to the unique pattern of stresses encountered during racing and training might impact upon the risk of injury.

Racing Greyhounds sustain a number of musculoskeletal injuries. Several of these, notably fatigue fractures of distal limb bones, are very similar to those seen in human athletes and military recruits (Armstrong *et al.* 2004; Beck *et al.* 2000; Brukner *et al.* 1996; Kowal 1980; Matheson *et al.* 1987). The most common, often leading to the dog being euthanatised, is fracture of the right tarsus. Evaluation of tarsal fractures via radiography alone frequently resulted in an underestimation of the severity of the injuries, whereas the use of computed tomography provided a more detailed, accurate assessment.

Evidence of asymmetric bone remodelling was found in the distal limb bones of racing Greyhounds. Rail-side bones had significantly higher bone density and increased levels of bone resorption and formation markers compared to contralateral bones. Greyhound bones also have regional differences in trabecular architecture. In contrast, Staffordshire Bull Terrier (SBT) bones did not show these differences. Additionally, Greyhound distal limb tendons appear well adapted to withstand the high stresses of racing; they are stronger, stiffer, and in the pelvic limbs, return more elastic strain energy than the corresponding SBT tendons. Greyhounds had left-to-right asymmetries in the tensile properties of their pelvic limb tendons, which SBTs did not. SBTs are not bred for racing and are unlikely to encounter asymmetric stresses. Therefore, the adaptive changes observed in the Greyhound bones and tendons appear to result from the asymmetric stresses encountered by the Greyhounds during racing around ovoid tracks.

Acknowledgements and Dedication

There are numerous people that I am indebted to, too many to personally mention here, but I would sincerely like to thank all my friends, family and colleagues for all their help and support throughout the past four years.

In particular, I would like to acknowledge and thank my supervisors, Dr Iain Young and Prof John Innes, for their invaluable support, advice and friendship throughout my PhD.

I would like to thank those who have contributed to this work: in particular, Diana Hodson (access to Greyhound cadavers and provided contacts to the Greyhound racing industry), Anne Vaughan-Thomas and Diane Isherwood (biochemical analysis). Alisa Dean, Martin Baker, Fraser McConnell, Alex German and Shelley Holden (training and access to the diagnostic imaging facilities at the Small Animal Teaching Hospital, Leahurst), Robin Crompton, Russ Savage and Anthony Channon (training and access to the micro-CT) and Robert Ker (mechanical testing).

Thanks also to the Biotechnology and Biological Sciences Research Council and the Greyhound Board of Greyhound Britain for providing me with the funding to carry out this work.

I would also like to thank all my friends, especially my fellow PhD student Rebecca Lewis, for all their support, advice and encouragement, and for all the much needed coffee breaks. I am especially grateful to my family; particularly my father Peter Hercock, and my brother Richard Hercock, whose love, support and encouragement throughout the last four years and my life have helped me to complete this PHD.

Finally, I wish to dedicate this thesis to the memory of my mother Wendy Hercock, whom I know would have been proud of what I have achieved.

Contents list

List of Figures

List of Tables

Chapter 1

GENERAL INTRODUCTION

The racing Greyhound is a superlative athlete produced by generations of selective breeding with the aim to increase its performance and principally its speed. Therefore, it presents us with an opportunity to study the characteristics of a successful athlete and the costs and risks such specialisation entails. This thesis investigates the nature of the injuries sustained by the racing Greyhound and how adaptation of the musculoskeletal system to the unique pattern of stresses encountered during racing and training might impact upon the risk of injury. The findings of this study, while clearly applicable to veterinary medicine, are equally applicable to human medicine and sports physiology. This first chapter will explain the aims and philosophy of the study and provide background information about functional adaption, the biomechanics of running, the musculoskeletal system, the Greyhound and Staffordshire Bull Terrier (SBT) (which provides a contrast and comparison with the Greyhound because they have been bred for fighting ability rather than speed), Greyhound racing and commonly sustained injuries.

1.1. Biomechanics of running, functional adaption and limb morphology

1.1.1 Cursorial locomotion

Cursorial animals travel easily at high speed or for long distances on the ground (Hildebrand and Goslow 2001). Adaptation for fast cursorial locomotion requires an animal to overcome the inertia of its body to attain speed, to overcome the movement and inertia of the legs and/or any other oscillating parts with every reversal in the direction of their motion, to support the body, to compensate for forces of deceleration, to control its course of motion and to maintain all of these functions for sustained periods (Hildebrand and Goslow 2001).

1.1.2 Forces acting on the limbs

When a terrestrial animal's limb contacts the ground it exerts and experiences a "ground reaction force". This force has three components: the vertical (G_V) component supports the animal's weight, the horizontal fore-aft (G_H) and mediolateral (G_{ML}) components allow the animal to accelerate, decelerate, manoeuvre and balance (Biewener 2003). Over a series of strides the average vertical force exerted on ground by the limbs must equal an animal's weight (Biewener 2003). At rest, the force acting on a limb is approximately equal to the animal's weight divided by the number of limbs that are supporting that weight. When an animal moves the forces exerted by the limbs on the ground rise and fall during limb support, and are zero when there are no limbs on the ground (aerial phase of a stride). Therefore, the maximum forces exerted on the ground by a single limb during movement are always much higher than those sustained when an animal is at rest. If the limbs are kept on the ground for longer periods of time then smaller maximum vertical forces are required, but this limits the speed of movement. To move faster, animals must move their limbs faster, which reduces the time of limb support and thus increases the magnitude of force that must be generated against the ground.

1.1.3 Running around a bend

Greyhounds are always raced anti-clockwise around ovoid tracks. These tracks have two straight sections and two semicircular banked bends. Running around a bend increases an animals' effective body weight because body mass experiences both gravity and centripetal acceleration. Usherwood and Wilson (2005) calculated that Greyhounds racing around a bend experience an increase in their effective weight of approximately 71.0% due to the high centripetal acceleration. Humans sprinting around banked bends compensate for this increase in effective body weight by increasing the duration of their limb support phase, spreading the time over which the load is applied to keep the force on their limbs constant

(Greene 1987); however, this results in a loss of speed. Greyhounds entering a bend do not alter their foot contact timings; therefore, all four limbs experience an increase in peak force of approximately 64.5% during bend running compared with straight line running, consequently they can maintain their speed more effectively (Usherwood and Wilson 2005). Greyhounds are thought to transfer their weight to the left side of their limbs when they corner (Boemo 1998); therefore, the distal limb bones of Greyhounds are thought to experience asymmetrical loading during racing, with the bones that are nearest to the inside of the track experiencing higher stresses than the contralateral bones.

1.1.4 Limb morphology and adaptation for speed

The locomotor cycle, or stride, can be divided into support and swing phases of the limb, and the time taken to complete one full locomotory cycle is known as the stride period (Biewener 2003). The relative fraction of the stride period that is represented by a limb's support phase is defined as the limb's duty cycle (Biewener 2003). As animals increase their speed they decrease the duty factor of their limbs which requires an increase in the maximum forces exerted against the ground. The maximum speed an animal can run is determined by stride length (the distance travelled over one stride cycle) and stride frequency: increases in stride length and frequency increase speed; therefore, adaptations of the limbs for speed are related to one or both of these factors. Increases in stride length are achieved primarily by increasing the length of the distal segments of the limbs, while increases in stride frequency are achieved via mechanisms that allow the limbs to swing forward and back more rapidly, for example, reduced muscle mass in the distal limb (Gregory 1912). Increasing the distal limb segments while keeping the proximal limb segments (i.e. the humerus or femur) short means that the muscles moving these bones with respect to the limb girdles act over a short distance. A given mass of muscle can contract powerfully over a short distance, hence, the short proximal segment can be moved

with a lot of power, and the proximal muscles used to swing the rest of the elongated limb. Concentrating the power in the proximal muscles means the distal limb muscles can be smaller reducing the weight of the distal limb and thus reducing the "pendulum effect" that has to be overcome when the foot is slowed, stopped, and accelerated in the opposite direction (as it must be at each end of each stride). Therefore, limbs that are built for speed have a short proximal segment with large powerful muscles and a slender distal segment with reduced muscle mass (Gregory 1912; Hildebrand and Goslow 2001; Hinchliffe and Johnson 1980)

1.2 Breed information

Racing Greyhounds and SBTs are both breeds of domestic dog (*Canis familiaris*).

1.2.1 Greyhounds

Greyhounds belong to the group of dogs known as sight-hounds or gaze-hounds. These dogs have been selectively bred to hunt using sight and speed rather than scent and endurance. This type of hunting with dogs is known as coursing. In the 1500's Queen Elizabeth I is credited with turning coursing into a competition, where two dogs were matched together against the game and bets were placed as to which dog would win. Modern day racing has its origins in coursing and the sport emerged in its recognisable form in Britain in 1926. Nowadays, the Greyhound is recognised as the fastest breed of domestic dog, capable of reaching speeds of up to 18 ms^{-1} during racing.

The conformation of the Greyhound is similar to that of the other sight-hounds. Generally, Greyhounds are strongly built, with a long head and neck, deep chest, slightly arched loin, long slender limbs, well developed muscles and a short fine coat (Figure 1.1). Bitches measure 68 to 71 cm at the withers and generally weigh between 23 and 30 kg; dogs measure 71 to 76 cm and weigh 27 to 37 kg. Greyhounds have been bred to have a gentle

even-tempered nature, as any sign of aggression during a trial or race will result in disqualification, with repeat incidents leading to the dog being permanently disqualified from racing. As the Greyhound is bred for performance rather than looks, it has escaped a lot of the genetic problems encountered by other pure breed dogs. Davis (1967) stated "The Greyhound is one of the few breeds unaffected by the show ring, as the test for survival is still ability to perform on the track".

The Greyhound is believed to be one of the oldest breeds of dog with a history dating back 4000 years although its exact origin is not really known. Many believe the Greyhound originated in Egypt, Greece and Persia, as depictions of smooth-coated sight-hound type dogs have been found which are typical of Saluki (Persian Greyhound) or Sloughi (North African sight-hound) (Beni Hasan tombs c. 2000 BC). However, recent DNA analysis of the purebred domestic dog suggests the Greyhound, along with a couple of other sight-hounds such as the Wolfhound and Borzoi, is closely related to herding dogs like the Belgium Sheepdog and Collie (Parker *et al.* 2004); their results suggest that although the Greyhounds and other similar sight-hounds resemble the ancient Egyptian sight-hounds in appearance, their genomes are very different. All modern pedigree Greyhounds are descendants of dogs recorded and registered, firstly in the private 18th century studbooks, and then in the public 19th century studbooks, which eventually became registered with the UK's coursing, racing, and kennel club authorities.

Information about the Greyhound breed was obtained from the UK Kennel Club (2009), Dalziel (1955) and Branigan (2003).

Figure 1.1: Photograph showing the general conformation of a Greyhound (Burton, courtesy of Fay Penrose).

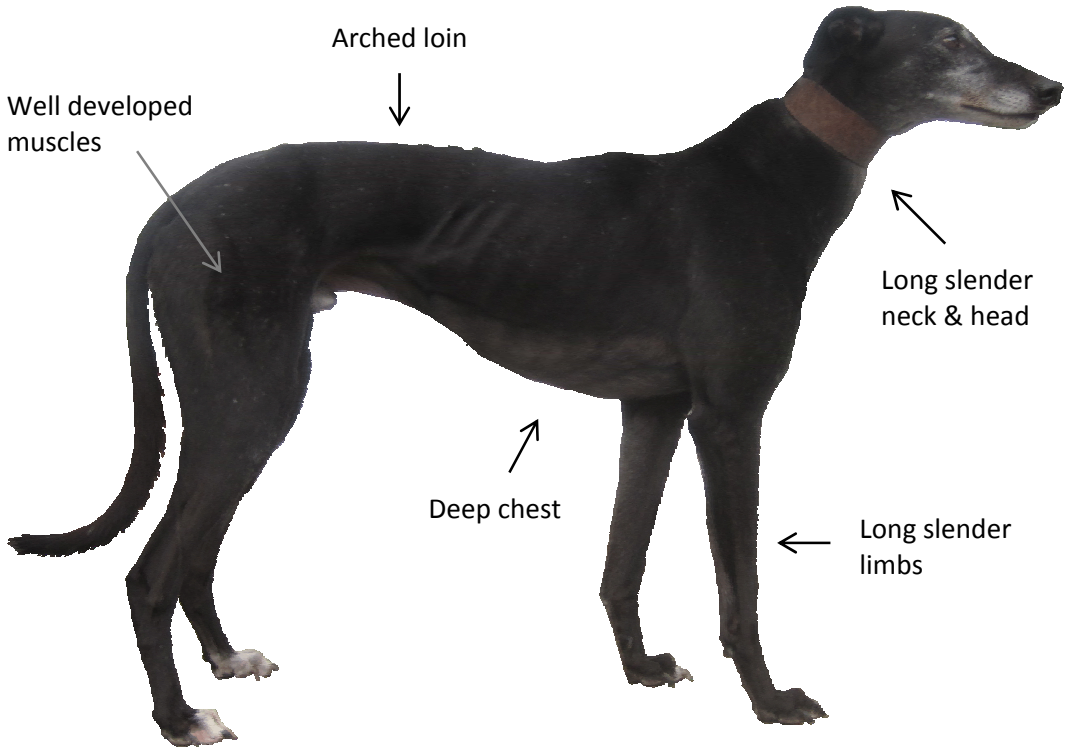

1.2.2 Staffordshire Bull Terriers

The SBT belongs to the terrier group of dogs. SBTs are medium-sized, stocky, well-muscled dogs. Generally they have a broad head with pronounced cheek muscles and short muzzle, a relatively short neck, heavyset body and relatively short limbs that are set rather wide apart. Both bitches and dogs stand 36 to 41 cm at the withers. Bitches generally weigh between 11 and 15 kg, while dogs can be heavier weighing 13 to 17 kg. Blood-sports such as bull-baiting and bear-baiting were common events before the 19th century. Dog fights with other animals such as bulls and bears were organised as entertainment for both commoners and royalty. The dogs that were used for these events were the ancestors of the modern day SBT. In the UK these blood-sports were officially eliminated in 1835 when

animal welfare laws began to be introduced. As dog fights were both cheaper to organise and easier to conceal from the authorities than bull-baiting or bear-baiting, blood-sport advocates began pitting their dogs against one another instead. The SBT is believed to have originated from crossbreeding the fighting bulldog of the day with a terrier to produce the "Bull and Terrier" or "Pit Dog". On the 25th May 1935 the SBT attained UK Kennel Club recognition and the UK Staffordshire Bull Terrier Club was formed a couple of months later in June 1935. Information about the SBT breed was obtained from the UK Kennel Club (2000) and the Staffordshire Bull Terrier Breed Council of Great Britain and Northern Ireland (2008).

1.3 Greyhound Racing

1.3.1 History

Greyhound racing was introduced to Britain in its modern day format by the American Owen Patrick Smith. Smith had invented the mechanical lure and circular track in the USA in 1925, and along with Charles Munn, set about promoting the sport in Britain. Together with Brigadier-General Alfred Critchley and Sir William Gentle they set up the Greyhound Racing Association (GRA). The very first purpose built Greyhound racing stadium, known as Belle Vue Stadium, was built by the GRA in Manchester in 1926. Its first meeting was held on the 24th July 1926. Following the introduction of Greyhound racing at Belle Vue, additional stadia were built around the country. To date there are 25 licensed Greyhound stadia in Britain and Greyhound racing is one of Britain's most highly attended spectator sports. The National Greyhound Racing Club (NGRC) was formed in January 1928 under the first steward Captain EAV Stanley and the Rules of Racing came into operation on 23rd April 1928. At that stage 43 stadia agreed to accept the discipline of the NGRC Stewards. The following year, in 1929, the British Greyhound Racing Board (BGRB) was set up to enable various stake holders in the sport to discuss the promotion and improvement of the

Greyhound racing industry, to consult with the NGRC regarding the rules of racing and to improve the care and welfare of the Greyhound. On the 1st January 2009 the Greyhound Board of Great Britain (GBGB) became operational, taking on and combining the functions of the BGRB and NGRC. Information about the history of racing was obtained from GBGB (2009).

1.3.2 Racing

In the UK Greyhounds are raced anti-clockwise over the flat or over hurdles around ovoid tracks. The term race refers to a simultaneous contest between a maximum of eight Greyhounds on a GBGB licensed racecourse, over a distance of no less than 210 metres and no more than 1105 metres (GBGB 2010). There are several different categories including open, graded and match: a full list of the different categories can be found in the GBGB rules of racing (GBGB 2010). A trial is any test run on a GBGB licensed racecourse other than a race. There are several trial types including schooling, sales and clearance trials (GBGB 2010). Greyhounds start racing once they reach the age of 15 months. A Greyhounds age is calculated based on the first day of the month in which it is whelped. For example, a Greyhound whelped in January cannot race before the 1st April in the following year. Once a Greyhound begins its racing career and has shown to be capable, it will usually be raced about once a week until it retires. Greyhounds either retire from racing because they are not good racers, they are "past their best" (this is usually around 5 to 6 years of age) or they have suffered a career-ending injury.

1.4 Injuries in racing Greyhounds

1.4.1 Injuries in the literature

Racing Greyhounds suffer injuries in training or during the course of a race or trial. They sustain a variety of musculoskeletal injuries that are rarely seen in pets or in other working

breeds of dogs (Davis 1967; Hickman 1975; Molyneux 2005; Prole 1976). It is assumed that the nature and consistency of the racing Greyhound's task, i.e. repetitively running in a counter-clockwise direction around a circular or ovoid track at high speed, leads to the injuries they sustain (Prole 1976). However, a whole range of factors including the speed at which the dogs race, track design (for example, the radius of the bends, how much the bends are banked and the composition of the track surface) and the weather, all contribute to injury development (Sicard *et al.* 1999). Racing injuries can result from either indirect trauma, such as fatigue fractures (Devas 1961; Gannon 1972; Wendelburg *et al.* 1988) or direct trauma, such as collision and falls (Sicard *et al.* 1999). Injuries caused by direct trauma appear to be rare and tend to result in fractures of the long bones of the limbs. Sicard *et al.* (1999) reported a 2% incidence of long bone fractures over a two year period at five Greyhound tracks in the USA; these fractures were consistently associated with falls, bumps and collisions. Injuries resulting from indirect trauma, i.e. fatigue fractures, are much more common, affecting bones such as the central tarsal and adjacent tarsal bones (Boudrieau *et al.* 1984; Dee *et al.* 1976; Devas 1961), metacarpal and metatarsal bones (Dee and Dee 1985; Gannon 1972) and the acetabulum (Wendelburg *et al.* 1988). The majority of racing injuries affect the limbs with most involving, or being distal to, the carpus in the thoracic limbs and the tarsus in the pelvic limbs. Prole (1976) reported 11% of all injuries sustained by racing Greyhounds involved the carpus and 6% the tarsus, and Sicard *et al.* (1999) reported 13% of injuries involved the carpus and 25% the tarsus.

Muscle injuries

Muscle injuries, ranging from a mild strain to a complete tear, are commonly seen in racing Greyhounds (Molyneux 2005). In the thoracic limb, the triceps brachii muscle which extends the elbow and flexes the shoulder, and in the pelvic limb the gracilis muscle which adducts the limb, are the most prone to injury (Davis 1973; Prole 1976). Triceps injuries do

not appear to affect one side in particular. However, the majority of gracilis injuries occur in the right limb in Greyhounds that are raced in the UK (Prole 1976; Vaughan 1969). However, this asymmetry is not found in Greyhounds raced in Australia (Davis 1973). Tears of the triceps and gracilis are often accompanied by the development of a haematoma that results in distortion of the lateral aspect of the shoulder or medial aspect of the thigh respectively, giving the impression of a disturbance of muscle contour and has led to the injuries being referred to as a "dropped muscle" (Bateman 1964; Davis 1967, 1973; Vaughan 1969). At present, it is not possible to relate any specific action or accident to account for tears of these muscles and therefore the factors common to all Greyhound injuries are implicated.

Tendon and ligament injuries

Tendon injuries are also common in racing Greyhounds and can range from strains to full disruptions (Molyneux 2005). In the thoracic limb, injuries to the digital flexor tendons account for 69% of all injuries to the metacarpus (Prole 1976). Additionally, the majority of carpal fractures, in particular fracture of the accessory carpal bone, are associated with avulsion of various tendons and/or ligaments (i.e. the tendon/ligament has pulled off a fragment of the bone) (Johnson 1987; Johnson *et al.* 1989; Johnson *et al.* 1988; Whitelock 2001). Other tendon injuries seen in the thoracic limbs of racing Greyhounds include avulsion or rupture of the biceps brachii and brachialis tendons of insertion (Schaaf *et al.* 2009), displacement of the biceps brachii tendon of origin (Boemo and Eaton-Wells 1995; Goring *et al.* 1984), sprain of the flexor carpi ulnaris tendon of insertion (Dee *et al.* 1990; Johnson 1987) and sprain and/or disorders of the attachment sites of the short radial collateral ligaments (Guilliard 1998; Guilliard and Mayo 2000a).

The common calcaneal tendon (CCT) in the pelvic limb results from the convergence of three distinct tendons: the gastrocnemius tendon, the superficial digital flexor (SDF) tendon

and the common tendon of the biceps femoris, gracilis and semitendinosus muscles (Evans and DeLahunta 1971; Miller *et al.* 1964). Injuries can be partial or complete and can involve any combination of these three tendons. Various injuries to the CCT have been reported in racing Greyhounds, ranging from strains and/or luxations of the individual SDF tendon (Dee *et al.* 1990; Prole 1976) to strains of the entire CCT (Prole 1976).

Fractures and dislocations

Fractures and/or dislocations of the carpus, metacarpus, tarsus and metatarsus make up a large proportion of distal limb injuries (Bateman 1960; Hickman 1975; Prole 1976). Prole (1976) reported approximately 12.5% of injuries to the distal thoracic limb and 32.0% of injuries to the distal pelvic limb were fractures or dislocations.

Fractures of the tarsus predominantly affect the right pelvic limb (Bateman 1960; Boudrieau *et al.* 1984; Gannon 1972; Guilliard 2000; Hickman 1975; Prole 1976), whereas fractures of the carpus in the thoracic limb do not seem to affect one side in particular. Some reports suggest the majority of carpal fractures occur in the left limb (Hickman 1975), while others suggest the right limb is most often injured (Bateman 1960; Dee and Dee 1985; Johnson *et al.* 1988; Poulter 1991; Prole 1976) and others report each side is equally affected (Gannon 1972).

In the thoracic limb racing Greyhounds are particularly prone to fracture of the right accessory carpal bone (Bateman 1960; Dee and Dee 1985; Johnson *et al.* 1988; Poulter 1991; Prole 1976; Vaughan 1985), usually associated with avulsion of one or more of the ligaments and/or tendons attached to the accessory carpal bone (Johnson 1987; Johnson *et al.* 1989; Johnson *et al.* 1988). Accessory carpal bone fractures have been classified into five types based on their radiographic and pathologic features; fracture type is determined by the fracture configuration and the ligaments and tendons that are involved (Johnson 1987).

The injury is believed to result from hyperextension of the carpus during the thoracic limb's stance phase of the gallop (Dee and Dee 1985). Guilliard and Mayo (2000b) determined that the forces acting on the carpus during thoracic limb stance phase cause the joint to hyperextend by up to 270°.

Fracture of the tarsus is one of the most commonly reported injuries in racing Greyhounds and it almost always involves the right limb (Bateman 1960; Boudrieau *et al.* 1984; Gannon 1972; Guilliard 2000; Hickman 1975; Poulter 1991; Prole 1976). The majority of tarsal injuries involve fracture of the central tarsal bone (CTB) (Boudrieau *et al.* 1984; Gannon 1972; Guilliard 2000; Hickman 1975), an anatomically important bone that articulates with all six of the other tarsal bones (Miller *et al.* 1964). Severe fracture of the CTB accounts for approximately 4% of all racing injuries (Gannon 1972) and is a common career ending injury in racing Greyhounds. Boudrieau *et al*. (1984) reported 34% of Greyhounds that had sustained a type IV or V CTB fracture were euthanatised or failed to return to competitive racing. Fractures of the adjacent tarsal bones are commonly associated with CTB fractures (Boudrieau *et al.* 1984; Guilliard 2000; Ost *et al.* 1987). A study by Ost *et al.* (1987) that looked at fractures of the calcaneus in 51 racing Greyhounds, found 80% of Greyhounds had sustained a fracture of both the CTB and the calcaneus. A review of 144 cases of CTB fracture in racing Greyhounds by Boudrieau *et al*. (1984) found 64% of the dogs also had fractures of the adjacent tarsal bones; T_4 and the calcaneus were the most often injured. Similarly, Guilliard (2000) described eight cases of CTB fracture in Greyhounds, half of which had sustained fractures of the adjacent tarsal bones with fracture of T_4 again being the most common. CTB fractures in racing Greyhounds have been classified into five types, ranging in severity from type I (dorsal slab fracture without displacement) to type V (severely comminuted and displaced), based upon radiographic evaluation of the fracture configuration (Dee *et al.* 1976). CTB fractures are thought to be fatigue fractures resulting

from the repetitive cycling loading encountered during training and racing (Johnson *et al.* 2000; Tomlin *et al.* 2000).

Metacarpal and metatarsal injuries are most often seen in young Greyhounds between 6 and 37 months of age (Bellenger *et al.* 1981; Ness 1993; Piras 2005). Male Greyhounds appear to be more susceptible to metacarpal and metatarsal fractures than female Greyhounds (Gannon 1972; Ness 1993; Piras 2005); this could be due to their heavier mass. These injuries usually occur on the rail-side of the affected foot, i.e. the side of the foot that is closest to the inside of the track (Figure 1.2). Left metacarpals four (MC_4) and five (MC_5), and right metacarpals two (MC_2) and three (MC_3) are the most often injured in the thoracic limbs (Bellenger *et al.* 1981; Dee and Dee 1985; Gannon 1972; Piras 2005). Left metatarsal five (MT_5) and right metatarsal three (MT_3) are the most often injured in the pelvic limbs (Dee and Dee 1985; Ness 1993; Piras 2005). Fractures of these rail-side metacarpals and metatarsals are believed to be fatigue fractures that result from the repetitive cyclic loading that occurs during training and racing (Johnson *et al.* 2001).

Figure 1.2: Diagram of the rail-side metacarpal and metatarsal bones within each distal limb of the racing Greyhound.

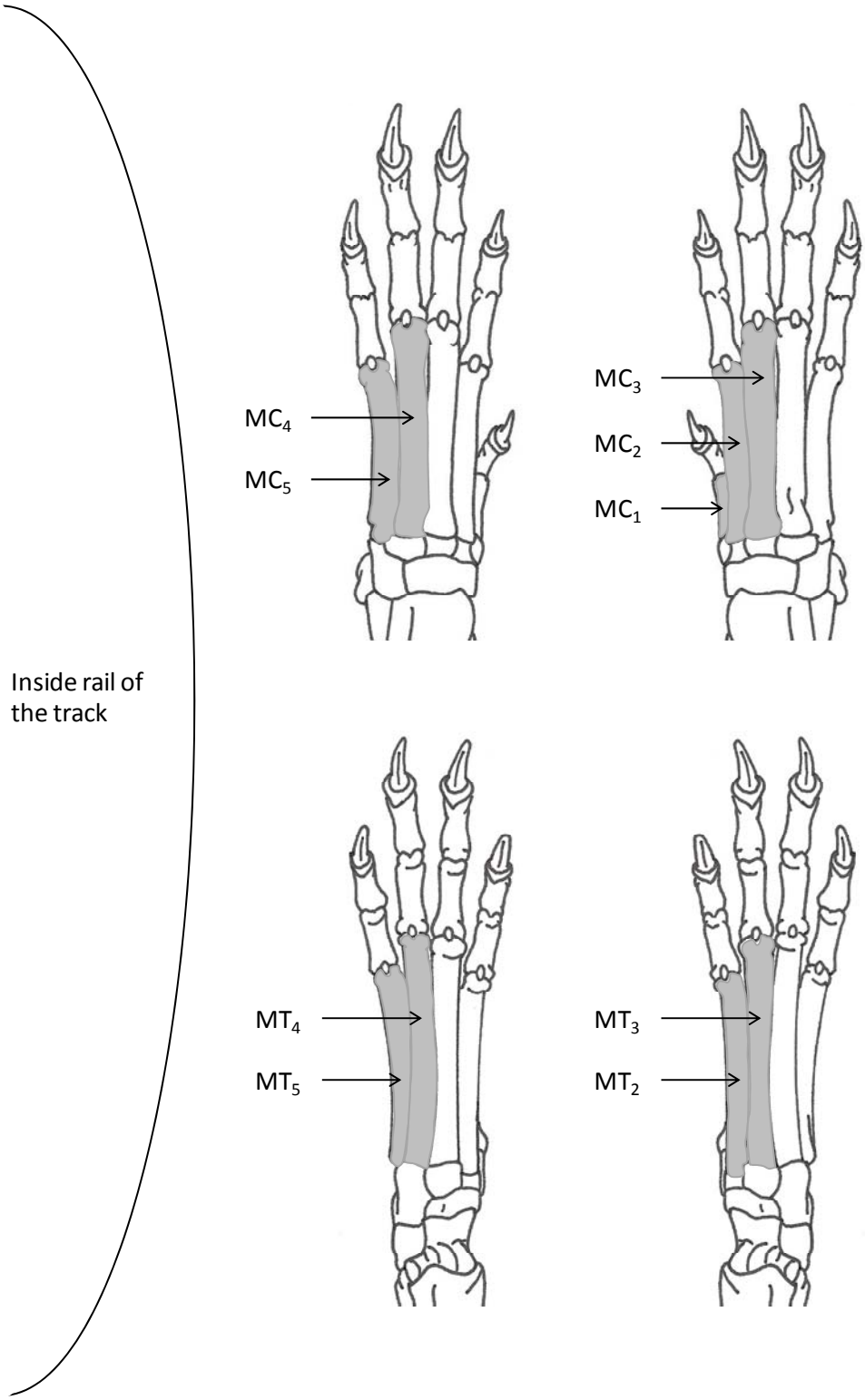

1.4.2 Injuries at a British track

From June 2007 to August 2010 a total of 87 Greyhounds (61 male and 26 female) were euthanatised at a GBGB registered track. The following information was obtained from post mortem examination and from pedigree and race data obtained from the online Greyhound database; www.greyhound-data.com.

Dog details and history

Mean age at euthanasia was 37 ± 10 months and mean weight was 30.0 ± 3.2 kg. The number of races run by the Greyhounds during their life was very variable, ranging from 0 to 137 with an average of 38 ± 28 races. Correspondingly, the total distance raced by the dogs during their life ranged from 0 to 65.3 Km, with an average of 18.4 ± 13.5 Km. All of the dogs were raced on the flat with the majority regularly being raced at a distance of 470 m. Trials were not included in any of the calculations of race history as they are inconsistently recorded on the online Greyhound database; www.greyhound-data.com. Pedigree information was available for these Greyhounds. Almost all of the Greyhounds that had been euthanatised were from different dams. However, these 87 Greyhounds had come from only 40 sires; none were full siblings. This is probably because breeders choose to breed from the more successful (male) dogs.

Reasons for euthanasia

There were three main reasons for euthanasia: severe injuries sustained during racing (80 dogs), health problems that resulted from racing (three dogs), and extreme behavioural problems such as aggression towards other dogs and/or people (11 dogs). The total number of dogs is less than the number of "reasons for euthanasia" as four dogs had sustained injuries to more than one region of their body and two other dogs had severe behaviour problems in addition to severe injuries sustained during a race. Racing injuries included soft

tissue injuries to various regions of the limbs, fractures and dislocations to various regions of the limbs and spinal fractures (Figure 1.3).

Figure 1.3: Pie chart detailing the most common reasons for euthanasia of racing Greyhounds at a GBGB registered British track.

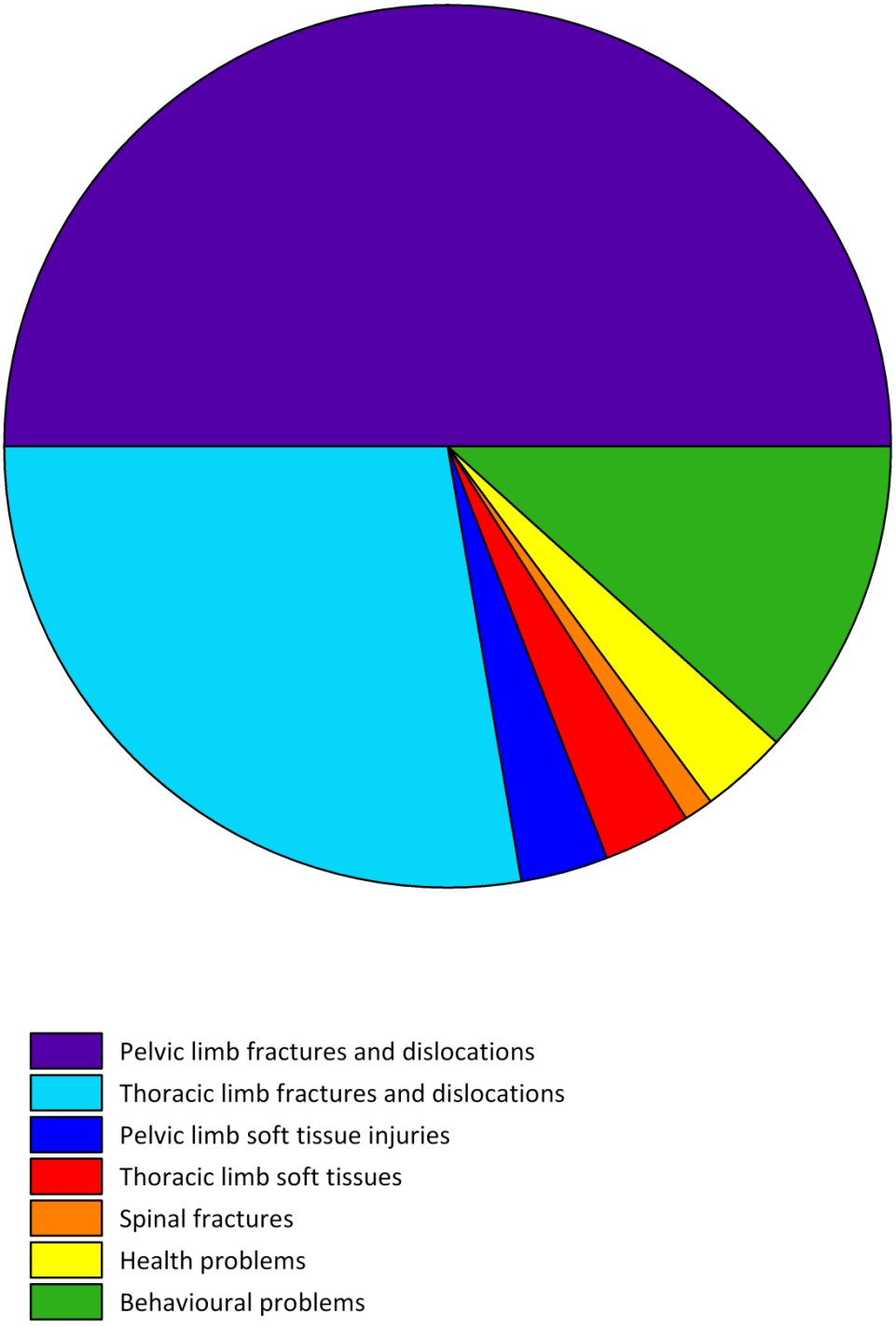

Consistent with the literature (Bateman 1960; Boudrieau *et al.* 1984; Gannon 1972; Guilliard 2000; Hickman 1975; Poulter 1991; Prole 1976), the most common reason for euthanasia was fracture of the right tarsus (Figure 1.4), accounting for 50.0% of all the racing injuries and 85.1% of all pelvic limb fractures/dislocations (Figure 1.5). Almost twice as many male dogs had been euthanatised due to fracture of the right tarsus as female dogs; 26 male versus 12 female. The second and third most common reasons for euthanasia were fracture of the radius and ulna, and fracture/dislocation of the carpus; accounting for 15.0% and 10.0% of all the racing injuries respectively. In contrast to the fractures of the tarsus, fractures of the antebrachium and carpus showed a bilateral distribution; nine dogs had injured their left and 11 their right limb. However, similar to the tarsal fractures, a much greater number of male dogs had been euthanatised than had female dogs; 16 male dogs versus four female.

In Greyhound racing male and female dogs are raced against each other. An analysis of one month of race meetings in 2010 at the same British track was carried out to see if more male dogs are raced than female dogs. Sixteen meetings consisting of 217 races were investigated. A total of 1297 Greyhounds were raced: 757 were male and 540 female, a ratio of 1.4 males for every female raced. This could partly explain the higher incidence of skeletal injuries in male dogs; however, the ratio of male to female dogs euthanatised due to injury was 2.4 : 1. A possible explanation for this could be that the heavier mass of the male places the musculoskeletal system under greater stresses which leads to a higher injury rate.

As the majority of the Greyhounds were euthanatised as a result of injuries to the distal limbs, we decided to focus on the bones, muscles and tendons within the distal limbs to see how they are adapted for the Greyhounds task and what effect training and racing has on these structures.

Figure 1.4: 3D reconstruction of computed tomography scans of the left (images on the right side of the page) and right (images on the left) tarsi from a Greyhound euthanatised due to a fractured right tarsus. The right central and fourth tarsal bones were fractured.

Dorsal views:

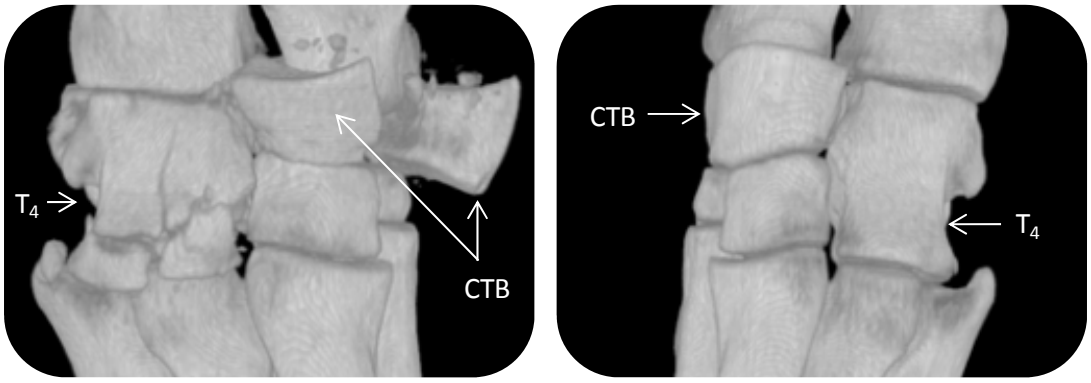

Medial views:

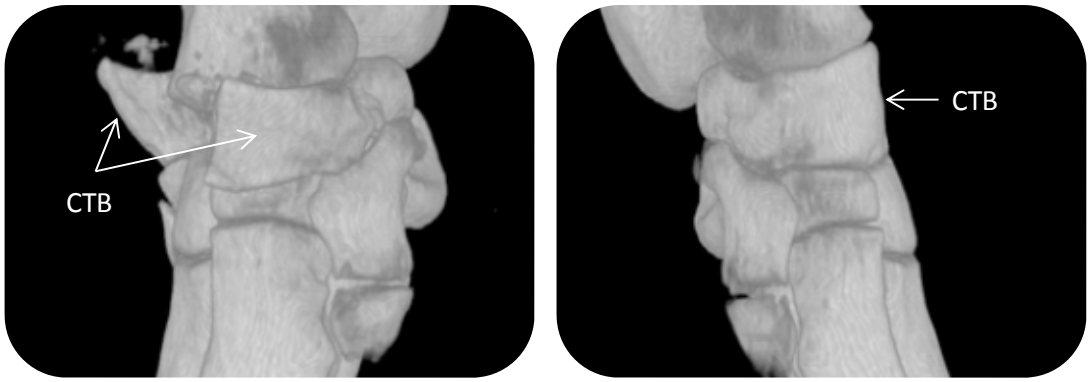

Lateral views:

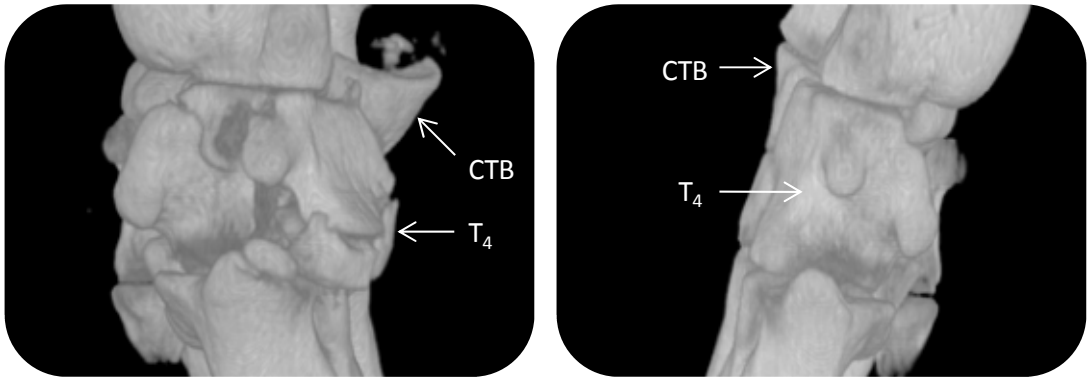

Figure 1.5: Breakdown of the most common sites of catastrophic fractures and/or dislocations in the pelvic limb of racing Greyhounds euthanatised at a British track. 42 dogs had sustained a fracture and/or dislocation of the pelvic limb, with the right tarsus being the most often injured.

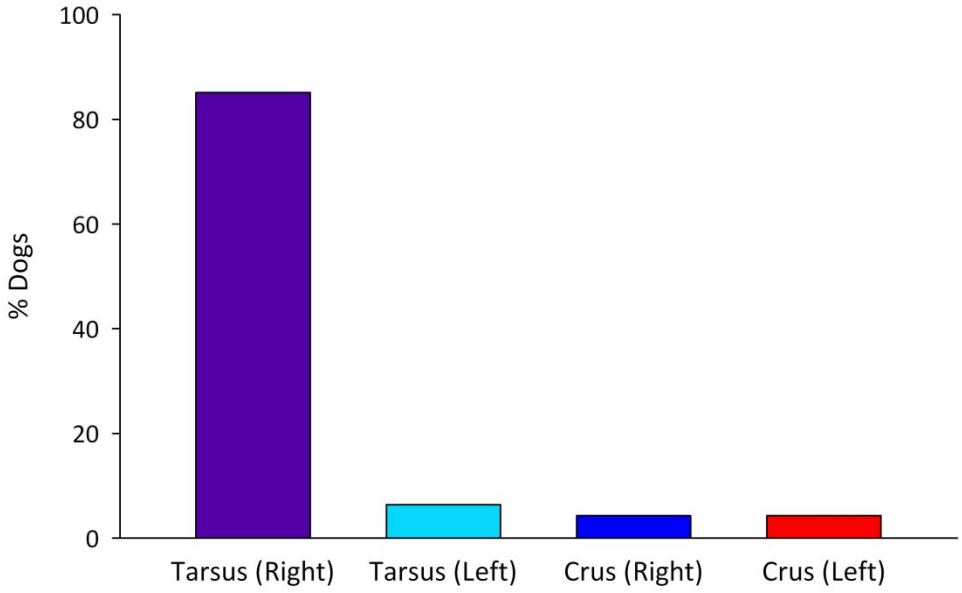

1.5 Anatomy of the thoracic distal limb

The distal thoracic limb is made up of the antebrachium, carpus, metacarpus and phalanges. The following anatomical information was obtained from Miller *et al.* (1964) and Evans and DeLahunta (1971).

1.5.1 Bones of the distal thoracic limb

The radius and ulna are the bones of the antebrachium, also known as the antebrachium. They cross each other obliquely so the proximal end of the ulna is medial to, and the distal end is lateral to, the radius. The radius is the shorter of the two bones. It articulates proximally with the humerus and distally with the carpus. It also articulates with the ulna, by its caudal surface proximally and near its lateral border distally. The ulna is located in the

caudal part of the forearm. It is longer than the radius and has an irregular shape, generally tapering from its proximal to its distal end. The ulna articulates proximally with the humerus and distally with the articular circumference of the radius.

The carpus refers to the section of the thoracic limb that lies between the forearm and metacarpus (Figure 1.6). There are seven small irregular bones arranged into a proximal and a distal row. The proximal row is made up of the radial, ulna and accessory carpal bones. The radial carpal bone lies on the medial side of the carpus and articulates proximally with the radius. The ulnar carpal bone lies on the lateral side of the carpus and articulates proximally with the styloid process of the ulna. The accessory carpal bone lies on the palmar aspect of the limb and articulates with the styloid process of the ulna and the ulnar carpal bone. The distal row of bones is made up of four bones that are numbered from medial to lateral. From the smallest bone on the medial side to the largest bone on the lateral side of the carpus they are known as the first, second, third and fourth carpal bones.

The metacarpus (Figure 1.6) contains five miniature long bones which have a slender body (diaphysis) and larger extremities (epiphyses). The proximal extremity is the base and the distal extremity is the head. As with the first to fourth carpal bones, the metacarpal bones are numbered from medial to lateral. Proximally, the first to fourth metacarpals articulate with the corresponding carpal bones. The fifth metacarpal bone articulates with the fourth carpal bone. Distally, all the metacarpals articulate with the corresponding proximal phalanges. The first metacarpal bone is atypical. It is a vestigial structure but, unlike the first metatarsal bone in the pelvic limb, it is always present.

There are three phalanges for each of the four main digits. The first digit has two phalanges. Each phalanx has a proximal head and a distal base.

Figure 1.6: Dorsal view of the bones of the distal thoracic limb. Adapted from Goody (1997).

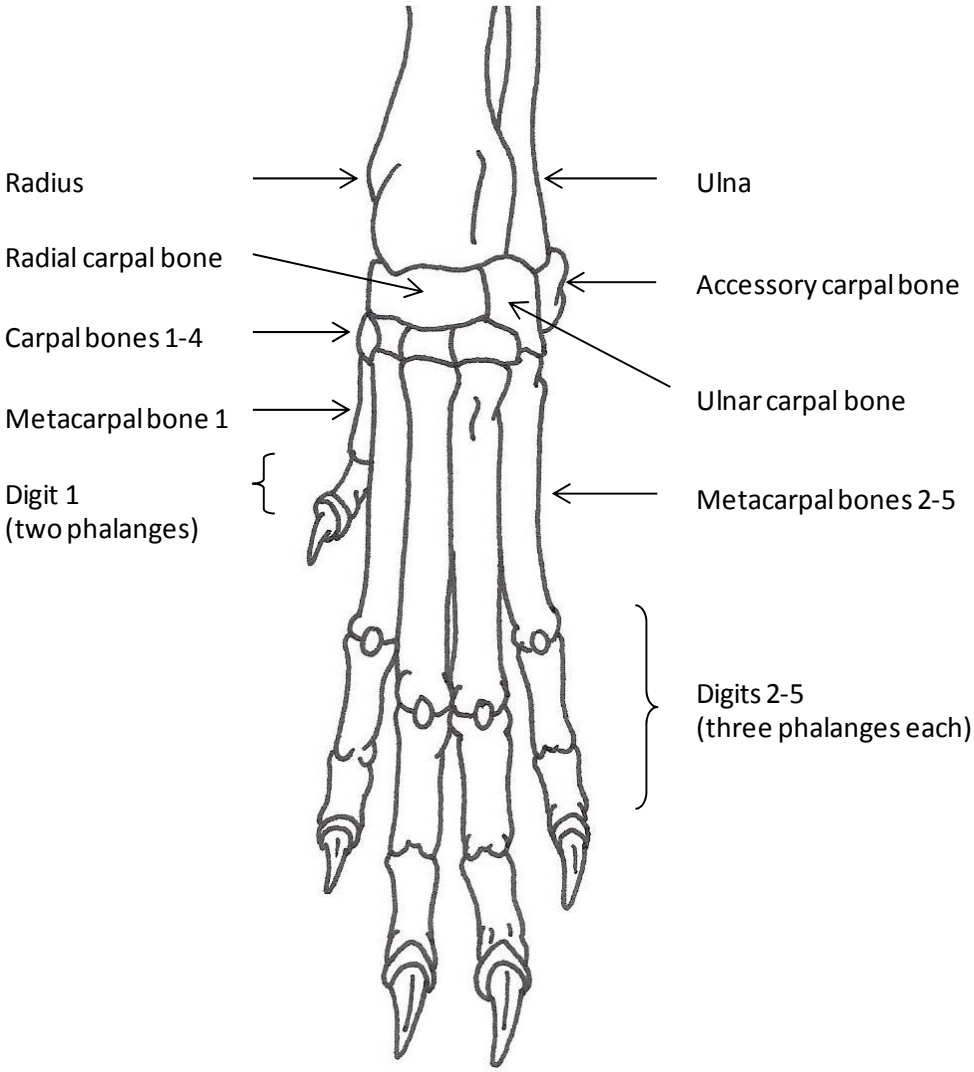

1.5.2 Muscles and tendons of interest in the distal thoracic limb

The superficial and deep digital flexor tendons and their corresponding muscles are the structures of interest (Figure 1.7).

The superficial digital flexor (SDF) lies between the skin and antebrachial fascia on the caudomedial side of the forearm. It originates from the medial epicondyle of the humerus, it covers the deep digital flexor (DDF) and the muscle belly extends almost to the carpus.

Figure 1.7: Palmar view of a canine (right) distal thoracic limb showing the muscles and tendons of interest. Only the ulnar head of the DDF is visible. The humeral and radial heads are out-of-view behind the SDF and other more superficial muscle-tendon units. Adapted from Evans and DeLahunta (1971).

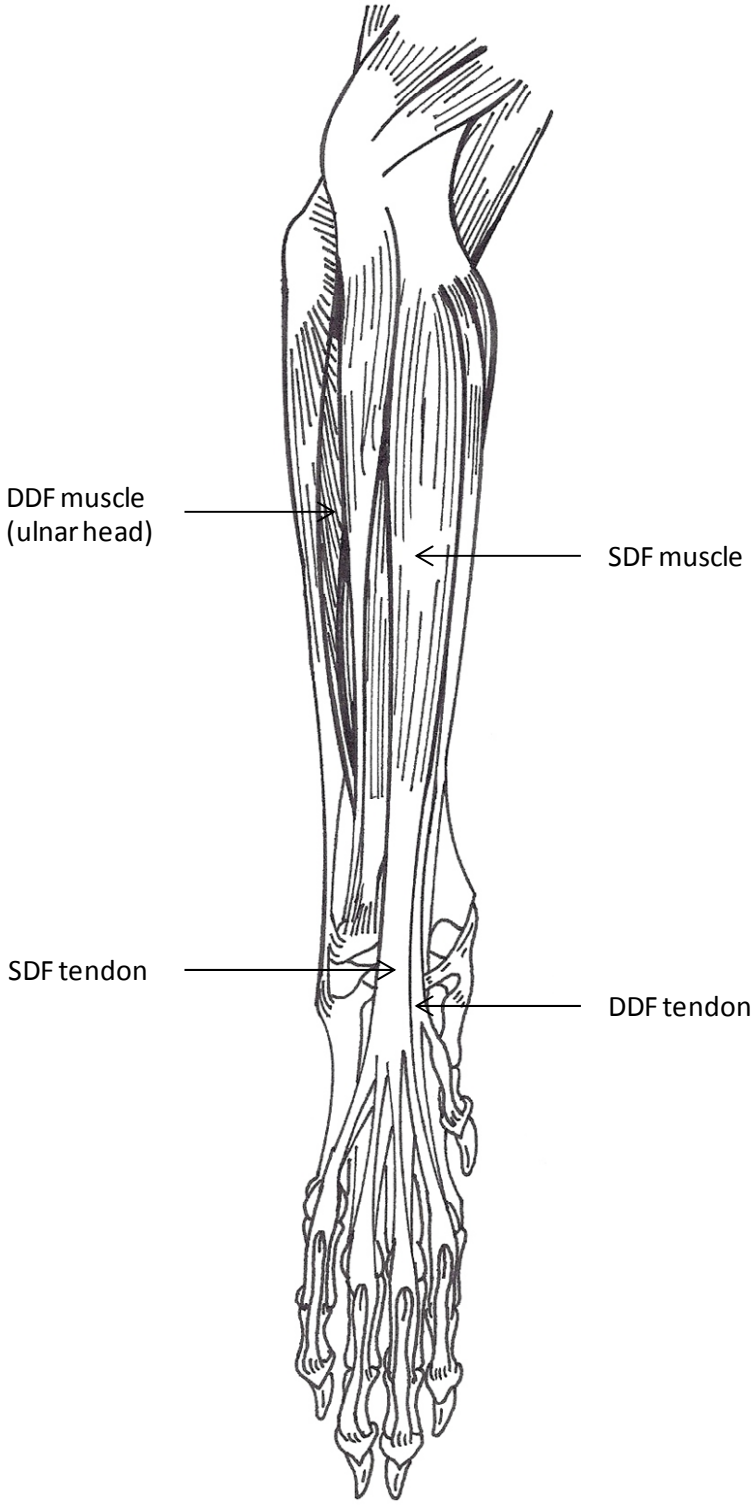

The SDF tendon is initially a single tendon. It crosses the flexor surface of the carpus medial to the accessory carpal bone, where it is covered by the superficial part of the flexor retinaculum, and branches into four tendons of nearly equal size. These four branches insert on the proximal palmar surfaces of the second phalanges of the four principle digits. At the metacarpophalangeal joint each tendon forms a collar around the DDF tendon which passes through it. Both the SDF and DDF tendons are held firmly in place at the metacarpophalangeal joint by palmar annular ligament. The SDF acts to flex digits two to five.

The DDF has three heads of origin which arise from the medial epicondyle of the humerus, the middle third of the medial border of the radius and the proximal three-fourths of the caudal border of the ulna. The humeral head is much larger than the other two, and the radial head is larger than the ulnar head. Their bellies lie on the caudal surfaces of the radius and ulna. The tendons of all three heads fuse at the carpus to form a single tendon, which is held in place in the carpal canal by the thick fibrous flexor retinaculum. The carpal canal is formed by the accessory carpal bone laterally, the joint capsule and carpal bones dorsally, and the flexor retinaculum on the palmar surface. Distal to the carpus the DDF tendon divides into five branches. Each branch goes to palmar surface of the base of the distal phalanx of its respective digit. The DDF acts to flex the digits.

1.6 Anatomy of the pelvic distal limb

The distal pelvic limb is made up of the crus (lower thigh), tarsus, metatarsus and phalanges. Anatomical information was obtained from Miller *et al.* (1964) and Evans and DeLahunta (1971).

1.6.1 Bones

The tibia and fibula are the bones of the crus, also known as the lower thigh or shank. The tibia is much larger than the fibular and lies in the medial part of the crus. It articulates proximally with the femur, distally with the tarsus and on its lateral side, both proximally and distally with the fibula. The fibula is a long, thin, laterally compressed bone located in the lateral part of the crus. It articulates proximally with the caudolateral part of the lateral condyle of the tibia and distally with the talus. It main purpose is muscle attachment as it supports little weight.

The tarsus refers to the section of the limb that lies between the crus and the metatarsus (Figure 1.8). There are seven bones arranged into three irregular rows. The proximal row is made up of a long, laterally located calcaneus and a shorter, medially located talus. Both the tibia and fibula articulate with the talus. There are four bones in the distal row numbered from medial to lateral. Three small bones, the first, second and third tarsal bones are located alongside each other and are separated from the proximal row by the central tarsal bone. The large fourth tarsal bone completes the distal row laterally and is as long as the combined lengths of the third and central tarsal bones against which it lies.

The metatarsus (Figure 1.8) contains five metatarsal bones that resemble the metacarpal bones. However, unlike the first metacarpal bone, the first metatarsal bone is not always present. The phalanges resemble those of the thoracic forepaw.

Figure 1.8: Dorsal view of the bones of the distal pelvic limb. Adapted from Goody (1997).

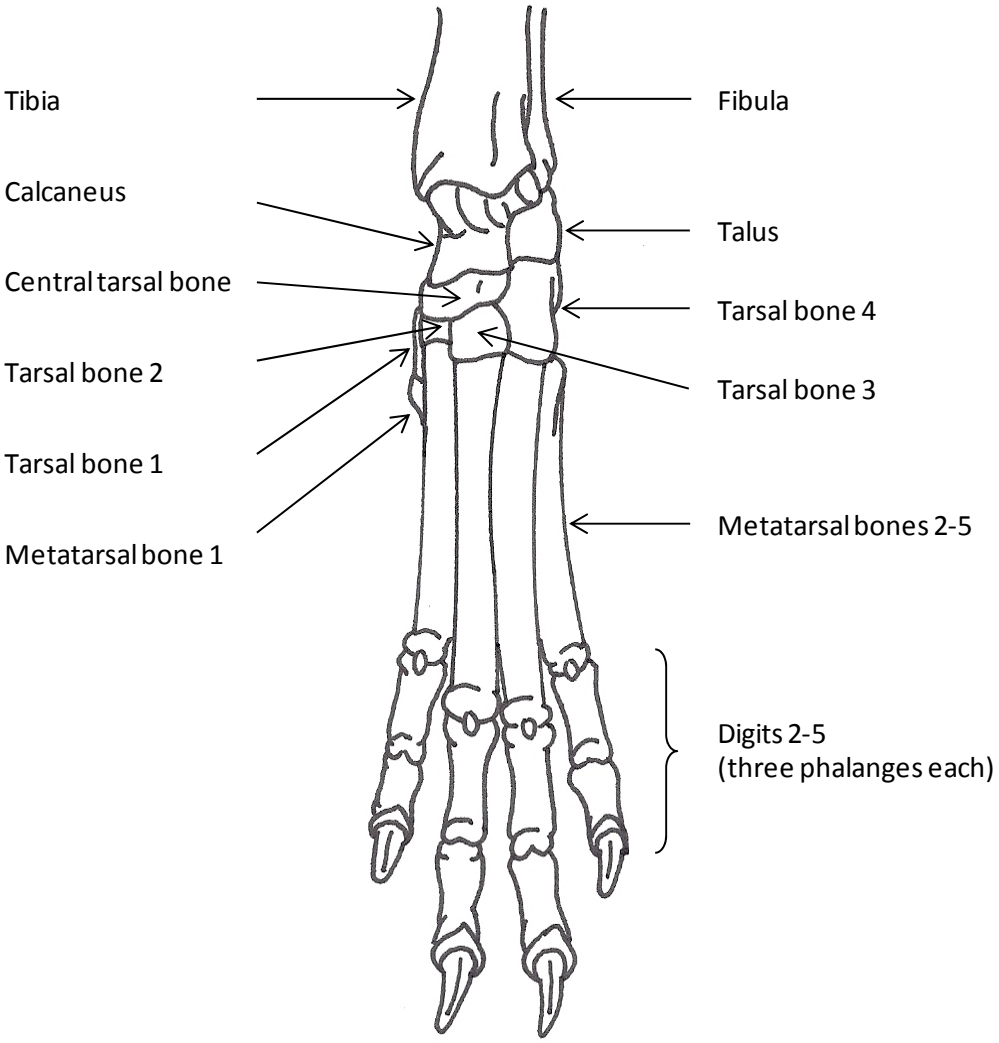

1.7.2 Muscles and tendons

The superficial and deep digital flexor tendons and their corresponding muscles are the structures of interest (Figure 1.9).

The SDF is a spindle shaped muscle arising from the lateral supracondylar tuberosity of the femur along with the lateral head of the gastrocnemius. Proximal to the calcaneal process the SDF tendon twists across the medial surface of the gastrocnemius. Further distally, the tendon widens, caps the tuber calcanei and attaches on each side of the tuber calcanei.

Figure 1.9: Plantar view of a canine (right) distal pelvic limb showing the muscles and tendons of interest. The medial and lateral deep digital flexor muscles are out-of-view behind the gastrocnemius muscles. Adapted from Evans and DeLahunta (1971).

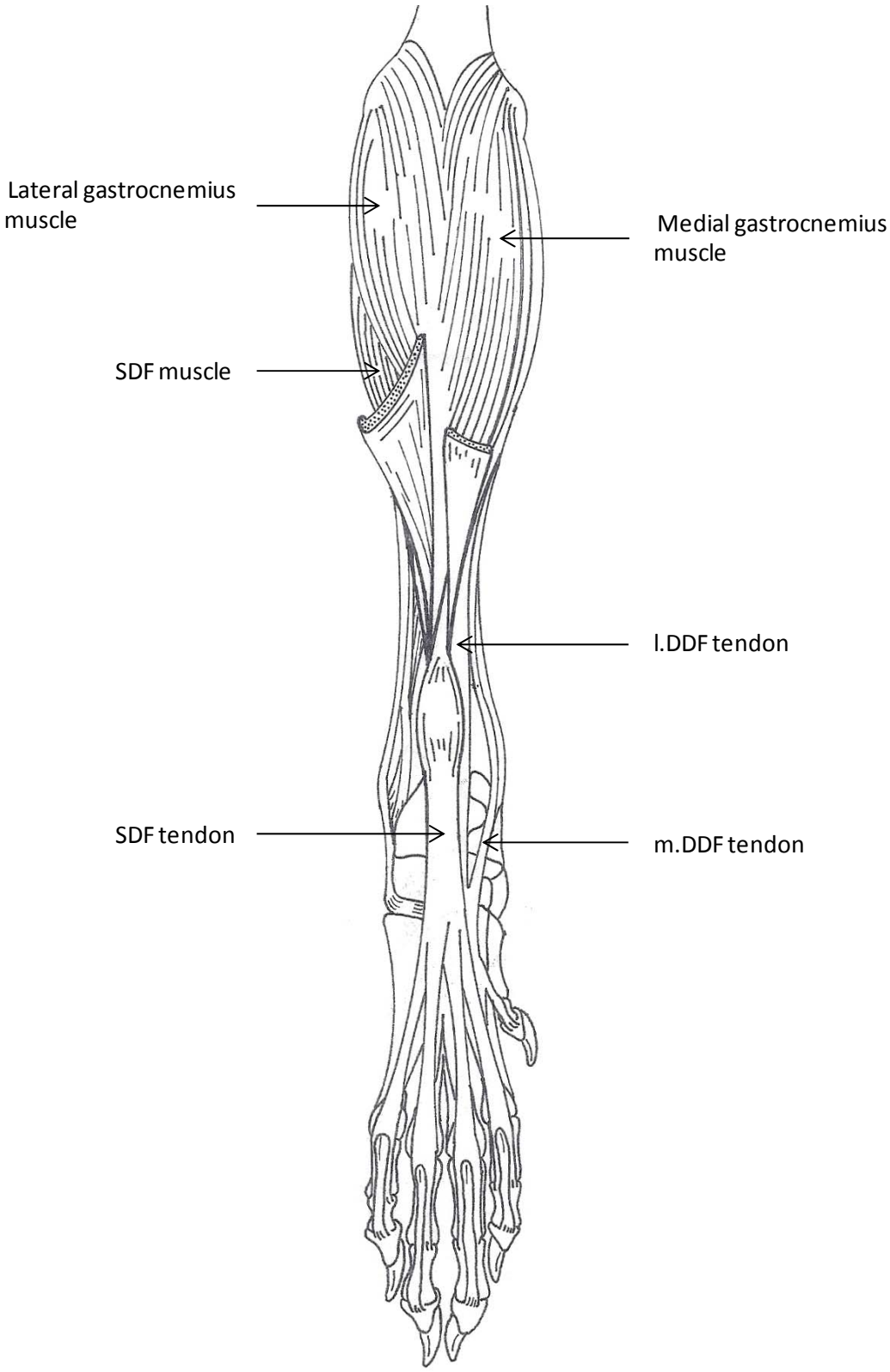

At the level of the distal row of tarsal bones, the tendon divides twice forming four tendons of nearly equal size. These extend distally over metatarsals two, three, four and five. At the metatarsophalangeal joints, each tendon forms a cylinder for the passage of the tendons of the DDF. The tendons insert at the bases of the second phalanges of digits two, three, four and five. The pelvic limb SDF acts to flex the digits and stifle, and to extend and fix the tarsus.

The gastrocnemius muscle is divided into a lateral and medial head. The lateral head arises by a large tendon on the lateral plantar tuberosity of the femur and the medial head from the medial plantar tuberosity. The two heads of the gastrocnemius almost totally enclose the SDF muscle; they all fuse together distally forming a flat muscle. After crossing the SDF tendon laterally, the tendon of the gastrocnemius inserts on the tuber calcanei.

The DDF consists of a large lateral head and a weaker medial head. The smaller medial head of the DDF lies between the lateral head and the popliteus muscle. It arises from the head of the fibula and the proximal end of the tibia and it runs distomedially. The medial DDF tendon lies on the caudomedial side of the tibia. At the level of the distal row of tarsal bones it unites with the tendon of the lateral head. The lateral head of the DDF arises from the caudolateral border of the proximal two-thirds of the tibia, most of the proximal half of the fibular and the adjacent interosseous membrane. The lateral DDF tendon begins as a wide expanse on the plantar side of the muscle which condenses distally. Medial to the tuber calcanei it is surrounded by the tarsal synovial sheath and bound in the groove over the sustentaculum tali of the calcaneus by the flexor reticulum. At the level of the distal row of tarsal bones the lateral DDF tendon fuses with the medial DDF tendon. At the middle of the metatarsus, the joined tendon then divides into four branches; these four branches behave in the same way as those of the DDF in the thoracic limb. The DDF acts to flex the digits and stifle and to extend the tarsus.

1.7 Hypothesis and aims

1.7.1 Hypothesis

Artificial selection has optimized the anatomy and physiology of the Greyhound to produce a supreme athlete designed specifically for fast cursorial locomotion. The extreme conditions encountered during racing test the Greyhounds musculoskeletal adaptations to the limit, often resulting in characteristic injuries, for example fracture of the right CTB.

1.7.2 Aims

- ***Determine what injuries are commonly sustained by racing Greyhounds***

There is a serious lack of data relating to injuries in racing Greyhounds in the United Kingdom (UK). Prole (1976) carried out a survey of injuries in Greyhounds racing at the London tracks. Track design is one of the contributing factors injury (Sicard *et al.* 1999) and since this survey was carried out by Prole (1976) advances have been made in track design. For example, tracks are now banked to some degree at each of the turns to reduce the centrifugal forces acting on the dogs at these points and tracks are now surfaced with a sand-composite rather than grass. More up to date data is required to determine what injuries Greyhounds racing in the UK are prone to and why. A literature review was carried out that details the most commonly reported injuries. The Greyhound Board of Great Britain (GBGB) was contacted to organise collection of Greyhound cadavers from a GBGB registered track in the UK. Data were collected and analysed regarding the reasons for euthanasia along with pedigree information and racing history. This provides information on the most common severe injuries sustained by Greyhounds raced in the UK. The most common injury, fracture of the right CTB, was examined in more detail. The ability of observers to evaluate CTB fractures accurately via two different imaging techniques, radiography and computed tomography (CT), was compared.

- ***Determine the effect of asymmetric cyclic loading on the bones in the Greyhound distal limb and compare to a non-raced breed of dog.***

The distal limb bones of Greyhounds experience asymmetrical loading because the dogs are always raced anti-clockwise around ovoid tracks. This pattern of loading leads to asymmetric adaptive remodelling of the distal limb bones, which involves phases of bone resorption followed by new bone formation. It is thought that the likelihood of fracture increases during skeletal remodelling, because the bone is mechanically weaker at this time and more susceptible to damage if subjected to further loading. We examined the effect of the stresses encountered during racing on the distal limb bones of Greyhounds and compared the Greyhound to a non-racing breed, the SBT. Dual-energy x-ray absorptiometry (DXA) was used to determine bone mineral density (BMD) and biochemical analysis was carried out to measure changes in the composition of the bone matrix and changes in the levels of markers of bone turnover. This allowed the extent of remodelling to be determined and provided information about how the fractures typically seen in racing Greyhounds could occur.

- ***Examine the effect of racing on the internal architecture of Greyhound distal limb bones and compare to a non-raced breed of dog.***

The internal architecture of bone is determined by anatomical site and the mechanical loads imposed upon the bone. Micro-CT scanning was used to examine the internal architecture of two of the distal limb bones that are especially prone to fatigue fracture in racing Greyhounds: the fifth metacarpal bone and the CTB. The SBT was used as a comparison.

- ***Determine how the muscles and tendons in the Greyhound distal limb are adapted for high speed running and compare to a breed of dog adapted for fighting.***

Animals adapted for fast cursorial locomotion, such as the racing Greyhound, have limbs with muscle-tendon units specialised for high acceleration and storage and recovery of elastic strain energy. Animals bred to fight, such as the SBT, have shorter tendons that do not function so well as springs. The architectural properties of the muscle-tendon units in the Greyhound distal limbs were examined and compared to the SBT. Morphometric analysis of the muscle-tendon units, as well as the results of mechanical testing of the digital flexor tendons, provides information on properties such as ultimate tensile strength, breaking stress, stiffness and ability to store elastic strain energy. This study details how the muscle-tendon units of Greyhounds have increased strength to withstand the high stresses and strains involved in high speed running, a higher capacity for elastic energy storage and increased efficiency of energy recovery compared to SBTs.

Chapter 2

COMPARISON OF RADIOGRAPHY AND COMPUTED TOMOGRAPHY FOR EVALUATING SEVERE CENTRAL TARSAL BONE FRACTURES IN RACING GREYHOUNDS

2.1 Abstract

Racing Greyhounds are prone to fracture of the right central tarsal bone (CTB). These fractures can be classified into five types based on configuration using radiographs. However, radiographs can be limited in their ability to evaluate complex joints. Computed tomography (CT) offers several advantages over conventional radiography. Our aim was to determine observer agreement on radiographic evaluation of severe CTB fractures and to compare this with evaluation of the same fractures using CT.

Radiographs and CT scans were obtained of the tarsi from right pelvic limbs of Greyhounds euthanatized after sustaining severe CTB fracture during racing. Four observers described and classified each fracture. Inter- and intra-observer agreements were calculated using the kappa and AC1 statistics.

Inter-observer agreement was higher for assessment of fractures using CT. Several fractures assessed by radiography were misclassified as a less severe type. Intra-observer agreement for assessment and classification of CTB fractures via radiography versus CT was variable. Overall agreement among all four observers was higher for CT than radiography. Additionally, when identifying fractures of the adjacent tarsal bones, observer agreement was higher for CT than radiography.

CT improved observer ability to correctly evaluate CTB fracture and detect the degree of displacement and extent of any comminution. Identification of fractures of adjacent tarsal bones was also improved when tarsi were assessed using CT. These data suggest that

treatment decisions based solely on radiographic assessment of CTB fractures may not produce the expected outcome. Therefore, based on the evaluation of the injuries carried out in this study, we propose that the current classification system requires review.

2.2 Introduction

2.2.1 Central tarsal bone fractures

Greyhounds are prone to distal limb injuries during training and racing (Sicard *et al.* 1999); particularly fractures of the right tarsus (Boudrieau *et al.* 1984; Guilliard 2000; Hickman 1975). The majority of these injuries involve fracture of the central tarsal bone (CTB) (Boudrieau *et al.* 1984; Gannon 1972; Guilliard 2000; Hickman 1975); an anatomically important bone that articulates with all six of the other tarsal bones (Miller *et al.* 1964) (Figure 1.8). Fractures of the adjacent tarsal bones, particularly the calcaneus and fourth tarsal bone (T_4) are often associated with CTB fracture (Boudrieau *et al.* 1984; Guilliard 2000). In racing Greyhounds, fractures of the CTB have been classified into five types (Figure 2.1, Table 2.1) based upon radiographic evaluation of the fracture configuration (Dee *et al.* 1976).

Figure 2.1: Types of central tarsal bone fracture as classified by Dee *et al.* (1976). Dashed lines represent fracture lines and arrows denote displacement.

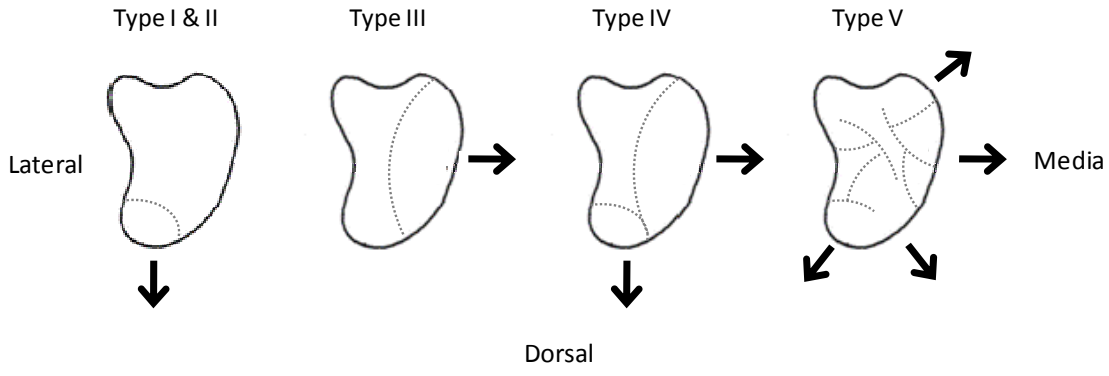

Table 2.1: Description of the five types of CTB fracture, as classified by Dee *et al.* (1976).

Type	Description
I	Dorsal slab fracture without displacement
II	Dorsal slab fracture with displacement
III	Dorsal and/or medial slab fracture with displacement
IV	Dorsal and medial slab fractures with displacement
V	Severely comminuted and displaced fractures

2.2.2 Imaging modalities

Radiography works on the principle that biological tissues are partially translucent with respect to X-ray photons. When a beam of X-rays is directed at a patient's body, a fraction of them will pass through while the rest will interact with, and be attenuated by, the biological tissues; the degree of attenuation depends on the type and quantity of the tissues present. The X-ray intensity produced behind the patient is measured to form a two-dimensional projection image (Guy and Ffytche 2005). Radiographs can be of limited use for the evaluation of complex joints such as the canine tarsus. Superimposition of the various bony structures, including the distal portion of the tibia and fibula, the talus, calcaneus, tarsal and metatarsal bones make identification of the structures difficult. Additionally overlapping structures can create radiolucent lines which can lead to misinterpretation of the image. The complexity of the tarsus means a detailed knowledge of the radiographic anatomy of the clinically normal canine tarsal joint is essential for correct interpretation of images (Carlisle and Reynolds 1990). Computed tomography (CT) scanning is based on and uses the same principles as conventional radiography. As a collimated high-kV X-ray beam is directed at the patient's body, fractions of the original beam are absorbed while others pass through, and a projection image is formed by measuring the X-ray intensity behind the patient (Guy and Ffytche 2005). The attenuation value along each ray from source to

detector can be calculated by comparing the primary beam intensity with the attenuated beam. The absorption of X-rays within a patient is directly proportional to the linear attenuation coefficient of the tissues through which the beam passes and the thickness of the object. The linear absorption in high kV beams is mainly due to electron density. Therefore high electron density tissues, such as bone, possess a higher linear absorption compared to low electron density tissue such as fat. The attenuation data obtained from the many different projections are re-calculated using a mathematical process called filtered back projection, and a matrix of the average relative X-ray absorptions in each volume element (short voxel) of the matrix in the slice of tissue examined is produced (Hathcock and Stickle 1993). The mean attenuation values in each element of this matrix, called Hounsfield Units (HU), are then displayed as picture elements (short pixels) in shades of grey in a two-dimensional digital image matrix. Therefore, each pixel represents a two-dimensional image of a three-dimensional voxel within the patient, with the third dimension being the slice thickness of the examined cross-section. CT scanning offers several advantages over conventional radiography, including the ability to produce detailed cross-sectional images, with improved resolution of the anatomical structures, which are free from distraction due to superimposed structures, as well as providing the facility for reconstruction of multi-planar images (Fitch *et al.* 1996; Gielen *et al.* 2001). CT is superior to radiography for the detection of small bone fragments and comminution in the injured limb (Morgan *et al.* 2006) and it is more reliable at detecting fracture displacements (Lozano-Calderon *et al.* 2006).

2.2.3 Study aim and hypothesis

The aim of this study was to compare radiographic and CT evaluation of CTB fractures in racing Greyhounds. This was achieved by evaluating and classifying the CTB fractures using the system described by Dee *et al.* (1976), then estimating and comparing intra- and inter-

observer agreements for each imaging modality. We also determined how effective radiography and CT were at identifying fractures of the adjacent tarsal bones, and compared the observer descriptions with post mortem findings. We hypothesised that CT would allow observers to describe and classify the fractured tarsi more accurately than radiography.

2.3 Materials and Methods

2.3.1 Specimens

Right pelvic limbs were collected from 14 racing Greyhounds (five females and nine males) that were euthanatized at their owners' request after they sustained a fracture of the right tarsus during a race. All of the tarsal fractures included fracture of the CTB. The mean age at euthanasia was 3.0 ± 0.7 years and mean bodyweight was 30.0 ± 2.8 kg. Limb specimens were disarticulated at the stifle and stored at -20 °C until required for further processing. Limbs were then thawed at room temperature prior to imaging by radiography and CT.

2.3.2 Digital radiography

Standard mediolateral and dorsoplantar radiographic views of the tarsi were obtained using a Siemens MULTIX TOP machine (Siemens Medical Solutions, Germany) linked to a computed radiography system (Fuji FCR-XG1, Fujifilm, UK). The CTB fracture classification system (Dee *et al.* 1976) was created based on mediolateral and dorsoplantar radiographic views, therefore oblique projections were not taken. All exposures were taken at 60kV and 1.80mAs, with 80% tube loading and each image was immediately reviewed to ensure diagnostic quality of exposure and positioning.

2.3.3 Computed tomography

Examinations were performed using a Siemens Somatom Volume Zoom 4 Slice Helical CT Scanner (Siemens Medical Solutions, Germany). Contiguous 0.5mm transverse slices were taken to generate multiple detailed, cross-sectional images of the tarsi. Slices were acquired at 120kV and 100mAs, collimation 0.5mm and table feed 1.0mm. Images were reconstructed using a window width of 4000, window centre of 700, very sharp (U90u) kernel, slice width of 0.5mm and a reconstruction increment of 0.5mm.

2.3.4 Post mortem observations

Soft tissues were removed from each limb. The limbs were disarticulated at the level of the talo-central joint and the proximal surface of the CTBs were described and photographed. CTBs were then carefully dissected free from the limbs, described and photographed. This process (disarticulation of the relevant joint, description and dissection) was repeated for all additional fractured tarsal bones.

2.3.5 Data evaluation

Radiographs and CT scans were evaluated by four observers (two boarded specialists in small animal orthopaedic surgery including one with extensive experience of working with injured Greyhounds, one boarded specialist in veterinary diagnostic imaging and one practising veterinary surgeon with extensive experience of working with injured Greyhounds). All observers were blinded to specimen identity. Each observer was asked to classify the type of CTB fracture present based on the classification system by Dee *et al.* (1976) and to describe any associated fractures. Radiographs and CT scans were evaluated in separate sessions in a randomised order with radiographs being evaluated first. Observers were allowed to describe the fractures at their own pace but discussion between observers was not allowed.

2.3.6 Statistical analysis

Classification of CTB fractures

Inter-observer and intra-observer agreements were initially calculated using the kappa statistic (Cohen 1960) and the quadratically weighted kappa statistic (Cohen 1968; Fleiss 1981). Both kappa and weighted kappa compare the observed measure of agreement with the level expected by chance alone; however, kappa does not take into account the degree of disagreement between all observers treating all disagreements equally (Cohen 1960). Weighted kappa is useful for ordered categories as it allows disagreements of varying gravity to be weighted accordingly by assigning a ratio-scaled degree of disagreement to each subject for which raters disagree by a number of categories (Cohen 1968; Fleiss 1981), i.e. greater emphasis is attached to large differences between ratings than to small differences. An overall kappa statistic was calculated for each imaging modality according to Fleiss' method of calculating kappa with multiple raters (Fleiss 1971). The kappa statistic is affected by parameters such as trait prevalence (Feinstein and Cicchetti 1990). Therefore, an alternative agreement coefficient, the AC1 statistic (Gwet 2001), was also used to calculate inter-observer and intra-observer agreements, and a generalised AC1 statistic (Gwet 2001) was calculated for each imaging modality. The kappa and AC1 values obtained were interpreted using the benchmark definitions of Landis and Koch (1977), whereby a value of one represents perfect agreement, a value of zero represents agreement equal to chance alone and a negative value implies that agreement is worse than chance alone. Full details of the definitions can be found in Table 2.2. The Landis and Koch definitions (poor, slight, fair, moderate, substantial and almost perfect) (Landis and Koch 1977) are commonly used to categorize observer agreement statistics. While these definitions are considered arbitrary, we used them to describe our data in order to allow a comparison of the Kappa and AC1 statistics.

Table 2.2: Definitions of the level of agreement according to the κ value, as described by Landis and Koch (1977).

κ value	Strength of agreement
≤ 0	Poor
0.01 – 0.20	Slight
0.21 – 0.40	Fair
0.41 – 0.60	Moderate
0.61 – 0.80	Substantial
0.81 – 1.00	Almost perfect

Identification of associated fractures

Observer agreement was calculated using the kappa statistic. Each observer's assessment was compared to the "gold standard", the post mortem findings. The benchmark definitions of Landis and Koch (1977) were again used to interpret the results.

2.4 Results

2.4.1 Post mortem observations

All 14 Greyhounds had sustained severely comminuted and displaced fractures of the CTB; examples of these can be seen in Figures 2.2 and 2.3. All of the dogs had sustained one or more fractures of the adjacent tarsal bones; these included the T_4 (11 dogs), calcaneus (seven), talus (three), third tarsal bone (T_3) (one) and second tarsal bone (T_2) (one). Fractures of the proximal head of the fourth metatarsal (MT_4) (two) and fifth metatarsal (MT_5) (one) bones were also found (Table 2.3).

Figure 2.2: View of the proximal surface of the CTB and T_4. A comminuted and displaced (dorsally and medially) fracture of the CTB is visible (black arrow). A chip fracture of T_4 can also be seen (white arrow).

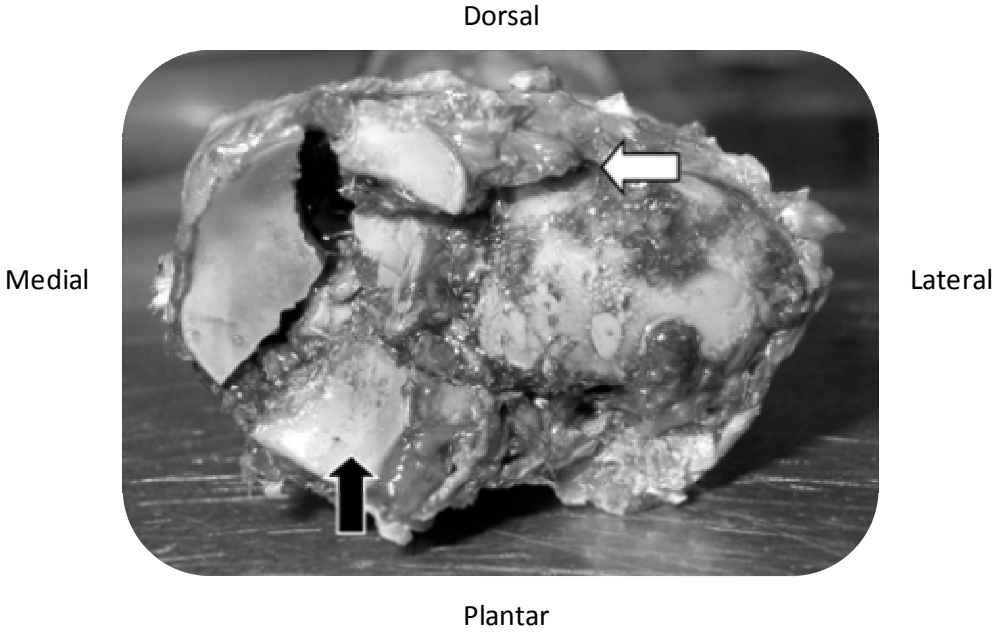

Figure 2.3: Image of an isolated CTB from one of the Greyhounds, showing the severity of the fracture sustained.

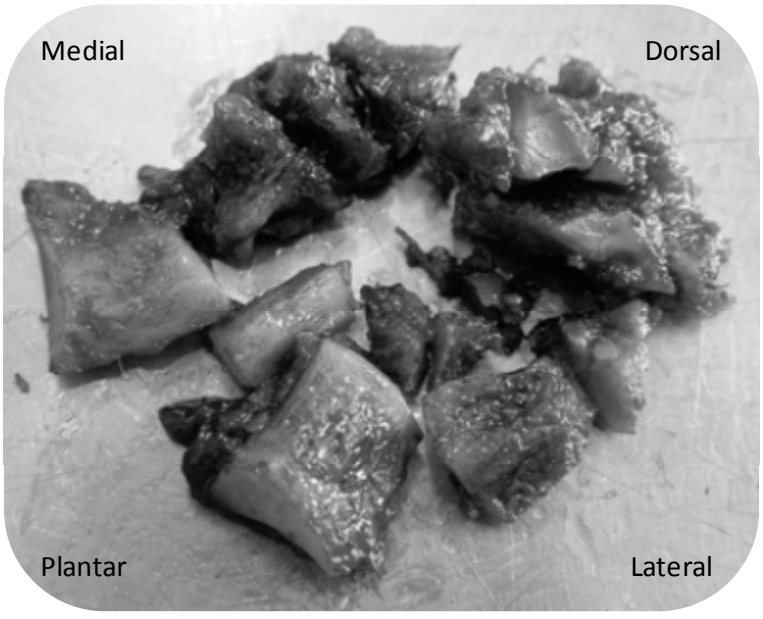

Table 2.3: Description of the CTB fracture type and details of the adjacent tarsal bones that were also fractured based upon post mortem findings.

Dog	Type of CTB fracture	Associated fractures
1	V: severely comminuted and displaced	T_3, T_4
2	V: severely comminuted and displaced	T_4
3	V: severely comminuted and displaced	Calcaneus, T_2
4	V: severely comminuted and displaced	Calcaneus, T_4
5	V: severely comminuted and displaced	T_4, MT_4
6	V: severely comminuted and displaced	Calcaneus
7	V: severely comminuted and displaced	Calcaneus, T_4
8	V: severely comminuted and displaced	Talus, T_4
9	V: severely comminuted and displaced	Talus, T_4
10	V: severely comminuted and displaced	Calcaneus, T_4
11	V: severely comminuted and displaced	Talus, T_4
12	V: severely comminuted and displaced	Calcaneus, T_4
13	V: severely comminuted and displaced	T_4, MT_4, MT_5
14	V: severely comminuted and displaced	Calcaneus

2.4.2 Classification of CTB fractures

Radiographs and then CT scans were used to assess and classify each of the 14 CTB fractures (Figure 2.4). A greater range of classifications were obtained from the observers when radiographs of the CTB fractures were assessed. This was more marked for observers I and II. Assessment of the CTB fractures using CT scans gave less variable results; three out of four of the observers classified all fractures as the most severe type of fracture, namely type V.

Figure 2.4: Frequencies with which the four observers allocated CTB fractures to each of the five different classifications when using radiographs (clear) and CT (hatched) scans.

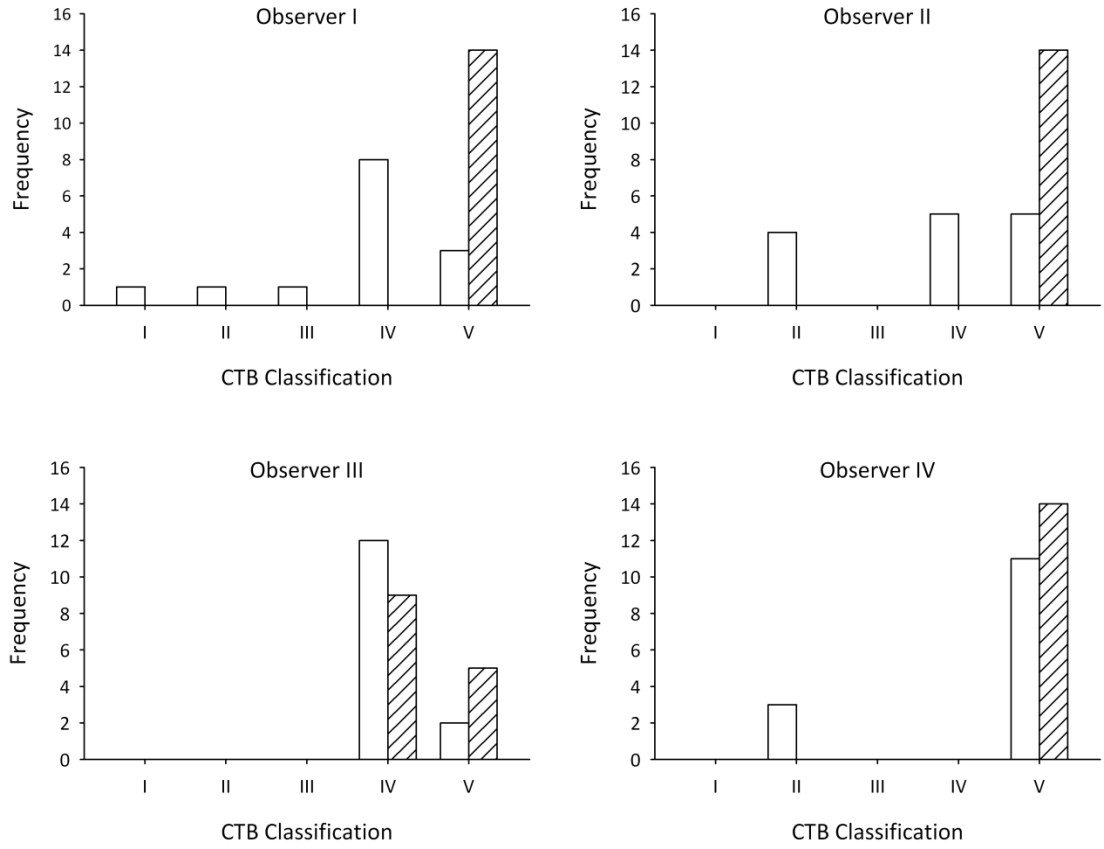

2.4.3 Identification of associated fractures

Observers were asked to describe any additional fractures present within the tarsus; their findings were compared to the post mortem observations (Table 2.4). Observer agreement was similar for identification of calcaneal fractures via CT and radiography, with mean values of κ = 0.714 ± 0.280 (95% confidence interval (CI)) (substantial agreement) for CT and κ = 0.786 ± 0.140 (substantial) for radiography. Observer agreement was higher for identification of fractures of the talus and T_4 (Figure 2.5) via CT assessment. Identification of talus fractures resulted in mean values of κ = 0.368 ± 0.141 (fair) for CT and κ = 0.051 ± 0.070 (slight) for radiography, and identification of T_4 fractures results in mean values of κ = 0.635 ± 0.358 (substantial) for CT and κ = 0.208 ± 0.109 (fair) for radiography. Observer agreement was higher for identification of T3 fractures using CT compared to radiography, with mean values of κ = 0.158 ± 0.309 (fair) for CT and κ = -0.019 ± 0.038 (poor) for radiography. However, observer agreement was higher for identification of fractures of T_2 using radiography, with mean values of κ = -0.038 ± 0.044 (poor) for CT and κ = 0.250 ± 0.490 (slight) for radiography.

Table 2.4: Observer agreement (each observer compared to post mortem findings) for evaluating adjacent tarsal bone fractures via radiography and CT. Values reported represent the kappa value ± 95% CI.

	Calcaneus	Talus	T_4	T_3	T_2
Radiography					
Observer I	0.714 ± 0.187	0.000 ± 0.512	0.263 ± 0.227	-0.077 ± 0.705	0.000 ± 0.964
Observer II	0.714 ± 0.187	0.000 ± 0.512	0.041 ± 0.162	0.000 ± 0.964	0.000 ± 0.964
Observer III	1.000 ± 0.000	0.054 ± 0.339	0.263 ± 0.227	0.000 ± 0.964	1.000 ± 0.000
Observer IV	0.714 ± 0.187	0.152 ± 0.359	0.263 ± 0.227	0.000 ± 0.964	0.000 ± 0.964
Mean	**0.786 ±0.140**	**0.051 ± 0.070**	**0.208 ± 0.109**	**-0.019 ± 0.038**	**0.250 ± 0.490**
CT Scans					
Observer I	0.857 ± 0.138	0.152 ± 0.359	0.576 ± 0.278	0.000 ± 0.964	0.000 ± 0.964
Observer II	0.286 ± 0.253	0.440 ± 0.367	0.152 ± 0.359	0.000 ± 0.964	0.000 ± 0.964
Observer III	0.857 ± 0.138	0.440 ± 0.367	0.811 ± 0.182	0.000 ± 0.964	-0.077 ± 0.705
Observer IV	0.857 ± 0.138	0.440 ± 0.367	1.000 ± 0.000	0.632 ± 0.355	-0.077 ± 0.705
Mean	**0.714 ± 0.280**	**0.368 ±0.141**	**0.635 ± 0.358**	**0.158 ± 0.309**	**-0.038 ± 0.044**

Figure 2.5: Frequencies with which the four observers correctly identified T_4 fractures using radiography (clear) and CT (hatched). During post mortem it was confirmed that 11 out of the 14 Greyhounds had T_4 fractures.

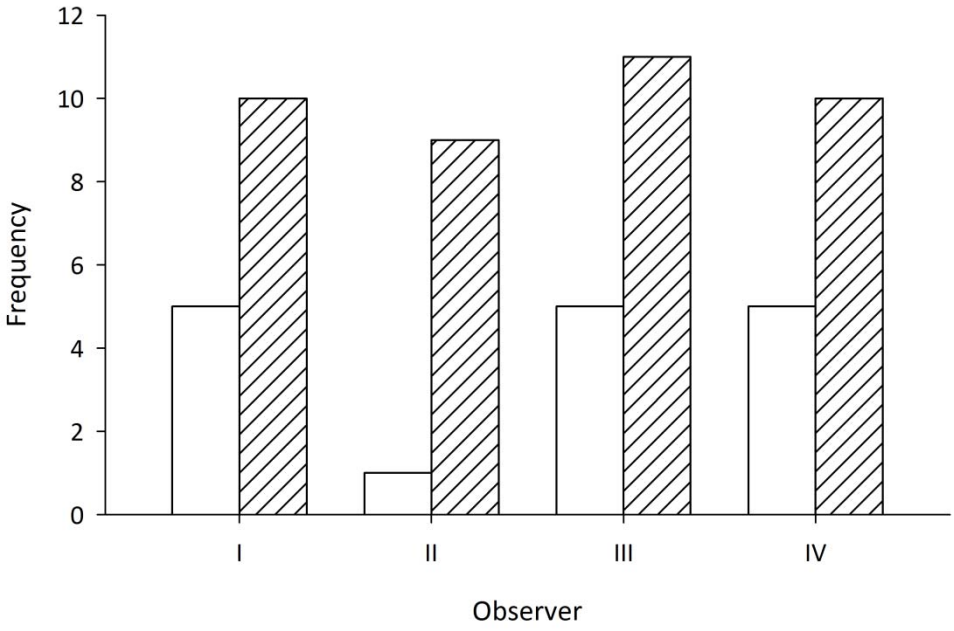

2.4.4 Inter-observer agreement for each imaging modality

Inter-observer agreement was higher for assessment of CTB fractures via CT than for assessment via radiography (Table 2.5). Mean values of κ = 0.500 ± 0.438 (95% CI) (moderate agreement), κ_ω = 0.500 ± 0.438 (moderate), AC1 = 0.639 ± 0.316 (substantial) for CT compared to mean values of κ = 0.102 ± 0.060 (slight), κ_ω = 0.269 ± 0.185 (fair), AC1 = 0.258 ± 0.164 (fair) for radiography.

Table 2.5: Inter-observer agreement in evaluating CTB fractures via radiography and CT. Values reported represent the agreement value ± 95% CI.

	P_o	κ	κ_w	AC1
Radiography				
Observer I vs. II	0.357	0.080 ± 0.601	0.455 ± 0.464	0.228 ± 0.313
Observer I vs. III	0.571	0.106 ± 0.905	0.144 ± 0.885	0.517 ± 0.303
Observer I vs. IV	0.214	0.038 ± 0.441	0.517 ± 0.363	0.056 ± 0.268
Observer II vs. III	0.429	0.111 ± 0.675	-0.048 ± 0.772	0.338 ± 0.312
Observer II vs. IV	0.500	0.240 ± 0.666	0.437 ± 0.491	0.415 ± 0.318
Observer III vs. IV	0.143	0.034 ± 0.346	0.109 ± 0.420	-0.005 ± 0.223
Mean		**0.102 ± 0.060**	**0.269 ± 0.185**	**0.258 ± 0.164**
CT Scans				
Observer I vs. II	1.000	1.000 ± 0.653	1.000 ± 0.390	1.000 ± 0.000
Observer I vs. III	0.357	0.000 ± 0.000	0.000 ± 0.000	0.278 ± 0.292
Observer I vs. IV	1.000	1.000 ± 0.653	1.000 ± 0.390	1.000 ± 0.000
Observer II vs. III	0.357	0.000 ± 0.000	0.000 ± 0.000	0.278 ± 0.292
Observer II vs. IV	1.000	1.000 ± 0.653	1.000 ± 0.390	1.000 ± 0.000
Observer III vs. IV	0.357	0.000 ± 0.000	0.000 ± 0.000	0.278 ± 0.292
Mean		**0.500 ± 0.438**	**0.500 ± 0.438**	**0.639 ± 0.316**

2.4.5 Comparison of radiography to CT

Assessment of the CTB fractures by radiography resulted in a number of CTB fractures being misclassified by the observers as a less severe type of CTB fracture (Figure 2.6). Figure 2.7 shows an example of a misclassified CTB fracture.

Figure 2.6: Frequencies with which CTB fractures were misclassified as the same or as a less severe type of CTB fracture when assessed by radiography compared to CT. (NB: 0 means the fracture was classified as the same type when assessed by radiography and CT. 1, 2, 3 or 4 means the fracture was misclassified as 1, 2, 3 or 4 classifications lower when assessed by radiography compared to CT).

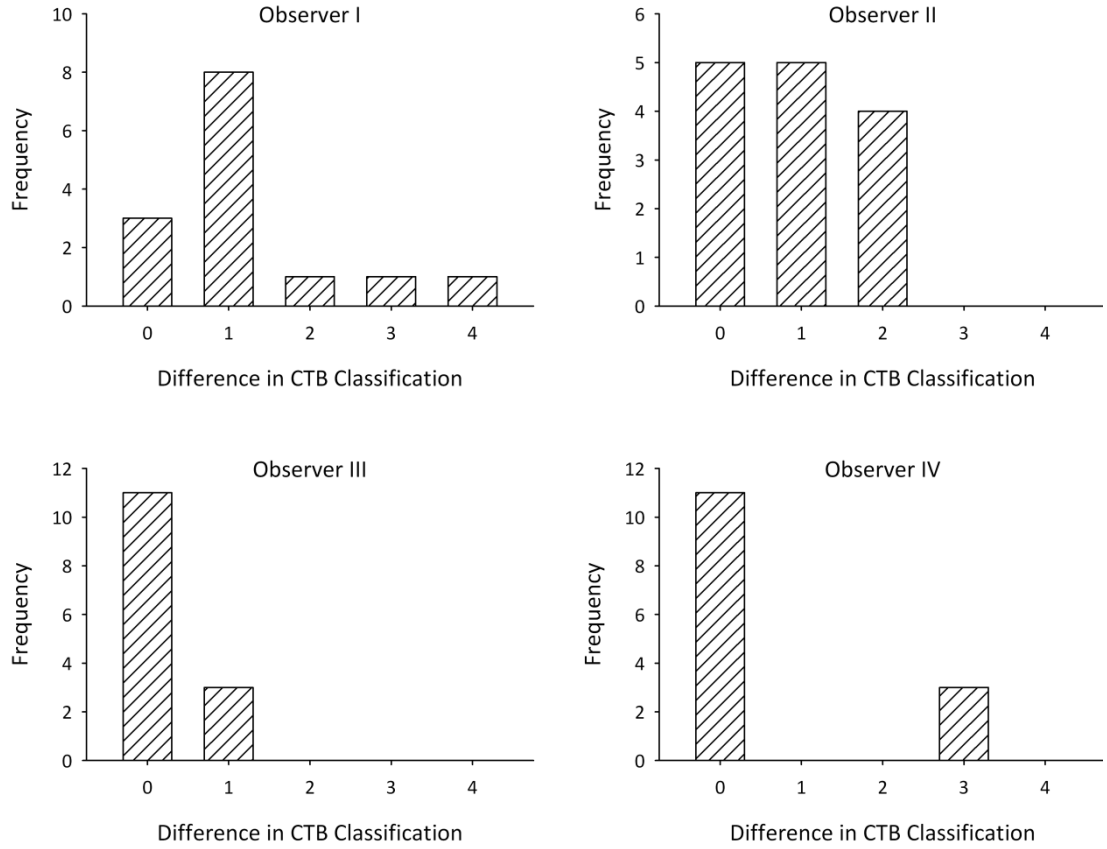

Figure 2.7: (a, b) Radiographic views and (c, d, e) CT images showing a CTB fracture that was misclassified as a less severe type of CTB fracture when initially assessed using radiographs. When this CTB fracture was assessed using radiographs, three out of the four observers classified the fracture as type I or II, i.e. a dorsal slab fracture with or without displacement. When the CT images were assessed, the fracture was classified as type V, i.e. severely comminuted and with displacement of the bone fragments.

2.4.6 Intra-observer agreement

Intra-observer agreement (Table 2.6) for assessment and classification of CTB fractures via radiography versus CT varied from poor to moderate when calculated using kappa (κ = 0 to 0.463) and weighted kappa (κ_ω = 0 to 0.462) and from slight to substantial when calculated using the AC1 statistic (AC1 = 0.090 to 0.775).

Table 2.6: Intra-observer agreement in evaluating CTB fractures: radiography versus CT scans. Values reported represent the agreement value ± 95% confidence interval (CI).

	P_o	κ	κ_w	AC1
Observer I	0.214	0.000 ± 0.458	0.000 ± 0.859	0.090 ± 0.258
Observer II	0.357	0.000 ± 0.653	0.000 ± 0.691	0.268 ± 0.297
Observer III	0.786	0.462 ± 0.904	0.462 ± 0.540	0.764 ± 0.246
Observer IV	0.786	0.000 ± 1.678	0.000 ± 1.003	0.775 ± 0.234

2.4.7 Overall agreement for multiple observers

Overall agreement among all four observers was calculated for each imaging modality. The generalised kappa statistic (Fleiss 1971) calculated for assessment of CTB fractures via radiography yielded a κ value of 0.013 ± 0.180 (95% CI) (slight agreement), whereas assessment via CT yielded a κ value of -0.191 ± 0.529 (poor). However, when calculated using the generalised AC1 statistic, radiography gave an AC1 value of 0.249 ± 0.083 (fair) and CT gave an AC1 value of 0.655 ± 0.140 (substantial).

2.5 Discussion

Racing Greyhounds are prone to fracture of the right CTB (Boudrieau *et al.* 1984; Gannon 1972; Hickman 1975). Severe fracture of the CTB forms approximately 4% of all racing injuries (Gannon 1972) and is a common career ending injury in racing Greyhounds. In a

previous study it was found that 34% of Greyhounds that had sustained a type IV or V CTB fracture were euthanatised or failed to return to competitive racing (Boudrieau *et al.* 1984). Fractures of the adjacent tarsal bones are commonly associated with CTB fractures (Boudrieau *et al.* 1984; Guilliard 2000). In a review of 144 cases of CTB fracture in racing Greyhounds, Boudrieau *et al*. (1984) found that 64 % of the dogs also had fractures of the adjacent tarsal bones, with the T_4 and calcaneus being the most often affected. Likewise, Guilliard (2000) described eight cases of CTB fracture in Greyhounds, half of which had sustained fractures of the adjacent tarsal bones, with fracture of T_4 again being the most common.

Fractures of the CTB in racing Greyhounds have been classified into five types based on the fracture configuration (Dee *et al.* 1976). Fracture classification systems such as this have an important role in orthopaedic practice: they allow for the description of fractures and provide guidelines for treatment and prognosis, as well as allowing comparison of different treatments among injuries of comparable severity. Therefore, it is important that a fracture classification system is robust.

The radiographic anatomy of the canine tarsus has been described in detail by Carlisle and Reynolds (1990). However, radiographic evaluation of such a complex joint remains problematic due to superimposition of the various bony structures. CT is able to provide several advantages over conventional radiography including improved resolution of the anatomical structures (Fitch *et al.* 1996; Gielen *et al.* 2001).

We looked at the classification and evaluation of CTB fractures in racing Greyhounds using radiography and CT, and calculated observer agreement for each imaging modality. We also looked at how well CT and radiography allowed fractures of the adjacent tarsal bones to be identified, and compared the observer descriptions with the post mortem findings.

Our study was limited to tarsal samples from Greyhounds euthanatised after they had sustained a severe fracture of the right tarsus, involving the CTB. CT and post mortem examination revealed all of the Greyhounds used in our study had the most severe type V fracture (Table 2.3), which led to prevalence bias. This prevalence bias could have been avoided if the study had included Greyhounds with less severe tarsal fractures; however, Greyhounds with less severe injuries are rarely euthanatised. Therefore, it would have limited the study as it would not have been possible to compare the observer agreements to the post mortem observations.

Cohen's kappa (Cohen 1960) is a well known chance-corrected measure of inter-observer agreement that compares the observed measure of agreement with the level expected by chance alone. However, there are several problems associated with using it, the best known of these are the two paradoxes presented by Feinstein and Ciccheti (1990). The first paradox results from the fact that the magnitude of the kappa statistic can be dramatically reduced by an unexpectedly high chance-agreement probability even when the observed probability is high. The second paradox occurs due to unbalanced marginal totals producing higher values of kappa than more balanced marginal totals (Feinstein and Cicchetti 1990). The marginal distributions describe how observers assign subjects to the response categories. Unbalanced marginal totals result when there is bias between the observers (i.e. the observers differ in their assessment of the frequency of occurrence of a condition). Thus, these two paradoxes arise because the kappa statistic is affected by any bias between observers and by the overall prevalence (i.e. the relative probability of the possible responses) (Brennan and Silman 1992; Byrt *et al.* 1993; Eugenio and Glass 2004). During data analysis it became apparent that due to bias in the overall prevalence, kappa would be an unsuitable statistic to use. To try and account for this we attempted to use weighted kappa because, while the categories used in the classification system were not strictly ordinal as normally required for this statistic, there is an increase in severity of the CTB

fracture from type I to type V. However, weighted kappa was unable to overcome the problems of bias, again yielding non-sensible results. Finally, an alternative chance-corrected agreement coefficient termed the AC1 statistic (Gwet 2001), which appears to be less sensitive to trait prevalence and marginal homogeneity compared with kappa (Gwet 2002; Gwet 2008), was used successfully , overcoming the problems of bias and providing sensible results. We did consider using the AC2 statistic (Gwet 2001) which, like the weighted kappa statistic, can be used for ordinal scales. However, the weightings that are applied when calculating these statistics are arbitrary. Additionally, the CTB fracture classification system is not truly ordinal as, while it represents increases in severity from type I to type V, the scale of severity does not necessarily represent a steady progression of even steps: for example, there is no evidence that type IV is twice as severe as type II. This is why weighted kappa was not ideal and did not correct for the prevalence bias in the study. Therefore, we decided to use the AC1 statistic.

We found that using CT scans to assess and classify the CTB fractures improved the observer's ability to correctly evaluate the fractures: CT improved the observer's ability to observe the degree of any displacements and the extent of any comminution (Table 2.5). Hence, the inter-observer agreement was greater: evaluation using CT scans gave an AC1 statistic of 0.639 compared to 0.258 using radiographs. The results for intra-observer agreement for assessment and classification of CTB fractures via radiography versus CT were variable (Table 2.6): Intra-observer agreement was highest for the two observers with extensive experience of working with injured Greyhounds. Overall agreement among all four observers was higher when CTB fractures were assessed and evaluated using CT scans suggesting that CT is the preferred method of evaluation of such fractures (Section 2.4.7).

CTB fracture classifications were more consistent between observers when CT scans were used to assess and evaluate the fractured tarsi. Assessment of the CTB fractures by

radiography resulted in a number of CTB fractures being misclassified by the observers as a less severe type of CTB fracture (Figure 2.4). It should be noted that all Greyhounds used in this study had the most severe type V fracture, therefore, the results of this study mainly relate to animals with severely fractured tarsi. Further investigation would be required to determine if simpler fractures are able to be accurately assessed by radiography alone. However, this underestimation of the severity of fracture has implications for practising veterinary surgeons, where a decision to treat the animal has to be made, as the prognosis may not be accurate if relying on radiographic imaging alone. For example, if a Greyhound is diagnosed with a less severe type of CTB fracture (type I or II as opposed to type V) then they will not receive the appropriate treatment, possibly resulting in deterioration of the injury, a prolonged recovery period and a decreased chance of successfully returning to racing. It is possible that the accuracy with which the fractures are assessed with plain radiography could be improved by using oblique projections in addition to standard orthogonal views.

We also found that identification of fractures of the calcaneus, talus, T_4 and T_3 bones was improved when observers assessed the tarsi using CT as opposed to radiographs (Table 2.4). A T_2 fracture was found in one dog; this fracture was identified by only one observer when the tarsus was assessed using radiographs and was missed by all when assessed using CT. We can only speculate as to why this occurred. It is possible that the fragments were thought to belong to the CTB due to the type of fracture (a small dorsal chip fracture) and the anatomical position directly under the (fractured) CTB. It is also possible that, due to the small size of the T_2, any malalignment in positioning could have led to the formation of artefacts and uncertainty over whether or not T_2 was fractured.

The current classification system, created by Dee *et al.* (1976), was produced by evaluating radiographs of Greyhounds with fractured tarsi. This study has shown that evaluation via

standard orthogonal radiographs can lead to an underestimation of the severity of type V CTB fractures; this may be particularly true when the clinician evaluating the radiographs has less experience with the specific injuries that occur in racing Greyhounds. All of the Greyhounds used in this study were found to have type V CTB fractures when evaluated using CT scans, whereas the initial evaluation via radiography produced a wide range of fracture classifications from type I to V. The results of this study indicate the current classification system is not very robust for the evaluation and classification of severe CTB fractures; however, as the results of this study only relate to type V fractures, it is not possible to say how well the classification system would perform for the less severe types of CTB fracture.

2.6. Summary

CT was shown to be superior to radiology for the assessment and classification of severe CTB fractures, and it improved observer ability to correctly identify the majority of adjacent tarsal bone fractures. However, it did not detect every pathologic feature and fractures of the smallest tarsal bones may still be missed. Additionally, notwithstanding the aforementioned limitations of this study, the results suggest that further CT-based investigation of CTB fractures is required to more accurately define the types of injuries that are sustained. This may allow a redefinition of the classification system.

Chapter 3

PHYSICAL AND BIOCHEMICAL EVIDENCE FOR ASYMMETRIC BONE REMODELLING IN THE DISTAL LIMB BONES OF RACING GREYHOUNDS

3.1. Abstract

The distal limb bones of Greyhounds experience asymmetrical loading because the dogs are always raced anti-clockwise around ovoid tracks with relatively tight bends. Repetitive loading leads to micro-damage formation, which stimulates bone turnover and repair by remodelling; however, the likelihood of fracture increases if the rate of resorption exceeds the rate of new bone formation, as it might if the dogs have insufficient recovery time between races. The aim of the study was to determine the extent of asymmetric remodelling of the distal limb bones and to see whether it could help explain the characteristic fractures typically seen in racing Greyhounds.

Distal thoracic and pelvic limbs were collected from racing Greyhounds and Staffordshire Bull Terriers (SBTs). Dual-energy x-ray absorptiometry (DXA) of the distal aspect of each limb and isolated bones was performed to obtain measurements of bone mineral density (BMD). Pairs of selected distal limb bones from both breeds were used to evaluate differences in their biochemical composition.

Increased bone resorption (increased matrix metalloproteinases (MMPs)) and bone formation (increased BMD, mineral content and bone specific alkaline phosphatase (BALP) levels) seen in the uninjured rail-side bones from racing Greyhounds suggests increased adaptive bone formation and remodelling is taking place. When central tarsal bones (CTB) from Greyhounds with a right CTB fracture were analysed, BMD and mineral content asymmetries were significantly reversed. The fractured bones had lower mineral content as well as high hydroxyproline content, indicating they are hypomineralised. These changes in

the bone matrix and the asymmetries between the left (uninjured) and right (fractured) bones could indicate that at some point an imbalance in the bone remodelling process has occurred, allowing micro-damage to accumulate, leading to weakening of the bone and structural failure. No asymmetries were present within SBT bones. This data supports the hypothesis that the physical and biochemical changes that take place within the Greyhound bones, and which can lead to characteristic fractures of those bones, occur as a result of the demands of racing.

3.2 Introduction

The racing Greyhound is an example of a superior sprint athlete that undergoes regular cyclic training, i.e. the dogs are regularly raced in one direction around an ovoid track subjecting their limbs to regular asymmetric cyclic loading. Greyhounds sustain injuries to their distal limbs that are similar to those seen in human athletes and military recruits, and, as such, provide a model to study the effect of repetitive loading on the properties of distal limb bones.

3.2.1 Bone turnover

Bone is a dynamic tissue continuously undergoing turnover throughout life. Bone turnover takes place via two processes; modelling and remodelling. Both involve the resorption of old bone by osteoclasts and the deposition of new bone by osteoblasts (Frost 1973; Lee *et al.* 2002; Martin and Burr 1989). When bone resorption and formation are spatially and temporally independent of one another, bone morphology changes to withstand the loads placed upon it. Frost (1990a) defined this as bone modelling. Bone remodelling involves the sequential removal and replacement of bone at discrete sites via the combined actions of the osteoclasts and osteoblasts that make up the bone multi-cellular unit (BMU) (Frost 1990b, 1992). A BMU forms in response to a signal or stimulus and follows the sequence;

origination and organisation of the BMU, activation of osteoclasts, resorption of the "old" bone, recruitment of osteoblasts, formation of new bone matrix (osteoid) and mineralisation (Frost 1966; Hattner *et al.* 1965; Parfitt 1994, 2000). The life span of the individual cells within a BMU is shorter than that of the BMU: as a BMU progresses along or through bone new cells are continually recruited to allow continued activation, resorption and formation. Once a BMU has been activated there are two phases of bone resorption. First there is a rapid phase lasting about eight days during which multi-nucleated osteoclasts begin to resorb a cavity, then a slower phase lasting about 34 days during which mononuclear cells continue resorption and pre-osteoblasts are stimulated to proliferate (Eriksen *et al.* 1984). Once the resorption cavity is at its maximum eroded depth there is a reversal phase lasting about nine days (Eriksen *et al.* 1984). The reversal phase signals the end of resorption and the initiation of formation. Osteoblasts converge at the bottom of the resorption cavity and start forming osteoid which begins to mineralise after 15 days (Eriksen *et al.* 1984). The osteoblasts continue to form and mineralise osteoid until the cavity is filled. The time to fill in the cavity at any point on the bone surface is between 124 and 168 days (Eriksen *et al.* 1984). The length of time for each of the bone remodelling phases appears to vary between species; the values reported here from Eriksen *et al.* (1984) refer to remodelling in human bone. Bone remodelling in rats is much shorter taking about 6 days in total (Guyomard and Baron 1974; Vignery and Baron 1980); the resorption phase takes 1.5 days (Vignery and Baron 1980), the reversal phase 3.5 days (Vignery and Baron 1980) and the formation phase 1 day (Guyomard and Baron 1974). Li *et al.* (1990) report a bone formation period of 27 days and a total bone formation period of 76 days, with mineralisation lagging behind the start of bone formation by 10 days. Bone remodelling preferentially occurs in regions of bone where micro-damage has formed: Mori and Burr (1993) demonstrated a significant increase in new remodelling events following the formation of micro-damage within canine radii. Therefore, remodelling enables bone

that is damaged by micro-fractures to be removed and replaced with healthy new bone (Burr 1993; Lee *et al.* 2002). The external morphology of the bone is not affected; however, its internal architecture (i.e. trabecular orientation, trabecular density etc.) may be subtly altered to increase the ability of the bone to resist the external loads placed upon it. During remodelling in skeletally mature animals, the processes of bone resorption and formation are balanced to prevent net changes in bone mass (Frost 1964); however, this balance can be affected by changes in the loading of bone with increased loading leading to increased bone mass and decreased loading causing a reduction in bone mass (Lanyon 1984; Rubin and Lanyon 1985). Additionally, the balance between micro-damage formation and repair by remodelling is important. Increased rates of damage formation or a deficient repair mechanism, such as what is seen in metabolic bone diseases likes Paget's disease or osteoporosis (Raisz 1999), can alter this balance. Imbalances in the rates of micro-damage formation and repair can cause micro-damage to accumulate until catastrophic structural failure occurs (Tomlin *et al.* 2000).

3.2.2 Mechanical loading of bone

The mechanical competence of whole bone can be characterised by the deformation it undergoes during loading (Figure 3.1). Generally, a linear relationship exists between the load imposed on the bone and the amount of bone deformation until the bone reaches its yield point (Khan 2001). Prior to the yield point bone is in its elastic region whereby if the bone was unloaded it would return to its original shape, i.e. applied forces in the elastic region cause temporary deformations. Beyond the yield point the slope of the load-deformation curve reaches a plateau and the area under this region of the curve is known as the plastic region. The plastic regions marks the point where permanent deformation occurs and where local fractures or other damage may result. If load is applied beyond the plastic region the failure load will be reached and the bone will fail completely.

Figure 3.1: The load-deformation curve of bone. Adapted from Khan (2001).

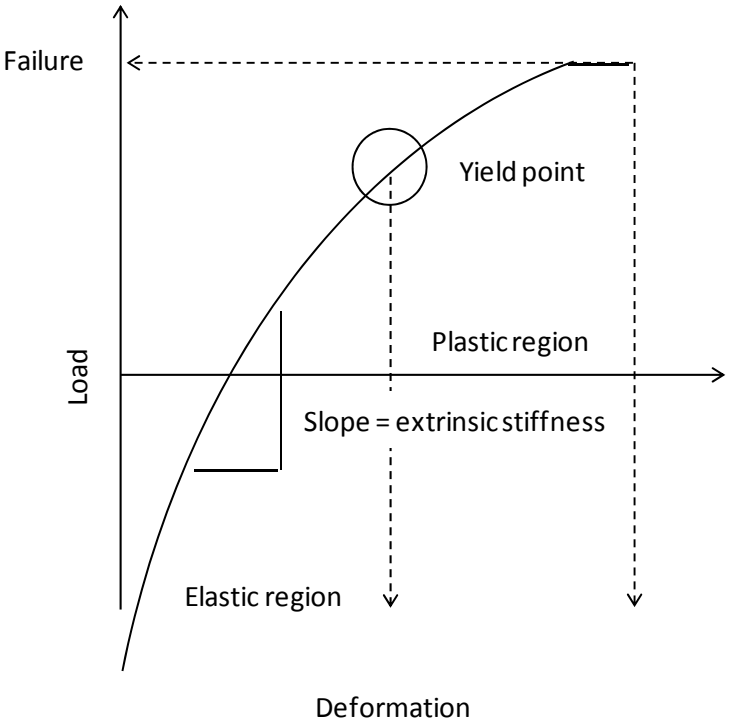

3.2.3 Effects of exercise on bone

Effects on bone mineral density

Mechanical loading of bone can elicit advantageous adaptations in bone mass and architecture (Lanyon 1992; Lanyon and Baggott 1976; Lanyon and Bourn 1979). Bone mineral density (BMD) (the ratio of bone mineral content (BMC) to size) is significantly higher in athletes taking part in higher intensity sports (Creighton *et al.* 2001; Heinonen *et al.* 1995; Heinonen *et al.* 1993; Heinonen *et al.* 1996), and in non-athletic individuals undertaking higher impact exercise programmes (Bassey and Ramsdale 1994), compared to less active individuals. Weight-training appears to be more effective at enhancing BMD than endurance activities (Heinonen *et al.* 1993). The increase in BMD seems to be site-specific according to the loading, i.e. bones within a specific region of the body (e.g. arm) may have left-to-right asymmetries in BMD. A comparison of the BMD of young female

athletes competing in two different impact loading sports, defined by Grimston *et al.* (1993) as sports producing ground reaction forces greater than or equal to three times the body weight, found BMD was significantly increased in the arms of gymnasts compared to volleyball players (Fehling *et al.* 1995). Additionally, both volleyball players and gymnasts had significantly increased BMD at several anatomical sites when compared to female swimmers (Fehling *et al.* 1995).Increases in BMD in response to high intensity exercise have also been reported in the distal limb bones of thoroughbred horses (Firth *et al.* 1999; Tidswell *et al.* 2008; Young *et al.* 1991). Asymmetries in BMD can result when bones on either side of the body experience differential loading. Such asymmetries have been observed in the arm bones of both male and female athletes participating in sports such as baseball, tennis and squash, with the dominant arm having increased density compared to the non-dominant (Haapasalo *et al.* 1994; Haapasalo *et al.* 1998; Haapasalo *et al.* 1996; Huddleston *et al.* 1980). Asymmetries in BMD have also been reported in the leg bones of young male athletes playing a wide variety of sports, with long-term exercise leading to greater cortical BMD in the non-dominant leg compared to the dominant leg (Sone *et al.* 2006). Similarly, left-to-right differences in BMD at the proximal femur have been reported in female gymnasts, with the left take-off leg having higher values than the right landing leg; these asymmetries were greater in gymnasts who practiced more (Wu *et al.* 1998). During sport, the dominant limb is used mainly for mobility or manipulation whereas the non-dominant limb helps support the actions of the dominant limb (Sadeghi *et al.* 2000). Therefore the two limbs could be subject to differences in mechanical loading with the type of limbs and type of repetitive action involved in the sport determining which side (dominant or non-dominant) would encounter increased loading and hence increased BMD. For example, female gymnasts experience greater vertical ground reaction forces during take-off than landing which creates a side-to-side asymmetry in BMD (Wu *et al.* 1998). In racing Greyhounds left-to-right asymmetries in BMD have been documented in the fifth

metacarpal bone (MC_5) (Emmerson *et al.* 2000; Johnson *et al.* 2001; Lipscomb *et al.* 2001) and in the central tarsal bone (CTB) (Johnson *et al.* 2000). These asymmetries are believed to result from the repetitive asymmetric cyclic loading that the dogs experience during racing. Asymmetries in BMD can also occur across a body part or region. Differences in BMD have been reported across the human foot from medial to lateral, with the tarsals and metatarsals on the medial side of the foot having lower BMD than the lateral side bones (Hastings *et al.* 2008; Sinacore *et al.* 2008). Assessment of barefoot plantar pressure during walking indicates the center of pressure line remains lateral to the anatomical longitudinal axis of the foot through the second metatarsal and digit until late in the stance phase (Hastings *et al.* 2008). Hastings *et al.* (2008) theorised that the long duration of lateral loading during stance phase may have contributed to an enhanced stimulus for bone formation in the lateral bones of the foot compared with the medial bones of the foot leading to the increased BMD laterally.

Effects on bone metabolism

Bone metabolic responses to mechanical loading have been studied with results varying depending on type and duration of training. Resistance exercise training in human males increases bone formation, while transiently suppressing bone resorption (Fujimura *et al.* 1997). A similar response to resistance training is seen in rats (Notomi *et al.* 2000). Athletes participating in high-impact sports, such as basketball, show increased bone formation compared to athletes who participate in low or non-impact sports such as swimming (Creighton *et al.* 2001). Similarly, high-impact exercise leads to a net increase in new bone formation and in bone collagen remodelling within the distal limb bones of racehorses (Tidswell *et al.* 2008).

3.2.4 Fatigue fractures

Fatigue (stress) fractures are partial or complete fractures that occur due to the application of cyclic stresses lower than that required to fracture normal bone in a single loading event (McBryde 1975). In human athletes (Brukner *et al.* 1996; Devas 1961; Iwamoto and Takeda 2003; Matheson *et al.* 1987; McBryde 1975; Orava *et al.* 1978) and military recruits (Armstrong *et al.* 2004; Beck *et al.* 2000; Hill *et al.* 1996; Kowal 1980) increased rates and magnitudes of loading lead to micro-damage accumulation and formation of fatigue fractures. Fatigue fractures have also been reported in the distal limb bones of equine (Nunamaker *et al.* 1990) and canine (Bellenger *et al.* 1981; Devas 1961; Gannon 1972) athletes. The repair mechanism of bone, i.e. bone remodelling, is instrumental in the development of a fatigue fracture (Martin 1995). During excessive cyclic loading, high rates of micro-damage formation may stimulate an intensive remodelling response, increasing porosity and decreasing stiffness of bone, which increases strain within the bone and further accelerates damage accumulation (Martin 1995), eventually leading to fracture. A high strain environment may inhibit this bone remodelling response (Frost 1987). Rubin and Lanyon (1985) found low levels of bone remodelling activity and increased periosteal and endosteal bone formation in the ulna of turkeys subjected to moderate to high functional strains, and high levels of remodelling activity with increased intra-cortical porosis in bones subjected to low strains. McCarthy and Jeffcott (1992) found young Thoroughbred horses subjected to a treadmill exercise programme had significantly less bone remodelling but increased sub-periosteal bone formation taking place in their third metacarpal bones compared to unexercised controls. Similarly, Verheyen *et al*. (2006) showed that accumulation of high-speed exercise (galloping) had a protective effect and decreased the risk of fatigue fractures in racehorses compared to accumulation of slow-speed exercise (cantering) suggesting high-impact exercise is better at eliciting a beneficial adaptive bone response. Therefore, continued high intensity exercise could act as a preventative measure

against micro-damage accumulated fatigue fracture. When exercise levels are decreased, remodelling is no longer inhibited and repair occurs. Circumstantial evidence is seen for this in racehorses; a rest period of 60 days or more prior to a return to training was a significant risk factor for racehorses that had sustained a catastrophic humeral fracture (Carrier *et al.* 1998). Once remodelling has been initiated, bone resorption takes place relatively quickly; the initial phase takes about 8 days (Eriksen *et al.* 1984). Bone formation is a much slower process and can take several months to complete (Eriksen *et al.* 1984; Li *et al.* 1990). Therefore, it is possible that the humeri of affected horses were predisposed to fracture when they returned to training due to high porosities associated with the on-going bone resorption process.

3.2.5 Asymmetrical damage in racing Greyhounds

Greyhounds are always raced anti-clockwise around ovoid tracks. This is thought to create asymmetric stresses in the left and right distal limb bones, with the rail-side bones, i.e. those bones within each paw which are closest to the inside of the Greyhound track, being subjected to the higher stresses. Previous studies examined left-to-right asymmetries in BMD of the metacarpals/metatarsals (Emmerson *et al.* 2000; Lipscomb *et al.* 2001), the accessory carpal bone (Emmerson *et al.* 2000) and the CTB (Emmerson *et al.* 2000; Johnson *et al.* 2000): the rail-side bones showed increased bone remodelling, indicated by increased BMD, compared to contralateral bones. Micro-damage formation within bone acts as a stimulus for bone remodelling (Bentolila *et al.* 1998; Mori and Burr 1993). Excessive cyclic loading is thought to increase the rate of micro-damage formation to faster than it is possible to repair by remodelling, eventually leading to fracture of the bone (Tomlin *et al.* 2000). As rail-side bones experience increased remodelling compared to the contralateral bones, they are more at risk of fatigue fracture due to excessive cyclic loading. Fractures of rail-side metacarpal and metatarsal bones are often reported in racing Greyhounds

(Bellenger *et al.* 1981; Dee and Dee 1985; Gannon 1972; Ness 1993; Piras 2005) and are believed to result from the repetitive cyclic loading that occurs during training and racing (Johnson *et al.* 2001). Fracture of the right CTB is one of the most common fractures seen in racing Greyhounds (Boudrieau *et al.* 1984; Gannon 1972; Guilliard 2000; Hickman 1975). This injury is also thought to be a fatigue fracture resulting from an imbalance between the rate of micro-damage formation and repair leading to micro-damage accumulation and structural failure (Tomlin *et al.* 2000).

3.2.6 Dual-energy x-ray absorptiometry

Dual-energy x-ray absorptiometry (DXA) scanners were first introduced in the late 1980s and DXA is now the most widely used and widely available method for bone densitometry (Blake and Fogelman 2007; Faulkner *et al.* 1991; Peel and Eastell 1993). DXA has several advantages over other imaging techniques for measuring BMD, including a more stable radiation source and the difference between the two energy levels is greater which increases resolution (Sartoris and Resnick 1990). During a DXA scan, the source which emits x-rays of 2 different energy levels (e.g. 70 kV and 40kV) and the detector move over the subject or specimen with the detector measuring the amount of x-rays that pass through the subject. X-rays of two energy levels are impeded by bone and soft tissue differently; therefore, DXA can distinguish between the type and quantity of tissue that is scanned. Correct positioning of the subject or specimen is the most critical part of bone densitometry, because DXA converts a 3D structure into a 2D image. The reproducibility of DXA can be expressed by the coefficient of variation values which take into account the range of measurements of the method (Gluer *et al.* 1995); ideally coefficient of variation values should be below 3%.

3.2.7 Determination of bone mineral density

BMD is the ratio of bone mineral content (BMC; reported as gcm^{-1}) to size and it is reported as gcm^{-2}. In humans and other animals, changes in BMD can be measured using DXA (Grier *et al.* 1996; Lauten *et al.* 2000; Lauten *et al.* 2001; McClure *et al.* 2001; Zotti *et al.* 2004). In dogs, DXA has been used to evaluate bone remodelling and healing (Markel *et al.* 1995), the effect of exercise on BMD (Puustjarvi *et al.* 1991), and left-to-right asymmetries *in vivo* (Muir *et al.* 1995) and *ex vivo* (Emmerson *et al.* 2000).

3.2.8 Biochemical markers of bone metabolism and bone matrix composition

Biochemical markers of bone cell activity can be classified into those which are markers of bone formation or resorption. Generally, suitable markers are enzymes expressed by osteoblasts or osteoclasts, or they are organic components released during bone synthesis or resorption. There are several reviews detailing markers of bone metabolism (Allen 2003; Looker *et al.* 2000; Risteli and Risteli 1993; Seibel 2000, 2005; Watts 1999). Table 3.1 provides details of the main markers of bone resorption and formation. There are some limitations associated with the use of biochemical markers to measure bone turnover in vivo, including variability associated with age (Lepage *et al.* 1990; Mora *et al.* 1998; Nishimoto *et al.* 1985; Wishart *et al.* 1995), diurnal rhythms (Gertz *et al.* 1998; Gundberg *et al.* 1985; Karlsson *et al.* 1992) and, in females, reproductive status (pregnant, menopausal etc.) (Karlsson *et al.* 1992; Rosenbrock *et al.* 2002). In addition, tissue specificity can be a problem as biomarkers are only relatively specific for bone. For example, alkaline phosphatase is derived from a wide variety of non-skeletal sources (Crofton 1982; Meyer-Sabellek *et al.* 1988). Therefore, it is preferable to assay a combination of markers to allow more detailed information on bone remodelling rates to be collected as each marker may reflect a different physiological process within bone. Biochemical markers can also be used to evaluate the composition of the bone matrix.

Table 3.1: Summary of biochemical markers of bone formation and resorption.

Bio-marker	Major source	Sample	References
Bone formation			
BALP	Osteoblasts	Serum/Plasma	Gomez *et al.* (1995), Mohamadnia *et al.* (2007)
Osteocalcin	Osteoblasts	Serum/Plasma	Lee *et al.* (2000), Brown *et al*. (1984)
PICP	Osteoblasts	Serum	Eriksen *et al.* (1993), Franke *et al.* (1998), Melkko *et al.* (1990)
PINP	Osteoblasts	Serum	Melkko *et al*.(1996)
BSP	Osteoblasts	Serum	Seibel *et al.* (1996)
Bone resorption			
Hydroxyproline	Collagen	Urine	Dull and Henneman (1963)
PYD	Collagen	Urine	Robins *et al.* (1996), Seyedin *et al.* (1993), Uebelhart *et al.* (1990)
DPD	Collagen	Urine	Robins *et al.*(1994), Robins *et al.* (1996)
ICTP / CTX-MMP	Collagen	Serum/Urine	Eriksen *et al.* (1993), Risteli *et al.* (1993)
NTX-I	Collagen	Serum/Urine	Franke *et al.* (1998)
TRAP	Osteoclasts	Serum/Plasma	Minkin (1982), Janckila *et al.* (2001)

Abbreviations: Carboxy-terminal propeptide of type I procollagen (PICP), amino-terminal propeptide of type I procollagen (PINP), bone sialoprotein (BSP), pyridinoline (PYD), deoxypyridinoline (DPD), carboxy-terminal cross-linked telopeptide of type I collagen (ICTP or CTX-MMP), amino-terminal cross-linked telopeptide of type I collagen (NTX-I) and tartrate resistant alkaline phosphatase (TRAP).

Matrix metalloproteinases

Matrix metalloproteinases (MMPs), also known as matrixins, are a family of zinc-dependent proteases that play a major role in the proteolytic degradation of structural components of the extracellular matrix (ECM) including collagen (Nagase and Woessner 1999; Sternlicht and Werb 2001). Most are secreted as inactive zymogens: these pro-MMPs are activated *in vitro* by proteinases and by non-proteolytic agents and once activated they degrade collagens and other ECM proteins (Nagase 1997; Nagase and Woessner 1999). Based on their structural and functional characteristics, human MMPs can be classified into several subfamilies, which include type IV collagenases, also known as gelatinases (Matrisian 1992; Vu and Werb 2000; Woessner 1991). There are two types of type IV collagenase; 72-kDa gelatinase (gelatinase A) or MMP-2 and 92-kDa gelatinase (gelatinase B) or MMP-9. MMP-2 and MMP-9 are responsible for the degradation of type IV and V collagen, and of denatured collagens such as type I collagen (Matrisian 1992). MMP-2 is expressed by osteoblasts (Meikle *et al.* 1992; Rifas *et al.* 1994; Rifas *et al.* 1989), while MMP-9 is highly expressed by osteoclasts (Tezuka *et al.* 1994; Wucherpfennig *et al.* 1994). In addition to being expressed by bone cells, both MMP-2 and MMP-9 are produced by immune cells such as macrophages and monocytes (Campbell *et al.* 1991; Garbisa *et al.* 1986). Inhibition of the gelatinases prevents bone resorption *in vitro* (Hill *et al.* 1995; Hill *et al.* 1994b). Approximately 95 % of the total collagen content of bone is type I collagen, with types III, V and VI present at low levels (Keene *et al.* 1991; Niyibizi and Eyre 1994). Therefore, increased expression of MMP-2 and MMP-9 indicates increased levels of collagen degradation and hence increased bone resorption.

Hydroxyproline

Hydroxyproline is formed by post-translational hydroxylation of the amino acid proline (Udenfriend 1966). It represents about 14% of the amino acid content of collagen (Eastoe

1955) and quantification of hydroxyproline can be used to estimate the total collagen content of bone.

Bone specific alkaline phosphatase

Alkaline phosphastase (ALP) is a zinc-containing glycoprotein enzyme synthesized by cells in a wide variety of tissues including bone (Crofton 1982; Meyer-Sabellek *et al.* 1988). Bone-specific ALP (BALP) is synthesised by, and expressed on the external surface of, osteoblasts during bone formation (Clarke 2008). BALP hydrolyses pyrophosphate, thereby removing an osteogenesis inhibitor and allowing bone mineralisation to proceed (Balcerzak *et al.* 2003). As such, BALP is one of the most frequently used non-collagenous markers of osteogenesis (Allen 2003; Magnusson *et al.* 1999; Watts 1999).

3.2.9 Study aim and hypothesis

We hypothesised that the asymmetric cyclic loading experienced by Greyhounds during racing would lead to left-to-right differences in the BMD and in the markers of bone resorption and new bone formation. In comparison, as they are not subjected to asymmetric stresses, we believed there would be no such left-to-right differences in SBTs. To test this we examined all of the carpal, metacarpal, tarsal and metatarsal bones, with the exceptions of the first tarsal (T_1) and first metatarsal (MT_1). These two bones are vestigial in the dog: the degree to which they are present vary greatly between individual dogs, in some they can be fused together, in others they may be absent (Miller *et al.* 1964). Therefore, any left-to-right differences observed in T_1 and MT_1 would more than likely be false.

PART A: DETERMINATION OF BONE MINERAL DENSITY

3.3 Materials and methods

3.3.1 Specimens

Distal thoracic (n = 21 pairs) and pelvic (n = 29 pairs) limbs were collected from 31 racing Greyhounds (10 male, 21 female) all with a complete racing history and pedigree information. All Greyhounds were skeletally mature animals; mean age was 3.05 ± 0.75 years; mean weight was 30.51 ± 3.15 kg. The average number of races ran by the dogs was 37. Fifteen of these Greyhounds had been euthanatised at their owners request after sustaining a severe fracture of the right tarsus whilst racing. The other 16 Greyhounds were euthanatised because they sustained other injuries during a race (11 dogs); were injured in a kennelling accident (one dog); or because they were unable to race or to be re-homed due to behavioural problems (i.e. extreme aggression) (four dogs).

Distal thoracic (n = 8 pairs) and pelvic (n = 8 pairs) limbs were also collected from eight SBTs (six male, two female), euthanatized at a local dogs home when severe behavioural problems prevented them from being re-homed. Age of the dogs was unknown, although external examination suggested that they were skeletally mature dogs in generally good condition; mean weight was 16.50 ± 2.29 kg. It was important that dogs were skeletally mature as several biochemical markers of bone metabolism, such as BALP, are highly expressed during skeletal development (Allen *et al.* 2000b; Lepage *et al.* 1990; Nishimoto *et al.* 1985).

Limb specimens were disarticulated at the elbow/stifle and stored at -20 °C until they were thawed at room temperature when required for processing.

3.3.2 Determination of injury status

Digital radiography

Standard mediolateral and dorsoplantar radiographic views of the tarsi were obtained using a Siemens MULTIX TOP machine (Siemens Medical Solutions, Germany) linked to a computed radiography system (Fuji FCR-XG1, Fujifilm, UK). All exposures were taken at 60 kV and 1.80 mAs, with 80% tube loading and each image was immediately reviewed to ensure diagnostic quality of exposure and positioning.

Computed tomography

Examinations were performed using a Siemens Somatom Volume Zoom 4 Slice Helical Scanner (Siemens Medical Solutions, Germany), which was calibrated using a calibration phantom prior to scanning of the limbs. Contiguous 0.5 mm transverse slices were taken to generate multiple detailed, cross-sectional images of the tarsi. Slices were acquired at 120 kV and 100 mAs, collimation 0.5 mm and table feed 1.0 mm. Images were reconstructed using a window width of 4000, window centre of 700, very sharp (U90u) kernel, slice width of 0.5 mm and a reconstruction increment of 0.5 mm.

3.3.3 DXA Protocol

Measurement of BMD was performed by use of a fan beam Lunar Prodigy© Bone Densitometer. Machine stability was tested prior to each scanning session by means of a Quality Assurance test followed by a scan of a calibration phantom. These ensured that the machine was able to detect what materials were being scanned accurately and hence calculate the correct density. Limbs and bones were positioned by the use of anatomic reference points. The entire distal aspect of each intact thoracic and pelvic limb was scanned from proximal to distal in a dorsopalmar/plantar plane; the limbs were held in the

correct dorsopalmar/plantar position by placing sandbags on either side of the limb (proximal to the regions scanned). The left/right hand scan protocols were used. Scans were started 5 cm proximal to the proximal end of the third metacarpal bone in the thoracic limbs and 5 cm proximal to the medial malleolus of the tibia in the pelvic limbs. Following DXA scanning of the intact limbs, the individual carpal, metacarpal, tarsal and metatarsal bones were completely dissected out of the limbs. Each bone was placed in a water bath containing water to a depth of 3 cm and scanned using the left/right hand scan protocols (the DXA scanner was unable to scan isolated bones on the table, the water bath allowed the scanner to "see" the bones). The water in the bath was changed after each set of bones (i.e. bones from one dog) was scanned to ensure each set was scanned in clean clear water. Fractured bones were scanned by placing the fragments in as correct an alignment as possible, scanning five times and calculating the mean BMD. Standard analysis software (Prodigy enCORETM 2004, ver 8.70.005) was used to determine the total BMD for regions-of-interest (ROI) in the entire distal limb (Figure 3.2) and the isolated bones. A multi-ROI analysis (Figure 3.3) was carried out on metacarpal bones two (MC_2) and MC_5 to determine if any asymmetries in BMD occurred in specific areas of the metacarpal bones.

Figure 3.2: Diagram of the canine (a) thoracic and (b) pelvic distal limb showing the areas and bones scanned using DXA. Adapted from Goody (1997).

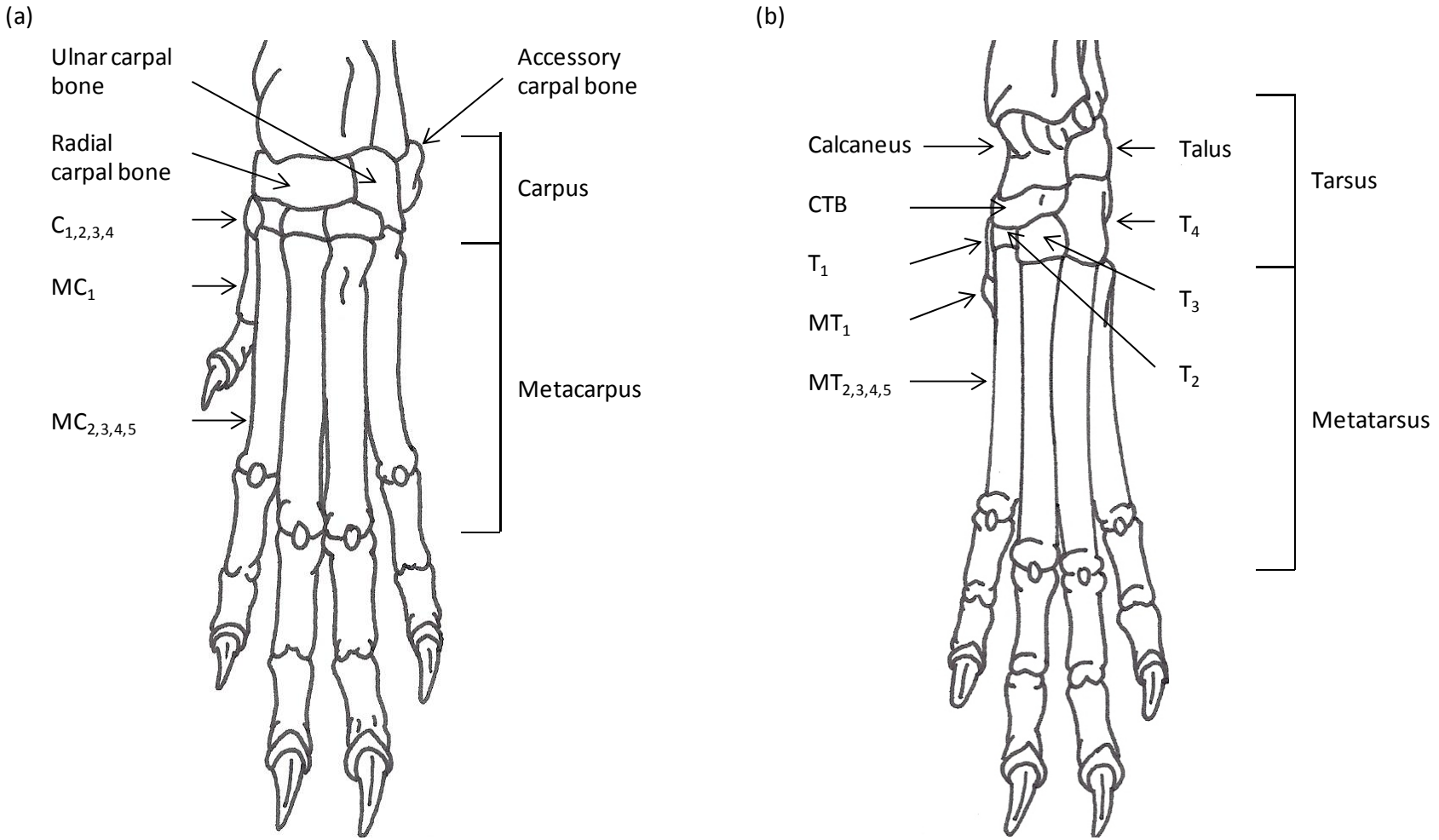

Figure 3.3: Diagram of a MC_2/MC_5 bone showing the three additional ROI scanned via DXA to determine if increases in BMD occurred in specific areas of the bones.

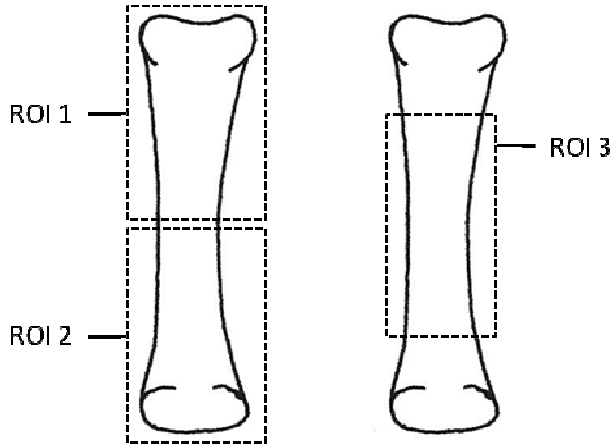

3.3.4 Statistical analysis

Mean and standard error of the mean were calculated for each parameter. The effect of side (left versus right) on BMD for each ROI (the carpus, tarsus, metacarpus, metatarsus, each individual bone and the regions examined in the multi-ROI analysis of MC_5 and MT_2) was examined using the two-tailed paired t-test. The effect of bone (carpal bones one to four (C_{1-4}), metacarpals (MC_{1-5}), tarsals two to four (T_{2-4}) and metatarsals two to five (MT_{2-5}) was examined using a one-way ANOVA with a post-hoc Tukey t-test. Differences were considered significant at $p < 0.05$. Representative limbs/bones from one Greyhound and one SBT were used to calculate the coefficient of variation (CV) for BMD measurement in each ROI; scanning of each ROI was repeated five times with repositioning of the limbs/bones between scans, the BMD was determined and the CV calculated.

3.4 Results

3.4.1 Racing Greyhounds

Injury status

During limb dissection it was confirmed that all the intact thoracic and pelvic limbs were free from injury, as were the left limbs from Greyhounds with a fractured right tarsus. The right limbs from these dogs had fractures of the following bones identified via radiography and CT scanning, and confirmed during limb dissection; CTB (14 dogs), T_4 (11 dogs), calcaneus (eight dogs), talus (three dogs), MT_4 (two dogs), T_2 (one dog), T_3 (one dog), and MT_5 (one dog).

Left-to-right asymmetries in BMD

There were no significant left-to-right asymmetries in total BMD of the entire carpus or metacarpus. When the thoracic limb bones were scanned individually, total BMD of the right C_2 ($p = 0.043$) and C_3 ($p = 0.025$), and the left C_4 ($p < 0.001$) bones was significantly higher than the corresponding bones in the contralateral limb. Total BMD was also significantly higher in the right MC_1 ($p = 0.001$), MC_2 ($p < 0.001$) and MC_3 ($p < 0.001$) as well as the left MC_4 ($p < 0.001$) and MC_5 ($p < 0.001$) bones, compared to the contralateral bones (Figure 3.4). Representative DXA scans of the left and right MC_5 bones can be seen in Figure 3.5. When the multi-ROI analysis was carried out on MC_2 and MC_5 BMD was significantly higher in the left MC_2 compared to the right for all three ROIs (ROI 1: $p = 0.015$; ROI 2: $p = 0.019$; ROI 3: $p = 0.035$). Similarly, BMD was significantly higher in all ROIs in the right limb MC_5 compared to the left (ROI 1: $p < 0.001$; ROI 2: $p = 0.001$; ROI 3: $p < 0.001$).

Figure 3.4: BMD values of the left (clear) and right (hatched) carpal and metacarpal bones of racing Greyhounds (n = 21 dogs). The error bars are standard error of the mean (SEM). Significant differences between the left and right limb bones are indicated by * $p < 0.05$.

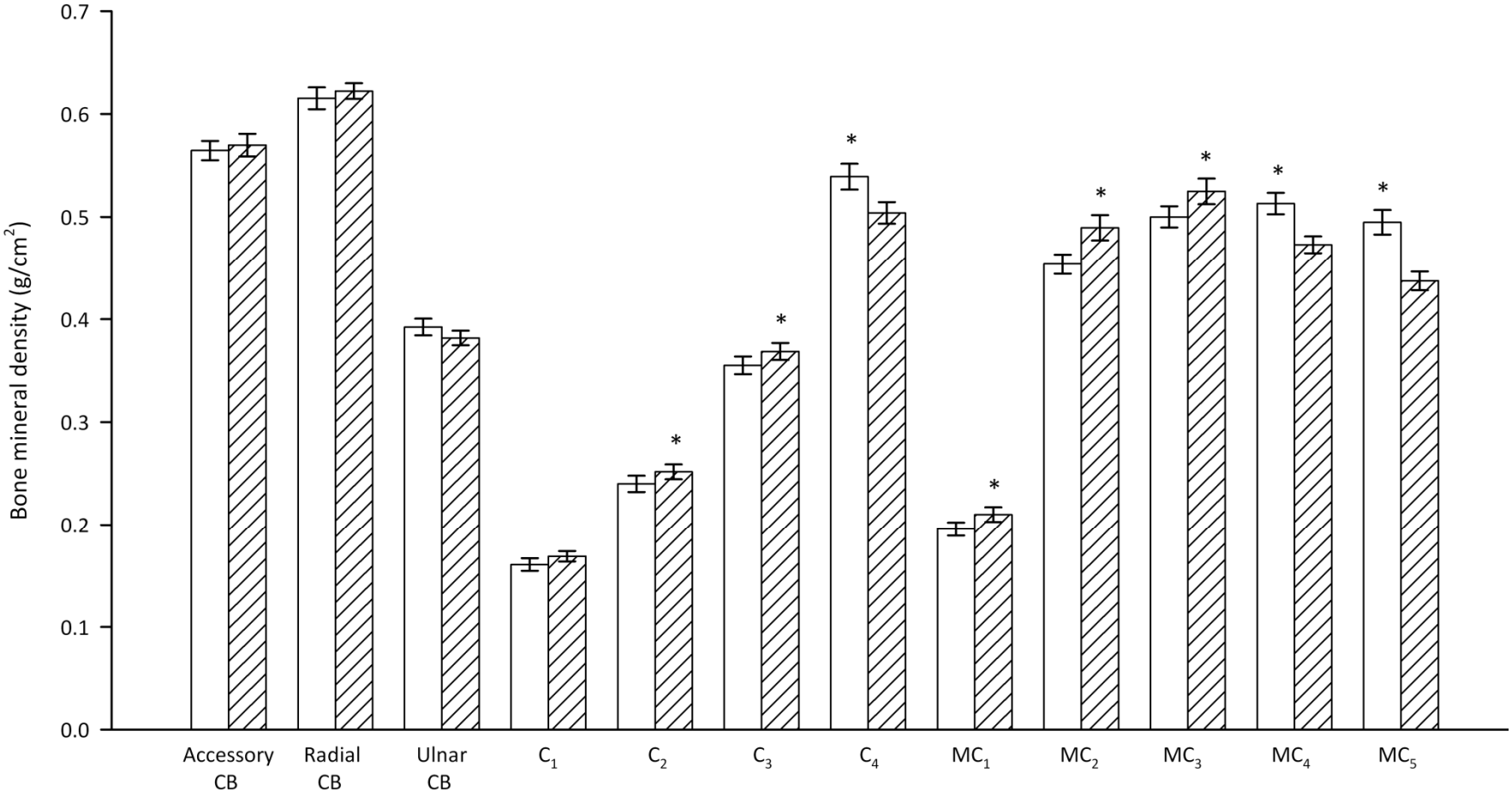

Figure 3.5: Representative DXA scans of the left and right MC_5 bones from a racing Greyhound. The increased BMD can be seen as increased light intensity, i.e. brightness, on the image of the left MC_5.

There were no significant asymmetries in total BMD of the entire tarsus or metatarsus regions. When the bones from Greyhounds without a right tarsal fracture were scanned and analysed, total BMD of the right CTB ($p = 0.034$), T_2 ($p = 0.012$), T_3 ($p = 0.003$), MT_2 ($p = 0.003$) and MT_3 ($p = 0.003$) bones were significantly higher than the contralateral limb bones (Figure 3.6). Similarly, when the pelvic limb bones from Greyhounds with a fracture of the right tarsus were scanned and analysed, total BMD of the right T_2 ($p = 0.020$), MT_2 ($p = 0.002$) and MT_3 ($p < 0.001$) and left CTB ($p < 0.001$) were significantly higher than those in the contralateral limb (Figure 3.7).

Figure 3.6: BMD values of the left (clear) and right (hatched) tarsal and metatarsal bones from racing Greyhounds with intact pelvic limbs (n = 14 dogs). The error bars are SEM. Significant differences between the left and right limb bones are indicated by * $p < 0.05$.

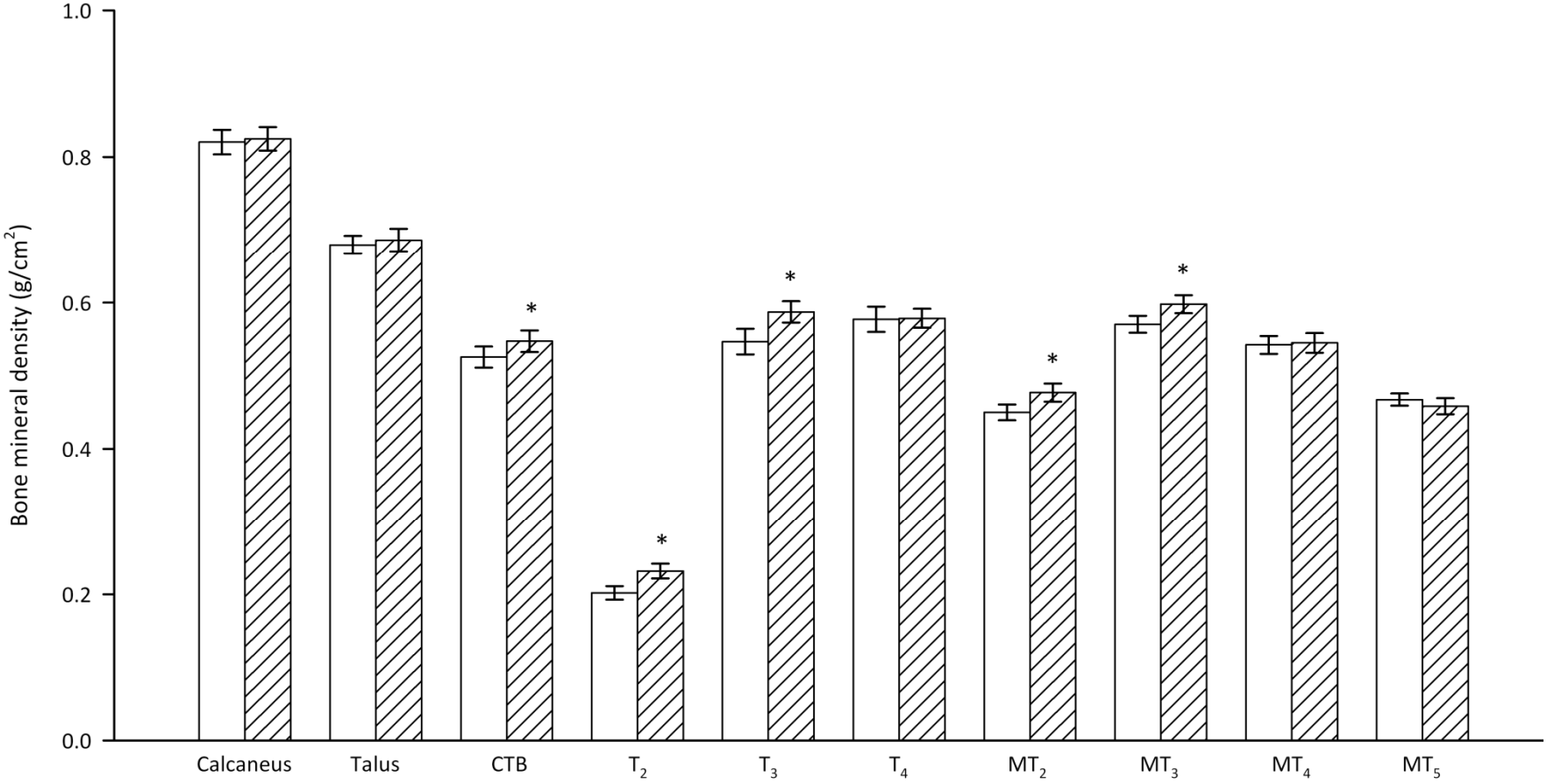

Figure 3.7: BMD values of the left (clear) and right (hatched) tarsal and metatarsal bones from racing Greyhounds with a fractured right tarsus (n = 15 dogs). The error bars are SEM. Significant differences between the left and right limb bones are indicated by * $p < 0.05$.

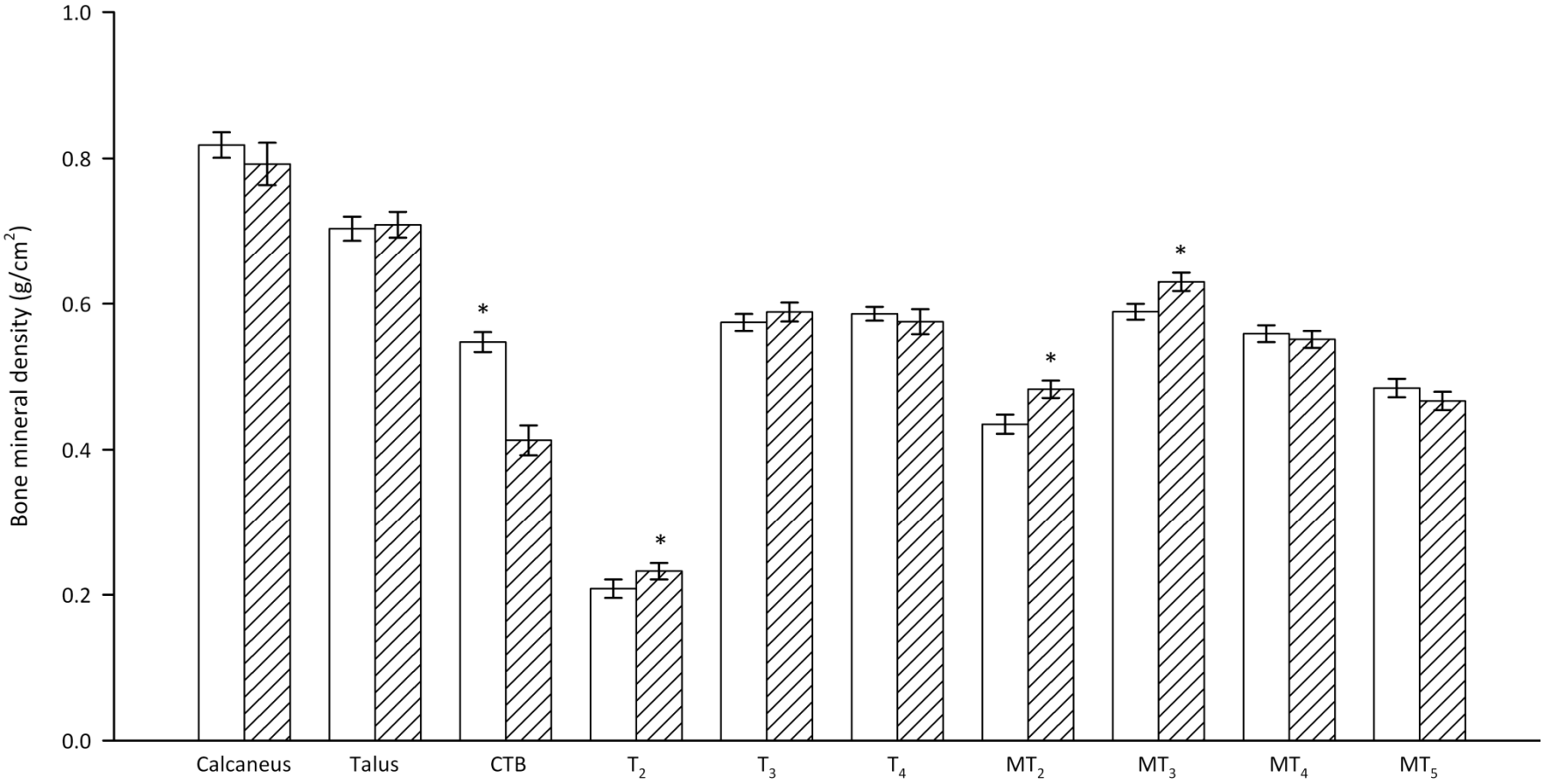

Medial-to-lateral differences in BMD

There was a significant effect of the specific carpal bone (C_1-C_4) ($p < 0.001$) and of the specific metacarpal bone (MC_{1-5}) ($p < 0.001$). BMD significantly increased across the carpal bones from medial (C_1) to lateral (C_4) in both left and right limbs (Figure 3.8). The pattern for the metacarpal bones differed between sides. BMD significantly increased from MC_1 to MC_3 and then remained similar from MC_3 to MC_5 in the left limbs, whereas in the right limbs, BMD significantly increased from MC_1 to MC_3 and then significantly decreased to MC_5 (Figure 3.9).

There was a significant effect of the specific tarsal bone (T_2-T_4) in Greyhounds with ($p < 0.001$) and without ($p < 0.001$) fracture, and of the specific metatarsal bone (MT_{2-5}) in Greyhounds with ($p < 0.001$) and without ($p < 0.001$) fracture. BMD significantly increased from T_2 to T_3 and then remained similar from T_3 to T_4 in left and right limbs from both Greyhounds with and without a right tarsal fracture. BMD significantly increased across the metatarsals from MT_2 to MT_3 and then decreased to MT_5 in left and right limbs from both Greyhounds with and without a right tarsal fracture. Figures 3.10 and 3.11 show the data for Greyhounds without a fracture, the pattern shown is similar for the injured Greyhounds.

Coefficients of variation

CV values for repeated BMD measurements were calculated for each ROI. CV values for ROI in the uninjured thoracic and pelvic limbs were generally less than 3.0%. The smallest distal limb bones (C_1, C_2, C_3, MC_1, T_2,) were more difficult to position correctly and had higher values. In the fractured limbs, CV values were higher in the tarsal and metatarsal ROI as the injuries made correct positioning awkward. CV values for the most commonly fractured bones (calcaneus, talus and CTB) were less than 2.0% despite requiring reconstruction of the fragments prior to scanning.

Figure 3.8: Medial-to-lateral BMD values across the carpal bones (C_1 = clear, C_2 = dotted, C_3 = hatched, C_4 = light grey) of Greyhounds and SBTs. The error bars are SEM. Within each limb, bones that are significantly different to C_1 are indicated by *, to C_2 are indicated by ¤ and to C_3 are indicated by +; $p < 0.05$.

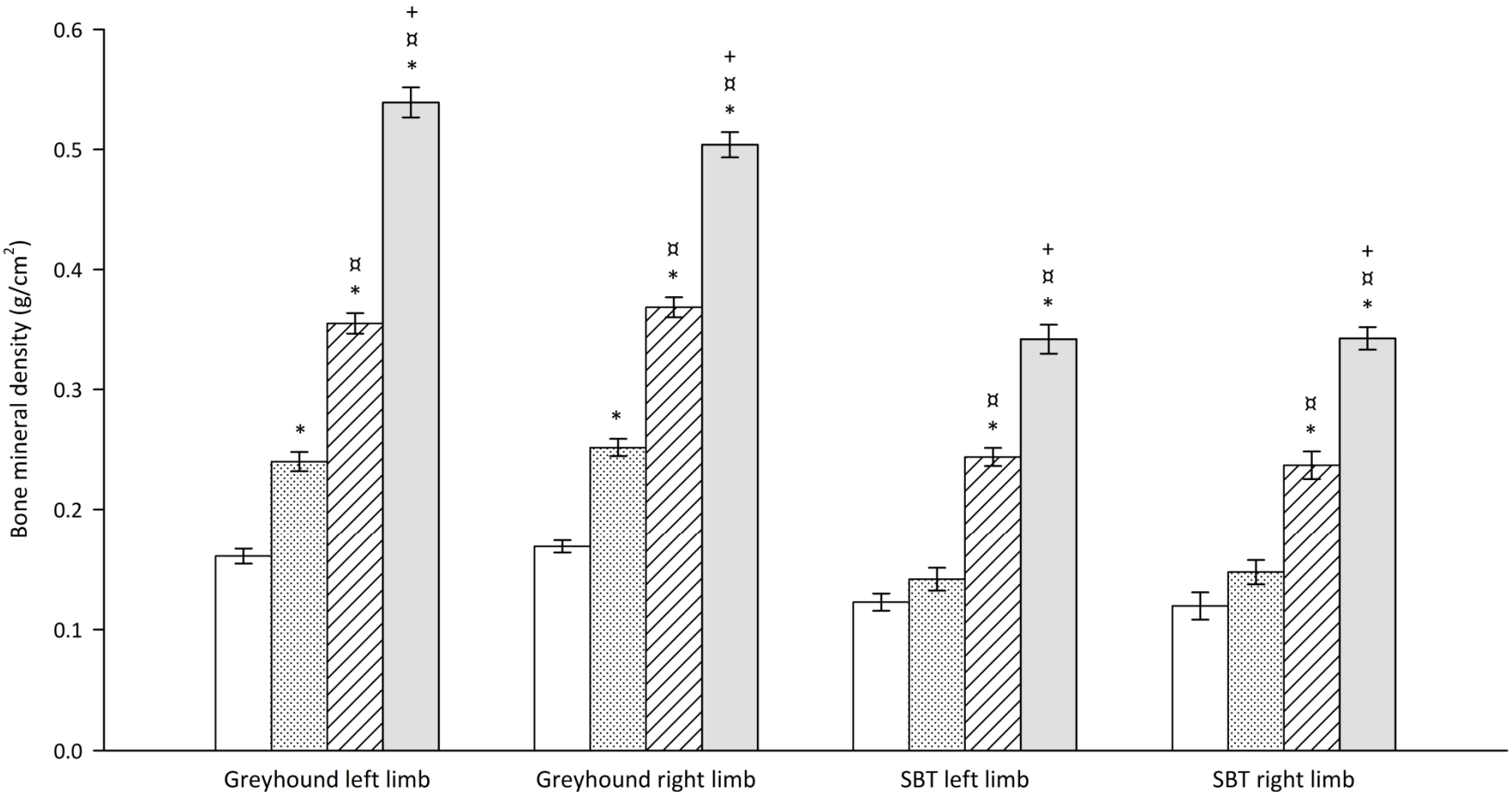

Figure 3.9: Medial-to-lateral BMD values across the metacarpal bones (MC_1 = clear, MC_2 = dotted, MC_3 = hatched, MC_4 = light grey, MC5 = dark grey) of Greyhounds and SBTs. The error bars are SEM. Within each limb, bones that are significantly different to MC_1 are indicated by *, to MC_2 by ¤, to MC_3 by + and to MC_4 by ‡; $p < 0.05$.

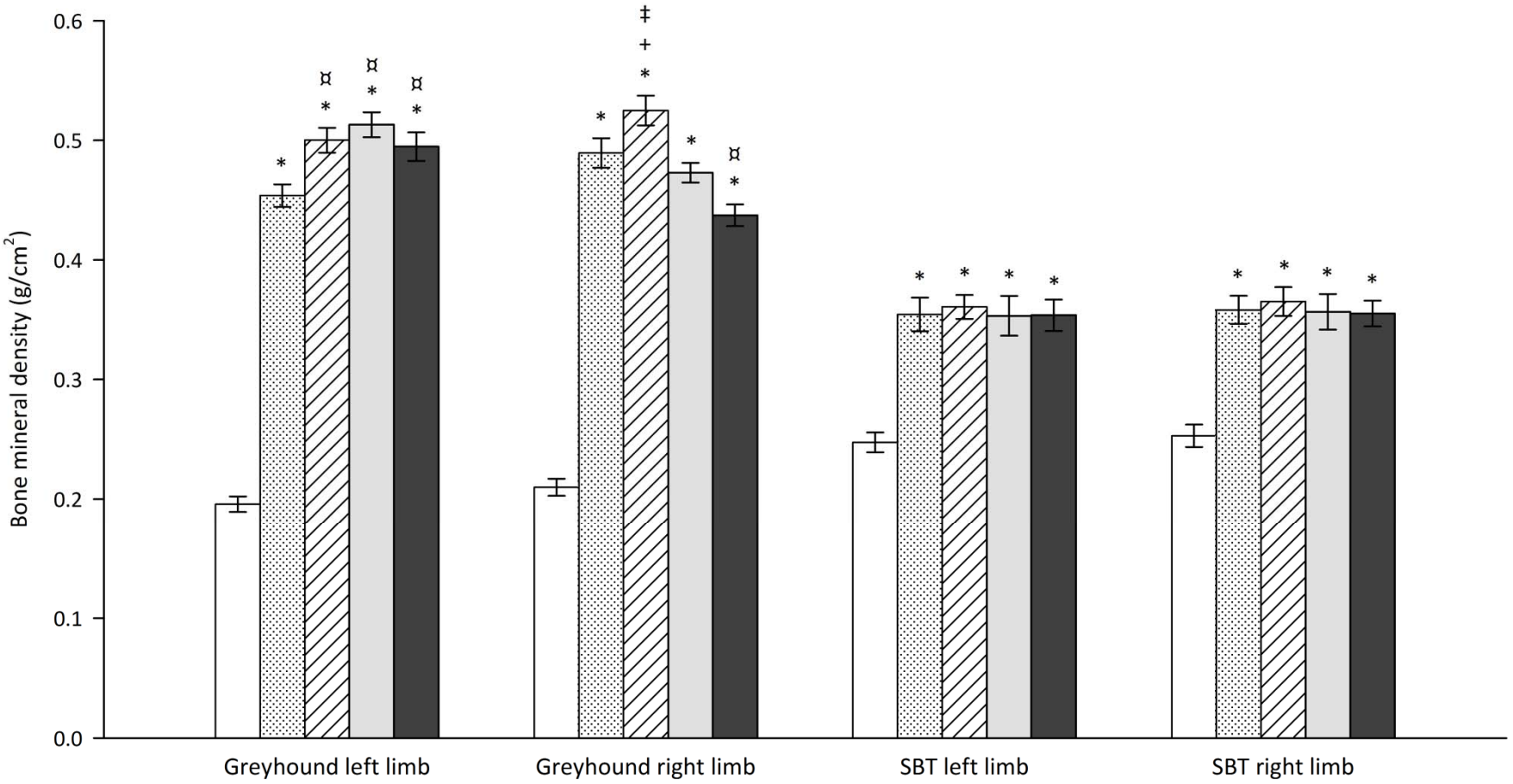

Figure 3.10: Medial-to-lateral BMD values across the tarsal bones (T_2 = clear, T_3 = dotted, T_4 = hatched) of uninjured Greyhounds and SBTs. The error bars are SEM. Within each limb, bones that are significantly different to T_2 are indicated by *; $p < 0.05$.

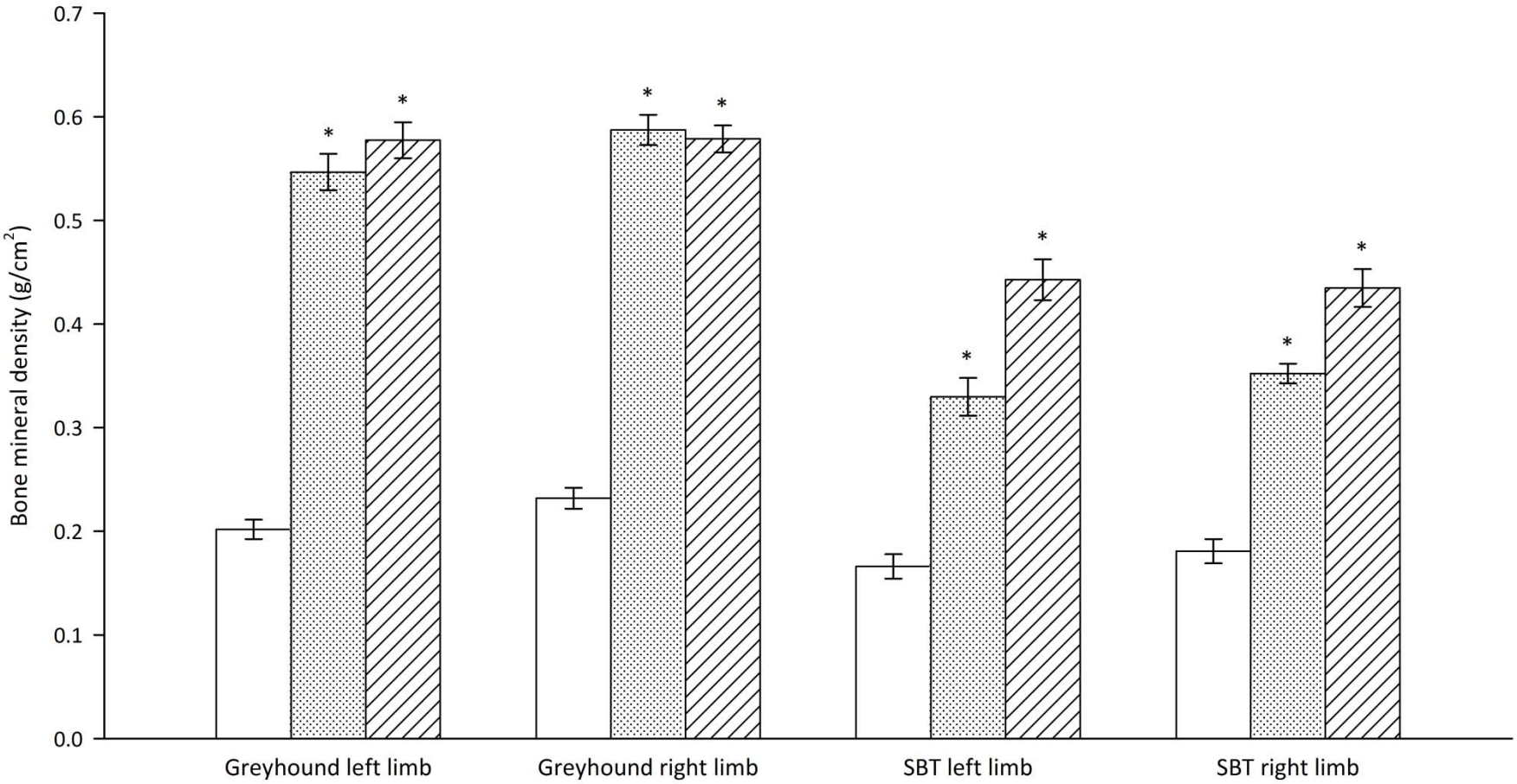

Figure 3.11: Medial-to-lateral BMD values across the metatarsal bones (MT_2 = clear, MT_3 = dotted, MT_4 = hatched, MT_5 = light grey) of uninjured Greyhounds and SBTs. The error bars are SEM. Within each limb, bones that are significantly different to MT_2 are indicated by *, to MT_3 by ¤ and to MT_4 by +; $p < 0.05$.

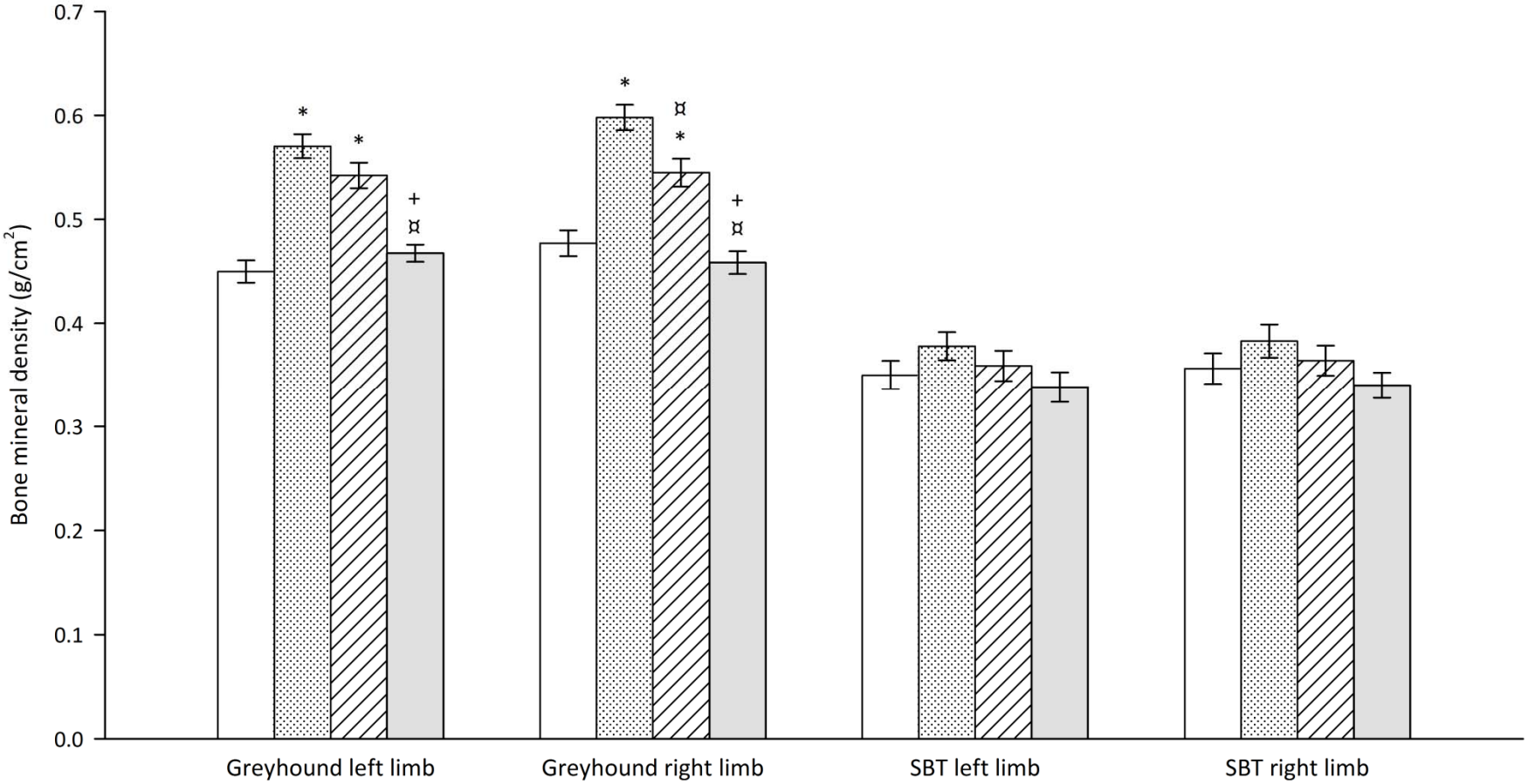

3.4.2 Staffordshire Bull Terriers

Injury status

During limb dissection it was confirmed that all 8 pairs of distal thoracic and pelvic limbs were free from injury.

Left-to-right asymmetries in BMD

No significant left-to-right differences were seen in total BMD of the entire carpus, metacarpus, tarsal or metatarsus regions, nor in any of the individual distal limb bones.

Medial-to-lateral differences in BMD

There was a significant effect of the specific carpal bone (C_1-C_4) ($p < 0.001$), metacarpal bone (MC_{1-5}) ($p < 0.001$), tarsal bone (T_2-T_4) ($p < 0.001$) and metatarsal bone (MT_2-MT_5) ($p < 0.001$). There were significant differences in BMD across the foot with an increase across the carpal bones from C_2 to C_4 in both the left and right limbs (Figure 3.8). There were no medial-to-lateral differences in BMD across MC_2 to MC_5. MC_1 had significantly lower BMD than the rest of the metacarpals (Figure 3.9). BMD significantly increased from T_2 to T_4 in both the left and right limbs (Figure 3.10). There were no medial-to-lateral differences in BMD across the metatarsals (Figure 3.11).

Coefficients of variation

Coefficients of variation for BMD measurements were calculated for each distal limb ROI. Values were generally less than 3.0%. As with the Greyhounds, the smallest bones (C_1, C_2, C_3, MC_1, T_2,) were more difficult to position correctly and therefore had higher values. In particular C_1, C_2 and T_2 produced values around 10.0% due to their very small size in the SBT.

PART B: BIOCHEMICAL ANALYSIS OF BONE

3.5 Materials and methods

3.5.1 Bone specimens

Several distal limb bones from both the thoracic and pelvic limbs of racing Greyhounds were selected and used to evaluate biochemical changes within the bones. Bones were selected that, in Greyhounds, showed significant left-to-right asymmetries in BMD and/or that are reported to be prone to fatigue fracture. Therefore, C_4 and MC_5 bones from the thoracic, and MT_2 and CTBs from the pelvic limb were chosen for analysis. Bones were selected from the six Greyhounds that had run the greatest distance during their lifetime in order to maximise the chances of demonstrating any differences between the left and right side bones. Pairs (left and right) of C_4, MC_5 and MT_2 bones from six Greyhounds were chosen to undergo analysis. 12 pairs (left and right) of CTB; six pairs were from Greyhounds with a fracture of the right CTB ($CTB_{(injured)}$) and six were from Greyhounds without a CTB fracture ($CTB_{(intact)}$), were also analysed.

Greyhound MC_5 bones had the largest left-to-right asymmetry in BMD, therefore to confirm no asymmetries were present within SBT bones, pairs of MC_5 bones were selected from six SBTs. These results were compared with those from the Greyhounds.

3.5.2 Tissue preparation

Bones were cut into required sections using an Exakt 300cl diamond coated band saw (Exakt, Germany). Metacarpal and metatarsal bones had a 1 cm long section cut out from the middle of the bone (i.e. the bones were cut at 0.5 cm from the mid-point of the bone in both the proximal and distal direction). The central section of the CTB (i.e. a 0.6 cm^2 piece was cut from the center of the bone) was used for biochemical analysis. Fractured CTBs

were pieced together as accurately as possible and each fragment was cut as required. Entire C_4 bones were analysed. Details of the sampling sites for intact bones can be seen in Table 3.2 and Figure 3.12.

Table 3.2: Sampling site information for the five bones that were used for biochemical analysis.

Bone	Bone sampling site
C_4	Entire bone
MC_5	Mid-diaphysis: 1cm^2 section
MT_2	Mid-diaphysis: 1cm^2 section
$CTB_{(intact)}$	Center of bone including cortical and trabecular bone: 0.6cm^2 section
$CTB_{(injured)}$	Center of bone including cortical and trabecular bone: 0.6cm^2 section

Figure 3.12: CTB and MC_5/MT_2 sampling sites. ROIs are indicated by dashed lines. (a) 1 cm section from the mid-diaphysis of the MC_5/MT_2 bones, (b) 0.6 cm^2 section from the center of intact CTBs and (c) 0.6 cm^2 section from the center of fractured CTBs were taken for biochemical analysis.

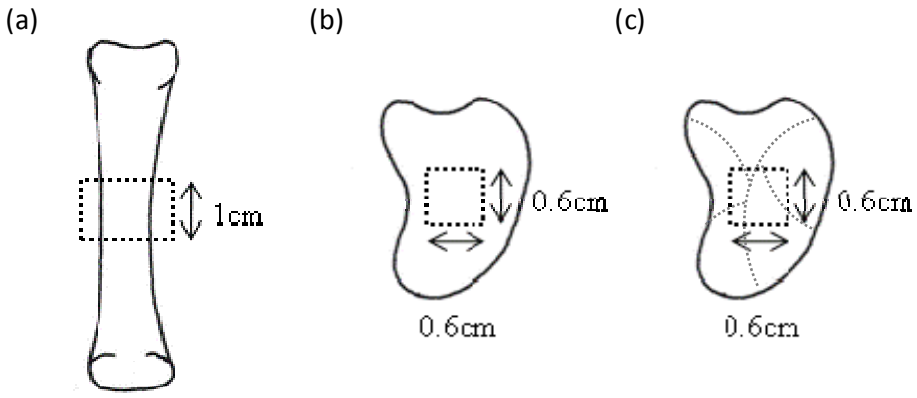

For biochemical analysis of the bone sections, samples were freeze-dried for 48 - 72 hours using a Heto Drywinner freeze dryer (Heto-Holten, Germany) connected to a Javac high-vacuum pump (Javac, UK), snap frozen in liquid nitrogen, reduced to a fine powder using a custom made stainless steel bone mill and re-freeze dried for 12 - 24 hours.

3.5.3 Extraction method

150 mg of the powdered bone was incubated with 3 ml of 20 mM Triethanolamine / 0.1 % Brij 35 (w/v) at 4 °C for 12-18 hours. Samples were then centrifuged at 7600 G for 20 min. The supernatant was divided into 100 µl aliquots, which were subsequently assayed for bone specific alkaline phosphatase (BALP) activity, MMP-2 and MMP-9 levels.

3.5.4 Hydrolysis method

100mg of the powdered bone was hydrolysed in 1 ml 6 M HCl at 110 °C for 12 - 18 hours. The bone hydrolysate was freeze dried for 24 - 72 hours and then re-suspended in 1 ml distilled water. 100 µl aliquots of the re-suspended hydrolysate were taken for hydroxyproline, calcium (Ca) and inorganic phosphate (Pi) quantification.

3.5.5 Matrix metalloproteinases 2 and 9

Quantification of MMP-2 and MMP-9 was by gelatin zymography (Heussen and Dowdle 1980). Briefly, 100 µl aliquots of the soluble protein extract were re-constituted in non-reducing sample buffer (0.2 M Tris-HCl (pH 6.8), 0.75% sodium dodecyl sulphate (SDS) (w/v), 25% glycerol (v/v)) at a ratio of 1:1. Samples were electrophoresed with MMP-2 and MMP-9 canine standards in a 7.5% SDS-polyacrylamide resolving gel containing 0.25% gelatin, using Mini Protean 3 system (Bio-Rad Laboratories Inc., Hertfordshire, Uk). Gels were incubated for 1 hour in 2.5% (v/v) Triton X-100 (pre-warmed to 37 °C), rinsed in distilled water and incubated for 18 - 24 hours in 30 ml MMP proteolysis buffer (5.0 mM

Tris, 0.5 mM $CaCl_2$, pH 7.6, 0.015% Brij 35). Gels were stained with Coomassie blue (0.2% w/v) in 10.0% (v/v) acetic acid and 30.0% (v/v) methanol and subsequently de-stained in 7.0% (v/v) acetic acid and 30.0% (v/v) methanol. Proteolytic activity was quantified by optical scanning of the gels and subsequent computer analysis of the band intensities (ImageJ 1.41o, National Institutes of Health, USA). Values were expressed as a percentage of the MMP standards.

3.5.6 Hydroxyproline

Hydroxyproline is produced as a post-translational product of proline hydroxylation. Quantification of hydroxyproline was by a colorimetric microassay system (Creemers *et al.* 1997) which utilises the ability to oxidise this amino acid to a pyrrolic compound that reacts with p-dimethylamino-benzaldehyde to form a chromophore that was measured spectrophotometrically.

3.5.7 Alkaline phosphatase

Total BALP activity was determined by analysing 100 µl aliquots of the soluble protein extract using the International Federation of Clinical Chemistry (IFCC) method (Tietz *et al.* 1983). BALP catalyses the hydrolysis of the substrate p-nitrophenylphosphate to form the coloured compound p-nitrophenol. The formation of p-nitrophenol in alkaline solution was followed by measuring absorbance at 405 nm using a Konelab 20i analyser (Labsystems Clinical Laboratory Division, Espoo, Finland). The rate of formation of p-nitrophenol is directly proportional to the amount of BALP present in the sample. BALP concentration was read from the resultant standard curve. Given that the levels of BALP have been quantified from bone extract, the concentration of BALP is assumed to be bone-specific.

3.5.8 Mineral content

For total calcium (Ca) determination, Arsenazo III reagent was added to 100 µl aliquots of the re-suspended bone hydrolysate. At neutral pH, calcium ions form a highly coloured complex with Arsenazo III. The amount of complex produced was determined by measuring absorbance at 660 nm using a Konelab 20i analyser (Labsystems Clinical Laboratory Division, Espoo, Finland). Total inorganic phosphate (Pi) was determined via a similar method. Ammonium molybdate was added to aliquots of the re-suspended hydrolysate. In acidic medium (sulphuric acid) phosphate forms a yellow coloured complex with ammonium molybdate. The intensity of this colour is proportional to the concentration of inorganic phosphate in the sample. The amount of coloured complex formed is determined by measuring absorbance at 340 nm using a Konelab 20i analyser (Labsystems Clinical Laboratory Division, Espoo, Finland).

3.5.9 Statistical analysis

The mean and standard error of the mean were calculated for each parameter. For each bone the effect of side (left versus right) on each parameter was examined using the two-tailed paired t-test, with differences considered significant at $P < 0.05$.

3.6 Results

3.6.1 Matrix metalloproteinases 2 and 9

An example of a typical gelatin zymography gel can be seen in Figure 3.13.

Figure 3.13: A gelatin zymography gel for $CTB_{(injured)}$ samples showing both forms of MMP-9 (active form: 92 kDa) and MMP-2 (active form: 72 kDa). The difference in MMP expression between the uninjured left (L) and the fractured right (R) bones can be seen.

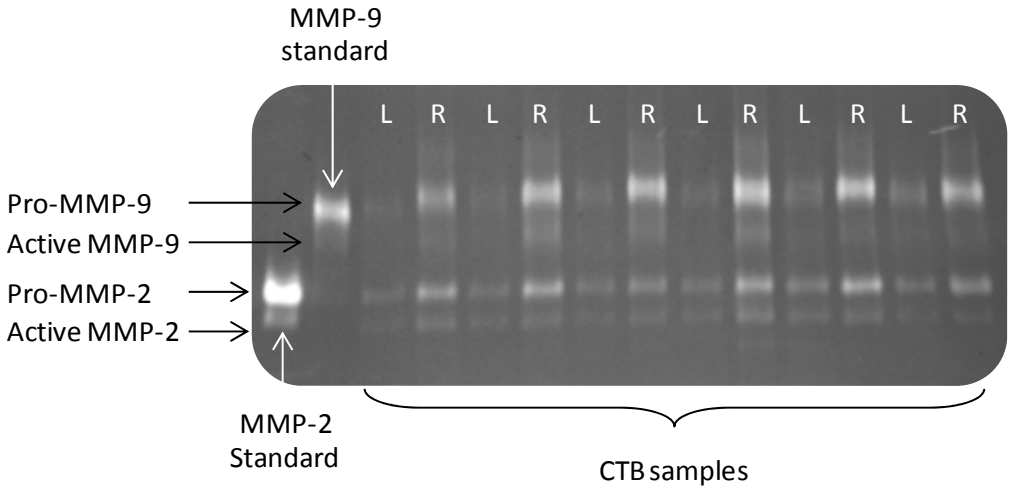

MMP-2

There were no significant left-to-right asymmetries in MMP-2 expression found within the SBT (control) MC_5 bones, or within the Greyhound MC_5, C_4, MT_2 and $CTB_{(intact)}$. Expression of pro-MMP-2 was significantly increased in right $CTB_{(injured)}$ compared to the left ($p = 0.001$) (Figure 3.14). Active MMP-2 expression in the left Greyhound MC_5 ($p = 0.046$) and right $CTB_{(injured)}$ ($p = 0.022$) was significantly increased compared to the contralateral limb bones (Figure 3.14).

MMP-9

No significant left-to-right asymmetries in MMP-9 expression were found within the SBT (control) MC_5 bones, the Greyhound MT_2 bones or the Greyhound $CTB_{(intact)}$. Expression of pro-MMP-9 was significantly increased in the left Greyhound C_4 ($p = 0.$), left MC_5 ($p = 0.036$), and right $CTB_{(injured)}$ ($p = 0.001$) compared to the contralateral bones (Figure 3.15). Active MMP-9 expression in the left Greyhound MC_5 ($p = 0.034$) and right $CTB_{(injured)}$ ($p = 0.028$) was significantly increased compared to the contralateral bones (Figure 3.15).

Figure 3.14: (a) Pro-MMP-2 amd (b) active MMP-2 expression in selected left (clear) and right (hatched) Greyhound and SBT bones. The error bars are SEM. Significant differences between the left and right limbs are indicated by * $p < 0.05$.

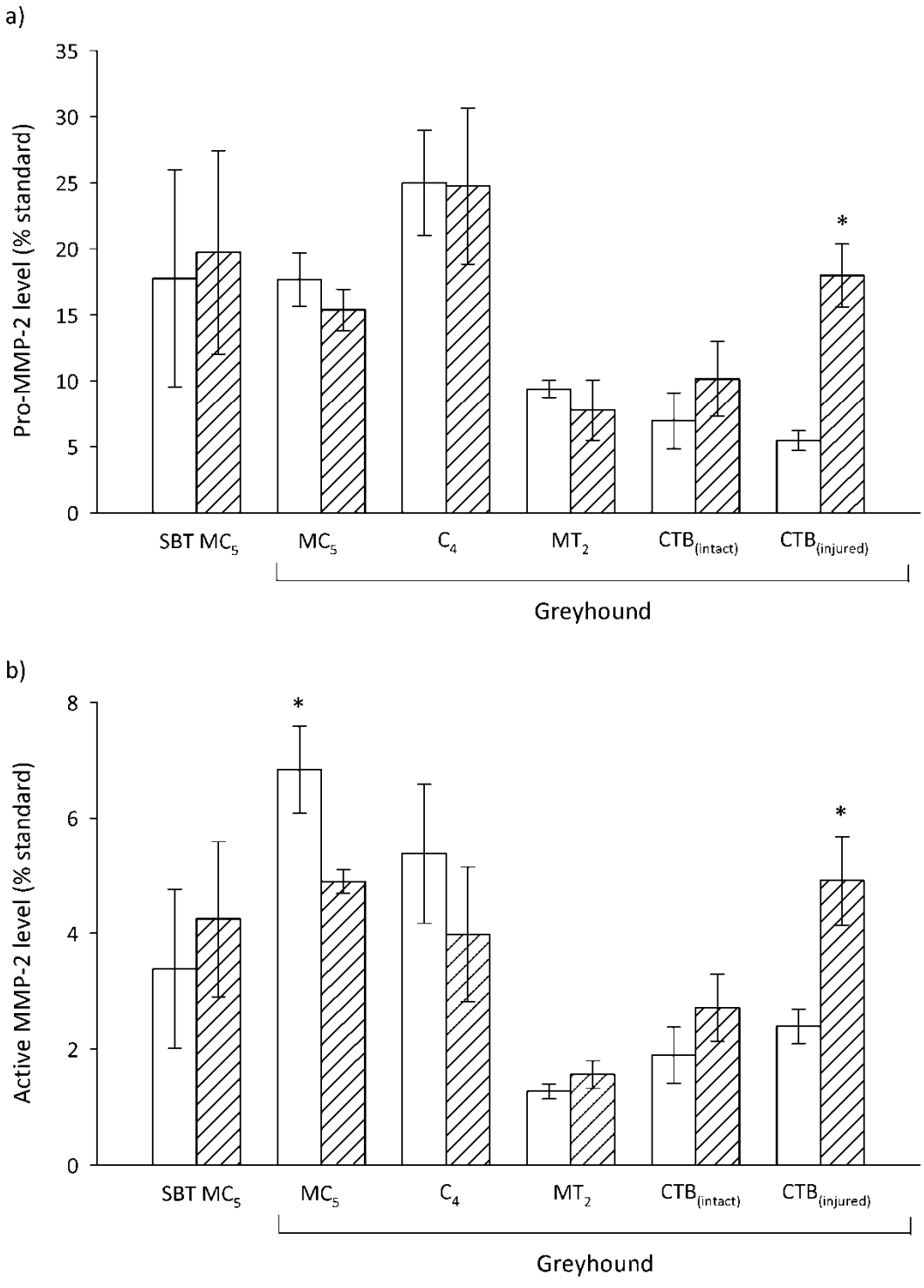

Figure 3.15: (a) Pro-MMP-9 and (b) active MMP-9 expression in selected left (clear) and right (hatched) Greyhound and SBT bones. The error bars are SEM. Significant differences between the left and right limbs are indicated by * $p < 0.05$.

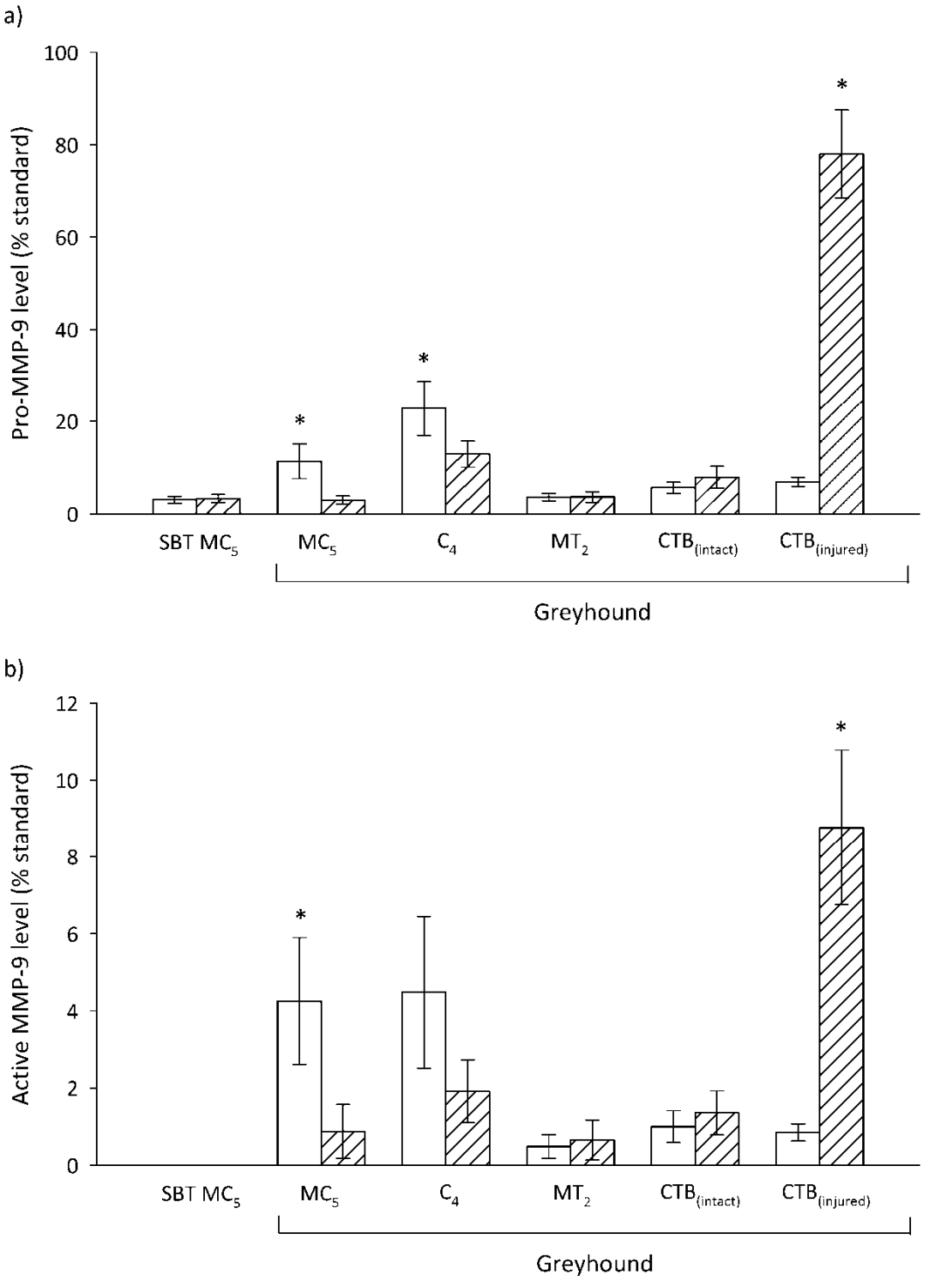

3.6.2 Hydroxyproline

There were no significant left-to-right asymmetries found in the hydroxyproline levels of the SBT MC_5 bones nor in the Greyhound MC_5, C_4 and $CTB_{(intact)}$. Hydroxyproline levels were significantly higher in right Greyhound MT_2 bones compared to the left ($p = 0.034$). Levels were also significantly higher in right $CTB_{(injured)}$ compared to the left ($p = 0.026$) (Figure 3.16).

Figure 3.16: Hydroxyproline levels in selected left (clear) and right (hatched) Greyhound and SBT bones. The error bars are SEM. Significant differences between the left and right limbs are indicated by * $p < 0.05$.

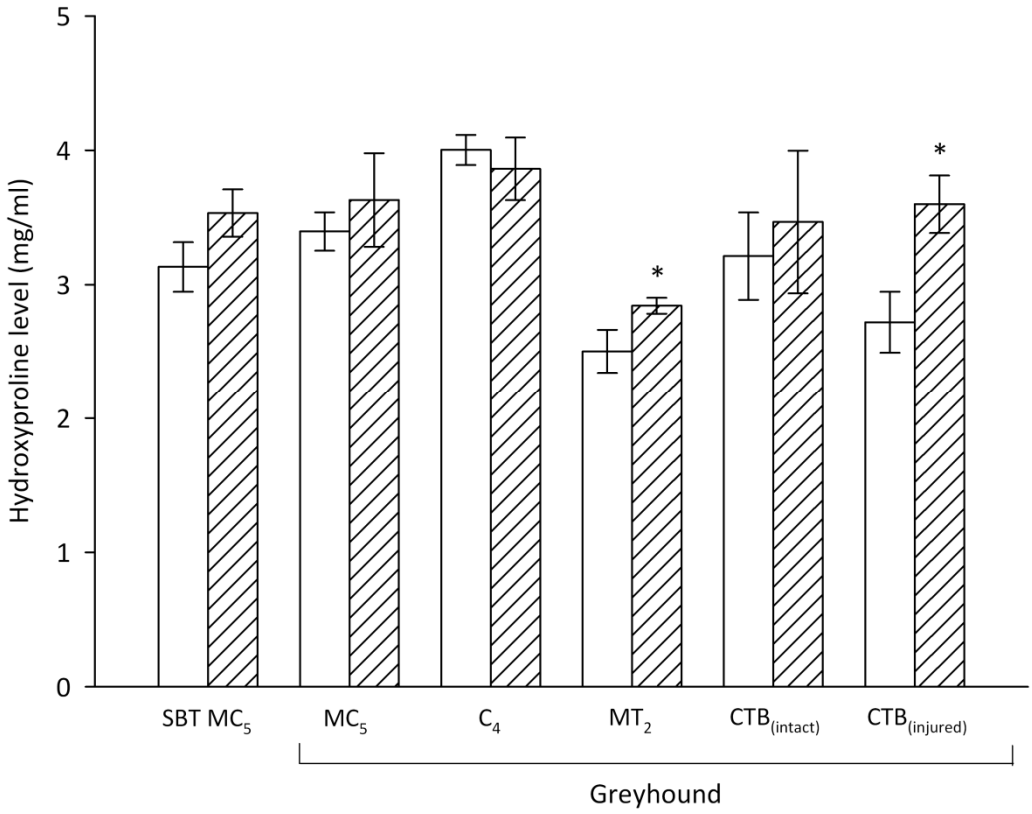

3.6.3 Alkaline Phosphatase

There were no significant left-to-right asymmetries in the BALP levels of the SBT MC_5 bones nor in the Greyhound C_4 and $CTB_{(intact)}$. BALP levels were significantly higher in the right Greyhound MT_2 ($p = 0.011$) and $CTB_{(injured)}$ ($p = 0.049$) compared to the left limb bones. Levels were also significantly higher in the left Greyhound MC_5 compared to the right ($p = 0.011$) (Figure 3.17).

Figure 3.17: BALP levels in selected left (clear) and right (hatched) Greyhound and SBT bones. The error bars are SEM. Significant differences between the left and right limbs are indicated by * $p < 0.05$.

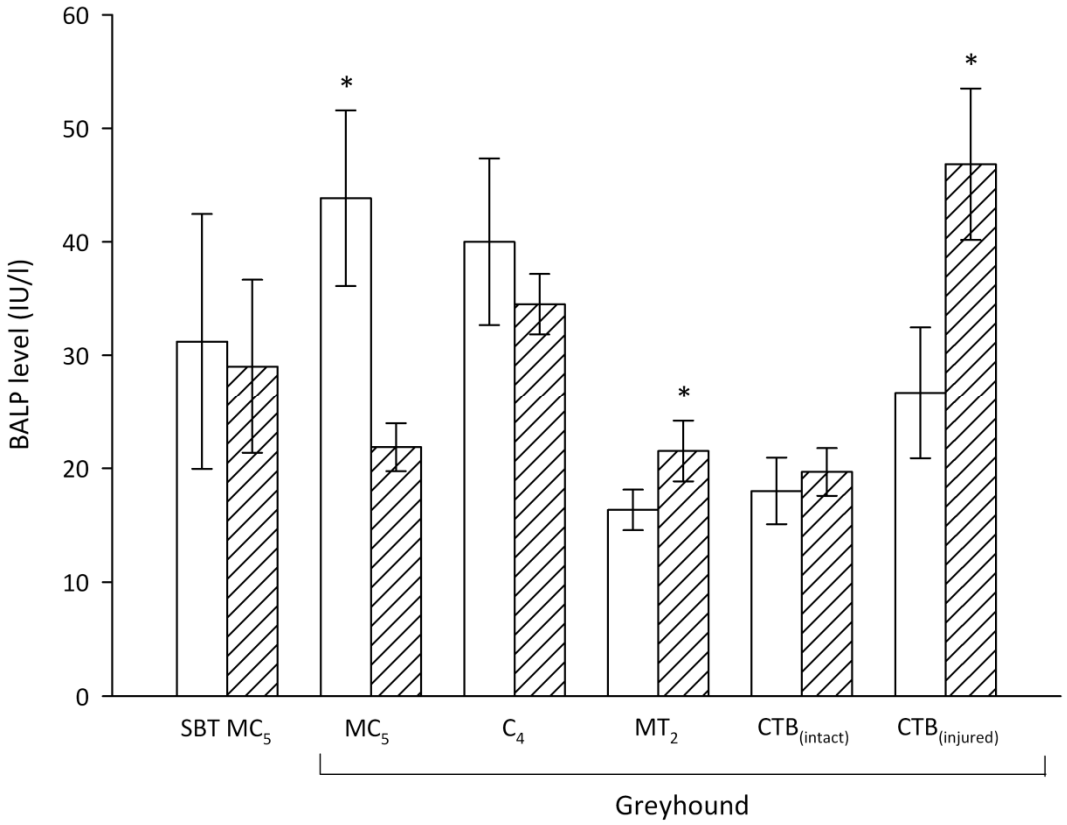

3.6.4 Mineral Content

There were no significant left-to-right asymmetries in the mineral content of the SBT MC_5 bones nor in the Greyhound MC_5, MT_2 and $CTB_{(intact)}$. Combined Ca and Pi content was significantly greater in the left Greyhound C_4 ($p = 0.003$) and $CTB_{(injured)}$ ($p = 0.010$) compared to the right limb bones (Figure 3.18).

Figure 3.18: Combined Ca and Pi levels in selected left (clear) and right (hatched) Greyhound and SBT bones. The error bars are SEM. Significant differences between the left and right limbs are indicated by * $p < 0.05$.

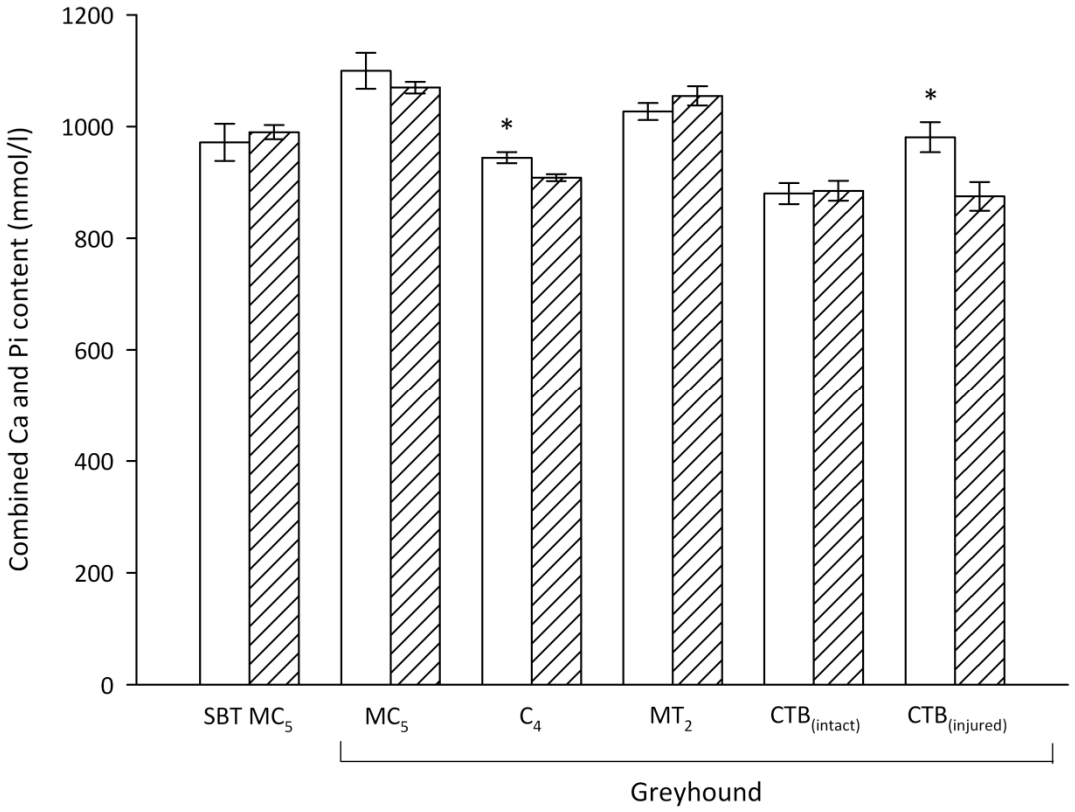

3.7 Discussion

3.7.1 Bone mineral density

Mechanical loading of bone due to physical exercise is an effective osteogenic stimulus that increases bone mass (Lanyon 1996). In human studies, athletes display increased BMD at anatomical sites that experience increased mechanical loading during training when compared to less active controls (Creighton *et al.* 2001; Heinonen *et al.* 1995; Heinonen *et al.* 1993; Heinonen *et al.* 1996). Similarly, Thoroughbred horses that have been raced show increased BMD in the C_3 bone compared to un-raced Thoroughbreds (Tidswell *et al.* 2008). Several sports impose unilateral loads on the limb bones of human athletes, leading to increased BMD at the skeletal sites experiencing greater loads. Athletes taking part in sports such as baseball, tennis and squash display greater BMD in their dominant arm (Haapasalo *et al.* 1994; Haapasalo *et al.* 1998; Haapasalo *et al.* 1996; Huddleston *et al.* 1980). Side-to-side differences in BMD have also been found in leg bones of male athletes playing football, tennis, baseball, volleyball and rugby have been reported, with increased cortical BMD being reported in the non-dominant leg (Sone *et al.* 2006). Similarly, left-to-right asymmetries in BMD have been documented in the fifth metacarpal bone (Emmerson *et al.* 2000; Johnson *et al.* 2001; Lipscomb *et al.* 2001) and in the central tarsal bone (Johnson *et al.* 2000) of racing Greyhounds. We found that Greyhounds with intact uninjured limbs had significant left-to-right differences in BMD in the majority of the thoracic distal limb bones with the rail-side bones having increased BMD compared to contralateral bones (Figure 3.4). These left-to-right asymmetries in BMD that develop in racing Greyhounds are similar to those reported in the limb bones of athletes participating in sports that unilaterally load the skeleton (Haapasalo *et al.* 1994; Haapasalo *et al.* 1998; Haapasalo *et al.* 1996; Huddleston *et al.* 1980; Sone *et al.* 2006; Wu *et al.* 1998); however, in Greyhounds, the asymmetry in BMD varies across the limb; it is not the bones within the

rail-side limbs that have the increased BMD, rather it is the rail-side bones within each limb. We found that the greatest left-to-right asymmetries in BMD were in the Greyhound C_4, MC_2, MC_4 and MC_5 bones (Figure 3.4), and in agreement with previous studies by Emmerson *et al.* (2000) and Lipscomb *et al.* (2001) the largest left-to-right asymmetry was found in the MC_5 bones. The left MC_5 is the most commonly fractured metacarpal bone in racing Greyhounds (Bellenger *et al.* 1981; Gannon 1972) and in addition to the asymmetries in BMD (Emmerson *et al.* 2000; Lipscomb *et al.* 2001) the MC_5 bones show the greatest asymmetries in microstructure (Johnson *et al.* 2001) and mechanical properties (Lipscomb *et al.* 2001) in response to the stresses of racing. This could be due to the anatomical position of the MC_5 bones within the thoracic limb causing the MC_5 bones to be subjected to the greatest degree of asymmetry in stresses when the dogs are raced; the left MC_5 is the closest metacarpal to the inside of the Greyhound track while the right is the furthest away. Asymmetries in the intact pelvic limbs of Greyhounds were less extensive than those found in the Greyhound thoracic limbs with only a few bones having significant left-to-right differences in BMD (Figure 3.5). Although, as in the thoracic limbs, it was the rail-side bones that displayed increased density compared to the contralateral bones. The thoracic and pelvic limbs of animals adapted for fast cursorial locomotion show functional specialisation: the thoracic limbs support the body and provide steering while the pelvic limbs provide the power for high accelerations (Brown *et al.* 2003; Payne *et al.* 2004; Williams *et al.* 2008a; Williams *et al.* 2008b). In addition, the percentage of body weight supported by the thoracic and pelvic limbs differs: approximately 60% of body weight is supported by the thoracic limbs and approximately 40% by the pelvic limbs at a trot (Lee *et al.* 1999) and at a gallop (Bryant *et al.* 1987; Walter and Carrier 2007). Greyhounds are thought to lean and shift their weight to the left during racing around bends (Boemo 1998). Therefore, because the thoracic limbs have a greater role in steering and because they support a greater percentage of the dogs' body weight, they are subjected to higher stresses and a greater

"lean" to the left, resulting in a more asymmetric distribution of forces across the thoracic limbs compared to the pelvic limbs. SBTs are not subjected to asymmetric stresses and, as expected, there were no left-to-right asymmetries in BMD found in the distal limb bones of the SBT.

In humans, medial-to-lateral differences in BMD have been reported across the tarsal and metatarsal bones. The lateral side bones had increased BMD compared to the medial side bones (Hastings *et al.* 2008; Sinacore *et al.* 2008). These differences in BMD are believed to result from the long duration of lateral loading during the stance phase of walking leading to increased bone formation and increased BMD in the lateral bones of the foot (Hastings *et al.* 2008). The carpal and tarsal bones of the two breeds of dog examined in the present study showed an increase in BMD from medial-to-lateral (Figure 3.8, 3.9, 3.10 and 3.11). This increase was more dramatic in the Greyhounds, suggesting their carpal bones experience a greater medial-to-lateral distribution of stresses during locomotion compared to SBTs. MC_1 had low BMD compared to all other metacarpals in both breeds, most likely because it is a much shorter bone that rarely touches the ground during locomotion. The left-to-right asymmetry seen in Greyhound MC_1 bones is probably a result of the dogs leaning to the left during racing and causing the right side MC_1 to bear some weight during racing. There were no medial-to-lateral differences across the main metacarpals (MC_2 to MC_5) nor across the metatarsals in SBTs; however, Greyhounds showed a pattern of increasing and decreasing BMD which varied depending on the limb and side examined. BMD increased from the medial to the mid bones (MC_2 to MC_3), and then decreased from the mid to the lateral bones (MC_3 to MC_5) in the right side Greyhound metacarpal bones (Figure 3.9). A similar result was found in the Greyhound left and right limb metatarsal bones: BMD increased from the medial to the mid bones (MT_2 to MT_3), and then decreased from the mid to the lateral bones (MT_3 to MT_5) (Figure 3.11). The Greyhound left limb metacarpal bones were slightly different. These bones demonstrated an increase in BMD

from the medial to the mid bones of the metacarpus (MC_1 to MC_3) with no decrease in BMD from the mid to the lateral bones (Figure 3.9). The larger middle metacarpals (MC_3 and MC_4) and metatarsals (MT_3 and MT_4) of Greyhounds provide the main weight-bearing support for the foot (Besancon *et al.* 2004). Therefore, these bones have had the highest BMD when examined medial-to-lateral because they are supporting the majority of the dog's weight as it runs and are therefore subject to higher stresses. Analysis of ground reaction forces applied by dogs galloping in a straight line found the thoracic limbs apply laterally directed forces for a longer duration than they apply medially directed forces during the stance phase of gallop (Walter and Carrier 2007). In contrast, the pelvic limbs apply medially directed forces for the majority of the stance phase (Walter and Carrier 2007). From this we can conclude that there is a medial-to-lateral distribution of forces across each foot during a straight line gallop. Greyhounds race round ovoid tracks where they run along straight sections of track as well as running around bends. Therefore it seems logical to assume that bend running, when the dog is subject to considerable centripetal accelerations, has a different distribution of forces to straight line running. Greyhounds are thought to transfer weight to the left side of their limbs when they corner around the bends of a track (Boemo 1998), placing more stresses on the metacarpals or metatarsals towards the inside of the track, e.g. left MC_5 and right MC_2. Analysis of the ground reaction forces during bend running would allow this to be confirmed. Additionally, the thoracic limbs of quadrupedal animals are thought to be mainly involved in support and steering during locomotion (Brown *et al.* 2003; Payne *et al.* 2004; Williams *et al.* 2008a), while the pelvic limbs provide the power (Pasi and Carrier 2003; Payne *et al.* 2005; Williams *et al.* 2008b). Therefore, when the dogs corner and shift their weight, the thoracic limbs could experience greater differences in stresses across the foot than the pelvic limbs due to the thoracic limbs role in supporting the animals' trunk. The functional difference between the thoracic and pelvic limbs could explain why the pelvic limbs had similar medial-to-

lateral differences in BMD across the left and right metatarsal bones, whereas the medial-to-lateral distribution of BMD across the metacarpal bones differed between the left and right thoracic limbs.

Racing Greyhounds are particularly prone to fractures of the right tarsus (Boudrieau *et al.* 1984; Guilliard 2000; Hickman 1975). The majority of these injuries involve fracture of the CTB (Boudrieau *et al.* 1984; Gannon 1972; Hickman 1975) as well as fracture of the adjacent tarsal bones, particularly the calcaneus and T_4 (Boudrieau *et al.* 1984; Guilliard 2000). Therefore, we also examined the distal pelvic limbs of Greyhounds with a right tarsal fracture. The majority of these Greyhounds had sustained fractures of the CTB, T_4, calcaneus and talus. The CTB is of particular interest as the left-to-right BMD asymmetry was reversed compared to CTBs from uninjured Greyhounds. In CTBs from Greyhounds without a right tarsal fracture the right CTB had significantly higher BMD than the left CTB (Figure 3.7); however, in CTBs from Greyhounds with a right tarsal fracture, BMD was 32.6 % lower in the right fractured CTB compared to the left uninjured CTB. This result is consistent with a previous study on Greyhound distal limb bones by Emmerson *et al.* (2000), who reported a 35.5% difference in BMD between the left (intact) and right (fractured) CTBs when isolated bones were scanned using DXA. The results from the biochemical quantification of mineral content (Figure 3.18) also showed that the fractured CTBs have significantly less mineral than the contralateral CTB supporting the results found using DXA. When the fractured bones were scanned, they were placed in as correct an alignment as possible. Imperfect reconstruction of bone fragments, especially from bones that are severely comminuted, will create some inaccuracy in the measurement of BMD. All CTB fractures were severely comminuted, making reconstruction of the fragments more difficult than other bones that had sustained simpler fractures. Imprecise measurement of BMD of fractured CTBs may be a possible explanation for the degree of asymmetry measured; however, several of the T_4 and calcaneal fractures were also highly comminuted

yet they had no significant asymmetry in BMD. In addition, coefficient of variation values for all of the fractured bones including the CTB were similar to those of intact bones, indicating that imprecise positioning was not the main reason for the measured difference. The degree of asymmetry measured in the CTBs from Greyhounds with a right tarsal fracture suggests that the adaptive remodelling process has failed in the bones from the injured dogs, leading to weakening of the bone and structural failure.

The CTB is a small cuboid bone containing both compact and trabecular bone. Adaptation of the CTB in response to cyclic loading causes the trabeculae to thicken and eventually coalesce into compact bone, especially in the dorsal region of the bone (Johnson *et al.* 2000). Adaptive remodelling of bone is targeted to the repair of fatigue micro-damage (Bentolila *et al.* 1998; Lee *et al.* 2002; Mori and Burr 1993). In the Greyhound CTB micro-damage is particularly prevalent in areas where trabecular bone has been extensively remodelled (Muir *et al.* 1999; Tomlin *et al.* 2000). Structural failure of Greyhound CTBs seems to result when cyclic loading causes an imbalance between the rate of micro-damage formation and the rate of repair by remodelling, which then leads to catastrophic failure via the accumulation and coalescence of micro-cracks through the remodelled bone (Johnson *et al.* 2000; Muir *et al.* 1999; Tomlin *et al.* 2000). The bone remodelling response to micro-damage formation may be inhibited by a high strain environment (Frost 1987), which acts as a preventative measure against micro-damage accumulated fatigue fracture. A rest period of 60 days or more prior to a return to training was a significant risk factor for racehorses that had sustained a catastrophic humeral fracture (Carrier *et al.* 1998). Once remodelling has been initiated, bone resorption takes place relatively quickly. Bone formation is a much slower process and can take several months to complete (Eriksen *et al.* 1984; Li *et al.* 1990). Therefore, it is possible that the humeri of affected horses were predisposed to fracture when they returned to training due to high porosities associated with the on-going bone resorption process. Racehorses either are train or race daily

providing a continuous stream of high intensity exercise; however, Greyhounds usually train or race only once or twice a week. It takes about 3 to 5 days for a BMU to be activated and start the bone resorption process (Martin *et al.* 1998), therefore, the length of time between training and racing sessions could be enough of a break between bouts of exercise to allow the bone remodelling process to begin, so that the next time the dog is raced the bone is undergoing resorption and is mechanically weaker and susceptible to further damage.

Why some Greyhounds experience fatigue fracture of certain bones and others do not is not known. In this study, uninjured Greyhounds had a positive adaptive response in their CTBs with increased BMD in the right limb bone, whereas CTBs from injured dogs had a reversal of this BMD asymmetry. Racing histories shed no light onto this matter as both dogs with and without right tarsal fracture had raced a similar number of times (41 versus 37 races) over a similar length of time (64 versus 72 weeks) (Appendix 1). Further information about the amount of cyclic training required to initiate an adaptive osteogenic response within Greyhound distal limb bones and the amount required to initiate micro-damage accumulation may help determine why some dogs are prone to fracture. It could be that some Greyhounds are genetically predisposed to fatigue fracture and analysis of their pedigree could help reveal this. In addition, information about the length of "rest" time needed to initiate bone remodelling and the length of time it takes for the bones to be mechanically strong enough to withstand racing following initiation of remodelling could help create training regimes for racing dogs that act as a preventative measure against fatigue fracture. Additional information such as the speed of the dogs when they race, the type of surface used on the Greyhound track and how the track is maintained, would also help in creating such training regimes.

3.7.2 Bone metabolism and matrix composition

Bone metabolic responses to mechanical loading have been studied with results varying depending on type and duration of training. Resistance exercise training increases bone formation, while transiently suppressing bone resorption (Fujimura *et al.* 1997; Notomi *et al.* 2000). High-impact exercise increases bone formation in humans (Creighton *et al.* 2001) and increases both new bone formation and bone collagen remodelling in racehorses (Tidswell *et al.* 2008). This study investigated the effect of repetitive cyclic loading on the metabolism and matrix composition of distal limb bones from racing Greyhounds, and we compared the Greyhound to a non-racing breed of dog; the SBT. The candidate markers selected were known to be quantifiable in bone extract based on a previous study by Tidswell *et al.* (2008) that examined the effects of exercise on equine distal limb bones.

The SBT bones showed no left-to-right asymmetries in any of the biochemical markers of bone turnover whereas the Greyhound bones had several, further supporting the hypothesis that the asymmetrical stresses experienced during racing are responsible for those seen in Greyhound distal limb bones.

Degradation of the organic matrix of bone involves two major classes of enzymes, lysosomal cysteine proteinases such as cathepsin B, L and K (Drake *et al.* 1996; Hill *et al.* 1994a) and MMPs, including collagenase and the gelatinases MMP-2 and MMP-9 (Hill *et al.* 1995). Increased expression of MMP-2 and MMP-9 indicates increased levels of collagen degradation and hence increased bone resorption. Increased MMP-2 and MMP-9 levels have been reported in the C_3 bone of racehorses, indicative of increased remodelling, in response to high intensity exercise (Tidswell *et al.* 2008). We found Greyhounds had increased expression of MMP-2 and MMP-9 in their rail-side bones indicating increased bone resorption is taking place within these bones compared to the contralateral bones (Figure 3.14 and 3.15). Additionally, in Greyhounds with a fractured right CTB, expression

of both forms of MMP-2 and MMP-9 were significantly increased in the fractured bones compared to the uninjured contralateral bones (Figure 3.14 and 3.15). As well as being produced by bone cells (Meikle *et al.* 1992; Rifas *et al.* 1994; Rifas *et al.* 1989; Tezuka *et al.* 1994; Wucherpfennig *et al.* 1994), both MMP-2 and MMP-9 are produced by macrophages, and their proteolytic activities are thought to be necessary for various functions of monocytes and macrophages such as extravasation, migration, and tissue remodelling during chronic inflammatory conditions (Campbell *et al.* 1991). Therefore, as well as indicating increased bone resorption within the right CTB, increased expression of MMP-2 and MMP-9 may be a response of the inflammatory cells to the increased mechanical loading imposed on the right CTB (and on the other rail-side bones) during racing. Additionally, MMP-9 has been shown to be essential for correct fracture repair; MMP-9 deficient mice display non-union or delayed union of fractures caused by persistence of cartilage at the injury site (Colnot *et al.* 2003). Therefore, MMP-2 and MMP-9 expression could be increased as result of the final catastrophic CTB fracture. However, all of the Greyhounds were euthanatised within half an hour of the fracture occurring and it is unlikely that such a significant up-regulation of not only the inactive, but also the active, form of the MMPs could have occurred within this short time span. Previous studies looking at the expression of MMPs post fracture have shown MMP-2 and MMP-9 expression is significantly elevated three days post fracture during the inflammatory phase of healing (Colnot *et al.* 2003; Wang *et al.* 2006) and the expression of MMP-2 precedes that of MMP-9 (Wang *et al.* 2006). MMP-2 and MMP-9 expression was also significantly increased in uninjured rail-side C_4 and MC_5 bones, indicating increased bone resorption taking place within these bones. Greyhound MC_5 bones are heavily remodelled in the mid-diaphyseal region (Johnson *et al.* 2001) and bone remodelling is initiated by micro-damage formation (Mori and Burr 1993). Therefore, it seems likely that, instead of being a result of the

catastrophic fracture, the increased MMP-2 and MMP-9 expression resulted from increased micro-damage formation acting as a stimulus for increased bone resorption.

BALP is one of the most frequently used non-collagenous markers of osteogenesis (Allen 2003; Magnusson *et al.* 1999; Watts 1999). Serum levels of BALP have been shown to increase in response to increased exercise in horses (Price *et al.* 1995), dogs (Puustjarvi *et al.* 1992) and humans (Fujimura *et al.* 1997) when compared to control subjects undertaking less intensive exercise; however, as type I collagen is present in many tissues, these values may not solely reflect bone activity. Tidswell *et al.* (2008) quantified BALP levels directly from bone and found BALP levels to be elevated in racehorses compared to unraced controls, indicating racing and race-training in horses increases bone formation. We found BALP levels were significantly elevated in the rail-side MC_5 and MT_2 bones of Greyhounds (Figure 3.16) indicating increased osteoblastic activity, and hence increased new bone formation, within these bones, as a result of the asymmetrical loading experienced during racing. Additionally, CTBs from Greyhounds with a fractured right CTB showed a significant asymmetry in BALP levels (Figure 3.16). Consistent with the other markers of bone turnover measured, the right side (fractured) bone had greatly increased levels of BALP compared to the left. This could be a response of the bone to the injury; however, as dogs were euthanatised quickly following injury and as other non-injured bones also display increased BALP, it is more likely that the increased BALP levels indicate increased bone formation in response to increased bone remodelling within these bones.

Approximately 14% of the amino acid content of collagen consists of hydroxyproline (Eastoe 1955). Therefore, quantification of hydroxyproline can provide an estimation of the total collagen content of a tissue. Hydroxyproline levels were significantly increased in rail-side MT_2 bones and in fractured CTBs (Figure 3.17), indicating increased total collagen content within these bones. Increased collagen content and decreased mineral content

indicates bone is hypomineralised (i.e. mineral deficient). Hypomineralisation of bone appears to be a consequence of high turnover and results in reduced strength and elastic modulus (Grynpas *et al.* 1991; Lane *et al.* 2006). A reduction in bone strength increases the fracture risk. Further information about the composition of the organic bone matrix could help determine exactly how the matrix is changing in response to the stresses of racing. Collagen cross-linking affects the mechanical strength of the collagen network and plays an important role in mineralization of collagen (Knott and Bailey 1998; Viguet-Carrin *et al.* 2006). The ratio of immature to mature cross-links provides details about the rate of turnover of the bones organic matrix: bones with more immature cross-links indicating an increased rate of turnover. Tidswell *et al.* (2008) found the ratio of immature to mature cross-links was higher in racehorses compared to unraced controls suggesting high-intensity exercise may be inducing elevated collagen turnover.

In Greyhounds, mineral content was significantly increased in rail-side C_4 bones, and decreased in fractured CTBs compared to the contralateral sides (Figure 3.18). Consistent with BMD data, mineral content was higher in the left rail-side C_4 bone and lower in the right fractured CTB. Mineral content is increased in the radial carpal and C_3 bones of racehorses compared to unraced controls (Tidswell *et al.* 2008) and in the metacarpophalangeal joint of trained compared to untrained foals (Brama *et al.* 2001). Increases in mineral content are correlated with increases in bone strength (Dalen *et al.* 1976; Hansson *et al.* 1980). Therefore, high intensity exercise leads to increased mineral content within certain bones which increases the strength of those bones. In the case of the Greyhound, the asymmetric stresses imposed on the bones within each distal limb result in increased mineral content in rail-side bones. The exception is in the right CTB from Greyhounds that have sustained a fracture of this bone; consistent with BMD data, and in contrast to the biochemical markers of bone turnover measured, the left side bone had increased mineral content compared to the right. This supports the idea that, despite the

increased bone turnover taking place within the right CTB, there is a net loss of bone leading to weakening and ultimately structural failure.

One gap in our knowledge is an understanding of the rate of bone remodelling and how factors, such as high intensity exercise, impact upon it. There are many applications for this information because human athletes and military recruits, in addition to Greyhounds, are susceptible to fatigue fracture. Further investigation into the *in vivo* rate of remodelling, for example using Tetracycline labelling (Milch *et al.* 1957) would be useful.

3.8 Summary

Racing Greyhounds develop left-to-right BMD asymmetries similar to those reported in the limb bones of athletes participating in sports that unilaterally load the skeleton. In Greyhounds, the asymmetry in BMD varies across the limb; it is not the bones within the rail-side limbs that have the increased BMD, rather it is the rail-side bones within each limb. Increased bone resorption and formation within the rail-side distal limb bones of racing Greyhounds suggests increased bone remodelling is taking place within these bones, most likely as a result of the asymmetric cyclic loading experienced during training and racing. These left-to-right asymmetries in BMD and bone turnover are not present in the distal limb bones of SBTs. In Greyhounds with a fractured right tarsus the fractured CTBs show evidence of increased bone resorption, bone formation, collagen content and yet decreased mineral content. This supports the idea that structural failure has resulted from a net loss of bone caused by an imbalance in the remodelling process.

Chapter 4

MICRO-COMPUTED TOMOGRAPHY ANALYSIS OF THE INTERNAL ARCHITECTURE OF DISTAL LIMB BONES FROM RACING GREYHOUNDS AND COMPARISON WITH STAFFORDSHIRE BULL TERRIERS

4.1 Abstract

The internal architecture of bone is influenced by anatomical site and the mechanical loads imposed upon the bone. We investigated the effects that the stresses imposed by racing had on the internal architecture of central tarsal bones (CTB) and fifth metacarpal (MC_5) bones from racing Greyhounds using micro-computed tomography (μCT) scanning. As a comparison we also examined bones from a non-racing breed of dog, the Staffordshire Bull Terrier (SBT).

The internal architecture of Greyhound CTBS was more heterogeneous than that of SBT bones. In the Greyhound a significant dorsal-to-plantar decrease in trabecular density and trabecular pore number, and increase in trabecular pore size was noted. Greyhound CTBs had a greater number of pores across the majority of the bone. In the plantar region the number of pores was similar across both breeds; however, those in Greyhound CTBs were over three times larger than those in SBT CTBs.

Although both breeds had regional differences in trabecular architecture of the MC_5 epiphysis, the trabecular pores were much larger in the palmar region of the epiphysis of the Greyhound bones. Additionally, the left MC_5 bones from Greyhounds had increased trabecular density and decreased trabecular pore size in the dorsal region of the bone and trabecular pores were smaller in the medial region compared to the right MC_5. Greyhounds also have a significant left-to-right asymmetry in the cortical thickness of the MC_5 diaphysis, which SBTs do not.

The regional differences in the internal architecture of the Greyhound bones appear to be an adaptive response to high stresses, unevenly distributed, across the bones during galloping. In support of this, SBTs, a non-racing breed of dog that we would not expect to experience the same uneven distribution of stresses, had CTBs with a homogeneous trabecular structure and had no left-to-right asymmetries in their MC_5 bones.

4.2 Introduction

4.2.1 Bone

Bone is a hierarchically structured composite material. Bone structure may be classified into five structural levels (Rho *et al.* 1998; Weiner and Wagner 1998) ranging from the macro-structure to the nano-structure (Figure 4.1).

Figure 4.1: Hierarchical structure of bone. Adapted from Rho *et al.* (1998).

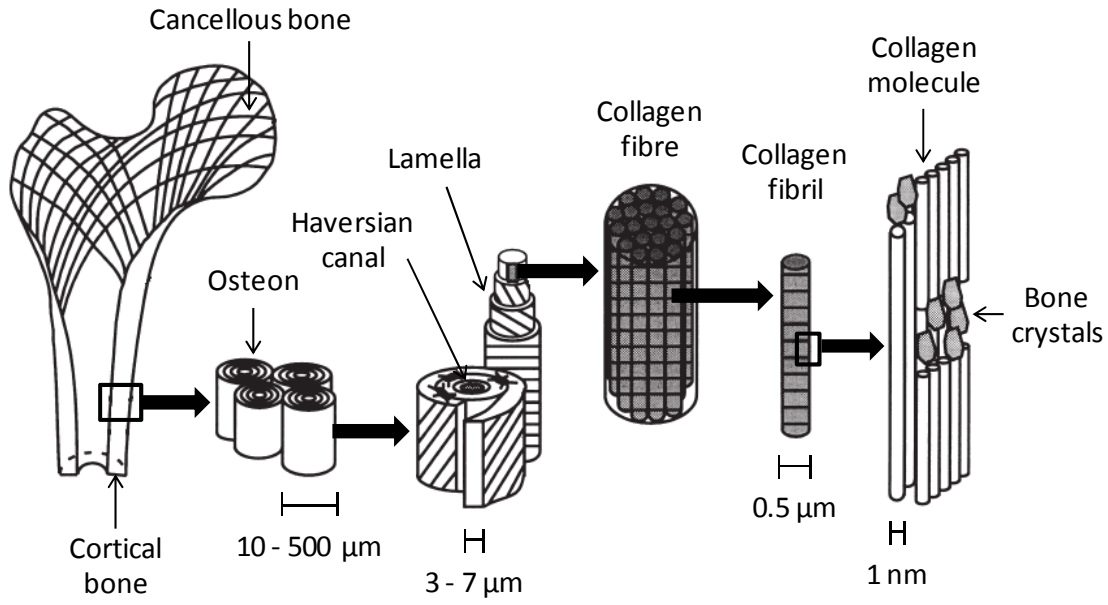

At the macrostructure level, it can be either cortical (compact) or cancellous (trabecular or spongy). This classification as cortical or cancellous is based on porosity; the proportion of the volume occupied by non-mineralised tissue. The literature is somewhat ambiguous,

with the distinction between very porous cortical and very dense cancellous bone fairly arbitrary (Martin 1972). However, in general terms, compact bone is said to have a porosity of between 5 and 30%, whereas trabecular bone can range from about 30% to more than 90%. Both mature compact and trabecular bone are made up of lamellae. Each lamellar unit is 3 to 5 µm thick and is composed of five sub-layers with each sub-layer being composed of an array of aligned mineralized collagen fibrils (Weiner *et al.* 1999). The orientations of these arrays differ in each sub-layer with respect to collagen fibril axes and crystal layers, forming a complex rotated plywood-like structure (Weiner *et al.* 1999). There are four general types of lamellar bone: trabecular lamellae, inner and outer circumferential lamellae and lamellae of osteons (interstitial lamellae). The last three types of lamellar are only found in compact bone (Buckwalter *et al.* 1996).

Cortical bone

Macroscopically, cortical or compact, bone appears as a solid continuous structure; however, microscopic examination shows it is composed of densely packed tubular structures called osteons or Haversian systems (Fawcett and Bloom 1994). Mature compact bone is made up of three types of lamellar bone: inner and outer circumferential lamellae, and interstitial lamellae (Buckwalter *et al.* 1996). Cross section through the mid-diaphysis of a long bone shows the cortical bone to be structured into three concentric systems: an outer circumferential system, an intermediate osteonic area and an inner circumferential system (An and Draughn 2000). Flat and short bones, as well as the epiphysis and metaphysis of the long bones, have a thin outer layer of compact bone that has both trabeculae and osteons, but the typical three-system arrangement of the long bones is not apparent (An and Draughn 2000).

Cancellous bone

Cancellous, or trabecular, bone is present in the medulla of flat and short bones and in the epiphysis and metaphysis of long bones. It is almost absent in the central part of the diaphysis of long bones. It is made up of columns (rods) and plates of bone known as trabeculae, which divide the inner region of the bone into intercommunicating pores of varying sizes, producing a structure of highly variable porosity and density (Galante *et al.* 1970). The dimensions of the holes (pores) in this lattice are extremely variable, with variation increasing with age (senescence) as trabeculae are lost (Aaron *et al.* 1987). The micro-architecture of the trabeculae appears to be random; however, their connections and the orientation of the trabeculae have particular patterns that are believed to be related to the specific mechanical properties of the bone (Kleerekoper *et al.* 1985). Trabeculae orientate themselves along lines of stress (Biewener *et al.* 1996; Huiskes *et al.* 2000; Wolff 1986) and there is a close relationship between the number and arrangement of trabeculae and bone strength (Kleerekoper *et al.* 1985). Trabecular architecture changes in response to exercise (Section 4.2.3) and in response to ageing (senescence). Trabeculae loss is selective: decreasing numbers of transverse trabeculae with little or no loss in the numbers of vertical trabeculae is seen in the central zone of osteoporotic vertebral bodies (Atkinson 1967). Complete loss of trabeculae have been observed in elderly women (Aaron *et al.* 1987) whereas in elderly men loss of trabeculae is less dramatic (Compston *et al.* 1987). As well as decreasing bone volume, this selective loss of trabeculae can cause a breakdown of the bones "connectivity" (Kleerekoper *et al.* 1985). The trabecular connectivity density can be interpreted as the trabeculae number per mm^3 (Feldkamp *et al.* 1989): a breakdown in trabecular connectivity decreases the strength of the bone, resulting in an increased risk of fracture (Legrand *et al.* 2000).

4.2.3 Bone remodelling

Bone remodelling involves the sequential removal and replacement of bone at discrete sites and is facilitated by small packets of cells known collectively as the bone multi-cellular unit (BMU) (Frost 1990b, 1992). Each BMU comprises a cutting cone of osteoclasts in front, a closing cone lined by osteoblasts behind, and connective tissue, blood vessels and nerves filling the cavity (Parfitt 1994). The organisation of a BMU differs in cortical and trabecular bone but these differences are mainly morphological rather than biological (Parfitt 1994). Intra-cortical BMUs form a tunnel and burrow through bone whereas cancellous BMUs lie along the surface and either form trenches (half-tunnels) or they spread out over an area (Jayasinghe *et al.* 1993; Parfitt 1994). BMUs form in response to a signal or stimulus and follow the sequence: origination and organisation of the BMU, activation of osteoclasts, resorption of old bone, recruitment of osteoblasts, formation of new bone matrix (osteoid) and mineralisation (Frost 1966; Hattner *et al.* 1965; Parfitt 1994, 2000). The life span of the individual cells within a BMU is shorter than that of the BMU; as a BMU progresses along or through bone new cells are continually recruited to allow continued activation, resorption and formation.

Remodelling of trabecular bone

Trabecular bone has a lattice-like structure made up of rods and plates of bone known as trabeculae. The overall structure does not necessarily change when it is remodelled; however, if bone resorption exceeds formation, then the resultant loss of bone causes thinning and/or perforation of trabeculae (Seeman 2003). The mechanical strength of bone is impaired to a greater extent with perforation of trabeculae than with trabeculae thinning (Guo and Kim 2002; Silva and Gibson 1997). Perforation of trabeculae can occur if the depth of the resorption cavity is deeper than the trabeculae thickness, or if there are two BMUs resorbing bone on opposite sides of the trabeculae at the same time (Parfitt *et al.* 1983).

Bone loss is amplified once the trabeculae have perforated because there is no "scaffolding" to support osteoblastic bone formation (Parfitt *et al.* 1983). Trabeculae are converted from a more plate-like structure into a more rod-like structure via this process, with a loss of surface available for bone formation (Parfitt *et al.* 1983). Once the trabeculae have become thinner and more rod-like, they can become disconnected from one other. This disconnection of trabeculae has been shown in scanning electron micrographs (Dempster 2000). Isolated trabeculae have no mechanical stimuli and are quickly severed from the osteocyte network and quickly resorbed (Mosekilde 1993).

4.2.3 Response to exercise

Effects on cortical bone

The diameter and the thickness of the cortex can have a dramatic impact on the biomechanical integrity of bone (Ammann *et al.* 1996; Turner 2002). Increases in cortical thickness and cross sectional area occur in response to increased exercise and training (Jones *et al.* 1977; McCarthy and Jeffcott 1992; Nunamaker *et al.* 1989; Woo *et al.* 1981b). Woo *et al.* (1981b) found femoral cortical thickness and cross-sectional area was significantly increased in pigs subjected to a 12 month long exercise program. Jones *et al.* (1977) found significantly increased cortical thickness in the humeri of the "playing" arm of tennis players compared to the contralateral arm. McCarthy and Jeffcott (1992) reported increased dorsal cortical thickness in the third metacarpal bone of Thoroughbred horses in response to treadmill exercise. Similarly, Nunamaker *et al.* (1989) found Thoroughbred horses have increased cortical thickness compared to Standardbred horses: Thoroughbred horses are trained at higher speeds than Standardbreds (gallop versus trot or pace) and therefore their bones are subjected to higher stresses. Individuals with thinner cortices are more at risk of fracture (Crabtree *et al.* 2001; Kaptoge *et al.* 2008). Therefore, increased

cortical thickness in response to exercise would appear to be an adaptive response to minimise the risk of fracture.

Effects on internal bone architecture

The internal architecture of bone is one of the major factors influencing its mechanical properties (Kleerekoper *et al.* 1985; Parfitt 1992). Mechanical loading due to exercise leads to an increase in trabecular bone mass, primarily via an increase in trabecular thickness (Holy and Zerath 2000; Notomi *et al.* 2000; Notomi *et al.* 2001). Holy and Zerath (2000) found trabecular thickness in the proximal tibial metaphysis increased following four weeks of exercise in growing rats; however, trabecular number was not affected. Similarly, Notomi *et al.* (2000) reported vertebral trabecular thickness increased, but trabecular number did not change in growing rats subjected to a resistance exercise program. These two studies were based on two-dimensional analysis of trabecular bone. In contrast, Joo *et al.* (2003) looked at the three-dimensional architecture of bone and found rats subjected to a 10 week exercise program had increased trabecular bone mass in the distal femoral metaphysis, due to the creation of new trabeculae, increased trabecular thickness and decreased trabecular separation. Similar results have been found in horses (Firth *et al.* 1999; Firth *et al.* 2000; Gabriel *et al.* 1998). Thoroughbred horses subjected to a high intensity treadmill exercise program (Firth *et al.* 1999) or race-trained (Firth *et al.* 2000) show increases in trabecular thickness and density in their carpal bones. A comparison of the architecture of the navicular bone in different breeds of horse found that athletic horses have more cortical and less cancellous bone than sedentary horses, with thickening of the cortex at the level of the distal and proximal borders and at the level of the flexor cortex (Gabriel *et al.* 1998).

4.2.4 Fatigue fractures in racing Greyhounds

Fatigue or "stress" fractures are partial or complete fractures that occur due to the application of cyclic stresses lower than those required to fracture normal bone in a single loading event (McBryde 1975). Some of the characteristic fractures seen in racing Greyhounds are believed to be fatigue fractures, in particular fracture of the central tarsal bone (CTB) and metacarpal bones (Devas 1961; Gannon 1972). Fracture of the right tarsus is one of the most commonly reported injuries in racing Greyhounds (Bateman 1960; Boudrieau *et al.* 1984; Gannon 1972; Guilliard 2000; Hickman 1975; Poulter 1991; Prole 1976) and it almost always involves fracture of the CTB (Boudrieau *et al.* 1984; Gannon 1972; Guilliard 2000; Hickman 1975). CTB fractures have been classified into five types ranging in severity from type I (dorsal slab fracture without displacement) to type V (severely comminuted and displaced) (Dee *et al.* 1976). CTB fractures are thought to be fatigue fractures resulting from the repetitive cycling loading encountered during training and racing causing catastrophic failure via the accumulation and coalescence of micro-damage (Johnson *et al.* 2000; Tomlin *et al.* 2000). Tomlin *et al.* (2000) found Greyhound CTBs exhibit arrays of branching micro-cracks in the compact bone failure surfaces, these arrays are similar to those seen after compressive fatigue loading of bovine compact bone *ex vivo* (Carter and Hayes 1977); such arrays were not found in the failure surfaces of long bones (Tomlin *et al.* 2000). Long bone fractures in Greyhounds are usually a result of direct trauma, i.e. a collision or a fall during racing (Sicard *et al.* 1999). The morphology of the failure surface of Greyhound long bone fractures supports the concept that induction of the fractures is not associated with the extensive accumulation of fatigue micro-damage (Tomlin *et al.* 2000). Metacarpal fractures are common in young Greyhounds between 6 and 37 months of age (Bellenger *et al.* 1981; Ness 1993; Piras 2005) and they usually occur on the rail-side of the affected foot, i.e. the side of the foot that is closest to the inside of the greyhound track. Left metacarpals four (MC_4) and five (MC_5), and right metacarpals two

(MC_2) and three (MC_3) are the most often injured (Bellenger *et al.* 1981; Dee and Dee 1985; Gannon 1972; Piras 2005). The left MC_5 is the most commonly affected metacarpal bone. Gannon (1972) reported 60.0%, and Bellenger *et al.* (1981) reported 57.1%, of metacarpal fractures involved the left MC_5. The bones usually fracture at the approximate junction of the proximal and middle one third of the metacarpal bones (near the attachment of the interosseous muscles) (Dee and Dee 1985). In the majority of dog breeds metacarpal fractures are the result of external trauma or falls (Phillips 1979); however, in racing Greyhounds, metacarpal fractures are believed to be fatigue fractures (Gannon 1972) resulting from the repetitive asymmetric cyclic loading that occurs during training and racing (Johnson *et al.* 2001). Evidence for this has been found in Greyhound MC_5 bones: the mid-diaphyseal region of the left MC_5 bones is heavily remodelled in response to micro-damage formation, having increased cortical thickness and osteonal density compared to the right MC_5.

4.2.5 Micro-computed tomography

The micro-computed tomography (µCT) was first introduced by Feldkamp (1989). A typical laboratory µCT scanner will consist of a tungsten-anode X-ray tube with a relatively small focal spot (~10 µm) coupled to a high-resolution X-ray detector system (~50 µm pixel spacing). A small X-ray focal spot is used with X-ray imaging systems that incorporate geometric magnification to minimize image blur (known as penumbral blurring) which would degrade the image resolution. To produce a 3D dataset, X-ray projection views are acquired at hundreds of equally spaced angular positions around the object of interest. These views are then used to reconstruct a CT image, typically by using a convolution back-projection approach (implemented in 3D) similar to that described by Feldkamp *et al.* (1984) and Lie *et al.* (2001). µCT techniques have been used for the non-destructive evaluation of trabecular bone structure (Borah *et al.* 2001; Gross *et al.* 1999) and µCT can

be used to precisely measure changes in bone stereology, volume and micro-architecture (Buchman *et al.* 1998).

4.2.6 Study aim and hypothesis

We hypothesised that the internal architecture of the Greyhound bones would show adaptive changes, such as coalescence and thickening of trabeculae and increased cortical thickness, as a result of the stresses imposed on them during racing and that such changes would not be present in bones from a non-racing breed, the Staffordshire Bull Terrier (SBT). To test this we used μCT scanning to examine the trabecular architecture of the CTBs and of the epiphysis of the MC_5 bones, and to examine the cortical thickness of the diaphysis of the MC_5 bone, from racing Greyhounds and SBTs.

PART A: CENTRAL TARSAL BONES

4.3 Materials and Methods

4.3.1 Central tarsal bone specimens

CTBs were collected from the distal pelvic limbs of five racing Greyhounds (four male, one female), euthanatised at their owners request after sustaining severe fractures of a thoracic limb (three dogs) or when severe behavioural problems (aggression) prevented them from racing or being re-homed (two dogs). All of the dogs had raced ≤ 23 times (range 7 to 23 races) during their lifetime (low-raced Greyhounds). Mean age of the dogs was 2.69 ± 0.19 years; mean weight was 30.34 ± 4.22 kg.

CTBs were also collected from five racing Greyhounds (three male, two female), euthanatised after sustaining severe fractures of one or both of the thoracic limbs, that had raced ≥ 45 times (range 45 to 61 races) during their lifetime (high-raced Greyhounds). Mean age of the dogs was 3.56 ± 0.68 years; mean weight was 29.96 ± 2.32 kg.

Additionally, CTBs were collected from five SBTs (four male, one female), euthanatised at a local dogs home when extreme behavioural problems prevented re-homing. Age of the dogs was unknown; mean weight was 16.95 ± 2.91 kg.

4.3.2 µCT protocol

Examinations were performed using a BIR ACTIS µCT scanner (Actis, Bio-Imaging Research Inc., Lincolnshire, IL, USA) which was calibrated using a series of calibration phantoms prior to scanning of the bones. Bones were positioned on the scanner stage using blue tack (Figure 4.2). Contiguous 0.1 mm transverse slices were taken to generate multiple, detailed, cross-sectional images of the bones. Entire CTBs were scanned from proximal to distal. Slices were acquired at 88.0 kV and 0.015 mA with 2400 views taken per rotation

Figure 4.2: (a) Photograph and (b) close-up showing how CTBs were set up on the stage ready for µCT scanning.

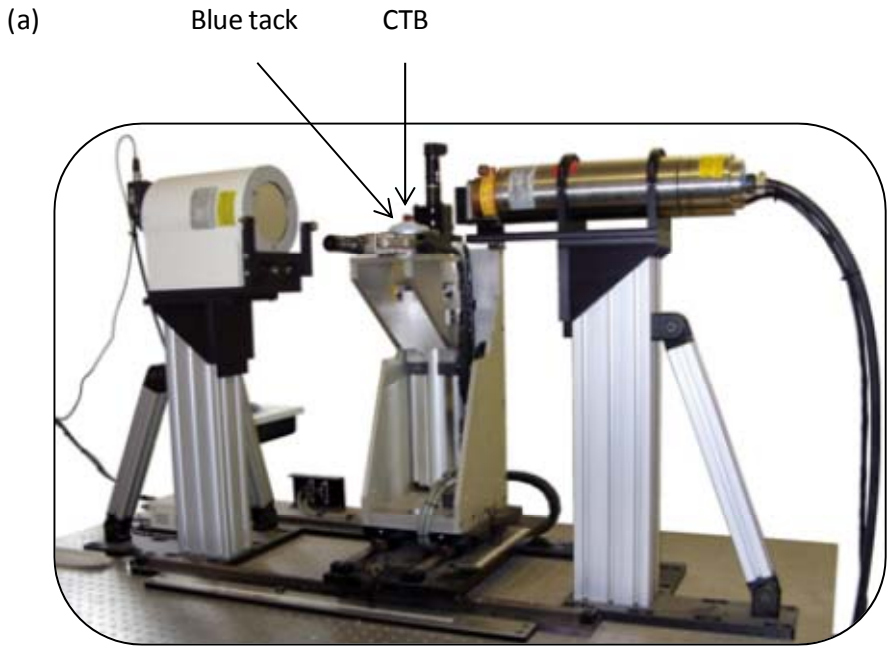

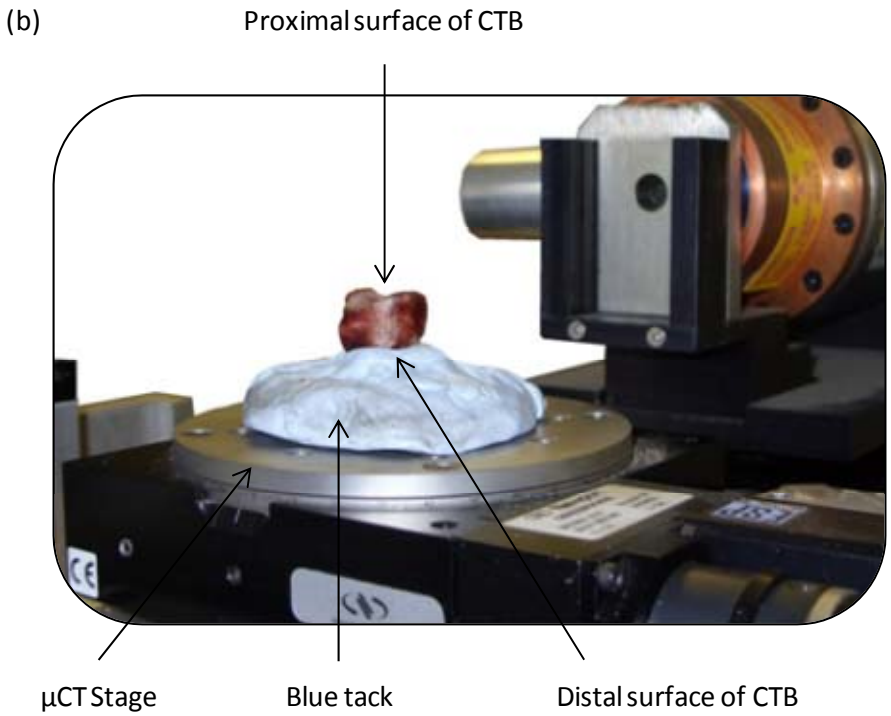

4.3.3 Image analysis

µCT images were analysed using ImageJ ver. 1.43s (National Institutes of Health, USA). Five regions-of-interest (ROI) across the CTB from dorsal-to-plantar were analysed (Figure 4.3). Dorsal-to-plantar ROI were 25 x 75 pixels in Greyhound CTBs and 20 x 60 pixels in SBT CTBs. The dorsal surface area of the SBT CTB was approximately 64% smaller than the Greyhound CTB, therefore, SBT ROI were 64% smaller than the Greyhound ROI. Additionally, three ROI across the CTB from medial-to-lateral were analysed (Figure 4.4). Medial-to-lateral ROI were 75 x 25 pixels in Greyhound CTBs and 60 x 20 pixels in SBT CTBs. The distribution of dorsal-to-plantar and medial-to-lateral ROI was consistent with respect to the overall dimension of the bone: the centre of the bone slice was determined via its Cartesian coordinates and the mid-ROI was positioned around it. The other ROI were then placed relative to that ROI contiguous to one another. The mid-point of each CTB from proximal to distal was determined and 30 (contiguous) slices around this point analysed; this ensured that only trabecular bone was analysed. Image-J was used to convert the greyscale µCT

images into black and white binary images. Trabecular density, trabecular pore size and trabecular pore distribution were then determined. Trabecular density was measured as the percentage of the ROI occupied by bony trabeculae; it does not refer to the mineral density of the scanned trabeculae. Trabecular pore size and distribution were calculated using the "analyse particles" tool as the number of pores and the pore sizes present within the ROI. Data is reported here in relation to pixels: 1mm = 11.8 pixels.

Figure 4.3: Measurements were taken in five ROI across the CTB from dorsal to plantar.

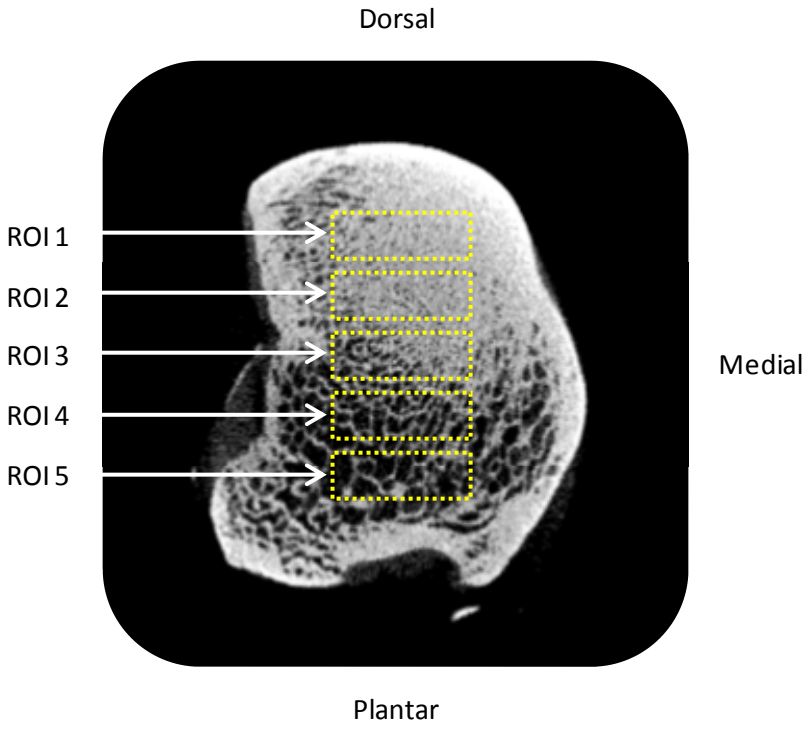

Figure 4.4: Measurements were taken in three ROI across the CTB from medial to lateral.

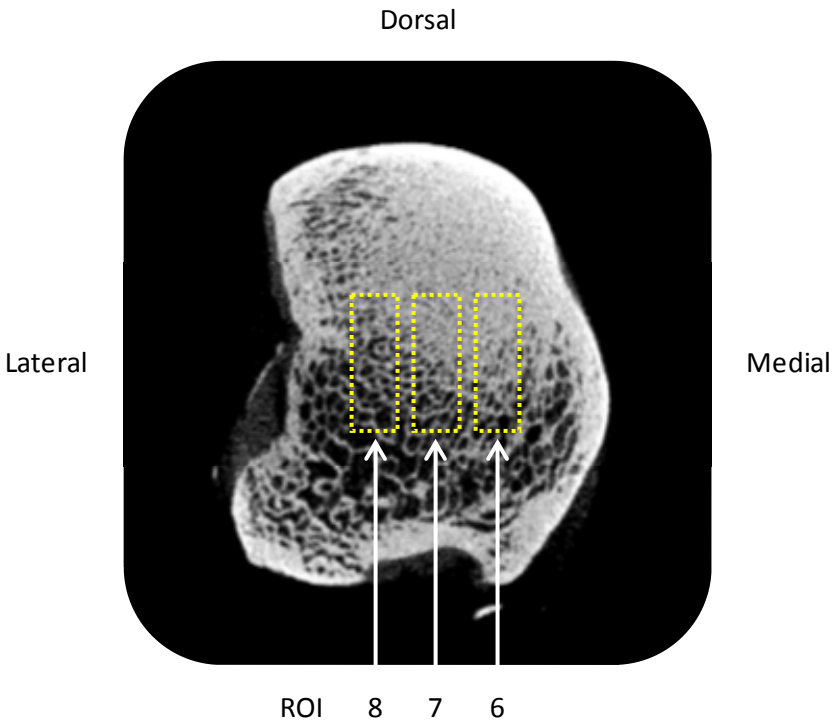

4.3.4 Statistical analysis

Mean and standard error of the mean (SEM) were calculated for each parameter (trabecular density, trabecular pore size and pore number). The effect of side (left versus right) on each parameter for each ROI was examined using a two-tailed paired t-test. Differences between low-raced and high-raced Greyhounds on each parameter for each ROI were examined using a two-tailed un-paired t-test. Differences between Greyhounds and SBTs on each parameter for each ROI were examined using a two-tailed un-paired t-test. A one-way ANOVA with a post-hoc Tukey's test was used to determine the effect of ROI (CTB: ROI 1 to 5 [1 = dorsal, 5 = plantar] and 6 to 8 [6 = medial, 8 = lateral]) on each parameter. Differences were considered significant at $p < 0.05$ for all statistical tests.

4.4 Results

Trabecular architecture data for the five dorsal-to-plantar ROI and the three medial-to-lateral ROI across the CTBs can be found in Table 4.1 and Table 4.2 respectively.

Table 4.1: Trabecular architecture data for the five dorsal-to-plantar ROI in the CTBs: mean (SEM) trabecular density, trabecular pore size and trabecular pore number. No significant differences were found between low and high-raced Greyhounds. † denotes a significant difference between the left and right limbs of a breed; $p<0.05$. Significant differences between high-raced Greyhounds and SBTs are indicated by *, and between low-raced Greyhounds and SBTs by +; $p < 0.05$.

ROI	Side	Trabecular density (area fraction)	Trabecular pore number	Trabecular pore size (pixels)
High Raced Greyhounds				
1	Left	80.1 (2.9) $^{+}$	32.6 (1.4) **	7.3 (1.0) **
	Right	81.4 (4.8) $^{+}$	28.3 (4.3) **	9.1 (1.7) **
2	Left	68.8 (3.9) $^{+}$	37.0 (2.4) †*	11.7 (1.0) **
	Right	69.3 (6.1) $^{+}$	30.7 (2.1) †*	15.8 (4.3) **
3	Left	53.4 (3.7) *	32.0 (2.5) **	25.5 (5.9) **
	Right	53.6 (3.5) *	27.8 (2.5) **	28.9 (4.3) **
4	Left	40.9 (2.4) *	22.4 (2.4) **	50.9 (10.4) *
	Right	41.5 (2.6) *	20.1 (2.6) **	57.4 (8.4) **
5	Left	34.0 (2.0) *	13.2 (1.3) **	99.9 (16.4) *
	Right	38.0 (2.0) *	14.0 (1.8) **	89.7 (15.7) *

Table 4.1 continued:

ROI	Side	Trabecular density (area fraction)	Trabecular pore number	Trabecular pore size (pixels)
Low Raced Greyhounds				
1	Left	84.1 (5.0) $^{++}$	29.2 (6.0)	7.4 (1.8) $^{+++}$
	Right	85.6 (3.6) $^{++}$	25.9 (3.6)	7.4 (1.3) $^{+++}$
2	Left	70.4 (5.6) $^{++}$	32.3 (1.6) $^{+}$	16.2 (4.3) $^{++}$
	Right	73.4 (5.7) $^{++}$	28.6 (1.8) $^{+}$	14.9 (3.6) $^{++}$
3	Left	54.8 (6.1) $^{++}$	27.3 (3.8) $^{+}$	44.9 (13.7) $^{+}$
	Right	56.9 (5.5) $^{++}$	28.5 (2.4) $^{+}$	31.0 (7.4) $^{++}$
4	Left	37.7 (4.5) $^{++}$	16.0 (3.3) $^{+}$	100.1 (22.7) $^{+}$
	Right	41.4 (4.5) $^{++}$	19.1 (2.9) $^{+}$	72.3 (16.9) $^{++}$
5	Left	33.7 (3.3) $^{++}$	10.4 (1.7) $^{+}$	162.2 (33.9) $^{+}$
	Right	35.2 (3.3) $^{++}$	11.4 (1.7) $^{+}$	161.8 (48.9) $^{+}$
SBT				
1	Left	78.8 (2.2) $^{++}$	25.4 (0.9) *	10.7 (1.4) $^{++}$
	Right	81.3 (3.6) $^{++}$	22.2 (1.5) $^{++}$	11.3 (2.6) $^{++}$
2	Left	77.6 (1.7) $^{++}$	21.7 (0.9) $^{*+}$	12.6 (1.3) $^{++}$
	Right	81.4 (3.5) $^{++}$	18.7 (1.4) $^{*+}$	12.6 (2.4) $^{++}$
3	Left	69.3 (3.5) *	19.2 (1.6) $^{*+}$	23.4 (4.1) $^{++}$
	Right	72.5 (4.0) *	18.0 (0.5) $^{*+}$	21.3 (3.4) $^{++}$
4	Left	60.4 (5.2) $^{*+}$	16.8 (1.0) $^{++}$	36.7 (5.5) $^{++}$
	Right	62.8 (3.7) $^{*+}$	15.0 (1.7) $^{++}$	44.1 (8.7) $^{++}$
6	Left	65.2 (6.5) $^{*+}$	13.8 (0.8) $^{++}$	35.7 (8.4) $^{*+}$
	Right	67.0 (4.1) $^{*+}$	13.0 (0.9) $^{++}$	37.2 (7.3) $^{*+}$

Table 4.2: Trabecular architecture data for the three medial-to-lateral ROI in the CTBs: mean (SEM) trabecular density, trabecular pore size and trabecular pore number. No significant differences were found between low and high-raced Greyhounds. † denotes a significant difference between the left and right limbs of a breed; $p<0.05$. Significant differences between high-raced Greyhounds and SBTs are indicated by *, and between low-raced Greyhounds and SBTs by +; $p < 0.05$.

ROI	Side	Trabecular density (area fraction)	Trabecular pore number	Trabecular pore size (pixels)
High Raced Greyhounds				
6	Left	55.6 (4.7) *+	30.7 (1.9) *	23.4 (3.7) *
	Right	61.7 (5.0) *+	27.4 (1.1) *	24.7 (4.8) *
7	Left	55.6 (3.1) *+	30.2 (1.8) *	24.7 (3.8) *
	Right	46.0 (2.3) *+	27.7 (1.2) *	28.4 (5.0) *
8	Left	52.1 (2.9) *+	30.1 (2.9) *	27. 5 (6.0) *
	Right	46.0 (2.3) *+	26.2 (1.8) *	36.8 (4.4) *
Low Raced Greyhounds				
6	Left	55.9 (5.0) ++	25.9 (2.9) +	33.9 (6.5) *
	Right	61.6 (4.5) ++	25.2 (1.9) +	28.8 (5.2) *
7	Left	52.9 (5.2) ++	24.0 (2.3) +	28.5 (7.6) *
	Right	58.1 (5.2) ++	25.4 (1.4) +	31.1 (5.3) *
8	Left	50.8 (5.2) ++	25.5 (3.4) +	40.0 (9.6) *
	Right	52.0 (5.2) ++	26.1 (3.3) +	37.2 (10.1)
SBT				
6	Left	71.9 (4.1) *+	19.8 (1.4) *+	19.1 (3.9) *
	Right	73.3 (4.2) *+	17.1 (0.7) *+	22.7 (4.8) *
7	Left	69.6 (3.3) *+	17.8 (1.0) *+	23.0 (3.3) *
	Right	71.7 (3.8) *+	16.1 (0.9) *+	24.2 (3.9) *
8	Left	65.9 (3.6) *+	20.1 (1.1) *+	23.3 (3.3) *
	Right	71.7 (3.6) *+	18.8 (0.9) *+	21.0 (2.6) *

4.4.1 Left-to-right asymmetries in trabecular architecture

There were no significant left-to-right asymmetries in trabecular density or in trabecular pore size of any ROI examined, from medial-to-lateral or from dorsal-to-plantar, in the SBT or in the Greyhound (low or high raced) CTBs. When the number of trabecular pores was examined, there were no significant left-to-right asymmetries in the CTBs from SBT or low-raced Greyhounds; however, high raced Greyhounds had significantly more trabecular pores in ROI 2 of their left CTBs compared to their right CTBs ($p = 0.04$) (Table 4.1. and Figure 4.5).

Figure 4.5: Mean number of trabecular pores in the dorsal-to-plantar ROI of left (clear) and right (hatched) CTBs from high raced Greyhounds. Error bars are SEM. Significant differences between the left and right side bones are indicated by * $p < 0.05$.

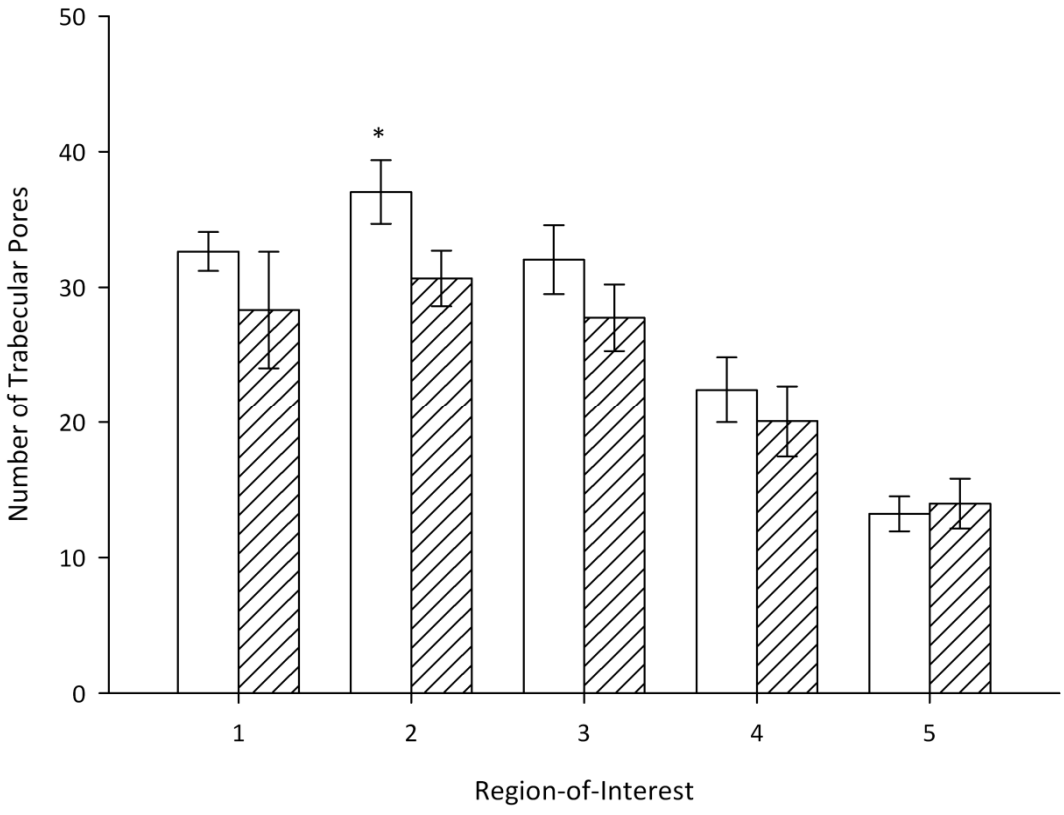

4.4.2 Breed differences in trabecular architecture (dorsal-to-plantar ROI)

Trabecular density

Trabecular density decreased across the bone from dorsal-to-plantar in CTBs from low and high raced Greyhounds, whereas it remained more or less constant across the SBT CTBs (Figure 4.6 and 4.7). Trabecular density did not differ between the low and high-raced Greyhounds in any of the dorsal-to-plantar ROI; however, both low and high raced Greyhounds had significantly lower trabecular density than SBTs in the mid-to-plantar regions of both the left (all $p \leq 0.010$) and right (all $p \leq 0.007$) CTBs (Table 4.1).

Figure 4.6: µCT images illustrating the dorsal-to-plantar changes in trabecular architecture across the Greyhound CTB and the homogenous trabecular architecture of the SBT CTB.

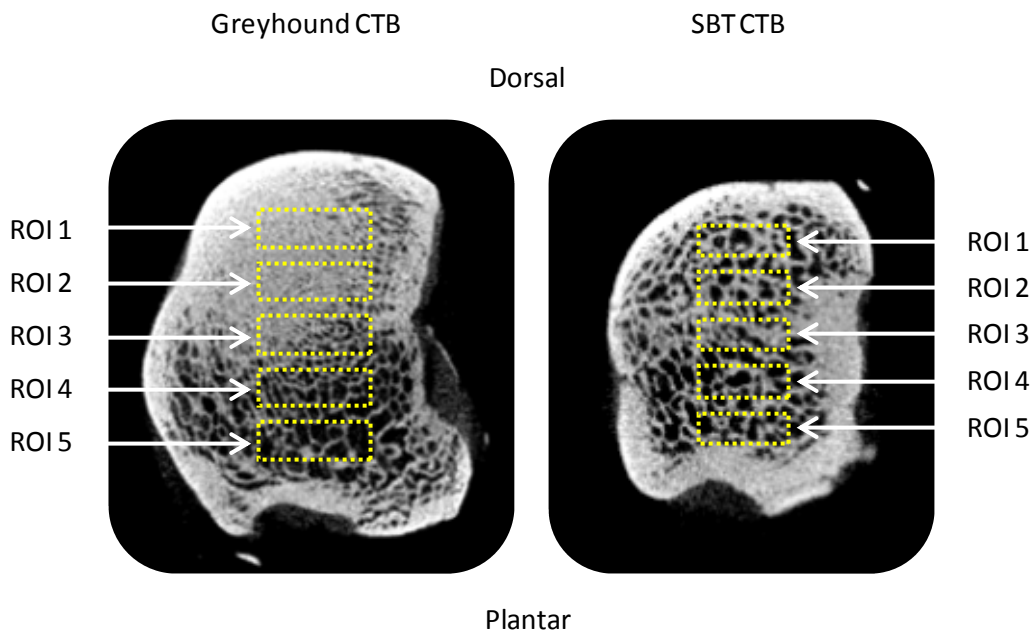

Figure 4.7: Mean trabecular density at the five dorsal-to-plantar ROI (1 = clear, 2 = dotted, 3 = hatched, 4 = light grey and 5 = dark grey) across CTBs from Greyhounds and SBTs. Error bars are SEM. Within each group of dogs, ROI that are significantly different to ROI 1 are indicated by *, to ROI 2 are indicated by ¤, and to ROI 3 are indicated by +; $p < 0.05$.

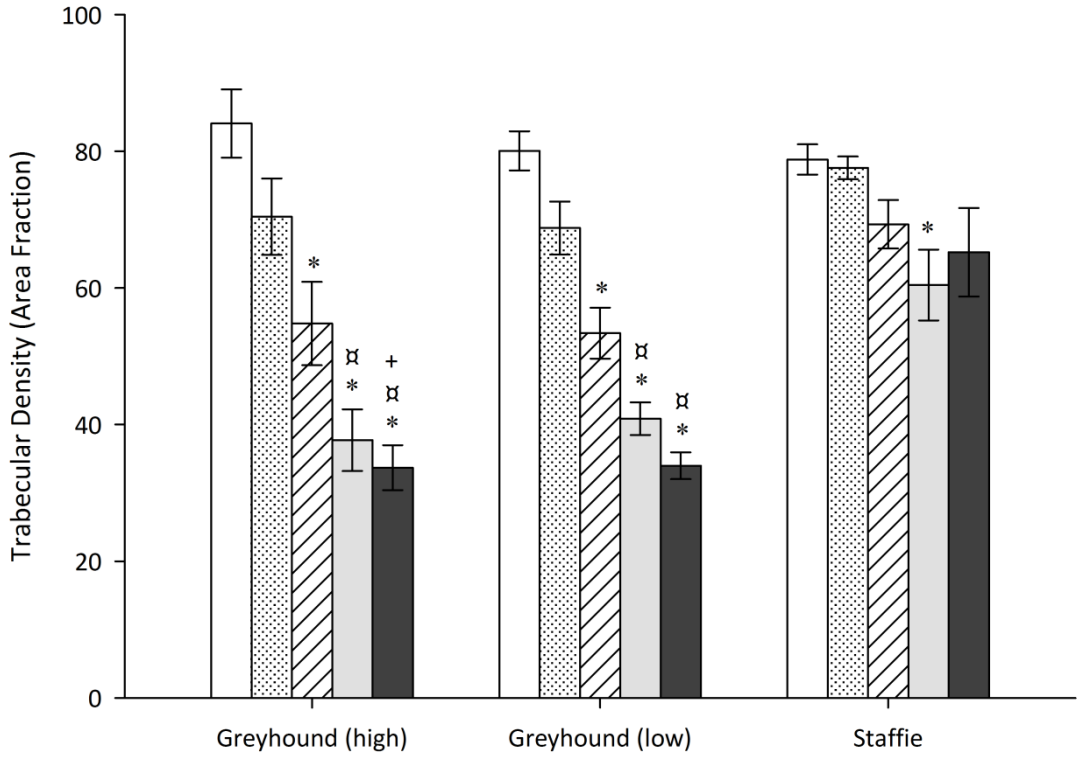

Trabecular pore number

The mean number of trabecular pores increased from ROI 1 to 2 and then decreased dramatically from ROI 2 to 5 in CTBs from low and high raced Greyhounds, whereas in SBT CTBS the number of trabecular pores gradually decreased across the bone from dorsal-to-plantar (Figure 4.6 and 4.8). The number of trabecular pores did not differ between the low and high-raced Greyhounds in any of the dorsal-to-plantar ROI; however, high raced Greyhounds had significantly more trabecular pores in ROI 1 (left CTB), 2 (left and right CTB) and 3 (left and right CTB), and low raced Greyhounds had significantly more trabecular pores in ROI 2 and 3 (left and right CTB), compared to SBT CTBs (all $p \leq 0.003$) (Table 4.1).

Figure 4.8: Mean number of trabecular pores in each of the five dorsal-to-plantar ROI (1 = clear, 2 = dotted, 3 = hatched, 4 = light grey and 5 = dark grey) across CTBs from Greyhounds and SBTs. Error bars are SEM. Within each group of dogs, ROI that are significantly different to ROI 1 are indicated by *, to ROI 2 are indicated by ¤, to ROI 3 are indicated by +, and to ROI 4 by ‡; $p < 0.05$.

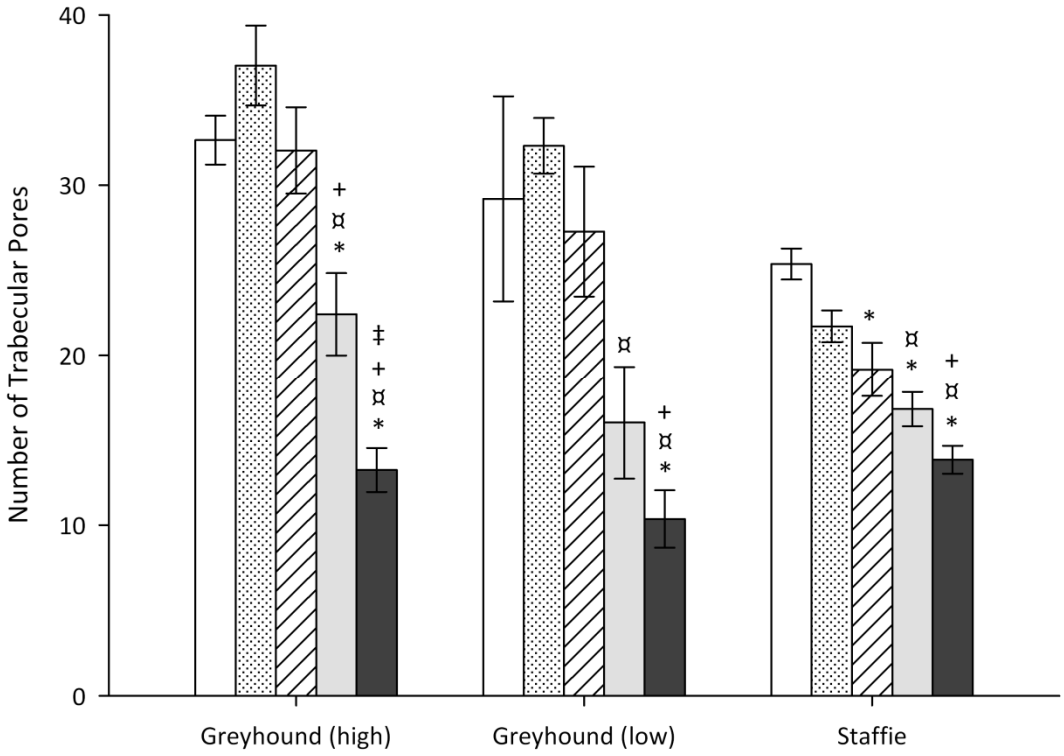

Trabecular pore size

Trabecular pore size increased dramatically across the CTBs from dorsal-to-plantar in both the low and high raced Greyhounds (Figure 4.6 and 4.9): trabecular pores were over 20 times larger in ROI 5 compared to ROI 1 in low raced Greyhounds and over 13 times larger in high raced Greyhounds. Trabecular pore size in SBT CTBs gradually increased across the bone from dorsal-to-plantar (Figure 4.6 and 4.9): pores were three times larger in ROI 5 compared to ROI 1. Trabecular pore size did not differ between the low and high raced Greyhounds in any of the dorsal-to-plantar ROI; however, trabecular pores were

significantly larger in ROI 5 of both the left and right side CTBs from both low and high raced Greyhounds compared to SBTs (all $p \leq 0.04$) (Table 4.1).

Figure 4.9: Mean trabecular pore size in each of the five dorsal-to-plantar ROI (1 = clear, 2 = dotted, 3 = hatched, 4 = light grey and 5 = dark grey) across CTBs from Greyhounds and SBTs. Error bars are SEM. Within each group of dogs, ROI that are significantly different to ROI 1 are indicated by *, to ROI 2 are indicated by ¤, to ROI 3 are indicated by +, and to ROI 4 by ‡; $p < 0.05$.

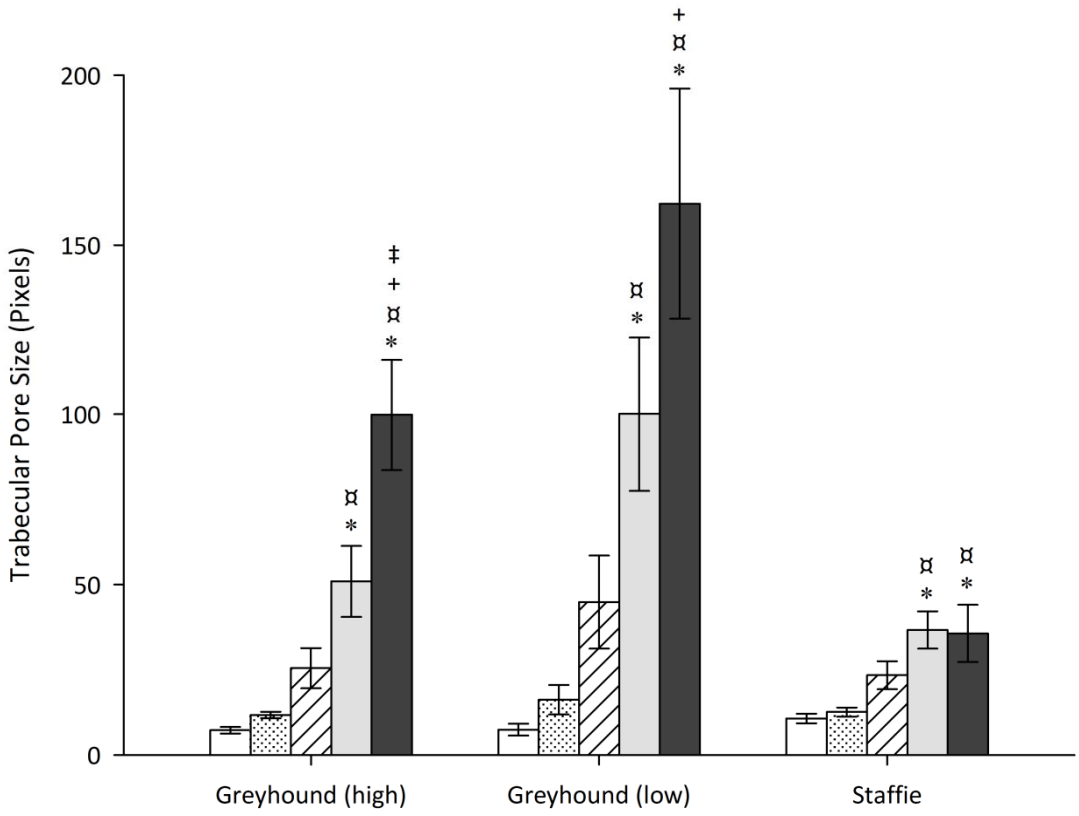

4.4.3 Breed differences in trabecular architecture (medial-to-lateral ROI)

Trabecular density

Trabecular density was not affected by the region (medial-to-lateral) of the CTB analysed in Greyhounds or SBTs, therefore, trabecular density was similar across the bones from medial-to-lateral in both breeds. Trabecular density did not differ between the low and high raced Greyhounds in any of the medial-to-lateral ROI; however, when the two breeds were compared, both groups of Greyhounds had significantly lower trabecular density than SBTs in all three ROI in the left side bones (all $p \leq 0.043$), as well as significantly lower trabecular density in ROI 7 and 8 in the right side bones (all $p \leq 0.034$) (Table 4.2).

Trabecular pore number

The number of trabecular pores was not affected by the region (medial-to-lateral) of the CTB analysed in Greyhounds or SBTs, i.e. the number of pores remained constant across the CTBs from medial-to-lateral in both breeds of dog. Trabecular pore number did not differ between the low and high raced Greyhounds in any of the medial-to-lateral ROI; however, high raced Greyhounds had significantly more trabecular pores in all three medial-to-lateral CTBs, and low raced Greyhounds had significantly more in ROI 6 and 7 compared to SBT CTBs (all $p \leq 0.035$) (Table 4.2).

Trabecular pore size

Trabecular pore size was not affected by the region (medial-to-lateral) of the CTB analysed; the pores were of a similar size across the CTBs from medial-to-lateral in both breeds. Trabecular pore size did not differ between the low and high raced Greyhounds in any of the medial-to-lateral ROI; however, trabecular pores were significantly larger in ROI 8 (right side bones) of CTBs from high raced Greyhounds compared to SBTs ($p = 0.015$) (Table 4.2).

PART B: FIFTH METACARPAL BONES

4.5 Materials and methods

4.5.1 Fifth metacarpal bone specimens

MC_5 bones were collected from five racing Greyhounds (four male, one female), euthanatised after sustaining severe injuries to the pelvic limbs. All five dogs had raced ≥ 40 times in their lifetime (range 40 to 49 races). Mean age of the dogs was 3.25 ± 0.68 years; mean weight was 33.20 ± 2.52 kg.

MC_5 bones were also collected from four SBTs (three male, one female), euthanatised at a local dogs home when extreme behavioural problems prevented re-homing. Age of the dogs was unknown; mean weight was 16.42 ± 1.37 kg.

4.5.2 µCT protocol

Examinations were performed using a BIR ACTIS µCT scanner (Actis, Bio-Imaging Research Inc., Lincolnshire, IL, USA); details can be found in section 4.3.2. MC_5 bones were scanned from the tip of the epiphysis at the proximal end to three quarters of the way down the diaphysis (Figure 4.10) to allow the areas in the MC_5 most often affected by fractures to be scanned, i.e. the proximal epiphysis to mid diaphysis (Gannon 1972; Newton and Nunamaker 1985).

Figure 4.10: Photograph showing how MC_5 bones were set up on the stage ready for µCT scanning.

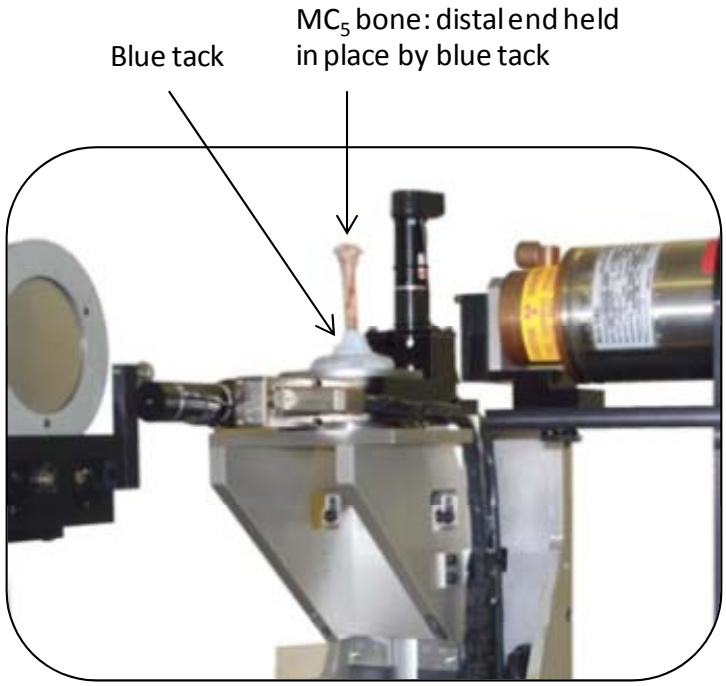

4.5.3 Image analysis

µCT images were analysed using ImageJ ver. 1.43s (National Institutes of Health, USA). Three ROI across the MC_5 epiphysis from dorsal-to-palmar were analysed (Figure 4.11). Dorsal-to-palmar ROIs were 40 x 20 pixels in Greyhound bones and 32 x 16 pixels in SBT bones. The epiphyses of the SBT MC_5 bones were approximately 64% smaller than those of Greyhounds, therefore, SBT ROI were 64% smaller than Greyhound ROI. Additionally, three ROI across the epiphysis from medial-to-lateral were analysed (Figure 4.11). Medial-to-lateral ROIs were 20 x 40 pixels in Greyhound bones and 16 x 32 pixels in SBT bones. The distribution of the dorsal-to-plantar and medial-to-lateral ROI was consistent with respect to the overall dimension of the bone: the centre of the bone slice was determined via its Cartesian coordinates and the mid-ROI was positioned around it. The other ROI were then placed relative to that ROI contiguous to one another. The mid-point of each MC_5 epiphysis was determined and 30 (contiguous) slices around this point analysed. Image-J was used to

convert the greyscale μCT images into black and white binary images. Trabecular density, trabecular pore size and trabecular pore distribution were then determined; details can be found in section 5.3.3. In addition, the average cortical thickness of the diaphysis was determined at four points around the circumference of the bone (dorsal, medial, palmar and lateral) (Figure 4.12). The width of the cortical bone was measured on five slices (each slice spaced equally along the length of the diaphysis) and the mean width calculated for each of the four points around the diaphysis.

Figure 4.11: Measurements were taken in three ROI across the MC5 epiphysis from (a) dorsal-to-palmar and (b) medial-to-lateral.

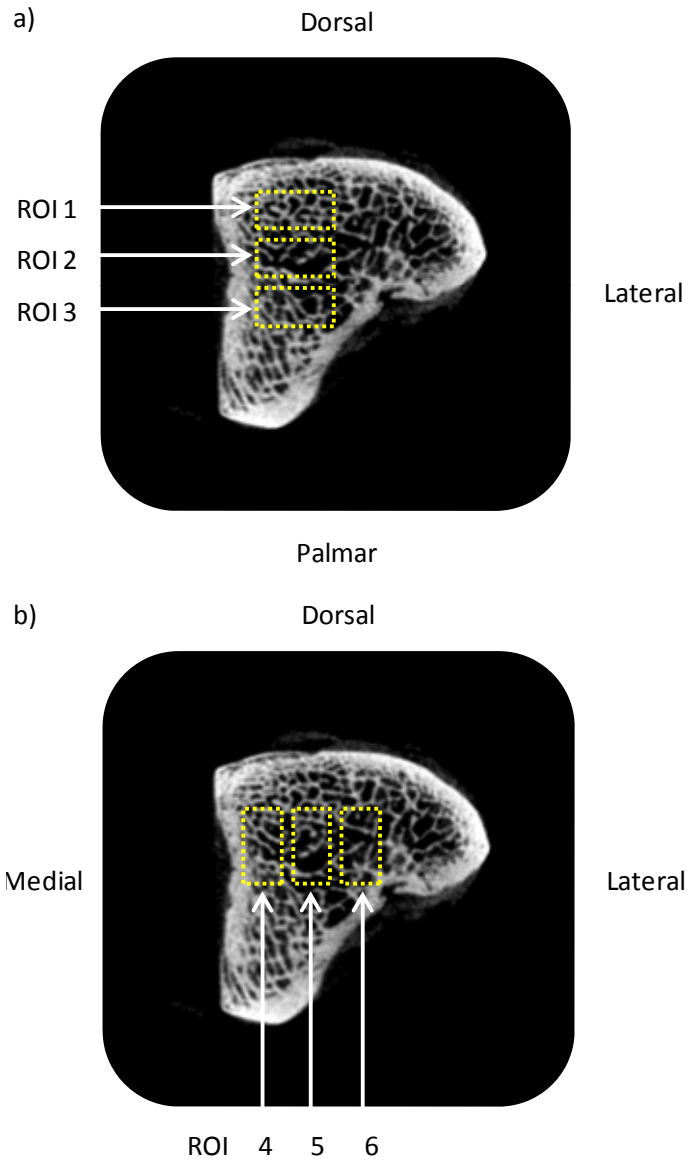

Figure 4.12: Measurements of the cortical thickness were taken at four points (dorsal, palmar, medial and lateral) around the MC_5 diaphysis.

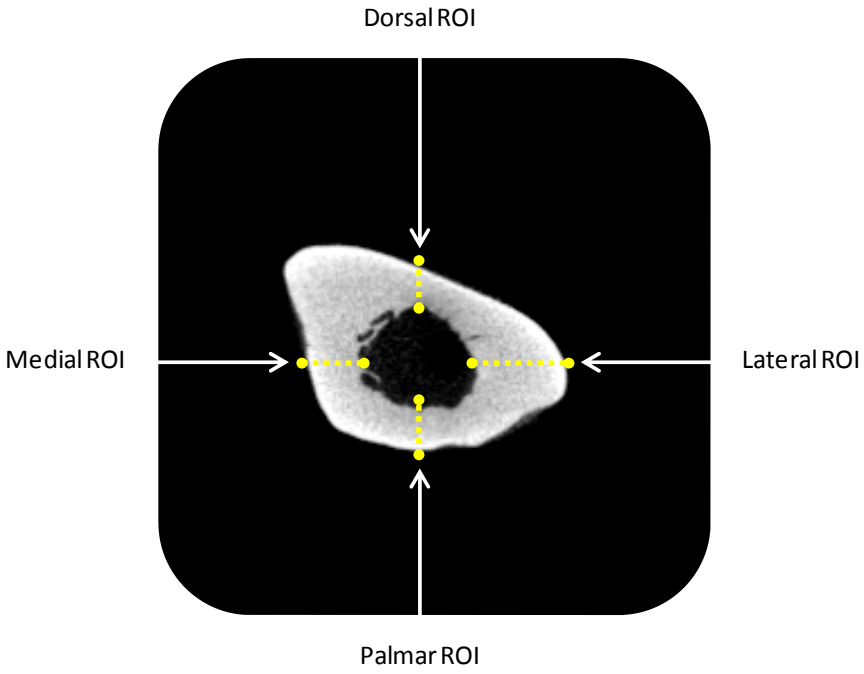

4.5.4 Statistical analysis

Mean and standard deviation were calculated for each parameter (trabecular density, trabecular pore size and the number of pores in the epiphysis, and cortical thickness in the diaphysis). The effect of side (left versus right) on each parameter for each ROI was examined using the two-tailed paired t-test. Differences between Greyhounds and SBTs on each parameter for each ROI were examined using the two-tailed un-paired t-test. A one-way ANOVA with a post-hoc Tukey's test was used to determine the effect of ROI (MC_5: ROI 1 to 3 [1 = dorsal, 3 = palmar] and 4 to 6 [4 = medial, 6 = lateral]) on each parameter. Differences were considered significant at $p < 0.05$.

4.6 Results

Trabecular architecture data for the three dorsal-to-plantar ROI and the three medial-to-lateral ROI across the MC_5 epiphysis can be found in Table 4.3 and Table 4.4 respectively.

Table 4.3: Trabecular architecture data for the three dorsal-to-plantar ROI in the CTBs: mean (SEM) trabecular density, trabecular pore size and trabecular pore number. † denotes a significant difference between the left and right limbs of a breed; $p<0.05$. * denotes a significant difference between the Greyhounds and SBTs; $p < 0.05$.

ROI	Side	Trabecular density (area fraction)	Trabecular pore number	Trabecular pore size (pixels)
Greyhounds				
1	Left	62.9 (4.6) †*	14.8 (1.1) *	20.4 (5.1) †*
	Right	48.8 (4.8) †*	13.5 (1.9) *	28.6 (4.1) †*
2	Left	38.8 (2.7) †*	9.0 (1.4) *	72.8 (19.0) *
	Right	34.7 (2.0) †*	7.3 (0.9) *	88.4 (11.5) *
3	Left	32.4 (1.9) *	6.9 (0.4) *	93.6 (7.0) **
	Right	33.0 (1.8) *	6.0 (0.4) *	98.0 (7.6) **
SBTs				
1	Left	78.1 (3.9) *	10.7 (0.6) *	14.7 (2.1) *
	Right	77.7 (4.5) *	10.3 (0.3) * *	15.1 (2.0) *
2	Left	47.5 (5.6) *	6.8 (0.6) *	64.6 (11.0) *
	Right	48.5 (2.1) *	6.2 (0.7) *	64.4 (12.3) *
3	Left	58.2 (2.0) *	7.8 (0.8) *	36.1 (5.2) *
	Right	57.4 (2.2) *	7.2 (0.7) *	40.9 (6.0) *

Table 4.4: Trabecular architecture data for the three medial-to-lateral ROI in the CTBs: mean (SEM) trabecular density, trabecular pore size and trabecular pore number. † denotes a significant difference between the left and right limbs of a breed; p<0.05. * denotes a significant difference between the Greyhounds and SBTs; p < 0.05.

ROI	Side	Trabecular density (area fraction)	Trabecular pore number	Trabecular pore size (pixels)
Greyhounds				
6	Left	49.9 (3.2) *	13.2 (0.7) †*	31.9 (4.1) **
	Right	43.0 (1.1) *	10.9 (0.8) †*	40.0 (1.0) **
7	Left	32.7 (2.3) *	7.1 (1.1) *	104.9 (24.6) *
	Right	31.5 (1.7) *	6.2 (0.6) *	103.8 (8.0) **
8	Left	37.5 (1.4) *	6.9 (0.8) *	86.8 (19.2) *
	Right	39.8 (1.3) *	6.3 (0.5) *	90.5 (14.5) *
SBTs				
6	Left	63.8 (5.2) *	10.6 (0.7) *	23.8 (2.8) *
	Right	63.3 (3.6) *	9.4 (0.7) *	27.3 (4.6) *
7	Left	47.0 (3.7) *	5.7 (0.8) *	73.3 (18.7) *
	Right	49.8 (1.7) *	6.1 (0.7) *	62.7 (10.6) *
8	Left	64.1 (3.1) *	6.2 (0.5) *	46.7 (4.8) *
	Right	61.2 (3.6) *	5.4 (0.1) *	51.1 (1.8) *

4.6.1 Left-to-right asymmetries in trabecular architecture (MC_5 epiphysis)

There were no left-to-right asymmetries in trabecular architecture of the SBT MC_5 bones; however, when the Greyhound bones were analysed the left MC_5 bones had significantly higher trabecular density compared to the right MC_5 bones in ROI 1 (dorsal region) ($p < 0.001$) and 2 (mid region) ($p = 0.014$) (Figure 4.13 and Table 4.3). Additionally, the epiphysis of the left MC_5 bones from Greyhounds had significantly more trabecular pores in ROI 4 (medial region) compared to the right MC_5 ($p = 0.017$) and trabecular pores were

significantly smaller in ROI 1 (dorsal region) in the left MC_5 epiphysis compared to the right ($p = 0.026$) (Figure 4.13 and Table 3.3).

Figure 4.13: µCT images illustrating the differences (a) dorsal-to-palmar and (b) medial-to-lateral across the left and right epiphyses of Greyhound MC_5 bones.

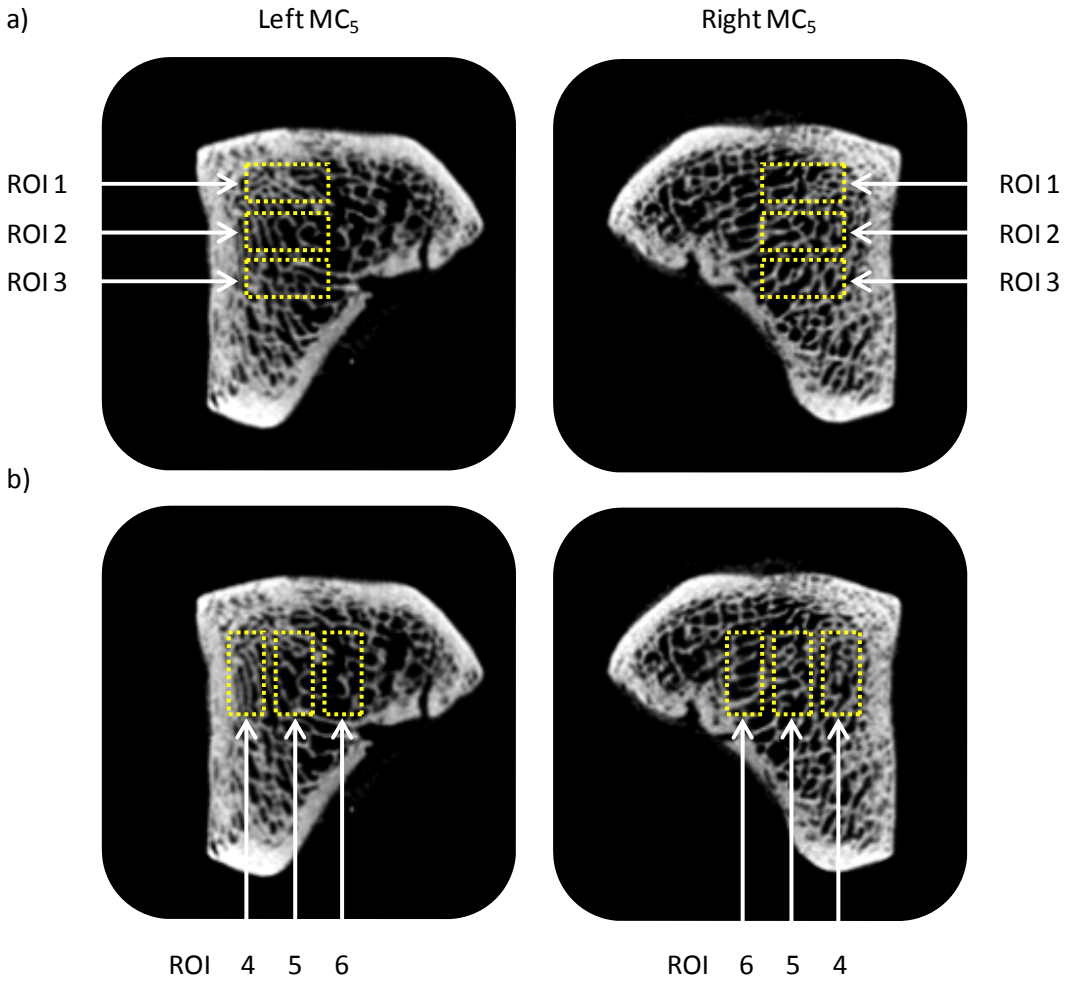

4.6.2 Breed differences in trabecular architecture (dorsal-to-palmar ROI; MC_5 epiphysis)

Trabecular density

The ROI examined had a significant effect on trabecular density: in both Greyhounds and SBTs trabecular density significantly decreased across the bone from dorsal-to-palmar (Figure 4.14 and 4.15). Trabecular density was significantly lower in Greyhound MC_5 bones

compared to SBT bones across all three dorsal-to-palmar ROI in the right side bones (all $p \leq 0.003$) and in ROI 1 and 3 in the left side bones (all $p \leq 0.046$) (Table 3.3).

Figure 4.14: µCT images illustrating the dorsal-to-palmar changes in trabecular architecture across the epiphysis of the Greyhound and SBT MC_5 bones.

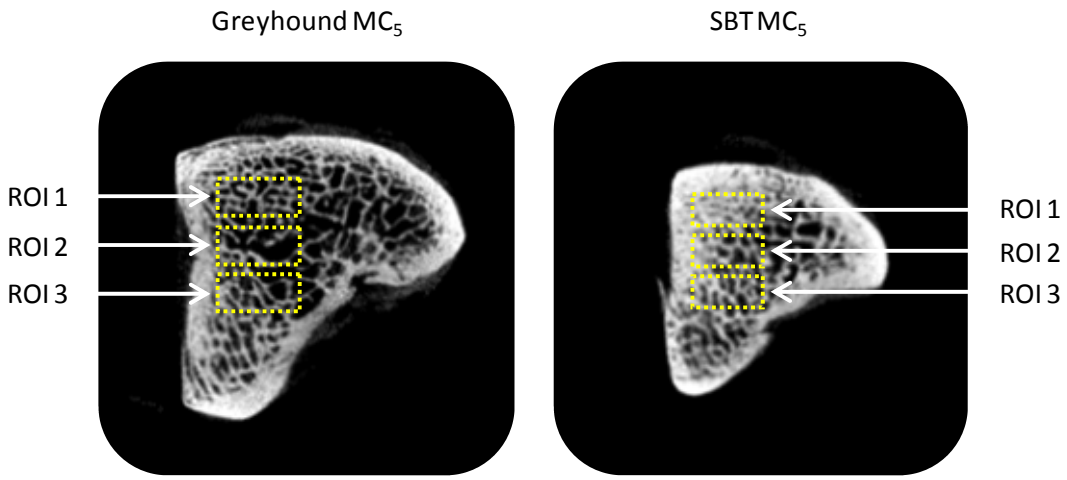

Figure 4.15: Mean trabecular density at the three dorsal-to-palmar ROI (1 = clear, 2 = dotted, 3 = hatched) across the epiphysis of MC_5 bones from Greyhounds and SBTs. Error bars are SEM. Within each group of dogs, ROI that are significantly different to ROI 1 are indicated by *, to ROI 2 are indicated by ¤, to ROI 3 are indicated by +; $p < 0.05$.

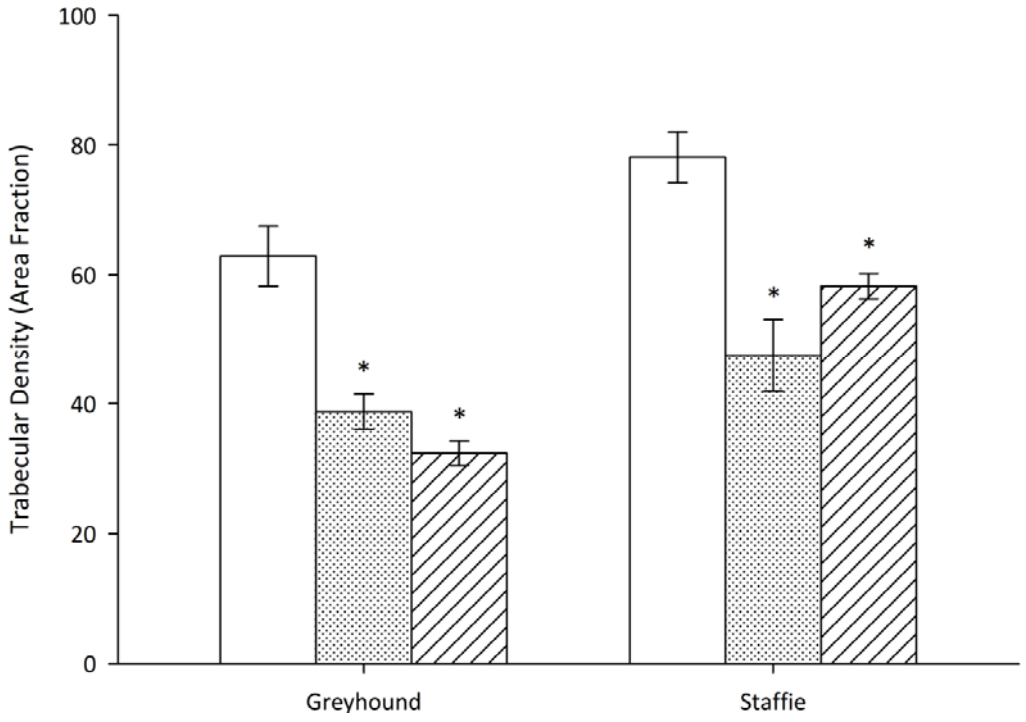

Trabecular pore number

The mean number of trabecular pores significantly decreases across the bone from dorsal-to-palmar in racing Greyhound whereas in SBT MC_5 bones the number of pores significantly decreases from ROI 1 to 2 and then increases again to ROI 3 (Figure 4.16). The epiphysis of the left side Greyhound MC_5 bones had significantly more trabecular pores present in ROI 1 (dorsal region) compared to SBT bones ($p = 0.019$) (Table 3.3).

Figure 4.16: Mean number of trabecular pores in each of the three dorsal-to-palmar ROI (1 = clear, 2 = dotted, 3 = hatched) across the epiphysis of MC_5 bones from Greyhounds and SBTs. Error bars are s SEM. Within each group of dogs, ROI that are significantly different to ROI 1 are indicated by *, to ROI 2 are indicated by ¤, to ROI 3 are indicated by +; $p < 0.05$.

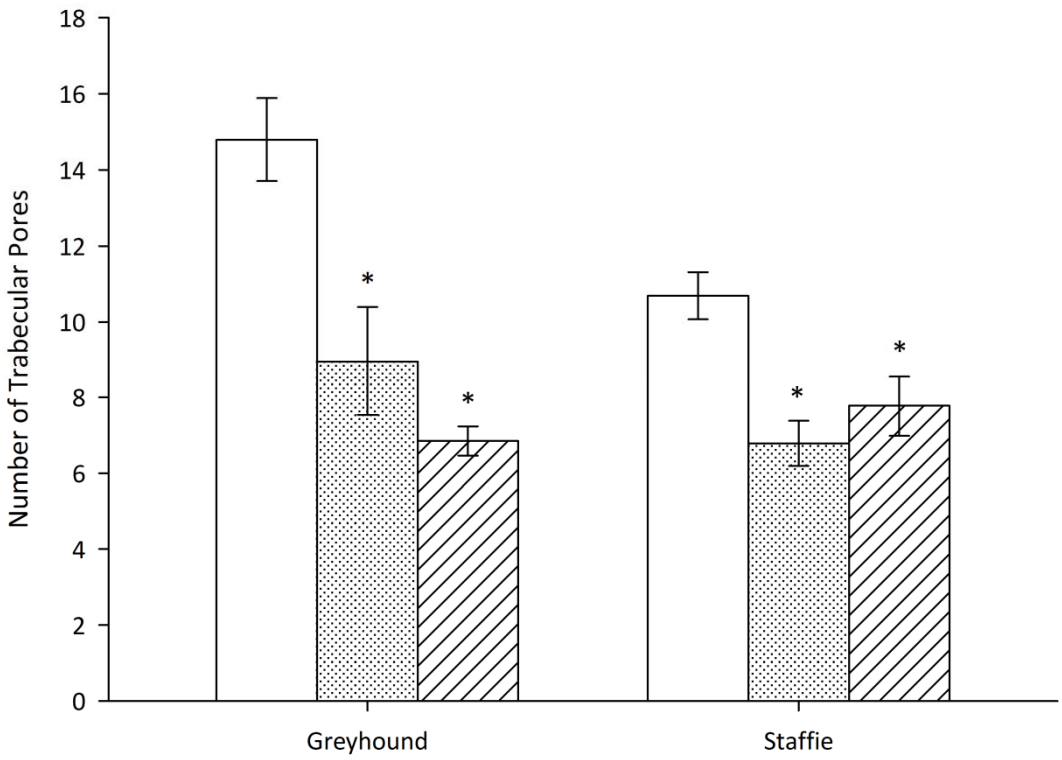

Trabecular pore size

Trabecular pore size increased dramatically from dorsal-to-palmar across the Greyhound MC_5 epiphysis (Figure 4.17): pores were over four times larger in ROI 3 compared to ROI 1. Trabecular pores significantly increased from ROI 1 to 2 and then decreased in size from ROI 2 to 3 in SBT MC_5 bones (Figure 4.17). Trabecular pores were significantly larger in ROI 1 (right side) and 3 (left and right side) of the MC_5 epiphysis in bones from Greyhounds compared to SBTs (all $p \leq 0.029$) (Table 3.3).

Figure 4.17: Mean trabecular pore size in each of the three dorsal-to-palmar ROI (1 = clear, 2 = dotted, 3 = hatched) across the epiphysis of the MC_5 bones from Greyhounds and SBTs. Error bars are SEM. Within each group of dogs, ROI that are significantly different to ROI 1 are indicated by *, to ROI 2 are indicated by ¤, to ROI 3 are indicated by +; $p < 0.05$.

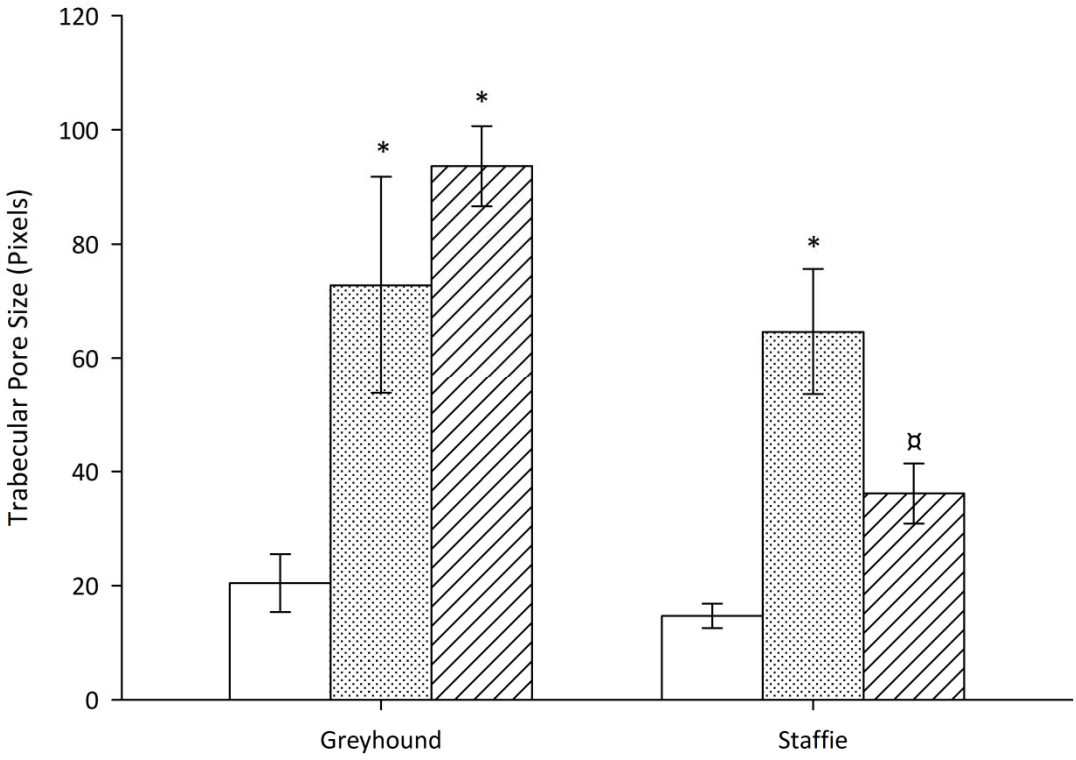

4.6.3 Breed differences in trabecular architecture (medial-to-lateral ROI; MC_5 epiphysis)

Trabecular density

The ROI examined had a significant effect on trabecular density: in both Greyhounds and SBTs trabecular density significantly decreased across the bone from ROI 4 (medial region) to ROI 5, and then increased from ROI 5 to 6 (lateral region) (Figure 4.18). Trabecular density was significantly lower in Greyhound MC_5 bones compared to SBT bones across all three medial-to-lateral ROI in both the left and right side bones (all $p \leq 0.048$) (Table 4.4).

Figure 4.18: Mean trabecular density at the three medial-to-lateral ROI (4 = clear, 5 = dotted, 6 = hatched) across the epiphysis of MC_5 bones from Greyhounds and SBTs. Error bars are SEM. Within each group of dogs, ROI that are significantly different to ROI 4 are indicated by *, to ROI 5 are indicated by ¤, to ROI 6 are indicated by +; $p < 0.05$.

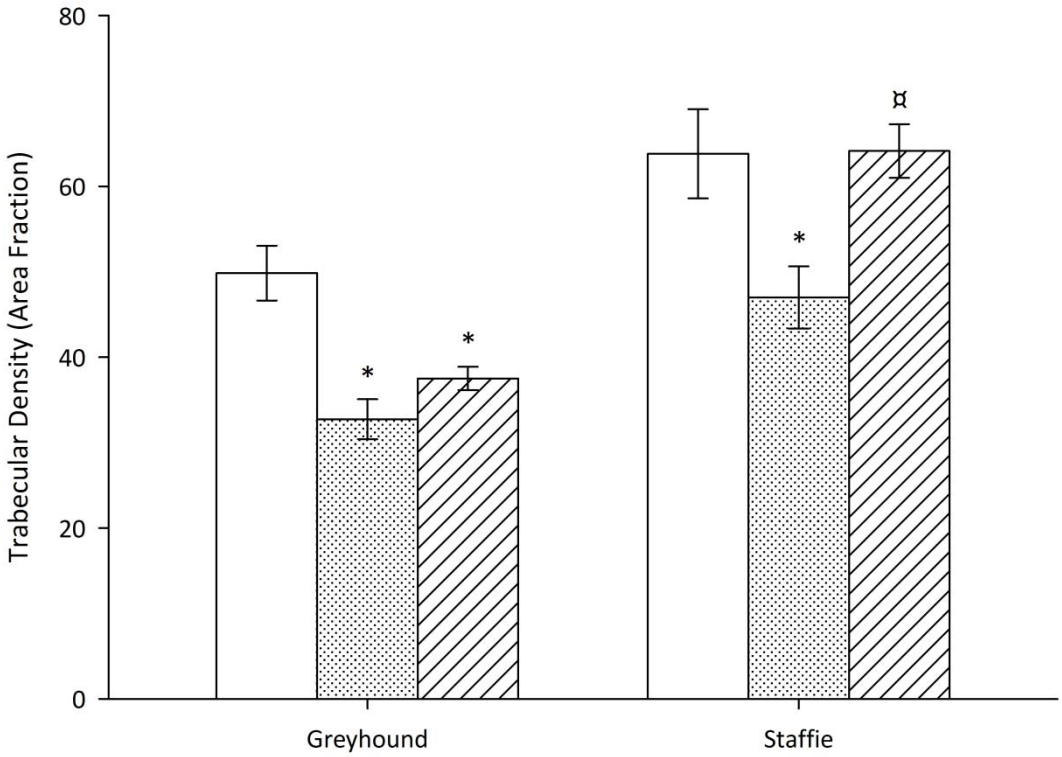

Trabecular pore number

The mean number of trabecular pores significantly decreases across the bone from medial-to-lateral in both breeds (Figure 4.19). The epiphysis of the left side Greyhound MC_5 bones had significantly more trabecular pores present in ROI 4 (medial region) compared to SBT bones ($p = 0.032$) (Table 4.4).

Figure 4.19: Mean number of trabecular pores in each of the three medial-to-lateral ROI (4 = clear, 5 = dotted, 6 = hatched) across the epiphysis of MC_5 bones from Greyhounds and SBTs. Error bars are SEM. Within each group of dogs, ROI that are significantly different to ROI 4 are indicated by *, to ROI 5 are indicated by ¤, to ROI 6 are indicated by +; $p < 0.05$.

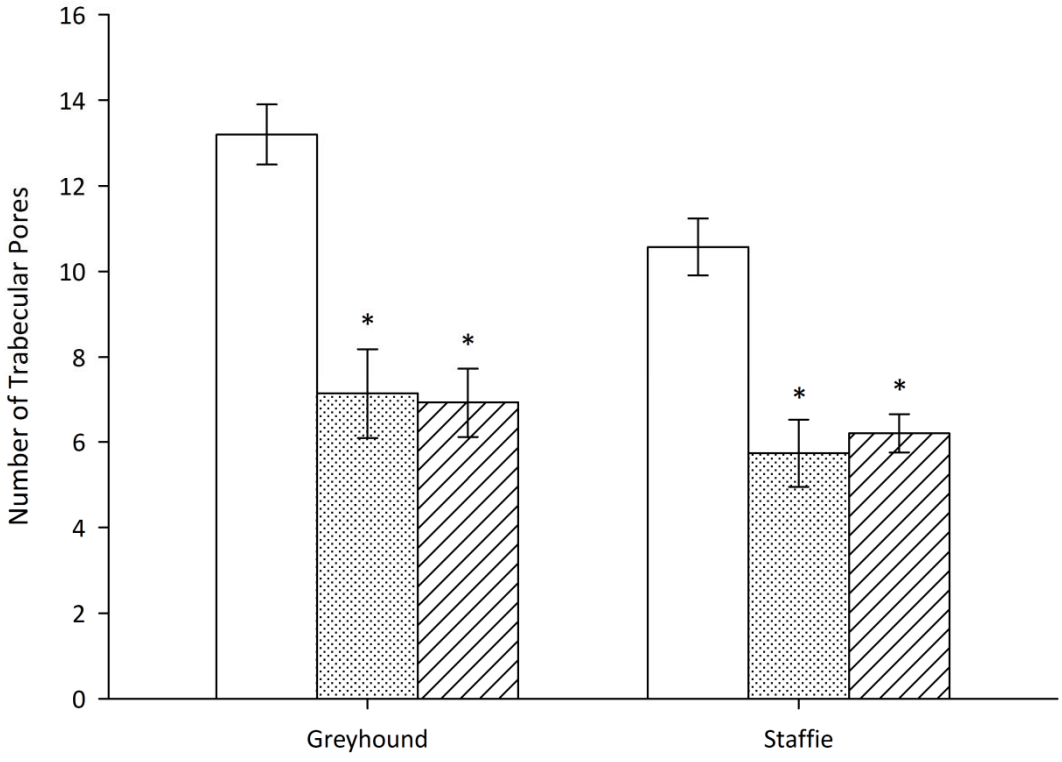

Trabecular pore size

Trabecular pore size significantly increased from ROI 4 to 5 in both breeds and then remained similar from ROI 5 to 6 (Figure 4.20). Trabecular pores were significantly larger in the epiphysis of the right side Greyhound MC_5 bones in all three of the medial-to-lateral ROI when compared to SBTs (all $p \leq 0.048$) (Table 4.4).

Figure 4.20: Mean trabecular pore size in each of the three medial-to-lateral ROI (4 = clear, 5 = dotted, 6 = hatched) across the epiphysis of MC_5 bones from Greyhounds and SBTs. Error bars are SEM. Within each group of dogs, ROI that are significantly different to ROI 4 are indicated by *, to ROI 5 are indicated by ¤, to ROI 6 are indicated by +; $p < 0.05$.

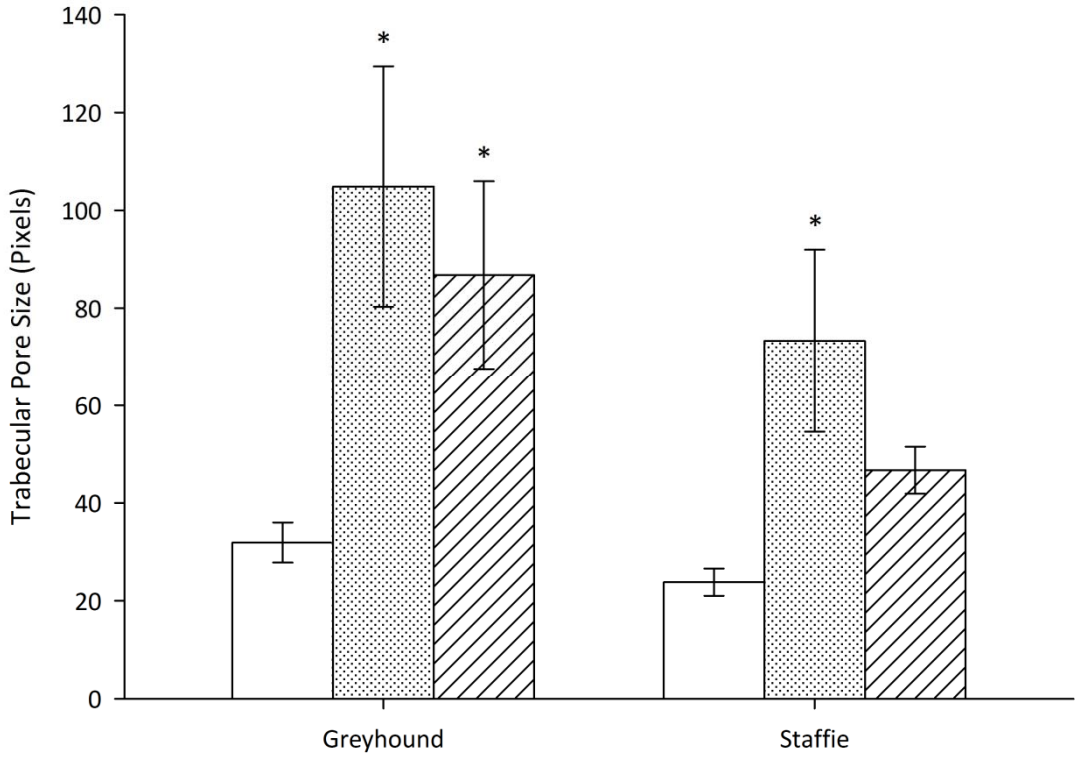

4.6.4 Cortical thickness of the MC_5 diaphysis

There were no asymmetries in cortical thickness in the SBT MC_5 bones; however, when Greyhound bones were analysed, cortical bone was significantly thicker in the left MC_5 compared to the right at all four of the ROI around the MC_5 diaphysis (all $p \leq 0.034$) (Figure 4.21).

Figure 4.21: Mean cortical thickness at each ROI around the MC_5 diaphysis in the left (clear) and right (hatched) diaphysis of MC_5 bones from racing Greyhounds. Error bars are SEM. Significant differences between the left and right side bones are indicated by * $p < 0.05$.

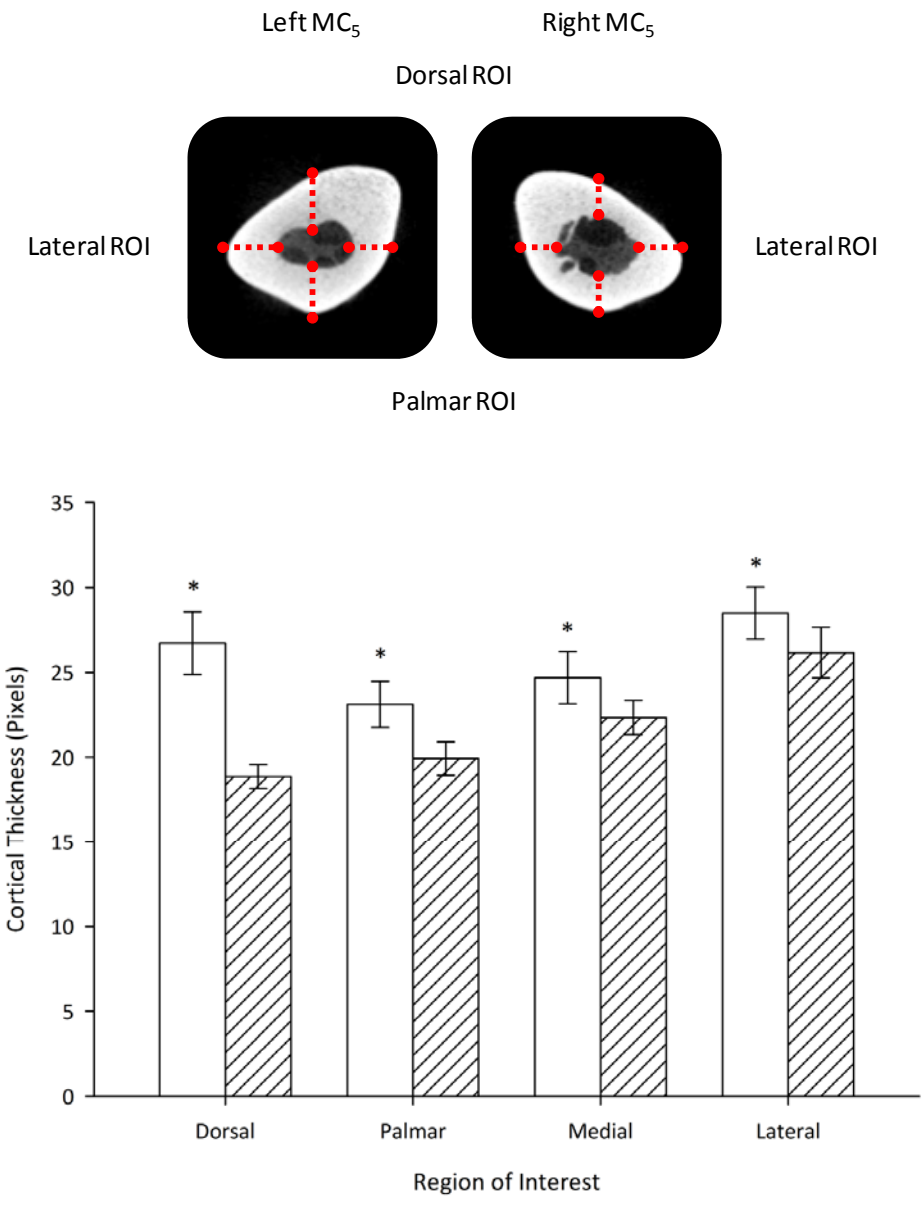

4.7 Discussion

The mechanical properties of bone are influenced by its internal architecture (Kleerekoper *et al.* 1985; Parfitt 1992), and in long bones, by cortical diameter and thickness (Jones *et al.* 1977; McCarthy and Jeffcott 1992; Nunamaker *et al.* 1989; Woo *et al.* 1981b). Mechanical loading due to exercise leads to increases in trabecular bone mass, primarily via increases in trabecular thickness (Firth *et al.* 1999; Firth *et al.* 2000; Gabriel *et al.* 1998; Holy and Zerath 2000; Notomi *et al.* 2000; Notomi *et al.* 2001) which results in increased stiffness of bone (Schaffler and Burr 1988). Increases in cortical thickness and cross sectional area occur in response to increased exercise and training (Jones *et al.* 1977; McCarthy and Jeffcott 1992; Nunamaker *et al.* 1989; Woo *et al.* 1981b) which increases bone strength.

4.7.1 Left-to-right asymmetries in bone architecture

Greyhound CTB

We showed that Greyhounds have increased total bone mineral density (BMD) in their right CTBs compared to their left CTBs in Chapter 3; however, when we examined the trabecular architecture of the CTB using µCT we found no significant left-to-right asymmetries in the trabecular density (measured as the percentage of the ROI occupied by bony trabeculae). Both the left and right side CTBs had a similar dorsal-to-plantar decrease in trabecular density and increase in trabecular porosity. The CTB is a cuboidal bone primarily composed of trabecular bone surrounded by an outer thin layer of compact bone and Greyhound CTBs consist of both remodelled cortical bone and remodelled inner trabecular bone (Muir *et al.* 1999). Johnson *et al.* (2000) reported the dorsal cortex of the right CTB was apparently thickened due to apposition of new lamellar bone on the outer periosteal surface in addition to thickening and compaction of trabeculae in deeper layers. We only looked at the trabecular bone of the CTB; we did not look at the thickness of surrounding compact

bone. Therefore, we are uncertain whether the left-to-right asymmetries in BMD that we observed in Chapter 4 resulted from increased formation of bone on the outer surface of the cortex of right side CTBs or increased trabecular density.

Greyhound MC_5 (epiphysis)

The epiphysis of the left Greyhound MC_5 bone had increased trabecular density and decreased trabecular pore size in the dorsal region and smaller pores in the medial region compared to the contralateral bone (Table 4.3 and 4.4). Increases in trabecular density and decreases in porosity are adaptive responses to increased loading. Studies on rats show mechanical loading of bone due to exercise increases trabecular bone mass which increases bone strength (Holy and Zerath 2000; Notomi *et al.* 2000; Notomi *et al.* 2001). Therefore, the increased trabecular density and reduced trabecular porosity in the dorso-medial regions of the left MC_5 epiphysis suggest these regions are subjected to higher stresses than the contralateral bone which then results in increased adaptive remodelling.

Greyhound MC_5 (diaphysis)

It is thought that the distal limbs of Greyhounds experience asymmetric stresses during racing with greater stresses imposed on those bones that are the closest to the inside rail of the track. Indirect evidence for this is provided by measurement of BMD. We found the rail-side bones have increased BMD compared to the contralateral bones (Chapter 3) and the greatest asymmetry in BMD was in the MC_5 bones, with increased BMD observed in the left side bone. These findings are consistent with previous studies by Emmerson *et al.* (2000) and Lipscomb *et al.* (2001) that showed the left MC_5 bones had significantly increased density compared to the right MC_5 bones. Greyhounds usually fracture metacarpal bones at the approximate junction of the proximal and middle one third of the bones (Dee and Dee 1985). Therefore, we decided to determine cortical thickness at specific points around the

cortex in the proximal half of the MC_5 diaphysis. We found that Greyhound left limb MC_5 bones had increased cortical thickness at all points measured around the diaphysis (dorsal, palmar, medial and lateral) compared to the right MC_5 (Figure 4.21). Increased cortical thickness occurs in response to the increased mechanical loading imposed on bone during exercise (Jones *et al.* 1977; McCarthy and Jeffcott 1992; Nunamaker *et al.* 1989; Woo *et al.* 1981b), therefore our data provides further evidence that the left MC_5 is subjected to higher stresses than the contralateral bone which leads to increased bone deposition.

4.7.2 Regional differences in trabecular architecture

Regional differences in trabecular architecture have previously been described in the carpal bones of Thoroughbred horses (Firth *et al.* 1999; Firth *et al.* 2000). The dorsal region of the third and radial carpal bones from Thoroughbred horses had increased trabecular thickness and density compared to the palmar region. This dorsal-to-palmar difference was increased when horses were subjected to a high intensity treadmill exercise program (Firth *et al.* 1999). Similarly, race-trained Thoroughbred horses had increased density in the dorsal aspect of the third and radial carpal bones when compared to un-exercised controls, whereas no differences were observed between the two groups of horses in the palmar aspect of the bones (Firth *et al.* 2000). Regional differences in trabecular architecture have also been found in the CTB of racing Greyhounds (Johnson *et al.* 2000; Muir *et al.* 1999). Muir *et al.* (1999) observed thickening and coalescence of the trabeculae in the dorsal and medial regions of both left and right CTBs, while Johnson *et al.* (2000) reported trabeculae in the dorsal region of right CTBs were thickened and compacted compared to contralateral bones. We found that the internal architecture of Greyhound CTBs was more heterogeneous than that of SBT bones. While Greyhound CTBs had a distinct dorsal-to-plantar decrease in trabecular density, a decrease in trabecular pore number and an increase in trabecular pore size, the SBT CTBs had a homogenous trabecular structure

across the entire bone (Figure 4.6 and 4.7). When the MC_5 epiphyses were examined, both breeds were found to have regional differences in trabecular architecture but the trabecular architecture of Greyhound bones was more heterogeneous than that of the SBT (Figure 4.14 and 4.15). Both breeds had significantly lower trabecular density in the middle and plantar regions compared to the rest of the epiphysis; however, while SBTs bones were more porous (higher numbers of trabecular pores and larger pore sizes) in the middle and lateral regions of the epiphysis, Greyhounds also had increased porosity in the palmar region. The increased trabecular density in the dorsal region of the Greyhound CTB appears to result from thickening and coalescence of trabecular bone into compact bone (Johnson *et al.* 2000; Muir *et al.* 1999), presumably as a result of this region experiencing higher stresses compared to the rest of the bone. Increased porosity, indicated by the very large pores in the plantar region of the Greyhound CTBs, could result from increased bone resorption in this region possibly as a result of this region experiencing lower stresses compared to the rest of the bone. In trotting dogs, peak vertical ground reaction force occurs about mid-stance. At this point the fore-aft force becomes positive (becomes an acceleration) and peaks at around 70% of the stance phase resulting in a forwardly-directed force (Ritter *et al.* 2001). Therefore, the dorsal regions of the limbs would experience higher forces during stance than the palmar/plantar regions and hence the dorsal regions of the bones would experience higher forces resulting in the adaptive remodelling seen in these areas. Information about how each area of the bone is loaded during galloping would help with understanding why some regions of the CTB and MC_5 epiphysis have increased resorption taking place while other regions have adaptive thickening of the trabeculae.

4.7.3 Breed differences in trabecular architecture

Trabecular density was similar in the dorsal region but significantly lower in the plantar region of Greyhound CTBs compared to SBTs (Table 4.1). Greyhound CTBs had a greater

number of pores across the majority of the bones and the trabecular pores in the plantar region were over three times as large as those in SBTs. When the MC_5 epiphyses were examined, Greyhounds had significantly lower trabecular density in all areas of the epiphysis and they had increased porosity compared to SBTs (Table 4.3 and 4.4). While these differences in trabecular architecture could result from intrinsic breed differences, previous studies of the carpal bones of Thoroughbred horses found adaptive changes in the trabecular structure of those subjected to high intensity exercise compared to un-exercised controls (Firth *et al.* 1999; Firth *et al.* 2000). Both the exercised and control horses were of the same breed, suggesting that the differences in trabecular structure were a result of the intensity of exercise. Additionally, Johnson *et al.* (2000) found that these adaptive changes were less apparent in Greyhounds that had been retired for several months compared to the CTBs of Greyhounds that had been racing up until they were euthanatised. Therefore, the differences in the trabecular structure of bones from Greyhounds and SBTs are most likely a result of the stresses of racing.

Examination of the trabecular structure from medial-to-lateral across the CTBs was confounded by the dorsal-to-plantar changes in architecture seen in the Greyhounds. The CTB is an irregularly shaped cuboidal bone and the shape varies between Greyhounds and SBTs (Figure 4.22). Each ROI was positioned in the center of the CTB to allow comparison of the trabecular architecture from medial-to-lateral; however, in Greyhounds this is the point where trabecular density and pore distribution changed from dorsal-to-plantar. Therefore, each medial-to-lateral ROI had an area of high trabecular density where trabecular pores were small and an area of low trabecular density where the pores were very large (Figure 4.23).

Figure 4.22: µCT scans showing how the two breeds of dog differ in the shape of their CTB bones.

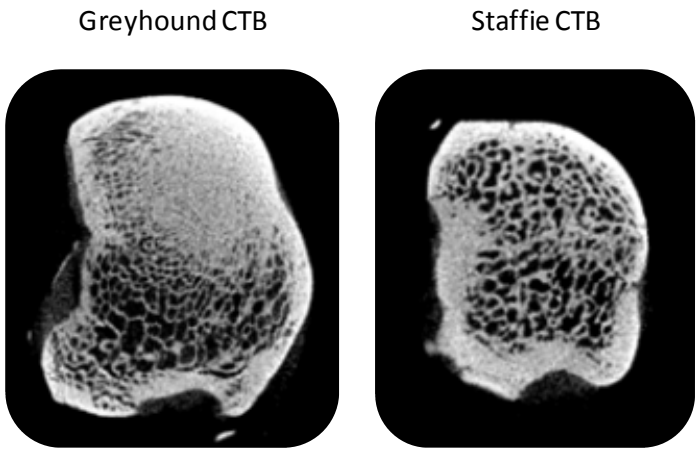

Figure 4.23: The three medial-to-lateral ROI. The approximate area where trabecular density and pore distribution changed from dorsal-to-plantar can be seen in the middle of each ROI; indicated by the dashed white line.

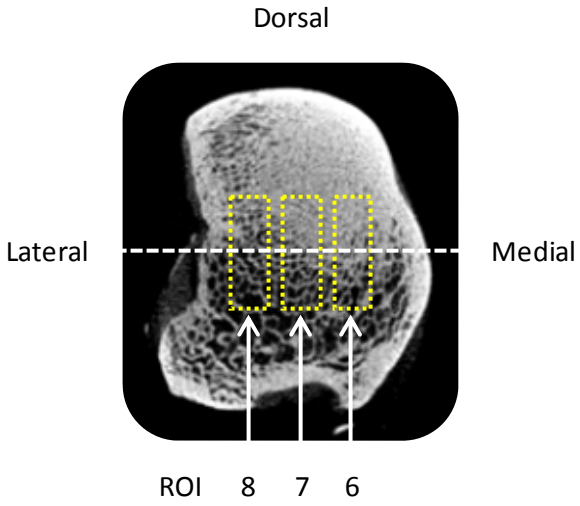

4.7.4 Fatigue fractures in Greyhounds

Racing Greyhounds are prone to fatigue fractures of the central tarsal bone (CTB) and metacarpal bones (Devas 1961; Gannon 1972). Evaluation of fractured CTBs reveals that catastrophic failure occurs via the accumulation and coalescence of micro-cracks through remodelled bone (Johnson *et al.* 2000; Muir *et al.* 1999; Tomlin *et al.* 2000). The dorsal (Johnson *et al.* 2000; Muir *et al.* 1999) and medial (Muir *et al.* 1999) regions of the CTB are heavily remodelled. Johnson *et al.* (2000) reported this adaptive bone remodelling occurs in regions of the CTB frequently affected by fracture. The majority of CTB fractures sustained by racing Greyhounds are type IV (Boudrieau *et al.* 1984), as classified by Dee *et al.* (1976). Type IV fractures result in two major fracture lines through the dorsal and mid regions of the CTB causing one slab of bone to be displaced medially and one to be displaced dorsally (Figure 4.24); however, in Chapter 3, we showed that all the Greyhounds used in our study had sustained type V fractures (severely comminuted and displaced).

Figure 4.24: Type IV central tarsal bone fracture as classified by Dee *et al.* (1976). Dashed lines represent fracture lines and arrows denote the direction the bone fragments are displaced.

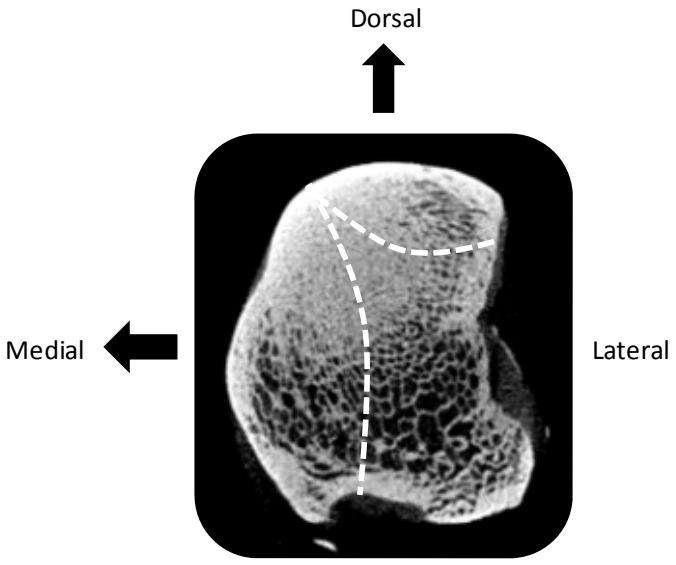

Most of these CTBs have several main fracture lines which, unlike the results presented by Johnson *et al.* (2000), appear to propagate through the region of the bone where, on our μCT scans, the trabecular architecture changes from high trabecular density and low porosity to low trabecular density and high porosity (Figure 4.25). This suggests that the area where the trabecular architecture changes is mechanically weaker, possibly due to changing material properties at this point, although destructive testing of the bones would be required to determine this.

Figure 4.25: Representative CT slices of six of the fractured CTBs used in Chapter 3. The major fracture lines can be seen to run through the dorsal region and the middle region of the bones. There were 14 Greyhounds with a fractured CTB and all were extremely comminuted; on 12 of the scans main fracture lines similar to those below were visible, the other two bones were so fragmented it was difficult to tell which the main fracture lines were.

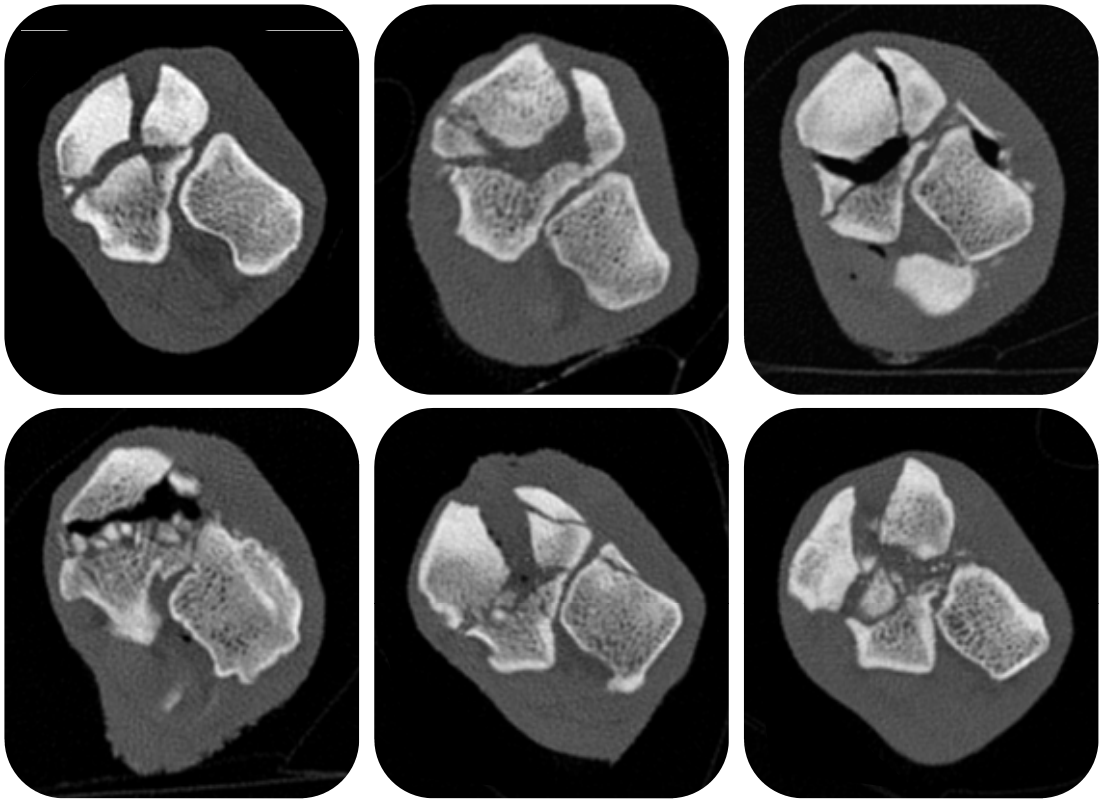

The reasons why the right CTB fractures while the left side bone does not is unclear as both left and right bones showed this regional difference in trabecular architecture. It could be that the right CTB has additional micro-damage targeted remodelling going on in the surrounding cortical bone.

Similarly, the reasons why some Greyhounds fracture their left MC_5 bones is not clear as the cortex was thickened around the entire diaphysis. Cortical bone at the mid-diaphysis region of MC_5 is heavily remodelled in Greyhounds, especially in the left limb (Johnson *et al.* 2001) and increased bone remodelling is stimulated by the formation of micro-damage (Burr 1993; Lee *et al.* 2002). Structural failure of Greyhound CTBs results from an imbalance in the rate of micro-damage formation and the rate of repair by remodelling, leading to catastrophic failure via the accumulation and coalescence of micro-cracks through the remodelled bone (Johnson *et al.* 2000; Muir *et al.* 1999; Tomlin *et al.* 2000). A similar process may be happening in the metacarpal bones; increased micro-damage formation leads to increased remodelling of the bone, but continued loading of the bone during racing causes micro-damage to accumulate eventually leading to structural failure.

4.7.5 Possible further studies

Further investigation of the trabecular architecture of the CTB, taking into account the three-dimensional structure of the trabeculae could prove useful in determining why some Greyhounds suffer a fracture of the right CTB and why other dogs just show adaptive remodelling. Three dimensional (3D) reconstruction of the μCT images followed by assessment of structural indices, including trabecular thickness, connectivity and anisotropy, would allow the 3D trabecular architecture to be characterised (Ulrich *et al.* 1999). In addition, Greyhounds that have sustained a CTB fracture often have fractures of the adjacent tarsal bones, in particular the calcaneus and fourth tarsal bone (Boudrieau *et al.* 1984; Guilliard 2000). Therefore, it could prove useful to study these adjacent bones to

see if they also have a heterogeneous trabecular structure. Additionally, while it appears likely that the heterogeneous trabecular structure of the CTB is due to an uneven distribution of stresses being distributed across the bone during the stance phase of gallop, analysis of how the bone is loaded during gallop would be required to say this for sure. Alternatively, examination of the trabecular structure of CTBs from young non-raced Greyhounds could help to determine the extent of the effect racing has on the internal architecture of the CTB. In addition, analysis of the thickness of the compact bone surrounding the CTB could provide more information as to how the CTB is adapting and why in some Greyhounds the CTB fractures. A similar analysis to what has been described above could be carried out on the MC_5 epiphysis to provide more information on adaptation in the metacarpal bones.

Examination of cross-sections of the MC_5 diaphysis via scanning electron microscopy, similar to what has been done for Greyhound CTBs (Muir *et al.* 1999; Tomlin *et al.* 2000), could allow determination of the amount of micro-damage present in the bones and would indicate if these bones also fail due to micro-damage accumulation and coalescence. Additionally, cross-sectional geometrical properties of long bones are often used to infer details about the mechanical adaptations of long bones (Burr *et al.* 1981; Burr *et al.* 1989; Ruff and Hayes 1983). Analysis of the cross-sectional geometric properties of Greyhound and SBT MC_5 bones could provide further information as to how these bones are loaded in raced and non-raced breeds of dog and could indicate where the greatest amount of loading is taking place. Greyhounds often fracture their metatarsal bones (Bellenger *et al.* 1981; Dee and Dee 1985; Ness 1993; Piras 2005) therefore a similar analysis of these bones would provide insights into how the pelvic limb bones are loaded during racing and why fractures are so common. While this study is clearly applicable to the welfare of racing Greyhounds, the principles of stress fracture development and micro-damage accumulation are equally applicable in human medicine and sports science. Many other professions and

pastimes involve sustained and repetitive activity and stress injuries are common: human athletes (including footballers) and military recruits and are particularly prone to fatigue fractures of the distal limb bones (Armstrong *et al.* 2004; Beck *et al.* 2000; Brukner *et al.* 1996; Kowal 1980; Matheson *et al.* 1987).

4.8 Summary

Regional differences in the trabecular architecture of Greyhound CTBs, and increases in trabecular density and cortical thickness of the left MC_5 bones, appear to be an adaptive response to high stresses, unevenly distributed, across the bones and limbs during galloping. Supporting this theory, SBTs, a non-racing breed of dog that we would not expect to experience the same uneven distribution of stresses, had CTBs with a homogeneous trabecular structure and MC_5 bones that had no left-to-right asymmetries in bone architecture.

Chapter 5

BUILT FOR FLIGHT OR BUILT TO FIGHT: A COMPARISON OF THE MECHANICAL PROPERTIES OF DISTAL LIMB TENDONS FROM RACING GREYHOUNDS AND STAFFORDSHIRE BULL TERRIERS

5.1 Abstract

Animals adapted for fast cursorial locomotion, such as the racing Greyhound, have limbs with muscles specialised for high acceleration and tendons that help save energy by functioning as springs. Animals bred to fight, such as the Staffordshire Bull Terrier (SBT), have shorter tendons that help stabilise the limbs but that do not function so well as springs. We investigated whether the distal limb muscle-tendon units (MTUs) of Greyhounds have the increased strength needed to withstand the high stresses and strains involved in running, a higher capacity for elastic energy storage and increased efficiency of energy recovery compared to SBT tendons.

Thoracic and pelvic distal limbs were collected from Greyhounds euthanatized after sustaining injuries during racing and from SBTs euthanatized when extreme behavioural problems prevented re-homing. MTUs were dissected out, their physical dimensions measured and the tensile properties of the tendons tested on an Instron E3000 ElectroPuls^{TM} servo-electric materials testing machine: stiffness, hysteresis at various strains, ultimate tensile strength (UTS) and breaking stress.

Greyhound thoracic and pelvic limb muscles show adaptations useful for high acceleration during running and their pelvic limb MTUs appear to be well suited for the storage and recovery of elastic strain energy. When tested mechanically, the left pelvic digital flexors were stronger and stiffer than the right tendons. This is likely an adaptive response to the asymmetrical loading of the limbs during racing. Comparison of the Greyhound and SBT

found Greyhound distal limb tendons appear well adapted to withstand the high stresses of racing; Greyhound tendons are stronger, stiffer, and in the pelvic limbs, more energy efficient than the corresponding tendons from a fighting breed of dog, the SBT. These results are consistent with the expected demands placed on the distal limbs due to high speed running and due to physical combat.

5.2 Introduction

5.2.1 Tendon composition and structure

Tendons are tough bands of fibrous connective that connect muscle to bone. Their primary role is to transmit forces from the muscle to the skeleton to drive movement and enhance joint stability (Butler *et al.* 1978). Tendons are composed of collagen (mainly type I collagen) and elastin embedded in a tendinous ground substance made up of proteoglycans, glycosaminoglycans, structural glycoproteins, a variety of other small molecules and water (Kannus 2000). Type I collagen makes up about 66% of the dry mass (Riley *et al.* 1994) and about 95% of the total collagen content of tendon (Riechert *et al.* 2001). Elastin accounts for 1-2% of the dry mass of tendon and its function is unclear; however, it may contribute to the recovery of the wavy configuration of the collagen fibres after the tendon has been stretched (Butler *et al.* 1978). All of these elements are produced by tenoblasts and tenocytes, the elongated fibroblasts and fibrocytes that lie between the collagen fibres (Hess *et al.* 1989). Tendons have a complex hierarchical structure (Figure 5.1): Soluble tropocollagen molecules form cross-links to create insoluble collagen molecules, which aggregate progressively into micro-fibrils and then into the collagen fibrils. These collagen fibrils are then organised into larger fibres aligned parallel to one another and orientated longitudinally between the muscle and bone (Elliott 1965; Kannus 2000; O'Brien 1997).

Figure 5.1: Hierarchical structure of tendon. Adapted from Kastelic *et al.* (1978).

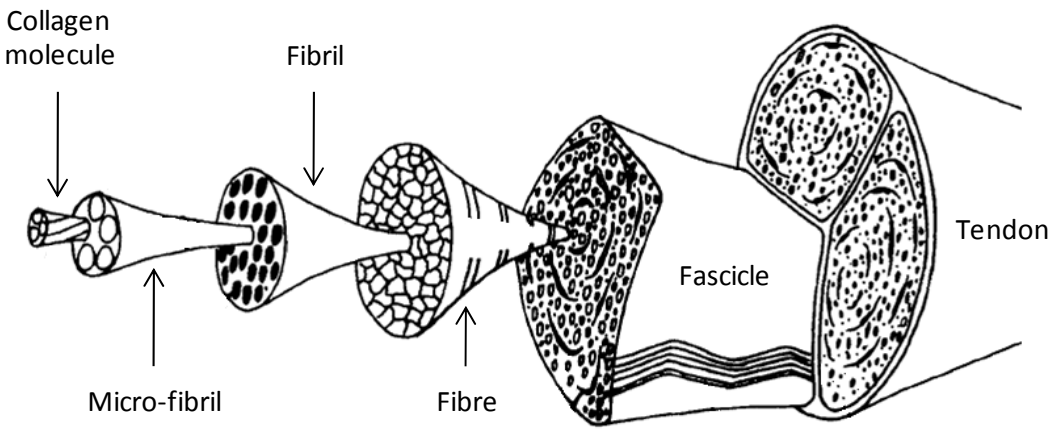

In a resting state, tendon collagen fibrils have a wavy configuration which is visible as regular bands across the fibre surface (Rowe 1985). This "crimp" configuration disappears if the tendon is stretched slightly, corresponding to straightening of the collagen fibres, and the tendon resumes its normal wavy appearance once the tensile force is released (Diamant *et al.* 1972; Rigby *et al.* 1959). Tendon "crimp" allows slight longitudinal elongation to occur without fibrous damage and acts as a shock absorber along the length of the tendon (O'Brien 1997).

5.2.2 Biomechanical properties of tendons

Tendons are described as being "viscoelastic" as they display both viscous (energy lost) and elastic (energy recovered) properties. When tendons are stretched and allowed to recoil, they can return up to 95% of the elastic energy stored during stretching, the slight energy-loss is known as the hysteresis (Bennett *et al.* 1986). Tendons also exhibit non-linear elastic properties which are reflected by their classic J-shaped stress-strain curves produced when they are stretched (Bennett *et al.* 1986; Shadwick 1990; Woo *et al.* 1982). When tendons are stretched, stiffness gradually increases during the initial "toe" region of the tendon stress-strain curve. Loads imposed on the tendon during the toe region elongate the

tendon by reducing the crimp angle of the resting collagen fibres. Therefore, loading within the toe region does not exceed the tendon elastic limit, and subsequent unloading restores the tendon to its initial length. Further elongation brings the tendon into the "linear" region of the stress-strain curve during which stiffness remains constant as a function of elongation; the slope of this region is referred to as the Young's modulus of the tendon. Tendon elongation in the linear region results from stretching of the aligned collagen fibres. At the end of the linear region some collagen fibres start to fail causing tendon stiffness to decrease; any subsequent loading does not restore the tendon to its original resting length. Elongation beyond the linear region eventually results in complete failure of the tendon (Butler *et al.* 1978; Rigby *et al.* 1959; Wang 2006).

5.2.3 Elastic energy savings, strength and stiffness

When an animal runs, each step involves a cycle of mechanical energy (Cavagna *et al.* 1977). Potential energy (PE) has to be supplied by an animal's muscles to raise and lower its body's center of mass during every step, and kinetic energy (KE) is required to reaccelerate the body's center of mass and reaccelerate the limbs relative to the body's center of mass (Cavagna *et al.* 1977; Raeke 2004). During running gaits such as trotting, hopping and galloping, the PE and KE of an animal's center of mass fluctuate in phase: during the first half of a step, PE and KE is absorbed by the limb as the animal's center of mass falls and decelerates, and during the second half mechanical energy must be provided to raise and reaccelerate the animal's center of mass (Cavagna *et al.* 1977; Raeke 2004). Rather than all of this energy being produced by the muscles doing work, a great deal can be stored and recovered in the elastic elements of the limbs, primarily in the tendons. Tendons are highly resilient elastic structures: when stretched and allowed to recoil they can return up to 95% of the elastic energy stored during stretching (Bennett *et al.* 1986). Many running and hopping animals lower their metabolic energy expenditure by utilizing elastic energy

storage and recovery in the long tendons of the limbs to reduce the amount of work that the limb muscles must do to restore an animal's PE and KE during locomotion (Alexander 1984). For example, it has been estimated that Tammar Wallabies hopping at 6 ms^{-1} (Biewener and Baudinette 1995) and Red Kangaroos hopping at 8 ms^{-1} (Cavagna *et al.* 1977) reduce their energy expenditure by approximately 50% by utilising elastic energy storage in their limb tendons. Further, female Tammar Wallabies are able to carry young weighing up to 15% of their own body weight for free (i.e. they do not have to expend any additional energy) by utilising this mechanism (Baudinette and Biewener 1998). This ability to carry loads for free by utilising elastic energy storage in their tendons is a unique feature of hopping compared to other modes of locomotion. Although, Nepalese porters (Bastien *et al.* 2005) and African women (Bastien *et al.* 2005; Maloiy *et al.* 1986) are able to carry loads of up to 20% of their bodyweight without increasing energy consumption; however, the mechanism by which they do so is unknown at the moment. Other running animals do not appear to achieve the same degree of energy savings as wallabies and kangaroos; however, elastic energy storage mechanisms are still important in helping to conserve energy. Horses, for example, have long distal limb tendons that can reduce muscle work by up to 40% at both the trot and gallop (Biewener 1998). In human runners, elastic energy savings in the Achilles tendon and ligaments of the foot are estimated to reduce muscle work by up to 50% (Ker *et al.* 1987). Tendons also need to be relatively stiff (i.e. have a high elastic modulus) and strong to withstand the stresses and strains of locomotion, especially as the peak stresses and strains acting in the long tendons of the limbs generally increase with increasing speed (Biewener 1998; Dimery *et al.* 1986; Stephens *et al.* 1989). For example, peak strains of 9.0 - 16.6% have been recorded in the superficial digital flexor (SDF) tendons of the horse at a gallop, compared to peak strains of 7.0 - 7.5% at a walk (Dimery *et al.* 1986; Stephens *et al.* 1989). Measurements of the stresses that various mammalian tendons experience during running, calculated from dynamic tensile tests, show the normal

range of tendon strain to be limited to a maximum of about 5 - 6% (Bennett *et al.* 1986) and stresses above 100 MPa, which correlates to a failure strain of about 8%, tends to lead to rupture of the tendon (Bennett *et al.* 1986). Tendon stiffness has been shown to increase from low values at low stresses to about 1500 MPa at stresses exceeding 30 MPa (Bennett *et al.* 1986).

5.2.4 Muscle architecture

Knowledge of muscle architecture (the organization of muscle fibres relative to the axis of force generation) can provide an insight into the relationship between musculoskeletal structure and function (Gans 1982). For example, a muscle with short muscle fibres and a long tendon, such as the digital flexor muscles, may be well suited for economical force generation and an enhance ability to utilise the storage and recovery of elastic strain energy, which can greatly improve locomotor efficiency (Biewener 1998). Muscles are generally divided into two types based on their architecture: parallel and pennate-fibered muscles. Muscles with parallel fibres generally have relatively long fibres that run end-to-end within the muscle in a direction parallel to the axis of force transmission and they attach to the skeleton with little or no tendon (Biewener 2003). In contrast, muscles with pennate fibres have a complex architecture comprising relatively short fibres that run at an angle to the muscles principle axis of force transmission and they attach to the skeleton via an external tendon that generally runs along the full length of the muscle (Biewener 2003). Pennate muscles can be uni-pennate (obliquely angled fibres attach to a distal tendon), bi-pennate (two sets of oblique fibres converge to both sides of a central tendon) or multi-pennate (complex with varying planes of angled fibres). The force developed by a muscle is proportional to its fibre cross-sectional area also known as its physiological cross sectional area (PCSA) (Knuttgen 1976; Maughan *et al.* 1983). The pennate arrangement of the muscle fibres increases the fibre cross sectional area which increases the force that the muscle can

exert and while pennate muscles suffer some loss of force transmission due to the angle of their fibres, this is more than compensated for by their greater fibre area (Biewener 2003). Therefore, pennate-fibred muscles have a larger PCSA and are able to generate greater forces and hence more power, than parallel-fibred muscles of an equal mass and volume. In addition, the energetic cost associated with generating a given force is reduced by using pennate-fibered muscles as a smaller volume of muscle is recruited to generate that force (Biewener 2003).

5.2.3 Effect of exercise on tendons

Tendons are able to respond to changing mechanical forces by changing their composition, structure and mechanical properties. The effects of exercise and training on the mechanical properties of tendons have been studied in a number of species. Long term physical activity improves the tensile mechanical properties of tendons (Buchanan and Marsh 2001; Reeves *et al.* 2003; Vilarta and Vidal Bde 1989; Woo *et al.* 1980), whereas disuse and immobilisation leads to deterioration of these properties (Loitz *et al.* 1989; Woo *et al.* 1982; Yamamoto *et al.* 1993). Endurance training appears to cause an increase in the tensile strength and stiffness of tendons. Following long term exercise, the extensor tendons of swine were significantly stronger and stiffer and exhibited hypertrophy (Woo *et al.* 1980). Interestingly, the same training regime had no effect on the digital flexor tendons (Woo *et al.* 1981a). Similarly, Vilarta and Vidal (1989) reported increased tensile strength in the Achilles tendon of rats after a 30 day exercise program, while Buchanan and Marsh (2001) reported increased stiffness in the Achilles tendon of Guinea fowl following a 12 week exercise program. There is limited data regarding tendon adaptation in response to strength training, i.e. training with large forces and few repetitions; however, a study by Reeves et al. (2003) showed strength training increased the stiffness of human patella tendons. Dimensional changes such as hypertrophy may account for some of these

changes; however, increases in ultimate tensile stress and strain indicate that improvement of tendon mechanical properties is also associated with changes in the intrinsic material properties.

5.2.6 Functional differences between thoracic and pelvic limbs

The thoracic and pelvic limbs of animals adapted for fast cursorial locomotion show functional specialisation. The equine thoracic limb supports and decelerates the body, is involved in joint stabilisation during the stance phase of gait, rapid flexion and extension of the limbs during swing phase, and utilises the storage and recovery of elastic strain energy (Brown *et al.* 2003; Payne *et al.* 2004). The equine pelvic limb appears to be specialised proximally for the production of large amounts of force and distally for economical force production (the distal muscles generate smaller forces over a greater range of motion) and elastic energy storage (Payne *et al.* 2005). Similar functional differences have been observed in the thoracic and pelvic limbs of racing Greyhounds. In the pelvic limb, the proximal muscles seem to be specialised for high power output and rapid acceleration, while the distal muscles appear to be specialised for elastic energy storage (Pasi and Carrier 2003; Williams *et al.* 2008b). Greyhound thoracic limbs show specialisation for increased limb support, enhanced sprint ability and greater manoeuvrability (Williams *et al.* 2008a). However, unlike the equivalent pelvic limb muscle-tendon units (MTUs) (Pasi and Carrier 2003; Williams *et al.* 2008b) or the equivalent MTUs in the equine thoracic limb (Brown *et al.* 2003), the Greyhound thoracic distal limb MTUs do not appear to be specialized for the storage and recovery of elastic strain energy (Williams *et al.* 2008a).

5.2.7 Function of the digital flexor tendons

The mechanical properties of the flexor tendons are believed to be correlated with their anatomic position and physiological function. The digital flexor tendons act as stiff

biological springs. When they are stretched during the stance and deceleration phase of a stride they store elastic strain energy that is returned when they recoil during the swing and acceleration phase (Alexander 1988; Alexander 1991). The anatomical position of the digital flexors (along the palmar/plantar aspect of the limbs) and their role in elastic energy storage and recovery, mean that they experience high strains. Strains up to 12.0% have been measured in the equine superficial digital flexor (SDF) tendons *in vitro* (Herrick *et al.* 1978), while peak strains of 9.0 - 16.6% have been recorded in the galloping horse (Dimery *et al.* 1986; Stephens *et al.* 1989). Failure strains of 12.3% have been recorded for equine SDF tendons *in vitro* (Riemersma and Schamhardt 1985). Predicted stresses and strains for Greyhound thoracic limb digital flexors (both superficial and deep) were 40 MPa and 2.7% (Williams *et al.* 2008a). Likewise, stresses of 27 MPa and 43 MPa, and strains of 1.8% and 2.8%, are predicted for the superficial and deep digital flexors of the Greyhound pelvic limb, respectively (Williams *et al.* 2008b).

5.2.8 Specialisation for different roles

Muscle and tendon properties vary greatly between species and breeds that are adapted for different roles. A study comparing muscle architecture in Quarter Horses (bred for acceleration) and Arabian Horses (bred for endurance) found that Quarter Horses have greater physiological cross-sectional areas and greater isometric force potential in their pelvic limb muscles, suggesting their muscles are better designed for acceleration than those of Arabian Horses (Crook *et al.* 2008). There are also functional differences relating to locomotor behaviour between limb musculature in humans and other primates. Human pelvic limb muscles appear to be optimised to generate large forces over a narrow range of joint positions, while muscles in chimpanzees (Thorpe *et al.* 1999) and great apes (Payne *et al.* 2006) are optimised toward generating moderate force over a wide range of joint positions. These features can be related to locomotor behaviour: humans are habitually

bipedal, predominantly moving on the horizontal and stable substrate provided by the ground; by contrast, non-human great apes, use various combinations of all four limbs, in numerous positions, to travel in an arboreal environment composed of unstable supports arranged in a complex three-dimensional manner.

As well as differences in locomotory behaviours (speed versus endurance, bipedal versus arboreal etc.), trade-offs between functionally opposing roles can lead to differences in muscle-tendon properties. One such trade-off is specialisation for fast, economical running versus specialisation for fighting ability. The physical demands of fast economical running are quite different from those required for fighting. Therefore, traits that make an individual good at fighting may limit locomotor performance and vice versa. In general, animals that are designed to run fast tend to have long gracile limbs with reduced muscle mass distally and long tendons designed for the storage and recovery of elastic strain energy (Hildebrand and Goslow 2001; Hildebrand and Hildebrand 1974; Payne *et al.* 2005; Williams *et al.* 2008a; Williams *et al.* 2008b). By contrast, specialisation for fighting seems to require short, stout limbs with muscles specialised for high force production and short stiff tendons that that can stabilise the limbs during fights, increase manipulative ability and enhance force transmission, but that are poorly suited for elastic energy storage (Pasi and Carrier 2003). A study comparing limb muscle architecture of Greyhounds (specialized for running) with Pit Bull Terriers (specialized for fighting), found Greyhounds to have relatively less muscle mass distally in their limbs compared to Pit Bull Terriers (Pasi and Carrier 2003). Greyhounds had weaker muscles in their thoracic limbs but stronger muscles in their pelvic limbs, while Pit Bull Terriers had muscles of equal or greater strength in their thoracic compared to pelvic limbs. Additionally, Greyhounds were estimated to have a greater capacity for elastic energy storage in their muscle-tendon systems (Pasi and Carrier 2003).

5.2.9 Study aim and hypothesis

Due to intense artificial selection (breeding), dogs provide an opportunity to compare the effects of differing specialisations on the mechanical properties of distal limb MTUs within the same species. Greyhounds are bred for maximum running speed: they are recognised as the fastest breed of domestic dog, capable of reaching speeds of up to 17.9 ms^{-1}. In contrast, Bull Terrier breeds have been bred for physical combat. The architectural properties of the digital flexor MTUs were measured and the tensile properties of the tendons mechanically tested. We hypothesised Greyhound MTUs would show adaptations for high acceleration and elastic energy storage. Further, their tendons would have increased strength to withstand the high stresses involved in running and a greater capacity for elastic energy storage and recovery when compared to SBT tendons.

PART A: PELVIC DIGITAL FLEXOR TENDONS

5.3 Materials and methods

5.3.1 Tendon specimens

Distal pelvic limbs were collected from 15 racing Greyhounds (12 male, three female) euthanatized at their owners request after sustaining a right tarsal (seven dogs), left carpal (two dogs), right carpal (two dogs) or left elbow (one dogs) fracture during a race, or due to severe behavioural problems preventing them from being re-homed (three dogs). Mean age of the dogs was 2.97 ± 0.56 years; mean weight was 29.79 ± 3.04 kg. Limbs were also collected from 11 SBTs (six male, five female) euthanatized and donated from a local dog pound when extreme behavioural problems prevented them from being re-homed. Age was unknown; mean weight was 16.00 ± 1.85 kg. The superficial (SDF), medial deep (m.DDF) and lateral deep (l.DDF) digital flexor tendons were dissected out from the pelvic limbs and stored at -20 °C until required for testing, at which point the tendons were

thawed at room temperature. The mechanical properties of tendons that undergo less than three freeze-thaw cycles are similar to those of fresh tendons, there is no significant reduction in tendon strength and stiffness (Huang *et al.* 2011). Therefore, it was assumed that the results obtained from our tendons were comparable to fresh samples.

5.3.2 Muscle-tendon architecture

Four pairs of the Greyhound and four pairs of the SBT distal pelvic limbs were initially used for measurements of the muscle-tendon unit (MTU) architecture. The SDF and both DDF tendons, and the muscles which they connect to (SDF, l.DDF, m.DDF, medial gastrocnemius (MG) and lateral gastrocnemius (LG)) were systematically removed from the limbs. Tendons were separated from the muscles at the point where the tendon inserts into the muscle-belly. The tendon and muscle-belly mass and length were measured. Incisions were made in the muscle bellies along the plane of the muscle fascicles. The lengths of a random selection of five fascicles from different areas of the belly were measured to provide an estimate of muscle fibre length. Resting pennation angle, defined as the angle between the internal tendon or aponeurosis and the muscle fascicles, was also measured (Figure 5.2).

Figure 5.2: Photograph detailing how the muscle belly length, muscle fibre length and pennation angle (θ) was measured.

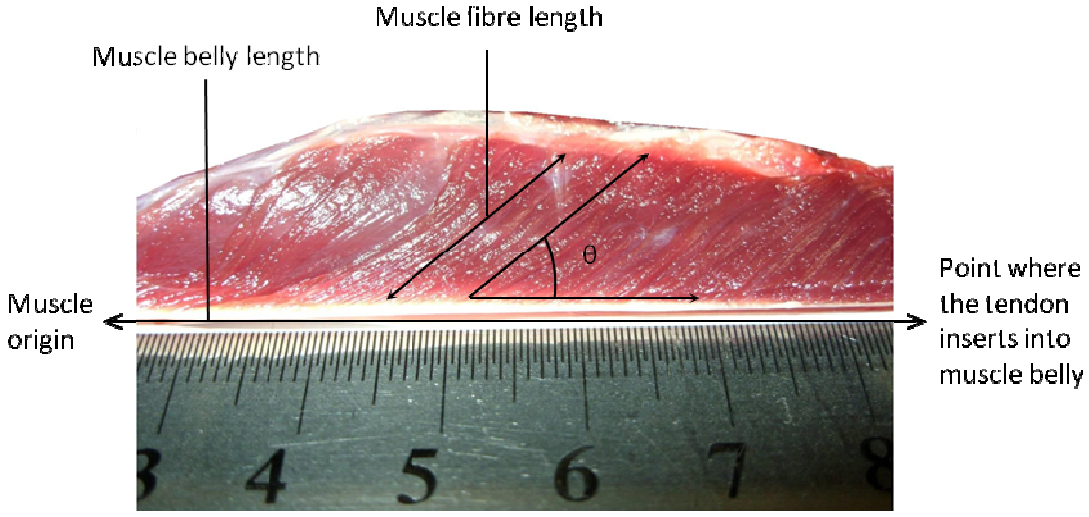

5.3.3 Tendon preparation and clamping

The collagen fibres of a tendon are largely independent, therefore clamping them securely can be difficult. Methods that only hold the outer fibres leave the inner fibres incompletely stressed making the material appear less stiff and less strong than it really is (Ker et al. 2000). To obtain valid test results the tendons must be squeezed by the clamp such that each individual fibre is held effectively independently (Vincent 1992). The best technique to achieve this is to air-dry the ends that are to be clamped (Haut 1983; Ker *et al.* 2000; Wang and Ker 1995). Therefore, tendons were prepared by air-drying the ends while the rest of the tendon was wrapped first in blue roll moistened with distilled water and then wrapped in cling film (Figure 5.3). The digital flexor tendons separate distally in order to insert separately onto each digit. Therefore, the tendons were dried 1 cm above the point at which they separate to ensure all tendon fibres were clamped securely.

Figure 5.3: Photograph detailing how the tendons were prepared for mechanical testing.

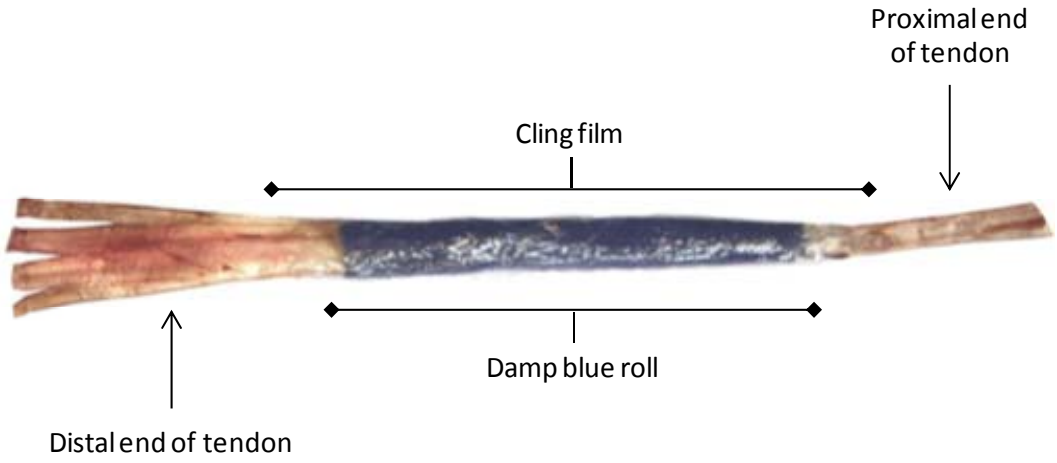

5.3.4 Mechanical tests

An Instron E3000 ElectropulsTM servo-electric materials testing machine (Instron, UK) was used for all tests. The machine was operated in digital position control for the majority of each test. This provided highly accurate control of the amplitudes imposed on the tendons

during the dynamic tests. Tests were carried out at room temperature. The dry ends of the tendons were clamped between serrated steel jaw faces, in mechanical wedge action clamps (Figure 5.4). The upper clamp was attached to the actuator and the lower was attached to the load cell, which was in turn connected to the stationary table of the load frame. Tensile force is applied to the tendons via the movement of the actuator.

Figure 5.4: Photograph of how tendons were set up ready for testing in the Instron.

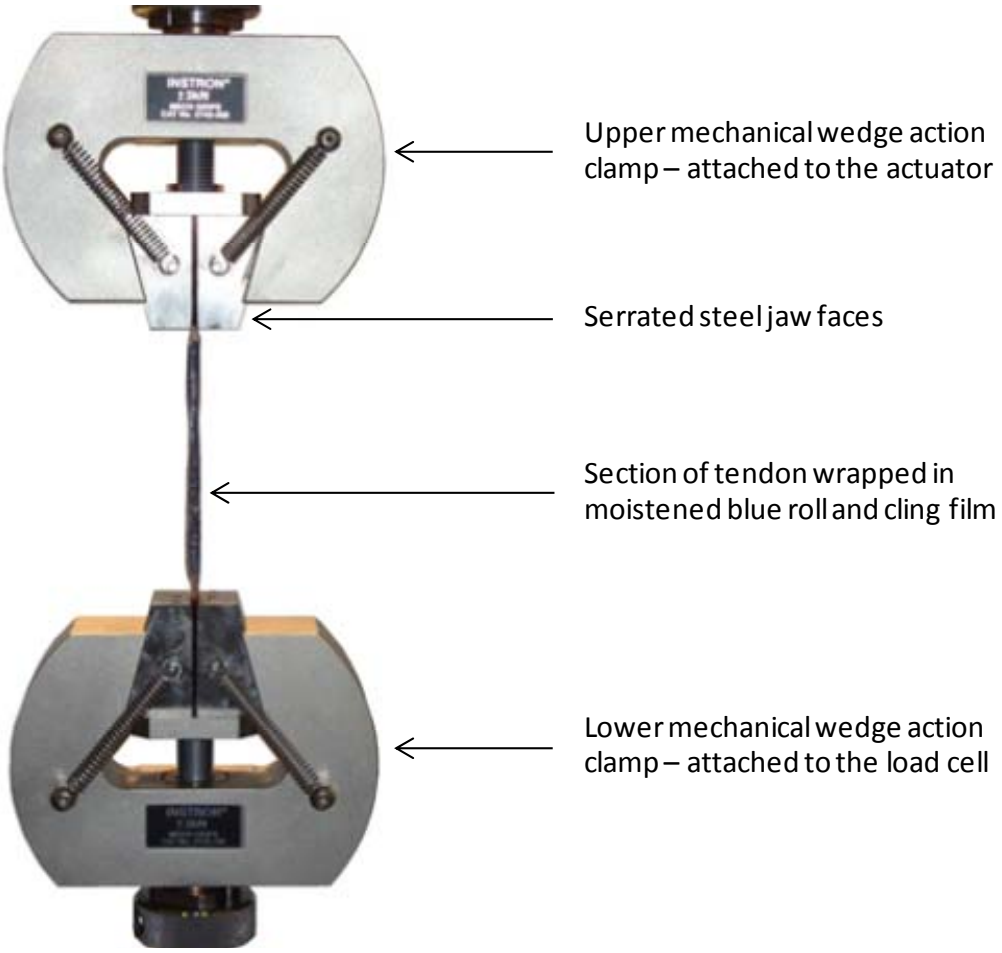

The normal range of mammalian tendon strain is limited to a maximum of about 5.0% (Bennett *et al.* 1986) and at strains above 8.0%, tendon tends to rupture (Bennett *et al.* 1986; Butler *et al.* 2000). Additionally, the maximum stresses and strains placed on the tendons by the muscles at F_{max} were calculated (Section 5.3.5 details the calculations) and used to provide an estimation of the physiological strains experienced by the tendons "in-

life" (all estimated to be less than 6.0%; Section 5.4.3). Animals have a preferred speed and stride frequency at each gait (walk, trot and gallop) and at each gait transition, which is scaled with size (Heglund and Taylor 1988; Heglund *et al.* 1974). The trot-gallop transition is often used to compare the speed and stride frequency of animals of different masses as it can be easily and precisely measured in the laboratory. The preferred stride frequency at the trot-gallop transmission is calculated as $4.19(M_b)^{-0.150}$ where M_b is the body mass in kg (Heglund and Taylor 1988). The preferred stride frequency at the trot-gallop transition was calculated using the average weight of the Greyhounds and SBTs in this study. Greyhounds had a preferred stride frequency of 2.5 Hz and SBTs had a preferred frequency of 2.7 Hz. This value was rounded down to 2.0 Hz for both breeds. Therefore, for the dynamic tests, SDF and l.DDF tendons were cycled sinusoidally at 2.0 Hz to 2, 3, 4 and 5% strain. Due to their small size, and based on preliminary data (not reported), m.DDF tendons were cycled to 2 and 3% strain only. Data was collected at a sampling frequency of 1000 Hz for 40 cycles; however, only data from cycle 20 was used for analysis. More energy is dissipated in the first cycle of a dynamic test than in subsequent cycles, after 10 or more cycles a steady state is achieved (Nigg *et al.* 2000), therefore, using cycle 20 allowed a stable hysteresis curve to be produced. Tendons were always tested in the same order (2.0%, 3.0%, 4.0% and then 5.0% strain). The lower strains were tested first as strains above 4.0% are thought to cause microscopic tearing of the collagen fibres (Butler *et al.* 2000). In addition, preliminary experiments showed that hysteresis did not increase from cycle 20 to cycle 40 when the tendons were tested at 5.0% strain. Therefore, it was assumed there was no experimental error introduced due to fatigue or creep of the tendons.

Following the dynamic tests, tendons were tested to failure by stretching the tendons at a rate of 1 mm/s until they broke or yielded irreversibly; the sampling frequency was 100 Hz.

5.3.5 Measurements and calculations

- ***Muscle cross sectional area and maximum isometric muscle force (F_{max})***

Muscle volume was estimated by dividing muscle mass by a muscle density of 1060 kg m^{-3} (Mendez and Keys 1960) and the physiological cross sectional area (PCSA) was calculated by dividing muscle volume by fascicle length. Isometric F_{max} was estimated by multiplying the PCSA by 0.3 MPa (the maximum isometric stress of vertebrate skeletal muscle (Medler 2002; Wells 1965). The calculation of PCSA, and hence F_{max}, was also corrected for pennation angle by calculating PCSA using the following equation; PCSA = (muscle mass . cos θ)/(muscle density . fibre length) where θ refers to the pennation angle. We present F_{max} results for both methods for comparison; however, our results and discussion refer to the values calculated without the correction as most pennation angles are small (i.e. less than 30°, and thus θ remains close to one).

- ***Muscle power***

Instantaneous muscle power was estimated as a tenth of the product of F_{max} and maximum fibre contraction velocity (V_{max}) (Hill 1938). V_{max} of dog muscle was taken to be 3.8 $L_o s^{-1}$, where L_o refers to muscle fibre resting length (Ameredes *et al.* 1992).

- ***Architectural Index***

The Architectural Index was calculated for muscles (Woittiez *et al.* 1983). This is an index that normalizes muscle fascicle lengths for muscle belly length. It allows comparison of relative fascicle lengths in muscles of different sizes, providing information about the configuration and shape of the muscle. It is calculated as the ratio of muscle fascicle length to total muscle belly length.

- ***Tendon cross sectional area***

The cross sectional area of each tendon was calculated using the following equation; $CSA_t = m_t . (d_t . l_t)^{-1}$ where m_t refers to the mass of the tendon in kilograms, d_t refers to the tendon density, assumed to be 1120 kg m^{-3} (Ker 1981), and l_t refers to the length of the tendon in meters.

- ***Estimated "in-life" tendon stress, strain and length change***

Tendon stress at F_{max} was estimated by dividing F_{max} by tendon CSA. The resultant value was then divided by the Young's modulus of tendon, taken as 1500 MPa (Bennett *et al.* 1986; Ker *et al.* 1988), to provide an estimate of tendon strain. Tendon length change was then estimated as the product of tendon rest length and tendon strain.

- ***Fibre length factor***

Muscle fibre length factor (FLF) is the ratio of muscle fibre length to tendon length change when the tendon is maximally loaded (Ker *et al.* 1988; Pollock and Shadwick 1994). FLF has been used to characterize muscle tendon units that favour elastic energy storage (FLF < 2) versus those that are better suited for force transmission and control of joint displacement (FLF > 4) (Ker *et al.* 1988; Pollock and Shadwick 1994).

- ***Stress and strain (mechanical tests)***

Readings of the load (N) and of the displacement (mm) of the actuator were available as functions of time. When required, load could be plotted against displacement. To account for differences in length and cross sectional area of the tendons tested, load was converted to stress (MPa) and displacement was converted to strain (strain is dimensionless and therefore has no units). Tendon stress was calculated by dividing load by the cross-sectional

area and strain was calculated by dividing the displacement by the original length of the tendon.

- ***Hysteresis***

The stress and strain data from the 20th cycle of each dynamic test was plotted as a hysteresis loop. The loop is formed in a clockwise direction, indicating the dissipation of energy. This energy loss (the hysteresis) was calculated as the work done on the tendon during stretching (represented as the area under the ascending limb of the loop) minus the work returned by the tendon during shortening (the area under the descending limb of the loop). The hysteresis is then presented as a percentage of the work done to stretch the tendon. This calculation of hysteresis indicated how energy efficient the tendons were.

- ***Young's modulus (Stiffness)***

A tangent to the load–displacement (stress-strain) curve created from the UTS test data provides an estimate of the stiffness of the specimen (Ker *et al.* 1986).

5.3.6 Statistical analysis

The mean and standard error of the mean (SEM) were calculated for each parameter. The effect of side (left versus right) on each parameter was examined using a two-tailed paired t-test (significance set at $p < 0.05$). The effect of breed (Greyhound versus SBT) on each parameter for each limb (left or right) was examined using a two-tailed un-paired t-test (significance set at $p < 0.05$).

5.4 Results

5.4.1 Muscle-tendon anatomy and architectural properties

The five major muscles that attach to the SDF and DDF tendons in the pelvic limb were considered (Figure 5.5). Measured and calculated architectural parameters for each of the muscles are given in Table 5.1 and 5.2, and for each tendon are provided in Table 5.3.

5.4.2 Left to right asymmetries in muscle-tendon properties

The muscle-tendon architectural properties were tested to determine if any left-to-right asymmetries were present. None were found in any SBT muscles or tendons. The m.DDF tendons from the Greyhound left limb of weighed significantly more ($p = 0.042$) and had a significantly greater volume ($p = 0.042$) than the m.DDF tendons from the right limb.

5.4.3 Breed comparison of muscle-tendon properties

Muscle-tendon architectural properties were also tested to determine if there were any significant breed differences. All of the muscles, except the m.DDF, were significantly heavier in Greyhounds ($p < 0.040$ for all muscles). Greyhounds had significantly heavier total body masses than SBTs ($p < 0.001$), therefore, the mass of each muscle was normalised relative to total body mass. Following this, only the right LG was found to be significantly heavier in Greyhounds compared to SBTs ($p = 0.009$).

Figure 5.5: Plantar view of a canine distal pelvic limb showing the muscles and tendons of interest. The medial and lateral deep digital flexor muscles are out-of-view behind the gastrocnemius. Adapted from Evans and DeLahunta (1971).

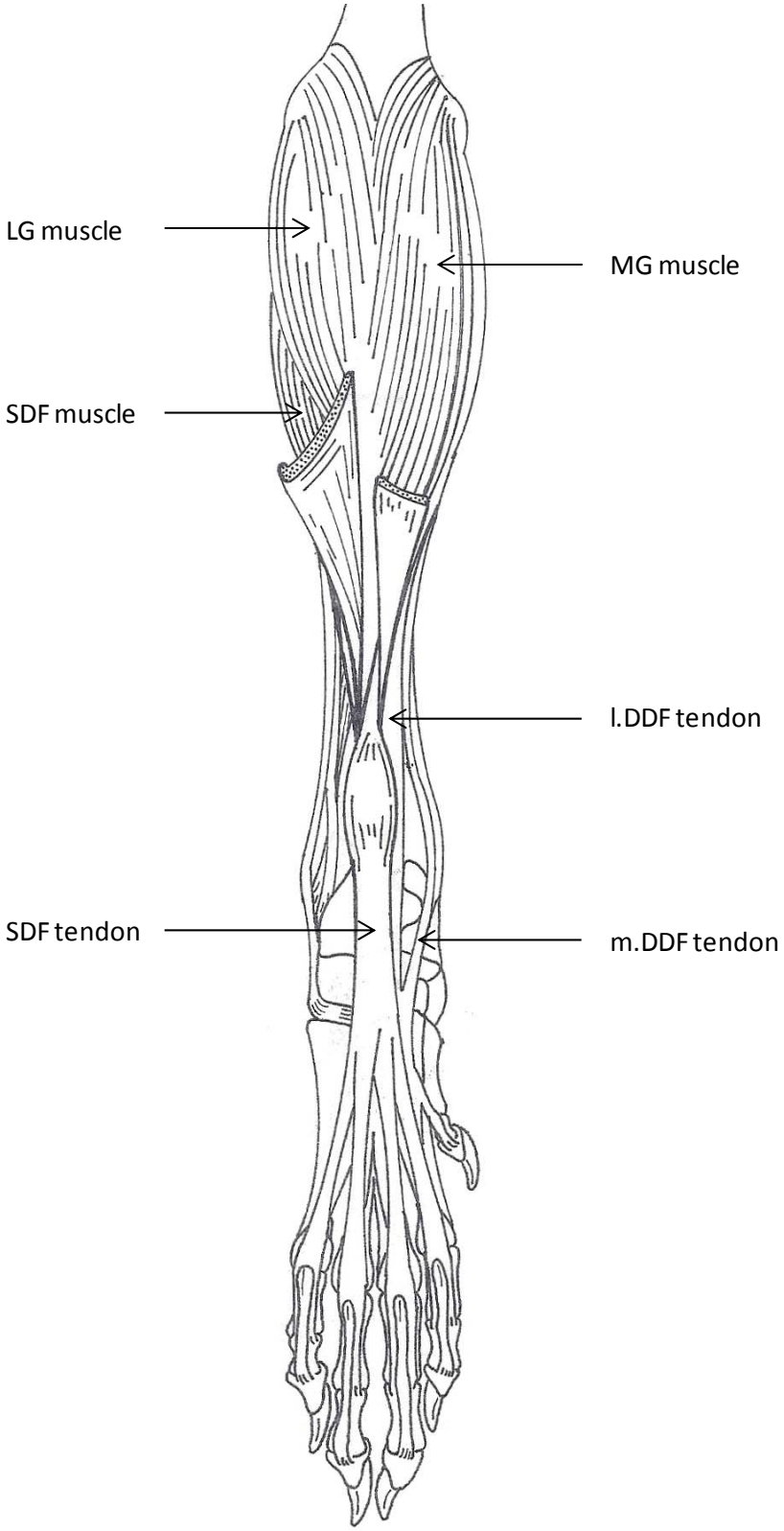

Table 5.1: Muscle data for the MG, LG and SDF muscles: Mean (SEM) muscle mass, belly length, fascicle length, physiological cross-sectional area (PCSA), pennation angle and estimated maximum isometric force (F_{max}) and power. No left-to-right asymmetries were found in Greyhounds or SBTs. * denotes a significant difference between the two breeds; $p < 0.05$.

Muscle	Side	Mass (g)	Belly Length (cm)	Fascicle Length (cm)	PCSA (cm^2)	Pennation Angle (°)	F_{max} (N)	Corrected F_{max} (N)	Power (W)
Greyhound									
MG	Left	43.9 (2.4) *	13.0 (0.4) *	1.9 (0.1)	21.9 (1.6) *	27.5 (2.5)*	657.7 (47.9) *	582.0 (44.7) *	4.7 (0.3) *
	Right	42.5 (2.6) *	12.6 (0.5) *	1.8 (0.1)	22.9 (1.9) *	32.5 (2.5)*	687.2 (56.9) *	577.8 (51.5) *	4.6 (0.3) *
LG	Left	50.4 (8.6) *	13.6 (0.9) *	1.8 (0.1)	27.2 (4.6) *	32.5 (3.2)*	637.0 (137.5) *	683.4 (111.7) *	5.4 (0.9) *
	Right	47.9 (5.3) *	13.7 (0.9) *	2.0 (0.1)	23.0 (2.7) *	30.0 (0.0)*	691.3 (80.0) **	598.7 (69.3) *	5.2 (0.6) *
SDF	Left	48.9 (8.8) *	16.8 (0.3) *	1.3 (0.1)	38.2 (8.8)	33.8 (2.4) *	1145.3 (263.1) *	934.0 (197.3) *	5.3 (1.0) *
	Right	48.0 (6.0) *	16.3 (0.7) *	1.2 (0.1)	39.5 (6.4)	37.5 (2.5) *	1184.7 (192.4) *	939.5 (115.8) *	5.2 (0.7) *
SBT									
MG	Left	19.4 (2.5) *	8.6 (0.5) *	1.8 (0.3)	10.6 (1.2) *	25.3 (0.6) *	317.3 (34.6) *	286.6 (29.9) *	2.1 (0.3) *
	Right	20.1 (2.7) *	8.6 (0.4) *	1.7 (0.2)	11.0 (1.2) *	28.3 (2.2) *	330.9 (36.6) *	288.9 (26.1) *	2.2 (0.3) *
LG	Left	18.8 (4.2) *	8.4 (0.5) *	1.4 (0.2)	12.2 (2.9) *	26.0 (3.2) *	364.4 (85.9) *	319.2 (76.1) *	2.0 (0.5) *
	Right	16.6 (1.4) *	8.4 (0.7) *	1.5 (0.2)	11.8 (2.7) *	24.3 (3.9) *	352.8 (79.9) *	315.6 (68.7) *	1.8 (0.2) *
SDF	Left	26.0 (3.2) *	10.3 (1.0) *	1.3 (0.1)	19.8 (2.7)	26.5 (2.0) *	594.6 (80.7) *	529.6 (68.0) *	2.8 (0.3) *
	Right	26.4 (5.7) *	10.3 (1.0) *	1.5 (0.2)	16.3 (2.5)	28.3 (2.3) *	487.5 (74.2) *	432.0 (70.9) *	2.8 (0.6) *

Table 5.2: Muscle data for the l.DDF and m.DDF muscles: Mean (SEM) muscle mass, belly length, fascicle length, physiological cross-sectional area (PCSA), pennation angle and estimated maximum isometric force (F_{max}) and power. No left-to-right asymmetries were found in Greyhounds or SBTs. * denotes a significant difference between the two breeds; $p < 0.05$.

Muscle	Side	Mass (g)	Belly Length (cm)	Fascicle Length (cm)	PCSA (cm^2)	Pennation Angle (°)	F_{max} (N)	Corrected F_{max} (N)	Power (W)
Greyhound									
m.DDF	Left	6.8 (0.7) *	9.7 (0.5) *	1.8 (0.1) *	3.6 (0.5) *	35.0 (6.5)	107.9 (16.2)	87.6 (16.7)*	0.7 (0.1) *
	Right	6.4 (1.0) *	9.8 (0.3) *	1.9 (0.1) *	3.3 (0.5) *	33.8 (2.4)	97.5 (13.4)*	81.8 (13.2)*	0.7 (0.1) *
l.DDF	Left	30.8 (1.4) *	18.1 (0.4) *	1.9 (0.1) *	15.7 (0.5) *	37.5 (2.5)	470.6 (16.1) *	371.3 (6.6)*	3.3 (0.2) *
	Right	30.9 (1.1) *	17.4 (0.6) *	1.9 (0.1) *	15.4 (1.0) *	42.5 (4.3)	462.8 (29.0) *	335.2 (15.0)	3.3 (0.1) *
SBT									
m.DDF	Left	4.3 (0.9) *	6.8 (0.2) *	1.5 (0.2) *	2.7 (0.6) *	21.8 (4.4)	82.2 (16.8) *	74.6 (14.1)*	0.5 (0.1) *
	Right	4.2 (0.8) *	6.7 (0.3) *	1.4 (0.1) *	2.8 (0.6) *	22.5 (3.1)	83.8 (18.5) *	76.2 (15.4)*	0.5 (0.1) *
l.DDF	Left	19.5 (1.9) *	12.2 (0.8) *	1.7 (0.2) *	11.4 (1.8) *	28.3 (3.1)	342.4 (52.7) *	303.2 (52.2)	2.1 (0.2) *
	Right	18.8 (2.5) *	11.4 (0.5) *	1.8 (0.1) *	10.2 (1.4) *	28.0 (2.5)	306.4 (42.8) *	270.3 (39.5)	2.0 (0.3) *

Table 5.3: Tendon data: Mean (SEM) mass, volume, and resting length, and estimated cross-sectional area (CSA_t), stress, strain, and length change. † denotes a significant difference between the left and right limbs of a breed; $p<0.05$. * denotes a significant difference between the two breeds; $p < 0.05$.

Tendon	Side	Mass (g)	Volume (cm^3)	Resting Length (cm)	CSA_t (cm^2)	Stress (MPa)	Strain (%)	Length Change (cm)
Greyhound								
SDF	Left	8.2 (0.5) *	7.3 (0.4) *	22.9 (0.2) *	0.32 (0.02) *	83.5 (10.6)	5.6 (0.0)	1.3 (0.2) *
	Right	9.3 (0.9) *	8.3 (0.8) *	23.2 (1.0) *	0.36 (0.03) *	74.6 (10.9)	5.0 (0.0)	1.2 (0.2) *
m.DDF	Left	0.6 (0.0) † *	0.6 (0.0) † *	17.9 (0.5) *	0.03 (0.00)	34.4 (4.9)	2.3 (0.3)	0.4 (0.1) *
	Right	0.5 (0.0) † *	0.5 (0.0) † *	17.3 (0.7) *	0.03 (0.00)	34.7 (3.9)	2.3 (0.3)	0.4 (0.1) *
l.DDF	Left	4.2 (0.3) *	3.8 (0.3) *	16.7 (0.2) *	0.23 (0.02) *	21.2 (1.7)	1.4 (0.1)	0.2 (0.0) *
	Right	3.9 (0.2) *	3.5 (0.2) *	16.1 (0.4) *	0.22 (0.01) *	21.2 (1.5)	1.4 (0.1)	0.2 (0.0) *
SBT								
SDF	Left	3.1 (0.3) *	2.7 (0.3) *	14.8 (1.0) *	0.19 (0.01) *	64.3 (11.3)	4.3 (0.8)	0.7 (0.2) *
	Right	3.0 (0.3) *	2.7 (0.3) *	15.4 (0.8) *	0.17 (0.01) *	67.9 (6.8)	4.5 (0.5)	0.7 (0.1) *
m.DDF	Left	0.3 (0.1) *	0.3 (0.0) *	10.1 (0.4) *	0.03 (0.01)	37.3 (12.9)	2.5 (0.9)	0.3 (0.1) *
	Right	0.5 (0.1) *	0.4 (0.1) *	10.6 (1.0) *	0.04 (0.01)	28.9 (14.6)	1.9 (1.0)	0.2 (0.1) *
l.DDF	Left	2.0 (0.1) *	1.8 (0.1) *	10.2 (0.3) *	0.18 (0.01) *	19.2 (2.2)	1.3 (0.2)	0.1 (0.0) *
	Right	2.2 (0.3) *	1.9 (0.2) *	10.4 (0.5) *	0.19 (0.02) *	17.8 (4.1)	1.2 (0.3)	0.1 (0.0) *

Greyhound left and right limb gastrocnemius muscles had significantly higher PCSAs ($p < 0.050$ for all muscles), F_{max} values (all $p \leq 0.024$) and estimated power outputs (all $p \leq 0.033$) than the corresponding SBT muscles, as did the right SDF (all $p \leq 0.041$) and l.DDF (all $p \leq 0.023$) muscles. Additionally, Greyhound muscles had significantly longer belly lengths than the SBT (all $p \leq 0.006$). When muscle fascicle lengths were compared only the right m.DDF was significantly longer in Greyhounds compared to SBTs ($p = 0.040$). Architectural Index values were significantly lower in left and right limb Greyhound MG (all $p \leq 0.049$) and SDF muscles (all $p \leq 0.018$) and in the right l.DDF muscle ($p = 0.018$), compared to the corresponding SBT muscles. Architectural Index data from the right limbs can be seen in Figure 5.6; the pattern for the left limbs is similar.

Figure 5.6: Architectural Index for MG, LG, SDF, m.DDF and l.DDF muscles from Greyhounds (clear) and SBTs (hatched). Error bars are standard error of the mean (SEM). * denotes a significant difference between the two breeds of dog; $p < 0.05$.

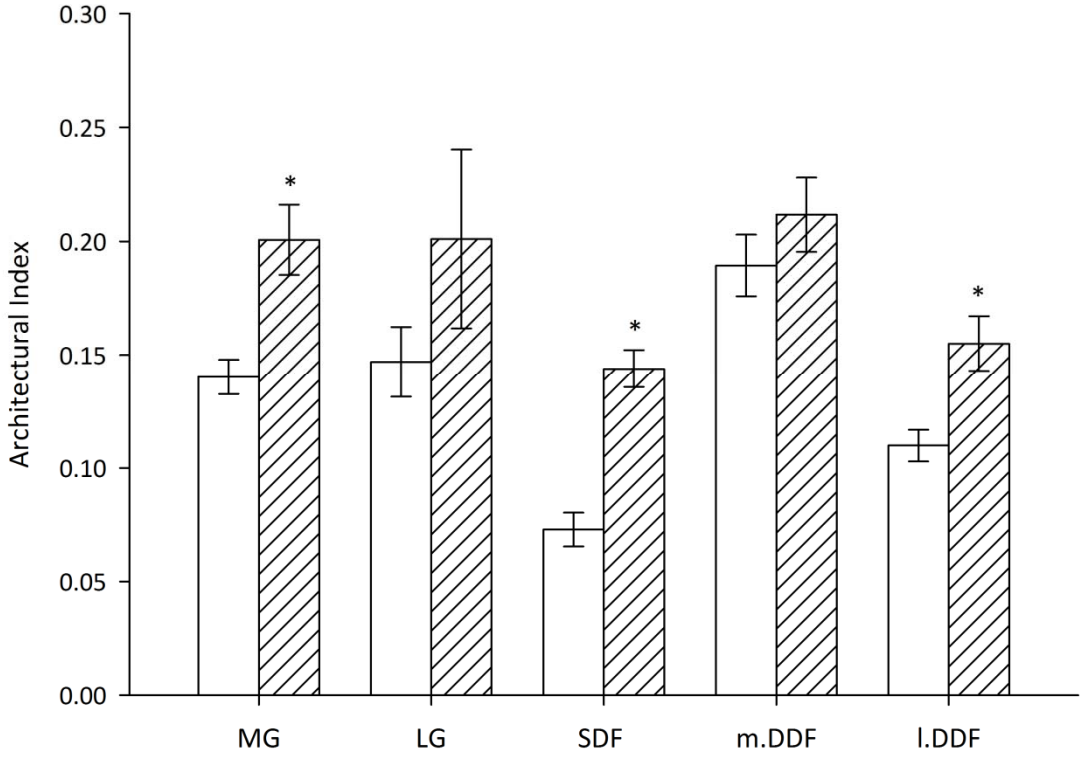

All Greyhound tendons had significantly longer resting lengths than the corresponding SBT tendons (all $p \leq 0.001$). Greyhound SDF and l.DDF tendons had significantly higher masses, volumes and CSA_ts than the SBT SDF and l.DDF tendons (all $p \leq 0.037$). Due to the left-to-right asymmetry, only the left Greyhound m.DDF tendons had significantly higher masses and volumes than the SBT m.DDF tendons (all $p \leq 0.001$). Predicted tendon stresses, strains and length changes were calculated using a value of tendon stiffness of 1500 MPa (Bennett *et al.* 1986; Ker *et al.* 1988). Greyhound and SBT tendons were predicted to experience similar stresses and strains. However, Greyhound l.DDF and SDF tendons were predicted to undergo significantly longer length changes than SBT tendons (all $p \leq 0.046$). All Greyhound MTUs had lower FLF values than SBT MTUs; the Greyhound SDF MTUs (both sides) had values < 2 indicating they may act effectively as springs (Ker *et al.* 1988; Pollock and Shadwick 1994).

5.4.4 Tendon mechanical properties

Data measured and calculated from the pull-to-failure tests can be found in Table 5.4 and Table 5.5.

5.4.5 Left to right asymmetries in tendon mechanical properties

There were no significant left-to-right asymmetries in any of the mechanical properties of the SBT tendons. There were also no significant asymmetries in the mechanical properties of Greyhound m.DDF tendons; however, the left limb Greyhound SDF ($p = 0.027$) and l.DDF ($p = 0.043$) tendons yielded at significantly higher loads than the right limb tendons. Additionally, the left limb Greyhound l.DDF tendons yielded at significantly higher breaking stresses ($p = 0.003$) and were significantly stiffer ($p < 0.001$) than the right l.DDF tendons.

Table 5.4: Mean (SEM) values for hysteresis (%) at 2, 3, 4 and 5% strain for Greyhound and SBT digital flexor tendons. No left-to-right asymmetries were found in Greyhounds or SBTs. * denotes a significant difference between the two breeds of dog; $p < 0.05$.

Tendon	Side	Hysteresis (%) at			
		2% Strain	3% Strain	4% Strain	5% Strain
Greyhound:					
SDF	Left	8.7 (0.4)	11.4 (0.3) *	12.2 (0.3) *	12.5 (0.3) *
	Right	8.7 (0.3)	12.2 (0.4) *	13.1 (0.5) *	12.8 (0.5) *
m. DDF	Left	14.3 (0.7)	14.6 (0.1)	-	-
	Right	14.7 (0.6)	13.4 (1.3)	-	-
l.DDF	Left	11.8 (0.4)	14.6 (0.3) *	15.4 (0.5) *	15.9 (0.5) *
	Right	12.4 (0.7)	15.6 (0.6) *	16.3 (0.7) *	16.6 (1.2) *
SBT:					
SDF	Left	9.1 (0.3)	12.7 (0.3) *	14.0 (0.4) *	14.6 (0.4) *
	Right	8.8 (0.5)	12.1 (0.4) *	13.6 (0.4) *	14.3 (0.4) *
m. DDF	Left	14.7 (0.6)	15.2 (0.2)	-	-
	Right	14.3 (1.1)	15.3 (0.3)	-	-
l.DDF	Left	11.7 (0.7)	16.6 (0.7) *	18.0 (0.7) *	18.7 (0.9) *
	Right	10.6 (0.7)	14.7 (0.7) *	16.6 (0.6) *	17.5 (0.7) *

Table 5.5: Mean (SEM) values for UTS, breaking stress and Young's Modulus (stiffness), for Greyhound and SBT digital flexor tendons. † denotes a significant difference between the left and right limbs of a breed; $p<0.05$. * denotes a significant difference between the two breeds of dog; $p < 0.05$.

Tendon	Side	UTS (N)	Breaking Stress (MPa)	Young's Modulus (MPa)
Greyhound:				
SDF	Left	1204.4 (41.9) † *	63.8 (5.4)*	743.1 (50.4) *
	Right	1148.7 (33.1) † *	60.1 (6.4)*	667.3 (45.3) *
m. DDF	Left	188.1 (14.1)	112.5 (11.1) *	1504.0 (107.6)
	Right	190.8 (16.4)	111.9 (11.5) *	1564.6 (130.8)
l.DDF	Left	1219.8 (81.9) † *	83.8 (4.7) †	1117.6 (30.1) †
	Right	1163.6 (75.1) † *	76.8 (4.8) †	993.0 (36.9) †
SBT:				
SDF	Left	649.9 (71.2) *	42.8 (2.7) *	467.2 (19.7) *
	Right	739.5 (18.8) *	50.6 (5.0)*	515.1 (34.8) *
m. DDF	Left	169.1 (9.9)*	158.8 (12.3) *	1883.8 (233.2)
	Right	152.8 (17.1)	137.4 (28.5) *	2004.4 (479.8)
l.DDF	Left	663.8 (44.8) *	80.4 (6.1)	953.9 (138.8)
	Right	673.8 (24.4) *	74.8 (5.8)	876.2 (81.3)*

5.4.6 Breed comparison of tendon mechanical properties

There were no significant differences in hysteresis between the Greyhound and SBT m.DDF tendons. Hysteresis was significantly lower in Greyhound SDF tendons (left limb) compared to the ipsilateral SBT SDF tendons at 3% ($p = 0.011$), 4% ($p = 0.004$) and 5% ($p = 0.002$) strain (Figure 5.7). Hysteresis was also significantly lower in Greyhound l.DDF tendons (left limb) compared to the ipsilateral SBT tendons at 3% ($p = 0.019$), 4% ($p = 0.013$) and 5% ($p = 0.017$) strain (Figure 5.8)

Greyhound SDF tendons had significantly higher UTS values (left and right limbs; all $p < 0.001$) and breaking stresses (left limb; $p = 0.008$) than SBT SDF tendons. Examples of typical breaking stress curves for Greyhound and SBT SDF tendons can be seen in Figure 5.9. Greyhound m.DDF tendons (left limb) had significantly lower breaking stresses than the ipsilateral SBT tendons ($p = 0.038$) and Greyhound l.DDF tendons yielded at significantly higher loads than SBT l.DDF tendons ($p < 0.001$).

There were no significant differences in stiffness between the Greyhound and SBT m.DDF and l.DDF tendons. Both the left ($p < 0.001$) and right ($p = 0.02$) SDF tendons from Greyhounds were significantly stiffer than the SDF tendons from SBTs.

Figure 5.7: Typical stress-strain curves for Greyhound (solid line) and SBT (dashed line) SDF tendons (left limb) cycled sinusoidally to (a) 3%: Mean hysteresis was 11.4% for Greyhound tendons and 12.7% for SBT tendons, (b) 4%: Mean hysteresis was 12.2% for Greyhounds and 14.0% for SBTs, and (c) 5% strain: Mean hysteresis was 12.5% for Greyhounds and 14.6% for SBTs. Greyhounds tendons had significantly lower hysteresis values at all strains compared to SBT.

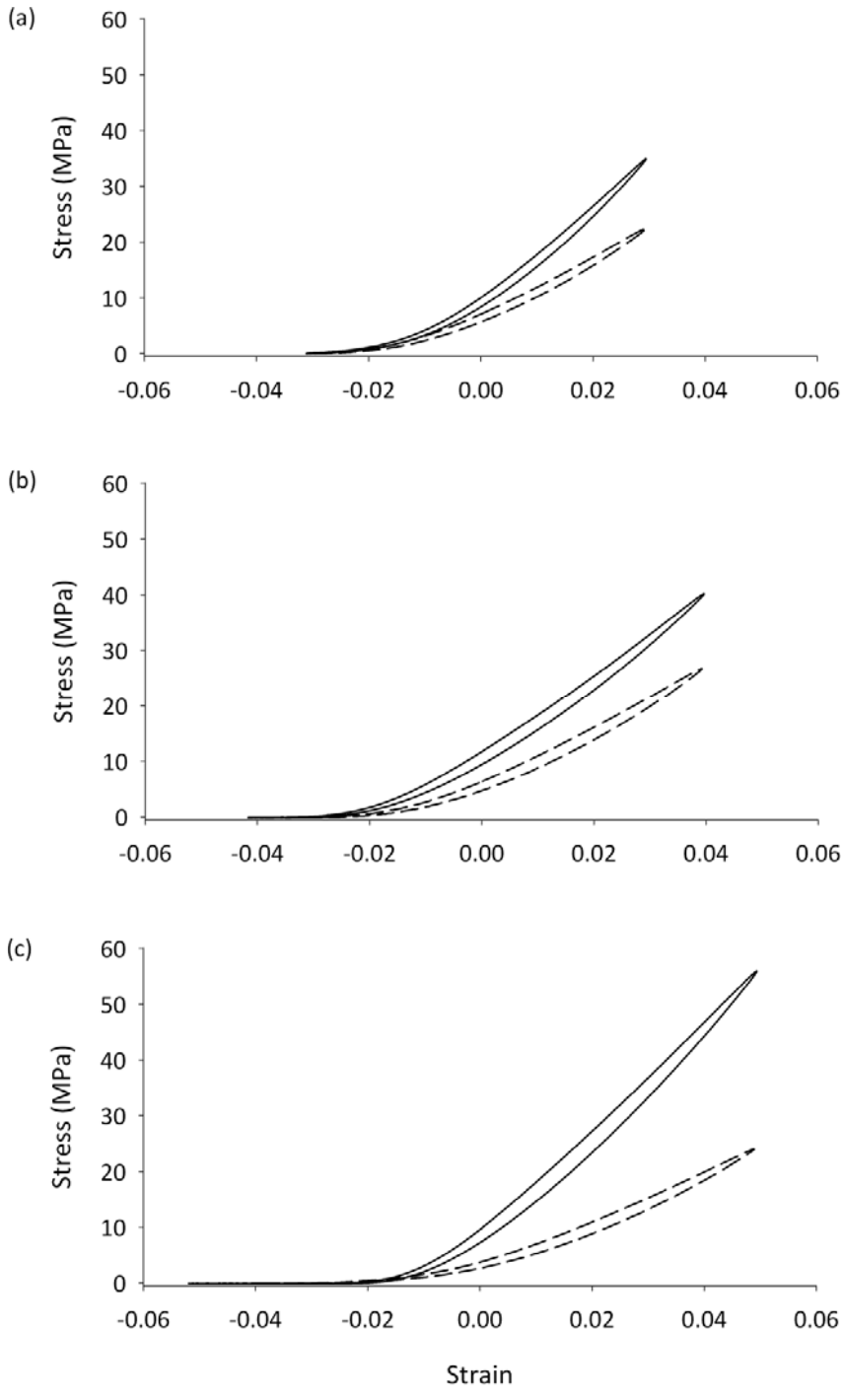

Figure 5.8: Typical stress-strain curves for Greyhound (solid line) and SBT (dashed line) l.DDF tendons (left limb) cycled sinusoidally to (a) 3%: Mean hysteresis was 14.6% for Greyhound tendons and 16.6% for SBT tendons; (b) 4%: Mean hysteresis was 15.4% for Greyhounds and 18.0% for SBTs, and (c) 5% strain: Mean hysteresis was 15.9% for Greyhounds and 18.7% for SBTs. Greyhounds tendons had significantly lower hysteresis values at all strains compared to SBT.

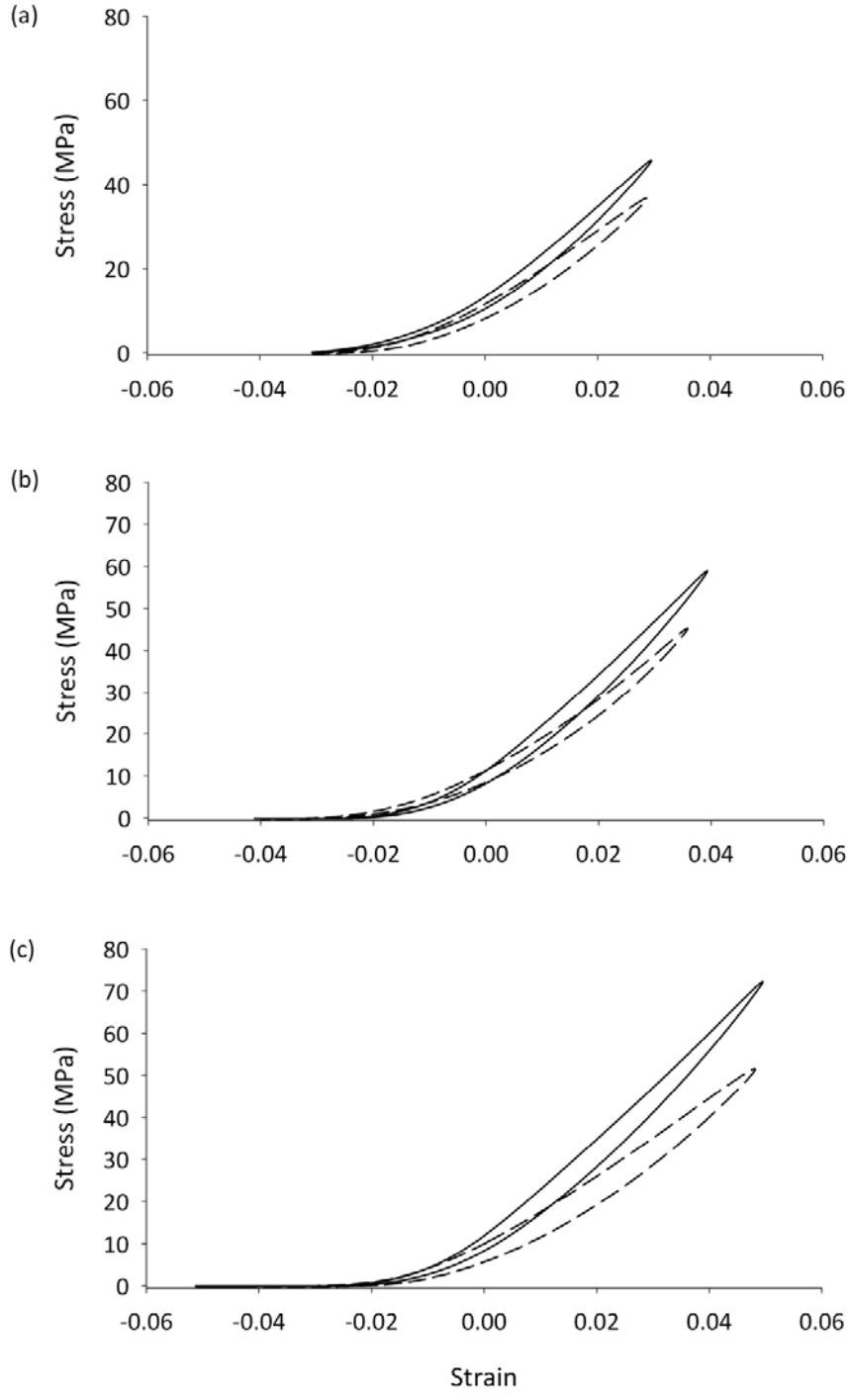

Figure 5.9: Typical curves for Greyhound (solid line) and SBT (dashed line) SDF tendons (left limb), which have been pulled at a rate of 1mm/s until yielding. Mean breaking stress for Greyhound SDF tendons was 64.0 MPa and for SBT tendons was 42.8 MPa. In this example the Greyhound SDF tendon yielded at 78.5 MPa and the SBT at 41.9 MPa.

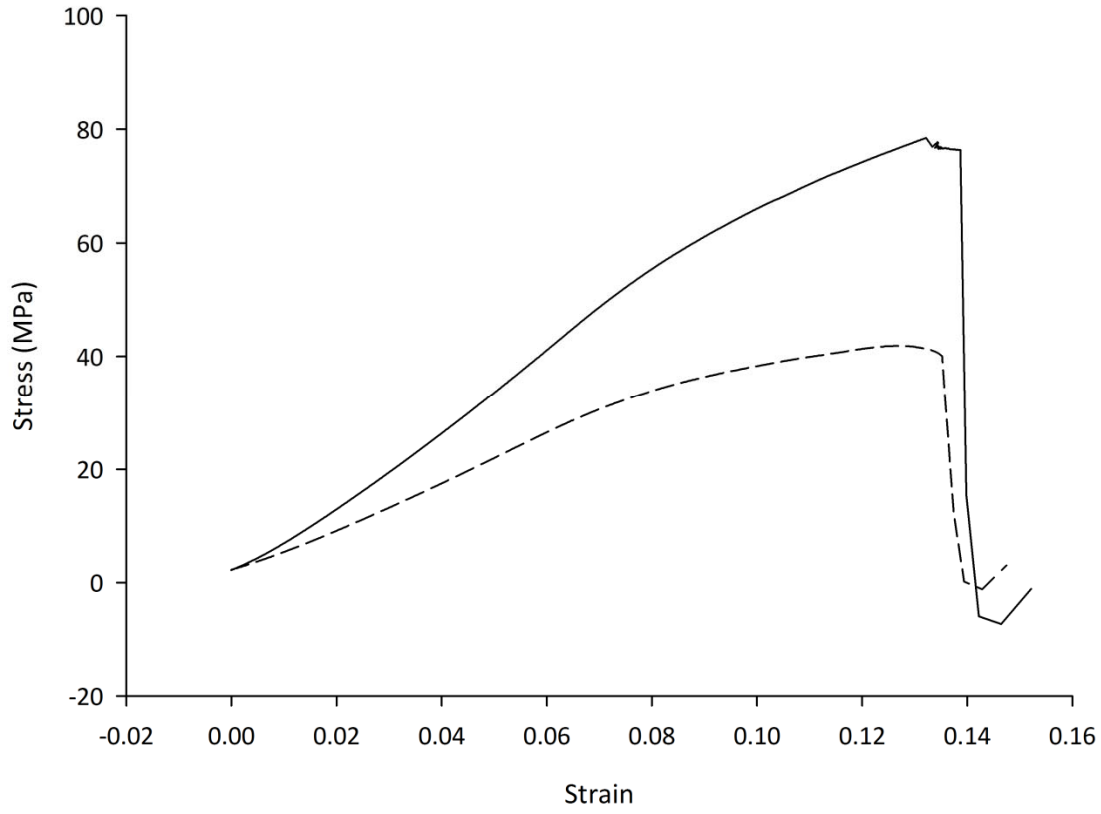

PART B: THORACIC DISTAL LIMB TENDONS

5.5 Materials and methods

5.5.1 Tendon specimens

Distal thoracic limbs were collected from 10 racing Greyhounds (seven male, three female) euthanatized at their owners request after sustaining a right tarsal fracture during a race (eight dogs) or due to severe behavioural problems preventing them from being re-homed (two dogs). Mean age of the dogs was 2.88 ± 0.37 years; mean weight was 29.88 ± 2.68 kg. Limbs were also collected from nine SBTs (seven male, two female) euthanatized and donated from a local dog pound when extreme behavioural problems prevented them from being re-homed. Age was unknown; mean weight was 16.90 ± 2.26 kg. The deep digital flexor (t.DDF) and superficial digital flexor (t.SDF) tendons were dissected out from the thoracic limbs and stored at -20 °C until required for testing, at which point the tendons were thawed at room temperature.

5.5.2 Muscle-tendon architecture

Five pairs of Greyhound, and four pairs of SBT, distal thoracic limbs were initially used for measurements of the MTU architecture. The t.SDF and t.DDF tendons, and the muscles they connect to, were systematically removed from the limbs as detailed in section 5.3.2. The t.DDF has three heads of origin. The tendons of these three heads fuse at the carpus to form a single tendon, therefore, muscle mass was calculated as the combined mass of the three heads.

5.5.3 Tendon preparation and clamping

Tendons were prepared by air-drying the ends while the rest of the tendon was wrapped first in blue roll moistened with distilled water and then wrapped in cling film.

5.5.4 Mechanical tests

An Instron E3000 ElectropulsTM servo-electric materials testing machine (Instron, UK) was used for all tests; details can be found in section 5.3.4. Pelvic limb tendons showed no asymmetries or breed differences at 2 and 3% strain, therefore, tendons were cycled sinusoidally at 2.0Hz to 4 and 5% strain. Data was collected in the same way as for the pelvic tendons; details can be found in section 5.4.3. Following the dynamic tests, tendons were tested to failure by stretching the tendons at a rate of 1mm/s until they broke or yielded irreversibly.

5.5.5 Measurements and calculations

Details of the measurements taken and calculations used can be found in section 5.3.5.

5.5.6 Statistics

The mean and standard deviation were calculated for each parameter. The effect of side (left versus right) on each parameter was examined using a two-tailed paired t-test (significance set at $p < 0.05$). The effect of breed (Greyhound versus SBT) on each parameter for each limb (left or right) was examined using a two-tailed un-paired t-test (significance set at $p < 0.05$).

5.6 Results

5.6.1 Muscle-tendon anatomy and architectural properties

The muscles that attach to the SDF and DDF tendons in the thoracic limb were considered (Figure 5.10). Measured and calculated architectural parameters for each of the muscles are given in Table 5.6 and for each tendon in Table 5.7.

Figure 5.10: Palmar view of a canine distal thoracic limb showing the muscles and tendons of interest. Only the ulnar head of the DDF is visible. The humeral and radial heads are out-of-view behind the SDF and other more superficial muscle-tendon units. Adapted from Evans and DeLahunta (1971).

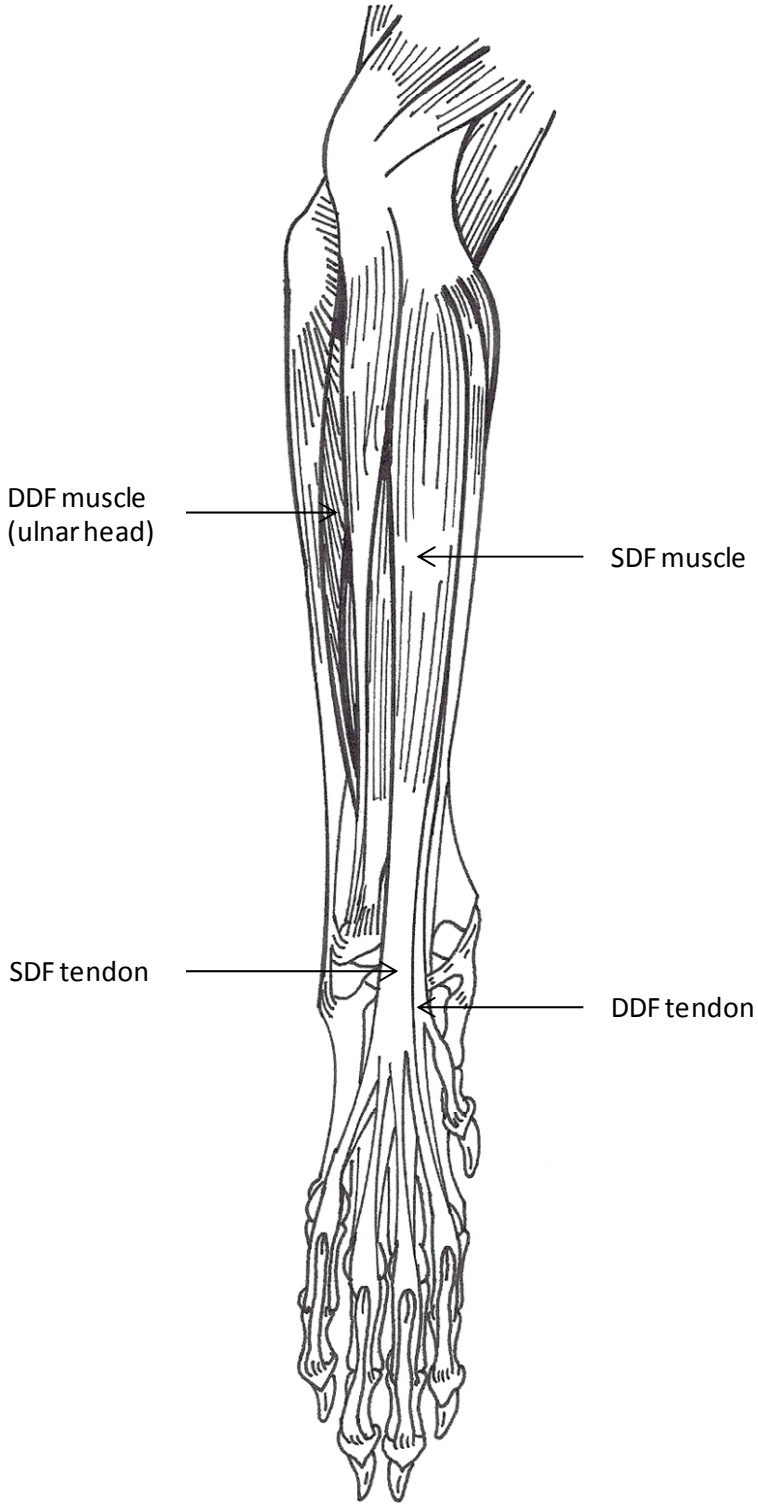

Table 5.6: Muscle data for the thoracic SDF and DDF muscles: Mean (SEM) muscle mass, belly length, fascicle length, physiological cross-sectional area (PCSA), pennation angle, and estimated maximum isometric force (F_{max}) and power. No left-to-right asymmetries were found in Greyhounds or SBTs. * denotes a significant difference between the two breeds of dog; $p < 0.05$.

Muscle	Side	Mass (g)	Belly Length (cm)	Fascicle Length (cm)	PCSA (cm^2)	Pennation Angle (°)	F_{max} (N)	Corrected F_{max} (N)	Power (W)
Greyhound:									
t.SDF	Left	17.7 (1.0) *	20.0 (0.4) *	1.0 (0.1)	16.9 (0.8) *	35.0 (2.3)	507.6 (24.1) *	415.5 (27.1) *	1.9 (0.1)*
	Right	17.0 (1.4) *	20.8 (0.7) *	1.0 (0.0)	15.6 (1.1) *	35.2 (1.0)	469.3 (32.8) *	382.9 (26.3) *	1.8 (0.2) *
t.DDF	Left	53.7 (3.1) *	22.6 (1.1) *	1.5 (0.1)	33.5 (2.3) *	25.0 (2.1)	1005.0 (69.6) *	907.9 (61.4) *	5.8 (0.3) *
	Right	53.2 (4.1) *	21.7 (1.0) *	1.4 (0.1)	36.3 (2.3) *	32.6 (1.4)	1089.6 (68.9) *	915.3 (52.8) *	5.7 (0.4) *
SBT:									
t.SDF	Left	12.7 (0.6) *	12.2 (0.3) *	1.0 (0.1)	12.1 (0.9) *	33.6 (2.7)	363.6 (28.2) *	304.2 (30.4) *	1.4 (0.1) *
	Right	12.6 (0.7) *	12.0 (0.4) *	1.0 (0.1)	12.2 (1.2) *	30.6 (1.9)	364.5 (36.7) *	315.1 (34.4) *	1.4 (0.1) *
t.DDF	Left	24.3 (1.9) *	12.4 () *	1.6 (0.2)	15.0 (1.0) *	30.6 (2.7)	448.8 (30.9) *	382.3 (23.5) *	2.6 (0.2) *
	Right	23.0 (1.1) *	12.6 () *	1.4 (0.1)	16.0 (1.2) *	29.3 (1.9)	479.1 (34.9) *	417.5 (33.2) *	2.5 (0.1) *

Table 5.7: Thoracic tendon data: Mean (SEM) mass, volume, and resting length, and estimated cross-sectional area (CSA_t), stress, strain, and length change. No left-to-right asymmetries were found in Greyhounds or SBTs. * denotes a significant difference between the two breeds of dog; $p < 0.05$.

Tendon	Side	Mass (g)	Volume (cm^3)	Resting Length (cm)	CSA_t (cm^2)	Stress (MPa)	Strain (%)	Length Change (cm)
Greyhound:								
t.SDF	Left	2.1 (0.2)*	1.9 (0.2)*	9.4 (0.3) *	0.20 (0.01) *	26.2 (2.3) **	1.8 (0.2) *	0.16 (0.01) *
	Right	2.0 (0.3)*	1.8 (0.2)*	9.0 (0.4) *	0.20 (0.03) *	23.9 (2.0) **	1.6 (0.1) *	0.14 (0.01) *
t.DDF	Left	2.4 (0.2) *	2.2 (0.2) *	8.2 (0.0) *	0.27 (0.02) *	39.2 (5.6) **	2.6 (0.4) *	0.21 (0.03) *
	Right	2.7 (0.2) *	2.4 (0.1) *	8.5 (0.3) *	0.28 (0.01) *	39.4 (2.9) **	2.6 (0.2) *	0.22 (0.02) *
SBT:								
t.SDF	Left	1.7 (0.2)*	1.5 (0.1) *	6.1 (0.4) *	0.25 (0.01) *	14.7 (1.0) **	1.0 (0.1) *	0.06 (0.01) *
	Right	1.7 (0.2)*	1.5 (0.2) *	6.5 (0.4) *	0.23 (0.02) *	16.8 (2.6) **	1.1 (0.2) *	0.07 (0.01) *
t.DDF	Left	2.3 (0.2)*	2.0 (0.2) *	6.6 (0.6) *	0.29 (0.01) *	15.4 (1.6) **	1.0 (0.1) *	0.07 (0.01) *
	Right	1.9 (0.2)*	1.7 (0.2) *	6.4 (0.5) *	0.26 (0.01) *	19.0 (2.1) **	1.3 (0.1) *	0.08 (0.01) *

5.6.2 Left to right asymmetries in muscle-tendon properties

There were no left-to-right asymmetries present in any of the architectural properties of thoracic MTUs from Greyhounds or SBTs.

5.6.3 Breed differences in muscle-tendon properties

Greyhound t.SDF and t.DDF muscles were significantly heavier compared to SBTs, even after being normalised relative to total body mass ($p \leq 0.019$ for all muscles). Greyhound muscles had significantly higher PCSAs, F_{max} values and estimated power outputs than SBT muscles (all $p \leq 0.013$). Additionally, Greyhound muscles had significantly longer belly lengths (all $p < 0.001$). When muscle fascicle lengths were compared, no breed differences were found. Architectural Index values were significantly lower in the Greyhound muscles compared to the corresponding SBT muscles (all $p \leq 0.033$) (Figure 5.11).

Figure 5.11: Architectural Index for left limb thoracic SDF and DDF muscles from Greyhounds (clear) and Staffies (hatched). Error bars are standard error of the mean (SEM). * denotes a significant difference between the two breeds of dog; $p < 0.05$.

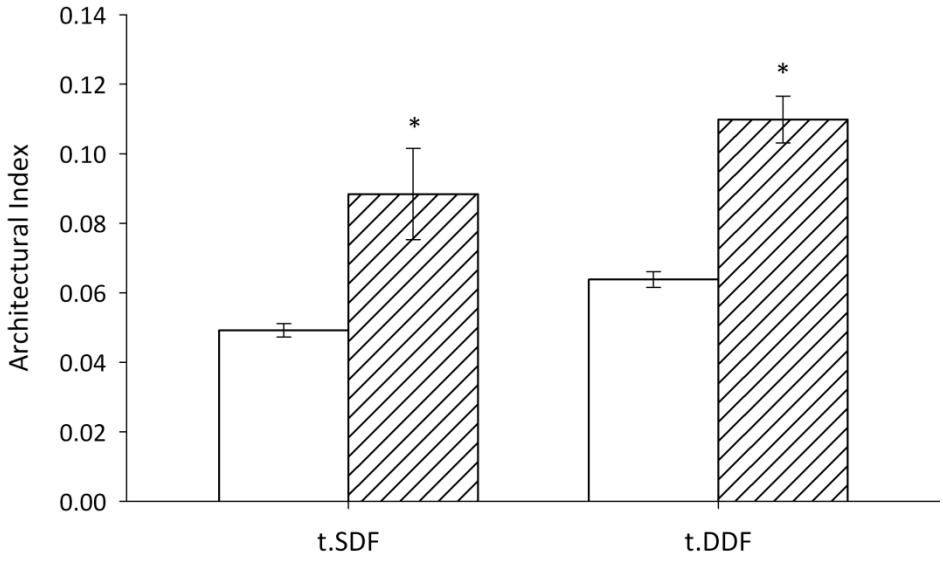

Greyhound t.SDF and t.DDF tendons had significantly longer resting lengths than SBT tendons (all $p \leq 0.033$). The tendons were of similar masses; only the right Greyhound t.DDF was significantly heavier ($p = 0.029$) and had a greater volume (all $p = 0.029$) than the corresponding SBT tendon. Greyhound tendons were predicted to experience higher stresses and strains, and undergo significantly longer length changes (all $p \leq 0.002$). CSA_ts were similar in both breeds; only the left t.SDF from SBTs had a significantly larger CSA_t than the corresponding Greyhound tendon ($p = 0.011$). FLF values were calculated for each MTU. Greyhound t.SDF (left limb; $p = 0.038$) and t.DDF (both limbs; all $p \leq 0.047$) MTUs had significantly lower FLF values than the SBT MTUs (Figure 5.12); however, both Greyhound and SBT thoracic MTUs had FLF values greater than 4 indicating the MTUs are designed for the control of joint displacement and force transmission (Ker *et al.* 1988; Pollock and Shadwick 1994).

Figure 5.12: FLF values for thoracic SDF and DDF MTUs from the left limbs of Greyhounds (clear) and Staffies (hatched). The pattern for the right limbs is similar. * denotes a significant difference between the two breeds of dog; $p < 0.05$.

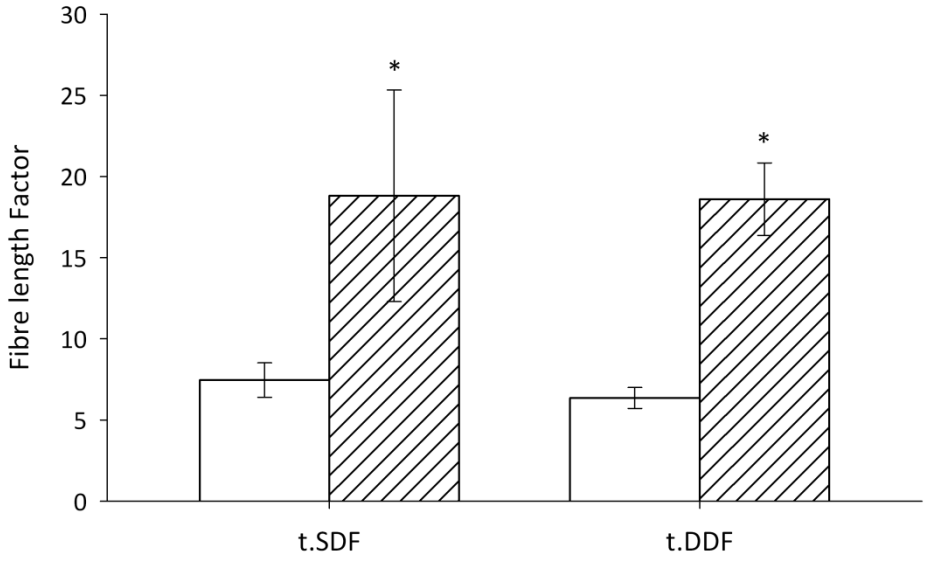

5.6.4 Tendon mechanical properties

Data calculated from the pull-to-failure tests can be found in Table 5.8.

5.6.5 Left to right asymmetries in tendon mechanical properties

There were no significant left-to-right asymmetries in any of the mechanical properties of any of the Greyhound or SBT distal thoracic limb tendons.

5.6.6 Breed comparison of tendon mechanical properties

Greyhound and SBT t.SDF tendons did not differ significantly in their hysteresis values. The Greyhound t.SDF tendons yielded at significantly higher loads than the corresponding SBT tendons (all $p \leq 0.045$). When the UTS values were corrected for CSA_t, Greyhound t.SDF tendons were still significantly stronger than the SBT tendons (all $p \leq 0.046$). Greyhound t.SDF tendons were also significantly stiffer than SBT tendons (all $p \leq 0.014$).

Left limb Greyhound t.DDF tendons had significantly higher hysteresis values than the corresponding SBT tendons at both 4% ($p = 0.026$) and 5% ($p = 0.027$) strain (Figure 5.13). Greyhound t.DDF tendons yielded at significantly higher loads than the corresponding SBT tendons (all $p \leq 0.011$). When CSA_t was accounted for, Greyhound tendons were still significantly stronger than the SBT tendons (all $p \leq 0.016$). Right limb Greyhound t.DDF tendons were also significantly stiffer than the corresponding SBT tendons ($p = 0.015$).

Table 5.8: Mean (SEM) values for hysteresis, UTS, breaking stress and Young's Modulus (stiffness), for Greyhound and SBT thoracic digital flexor tendons. No left-to-right asymmetries were found in Greyhounds or SBTs. * denotes a significant difference between the two breeds of dog; $p < 0.05$.

Tendon	Side	Hysteresis (%) at		UTS (N)	Breaking Stress (MPa)	Young's Modulus (MPa)
		4% strain	5% strain			
Greyhound:						
t.SDF	Left	16.7 (0.6)	18.6 (0.6)	840.0 (45.8) *	53.9 (4.5) *	545.3 (37.6) *
	Right	17.6 (0.4)	18.5 (0.6)	780.4 (37.8) *	48.0 (7.6) *	562.5 (87.1) *
t.DDF	Left	20.6 (0.4) *	20.8 (0.3) *	1232.3 (54.8) *	54.2 (2.7) *	663.9 (40.7) *
	Right	20.3 (0.7) *	20.1 (0.4) *	1187.7 (51.6) *	52.7 (2.5) *	631.6 (43.6) *
SBT:						
t.SDF	Left	16.8 (1.1)	20.0 (2.2)	676.4 (57.5) *	39.3 (4.0) *	353.7 (47.4) *
	Right	16.5 (0.4)	18.0 (0.7)	614.8 (71.4) *	29.3 (1.9) *	289.1 (16.5) *
t.DDF	Left	18.6 (0.8) *	18.8 (0.7) *	915.9 (61.0) *	41.4 (3.6) *	534.2 (57.8) *
	Right	18.3 (0.6) *	19.5 (0.7) *	927.7 (67.3) *	39.7 (2.4) *	449.2 (51.4) *

Figure 5.13: Typical stress-strain curves for Greyhound (solid line) and SBT (dashed line) t.DDF tendons (left limb) cycled sinusoidally at 2Hz to 4 and 5% strain. Typical curves at (a) 4% strain: Greyhound SDF tendons had a mean hysteresis of 20.6% compared to 18.6% for SBT tendons, and (b) 5% strain: Greyhound SDF tendons had a mean hysteresis of 20.8% compared to 18.8% for SBT tendons. Greyhound tendons had significantly higher hysteresis values compared to SBT tendons at both 4 and 5% strain.

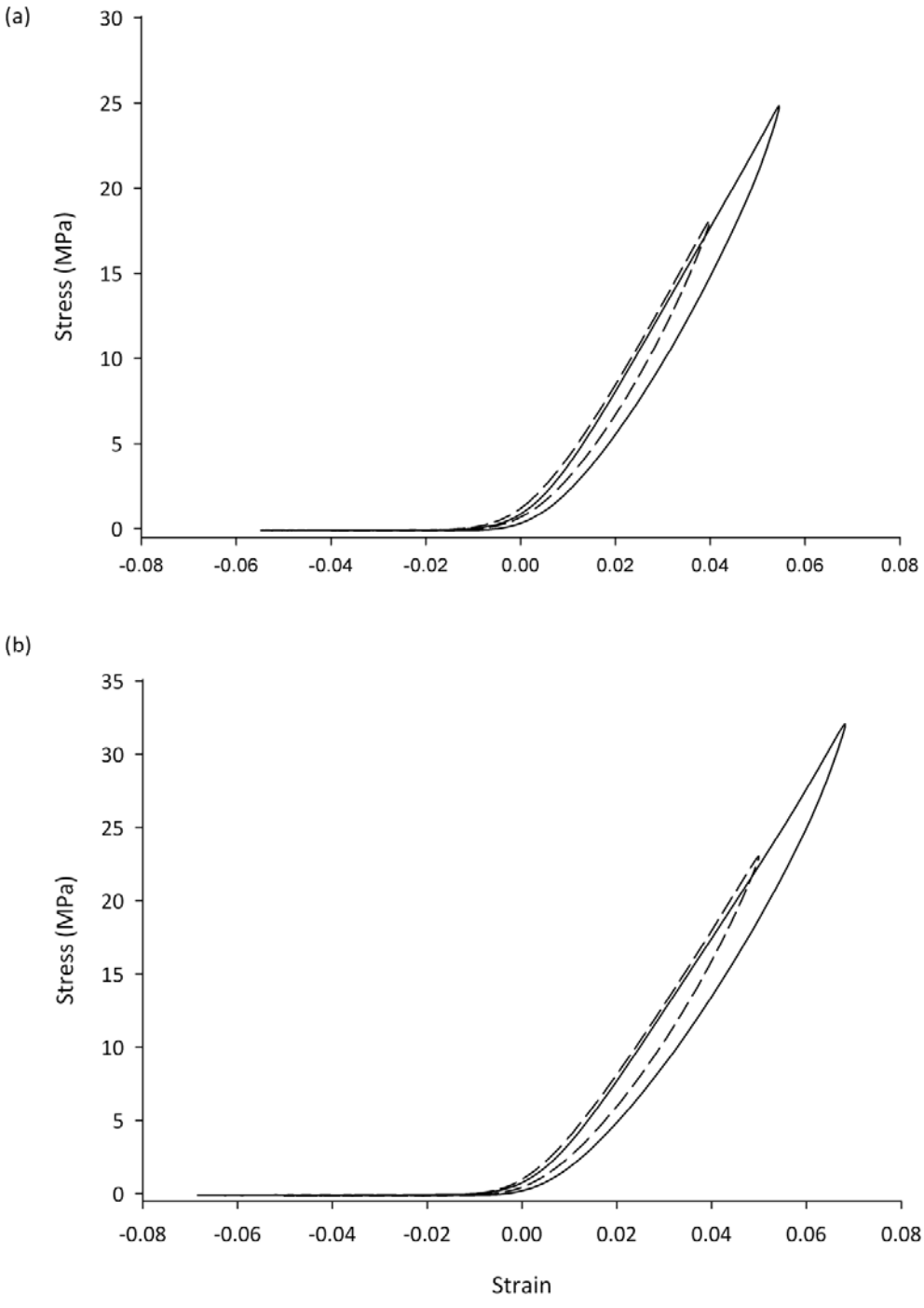

5.7 Discussion

5.7.1 Muscle-tendon architecture

Asymmetries in muscle-tendon architecture

The left pelvic digital flexors of Greyhounds were found to be stronger and stiffer than the right (Table 5.5). Increases in tendon stiffness and strength following long-term exercise could be attributed to tendon hypertrophy; however, current literature does not provide conclusive evidence to support this idea. Indeed, there is evidence to the contrary: exercise and training appear to have no effect on the dry weight of rat patella tendons (Vailas *et al.* 1985), the fresh or dry weights of rabbit distal limb tendons (Viidik 1967) or on the fresh weight of Guinea fowl Achilles tendon (Buchanan and Marsh 2001). Greyhounds have no left-to-right differences in size, nor any other property of muscle-tendon architecture. Therefore the increased stiffness and strength of the left pelvic digital flexors cannot be a result of hypertrophy of the left MTUs.

Breed differences in muscle-tendon architecture

The distal pelvic limb muscles of fast running quadrupeds, such as horses (Payne *et al.* 2005), hares (Williams *et al.* 2007a) and Greyhounds (Williams *et al.* 2008b), appear to be specialised for high force production. Within a species, breeds adapted for high acceleration tend to have muscles with larger PCSAs that are capable of producing greater forces than breeds adapted for traits such as endurance (Crook *et al.* 2008) or breeds that are not bred for a specific task (Williams *et al.* 2008b). Greyhound MTU architecture was comparable with previous studies by Williams *et al.* (2008a) and Williams *et al.* (2008b); SBT MTU architecture has not been studied before. We found that predicted “in-life” stresses and strains were higher for the Greyhound distal limb MTUs than they were for the SBT MTUs (Table 5.3 and 5.7) ranging from 21 MPa and 1.4% (l.DDF) to 77 MPa and 5.3% (SDF)

for the Greyhounds, compared to 19 MPa and 1.3% (l.DDF) to 66 MPa and 4.4% (SDF) for the SBTs. This is likely an adaptation for the Greyhound digital flexors to withstand the increased forces that are encountered during high speed running (Biewener 1998). We found that Greyhounds have distal limb muscles (both pelvic and thoracic) with larger PCSAs that are capable of producing greater forces than SBTs (Table 5.1, 5.2 and 5.6). Architectural index values were lower in the Greyhound pelvic and thoracic MTUs compared to SBTs (Figure 5.6 and 5.11), indicating the Greyhound muscles have relatively shorter muscle fascicles with a higher capacity for force generation. Therefore, Greyhounds seem to be well adapted for high acceleration with distal limb muscles that are able to produce greater forces and more power compared to SBTs. The distal pelvic limbs of fast running quadrupeds also appear specialised for the storage and recovery of elastic strain energy (Pasi and Carrier 2003; Payne *et al.* 2005; Williams *et al.* 2007a; Williams *et al.* 2008b). The FLF was calculated for each MTU of interest. FLF is the ratio of muscle fibre length to tendon length change (Ker *et al.* 1988; Pollock and Shadwick 1994). A value below 2 indicates MTUs are adapted for the storage and recovery of elastic strain energy, between 2 and 4 indicates an intermediate role and a value above 4 indicates the MTUs are adapted for force transmission and control of joint displacement (Ker *et al.* 1988; Pollock and Shadwick 1994). All Greyhound pelvic limb MTUs had FLF values lower than the SBTs, indicating SBT MTUs are designed more for limb control while the Greyhounds' MTUs are somewhat better designed for elastic energy storage; however, only the Greyhound SDF had a FLF value less than 2; which suggests that the Greyhound SDF has a more important role in the storage and recovery of elastic strain energy. This is consistent with previous studies comparing the Greyhound to other non-racing breeds of dog (Pasi and Carrier 2003; Williams *et al.* 2008b). In both Greyhounds and SBTs, the thoracic digital flexor tendons were shorter than their equivalent tendons in the pelvic limb and both breeds show little potential for elastic energy storage compared to their equivalents in the pelvic limb. All

Greyhound and SBT thoracic limb MTUs have FLF values above 4, and Greyhounds have significantly higher FLF values compared to SBTs (Figure 5.12). This data indicates that, in both breeds, the thoracic MTUs are involved in limb control allowing greater limb support and increased manipulative ability. This is consistent with previous studies on the thoracic limb of Greyhounds (Williams *et al.* 2008a) and hares (Williams *et al.* 2007b). The similarities between the thoracic limb MTUs of Greyhounds and SBTs could be explained by the role that the thoracic limbs play. Originally, Greyhounds were bred to chase highly manoeuvrable prey such as hares and rabbits. Nowadays they are bred to race around ovoid tracks with relatively sharp bends. It seems sensible that the thoracic limbs are designed for steering and the tendons adapted to provide increased limb control enhancing the Greyhound's manoeuvrability and cornering ability. SBTs were originally bred for bull-baiting and dog fighting, during which they would use their thoracic limbs to grapple with an opponent. Presumably increased control of the thoracic limbs would help with their balance, agility and opponent manipulation. Retaining manipulative ability in the thoracic limb may also be beneficial for other tasks that both breeds of dog would perform such as mating.

5.7.2 Asymmetries in the mechanical properties of Greyhound tendons

Several sports impose unilateral loads on the limb bones of human athletes, leading to left-to-right asymmetries in bone mineral density at skeletal sites experiencing the greater loads (Haapasalo *et al.* 1994; Haapasalo *et al.* 1998; Haapasalo *et al.* 1996; Huddleston *et al.* 1980; Sone *et al.* 2006). Similarly, left-to-right differences in bone density have been reported in the distal limb bones of racing Greyhounds (Emmerson *et al.* 2000; Hercock *et al.* 2008; Johnson *et al.* 2000; Lipscomb *et al.* 2001). Left-to-right asymmetries have also been reported in muscle strength of athletes taking part in sports such as football (Rahnama *et al.* 2005) and volleyball (Wang and Cochrane 2001). Rahnama *et al.* (2005)

found the knee flexor muscles of the leg football players preferred to kick the ball with were weaker than those of the contralateral leg. In a similar study on volleyball players, Wang and Cochrane (2001) reported eccentric muscle strength was weaker in shoulder rotator muscles of the dominant arm of volleyball players. We found asymmetries in UTS, breaking stress and Young's modulus (stiffness) values of the Greyhound SDF and l.DDF tendons: the left limb tendons were stronger and stiffer. To our knowledge, this is the first time left-to-right asymmetries have been reported in the tensile properties of tendons from athletes that experience asymmetric stresses. It is well established that long term physical activity improves the tensile mechanical properties of tendons demonstrated by increases in UTS and stiffness (Buchanan and Marsh 2001; Reeves *et al.* 2003; Vilarta and Vidal Bde 1989; Woo *et al.* 1980). The Greyhound's left limbs (that are closest to the inside of the Greyhound track) are thought to experience higher stresses during racing because the dogs are always raced in the same direction around ovoid tracks. There is a 64.5% increase in the forces acting on the limbs when the dogs enter a bend (Usherwood and Wilson 2005). Therefore, any asymmetrical loading experienced is likely to be increased when the dogs race around the bends compared to when they race along the straight sections of the track. Additionally, when they race Greyhounds utilise a double suspension rotary gallop. Along the straight sections of the track the dogs gallop with the feet contacting the surface in a clockwise fashion as follows: right pelvic limb stance phase, left pelvic limb stance phase, 1st suspension phase (limbs fully extended), left thoracic limb stance phase, right thoracic limb stance phase, 2nd suspension phase (limbs fully contracted) (Figure 5.14). However, when cornering, the sequence changes to: left pelvic limb stance phase, right pelvic limb stance phase, 1st suspension phase (limbs fully extended), right thoracic limb stance phase, left thoracic limb stance phase, 2nd suspension phase (limbs fully contracted) (Figure 5.15).

Figure 5.14: As Greyhounds race along the straight sections of the track, their gallop sequence is (a) right pelvic limb stance phase, (b) left pelvic limb stance phase, (c) 1st suspension phase (limbs fully extended), (d) left thoracic limb stance phase, (e) right thoracic limb stance phase, (f) 2nd suspension phase (limbs fully contracted).

Figure 5.15: As Greyhounds race around the bends of the track, their gallop sequence is (a) left pelvic limb stance phase, (b) right pelvic limb stance phase, (c) 1st suspension phase (limbs fully extended), (d) right thoracic limb stance phase, (e) left thoracic limb stance phase, (f) 2nd suspension phase (limbs fully contracted).

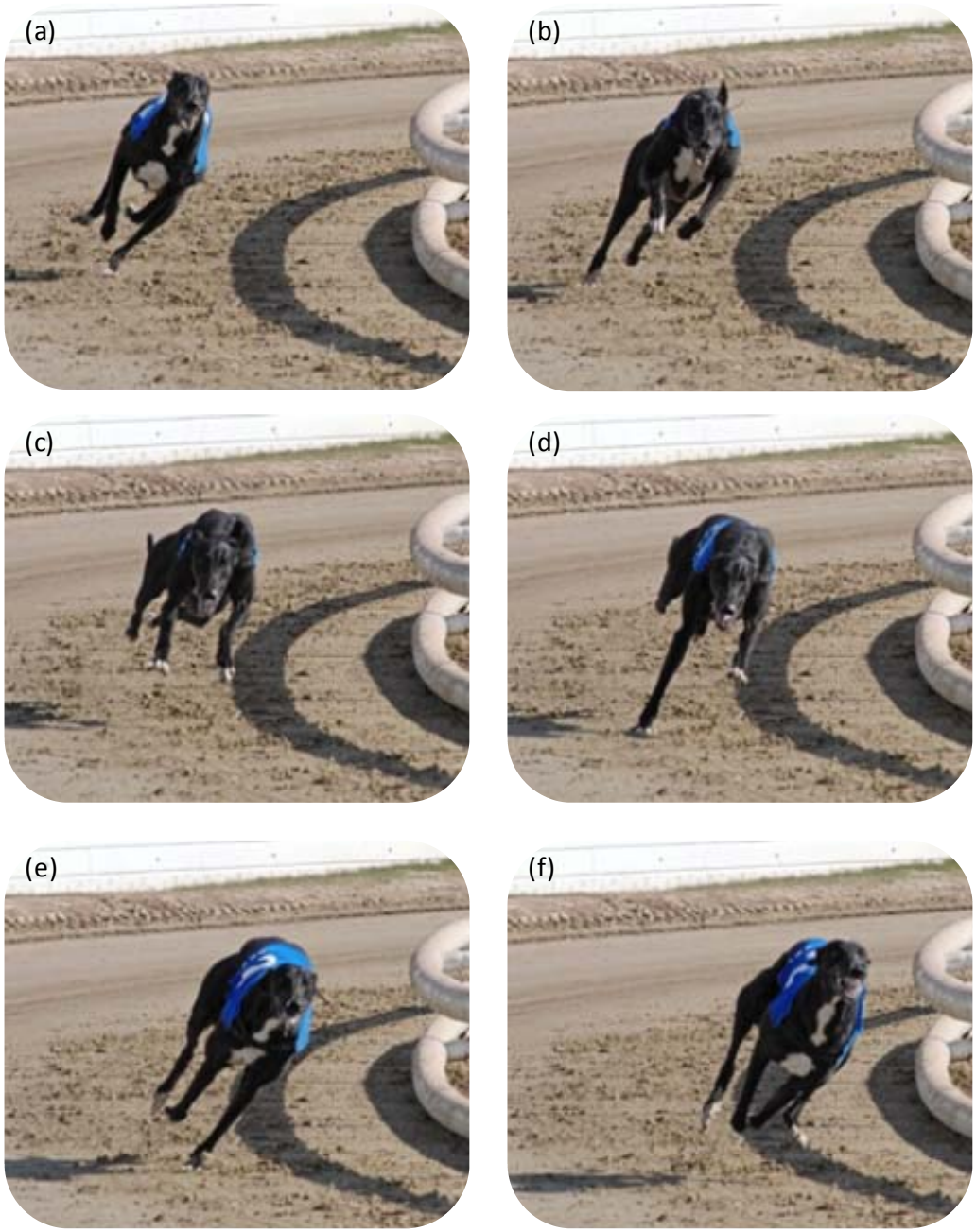

Therefore, the left pelvic limbs are likely to experience increased stresses compared to the right as a result of the asymmetrical loading being increased during cornering, and because the dogs change their gait while cornering so that the left pelvic limb is leading and bearing the dogs weight during the first stance phase. It would seem sensible to conclude that the left pelvic limb tendons adapt to this increase in stress by becoming stronger and stiffer.

In contrast, there were no left-to-right asymmetries in any of the mechanical properties of the thoracic digital flexor tendons. The thoracic limbs need to be able to support and balance the Greyhound during cornering. Consistent with previous findings (Williams *et al.* 2008a), the thoracic digital flexor MTUs seem to be specialised for support, manoeuvrability and force transmission; this multifarious role seems less likely to require asymmetrical adaptation.

5.6.3 Breed differences in tendon mechanical properties

Studies looking at the architectural properties of muscle and tendon from racing Greyhounds predicted that the pelvic limb SDF but not the DDF tendon should play a significant role in elastic energy storage (Williams *et al.* 2008b). Similarly, Pasi and Carrier (2003) compared the limb muscle architecture of Greyhounds with Pit Bull Terriers and estimated Greyhounds to have a greater capacity for elastic energy storage in the elastic extensor MTUs (i.e. the digital flexor MTUs). As predicted, from previous studies and from the muscle-tendon architectural properties measured in this study, the Greyhound pelvic limb SDF tendons were more energy efficient (conserved more elastic strain energy) than the corresponding SBT tendons over a range of different strains. Additionally, while the l.DDF tendons were not as energy efficient as the SDF tendons, they were more efficient than the SBT tendons. Canine thoracic digital flexor tendons are not thought to have an important role in elastic energy storage and recovery (Williams *et al.* 2008a) which agreed well with their relatively high energy losses when they were tested mechanically.

Tendons require increased strength and stiffness to withstand the increased forces encountered during high speed running (Biewener 1998).The large Greyhound SDF and l.DDF tendons were stronger than the corresponding SBT tendons, and the Greyhound SDF tendons were much stiffer than those from SBTs. The Greyhound thoracic digital flexor tendons were also stronger and stiffer than the corresponding SBT tendons. This increased strength and stiffness would allow these tendons to withstand the high forces imposed on the limbs during racing. Additionally, very elastic elements such as tendons can interfere with the transmission of muscle force to skeletal movement; therefore MTUs with stiffer tendons are thought to be good for powering high accelerations (Biewener and Roberts 2000; Ker *et al.* 1988) such as those produced by the Greyhound during racing. In contrast, the smaller m.DDF tendons from both breeds had very similar mechanical properties. This could be due to the small uniform size of the tendon and its anatomical position within the limb. The large digital flexor tendons are positioned along the plantar/palmar aspect of the limb. However, the m.DDF tendon is positioned further medially and it is possible that it experiences smaller forces than the SDF and l.DDF during locomotion.

Exercise and training can also alter the structural and mechanical properties of muscles and tendons. Increased strength and stiffness in response to long term exercise has been observed in the swine extensor tendons (Woo *et al.* 1980) and in the Achilles tendons of rats (Vilarta and Vidal Bde 1989) and birds (Buchanan and Marsh 2001). The large pelvic digital and the thoracic digital flexor tendons of Greyhounds had increased strength and stiffness compared to the SBT tendons. Undoubtedly, this is due to a combination of intrinsic breed differences and the effects of training and racing. Our study cannot determine how, or to what extent breed and exercise training account for these differences in strength and stiffness. However, this seems likely to be a fruitful direction for further work. Comparing un-raced versus raced Greyhounds would help us to determine the extent of the effects of training on muscle and tendon architecture and mechanical properties.

Additionally, it would be useful to look at what is changing in the Greyhound tendons to make them stronger and stiffer than the SBTs. There is limited and contradicting data regarding the long term effects of exercise on the biochemical and structural properties of tendons; for a review see Buchanan and Marsh (2002). Further investigation could determine whether increases in the tendon tensile properties result from changes in properties such as collagen content, proteoglycan concentration, collagen cross-linking and collagen fibril diameter.

5.7 Summary

Greyhound muscles appear to be adapted towards the production of greater forces and higher power than SBT muscles, which could be useful for high acceleration during running. Greyhound pelvic MTUs seem to be more adapted for the storage and recovery of elastic strain energy than SBT MTUs; this would allow the Greyhound to minimise the amount of work its muscles need to do during high speed running. Both Greyhound and SBT thoracic MTUs appear to be adapted for increased limb support and manoeuvrability. This similarity between the breeds is probably because the thoracic limbs have a similar functional role in balance and support despite the very different behaviours each breed is specifically bred for, and because the thoracic limbs are required for other more generic behaviours.

Greyhound SDF and l.DDF tendons from the left pelvic limbs were stronger and stiffer than those from the right. This is likely an adaptive response to the increased stresses acting on the left pelvic limb during cornering of bends. Greyhound SDF and l.DDF tendons were stronger, stiffer and more energy efficient than the ipsilateral SBT tendons, allowing the Greyhound tendons to be economical and to withstand the increased stresses and strains imposed on the limbs during racing. The m.DDF tendons displayed similar tensile properties presumably as a result of their anatomical position and role within the distal limb. Greyhound thoracic limb tendons were stronger and stiffer than the ipsilateral SBT

tendons; this would allow the Greyhound tendons to withstand the increased stresses and strains imposed on the limbs during racing. Neither Greyhounds nor SBTs have thoracic tendons that are elastic and energy efficient (compared to the pelvic limb tendons), possibly because the thoracic limbs have a similar functional role in both breeds; they act as a support and help with balance during both running and fighting.

Chapter 6

GENERAL DISCUSSION

6.1. Overall findings

Racing Greyhounds commonly sustain a number of musculoskeletal injuries that are rarely seen in pets or other working breeds of dogs (Davis 1967; Hickman 1975; Molyneux 2005; Prole 1976). Several of these, notably fatigue fractures of the distal limb bones, are very similar to those seen in human athletes and military recruits (Armstrong *et al.* 2004; Beck *et al.* 2000; Brukner *et al.* 1996; Kowal 1980; Matheson *et al.* 1987). The most common severe injury, often leading to the dog being euthanatized, is fracture of the right tarsus, and consistent with the literature (Boudrieau *et al.* 1984; Gannon 1972; Guilliard 2000; Hickman 1975), this injury nearly always involves fracture of the central tarsal bone and of one or more of the adjacent tarsal bones. One of our key objectives in this study was to characterise and evaluate these injuries. Consistent with the literature (Bateman 1960; Boudrieau *et al.* 1984; Gannon 1972; Guilliard 2000; Hickman 1975; Poulter 1991; Prole 1976), we found that the most common injury sustained by racing Greyhounds was fracture of the right tarsus (Chapter 1). In Chapter 2 we showed that evaluating these tarsal fractures via radiography alone frequently resulted in an underestimation of the severity of the injuries, whereas the use of computed tomography (CT) provided a more detailed, accurate assessment of the extent of the injuries. These results have implications for practising veterinary surgeons, where a decision to treat the animal has to be made. If the treatment decisions are based solely on radiographs, where the severity of the injuries has been underestimated, then the prognosis for the injured animal may not be accurate possibly resulting in a prolonged recovery period and, in the case of Greyhounds, a decreased chance of successfully returning to racing.

The adaptations of the Greyhound musculoskeletal system to the stresses and strains encountered during racing were examined in Chapters 3, 4 and 5. Greyhound distal limb bones were found to have significant left-to-right differences in bone mineral (BMD), collagen content and markers of bone metabolism (Chapter 3): Greyhound rail-side bones (i.e. those within each limb that are closest to the inside of the track) had significantly higher BMD and increased levels of bone resorption and formation markers compared to the contralateral bones. In addition, the diaphysis of the fifth metacarpal bone (MC_5) was much thicker in the rail-side (left) bone compared to the contralateral bone (Chapter 4). In contrast, bones from Staffordshire Bull Terriers (SBTs) did not show these differences. SBTs were originally bred for fighting and are now kept mainly as pets; they have not been raced, therefore, they are unlikely to encounter regular asymmetric stresses. The left-to-right differences observed in Greyhound distal limb bones, therefore, appear to result from the unique pattern of asymmetric stresses the left and right limbs are subjected to during racing. CTBs from Greyhounds with a right CTB fracture were also analysed using DXA and markers of bone metabolism (Chapter 3): BMD and mineral content asymmetries were reversed compared to uninjured CTBs. In addition, the fractured bones showed evidence of being hypomineralised (i.e. low mineral and high collagen content). These changes in the bone matrix and the asymmetries between the left (uninjured) and right (fractured) bones indicate an imbalance in the bone remodelling process has occurred leading to weakening of the bone and structural failure.

The effect of racing on the internal (trabecular) architecture of the fifth metacarpal (MC_5) and central tarsal (CTB) bones was further investigated using micro-CT (Chapter 4). Greyhound CTBs have dorsal-to-plantar changes in trabecular architecture whereas SBT CTBs have a homogeneous trabecular structure. The regional differences seen in Greyhound CTBs, like the differences in BMD and markers of turnover reported in Chapter 3, presumably reflect the pattern of stresses imposed on the bones during galloping. Forces

are forwardly (dorsally) directed for approximately 50% of the stance phase during trotting in dogs (Ritter *et al.* 2001), hence, the dorsal regions of the distal limb bones experience higher forces during stance compared to the plantar regions resulting in increased adaptive remodelling in these areas. Similarly, the epiphysis of Greyhound MC_5 bones show regional changes in trabecular architecture, although how much this is due to racing is unclear, as SBTs also show some regional differences in trabecular architecture. Greyhounds also have left-to-right differences in the trabecular architecture of the MC_5 epiphysis (which SBTs do not) with increased trabecular density and decreased porosity in the dorso-medial regions of the left side bones. Greyhounds transfer their weight to the left side of their limbs during cornering (Boemo 1998) causing an asymmetric distribution of stresses. In addition, the limbs are subjected to dorsally directed forces for a large percentage of stance (Ritter *et al.* 2001). Therefore, the left MC_5 bones are subjected to higher stresses compared to the right MC_5 bones and the left MC_5 bones experience higher stresses in their dorso-medial regions. This data supports the idea that the asymmetric patterns of stresses that the Greyhounds experience during racing drive the adaptive changes seen in the rail-side bones.

The effect of racing on the muscles and tendons within the Greyhound distal limb was also studied (Chapter 5). Greyhound distal limb tendons appear to be well adapted to withstand the high stresses of racing. They are stronger, stiffer and, in the pelvic limbs, return more elastic strain energy than the corresponding SBT tendons. These findings are consistent with the different demands of high speed running and fighting. Similar to the distal limb bones, we found marked left-to-right asymmetries in the tensile properties of the Greyhound's pelvic digital flexor tendons. SBTs had no such differences between their left and right limb tendons. These left-to-right asymmetries in the mechanical properties of tendons are additional evidence that the Greyhounds are subjected, and adapt, to asymmetric stresses during racing.

The adaptations of the Greyhound musculoskeletal system reported in this thesis are most likely due to a combination of intrinsic breed differences and the effects of training and racing. Our studies cannot determine how, or to what extent breed and exercise training account for the adaptations; however, this seems likely to be a fruitful direction for further work. For example, a comparison of Greyhounds that have never been raced with Greyhounds that have been raced around ovoid tracks would allow the effects of asymmetrical loading due to training on the musculoskeletal system to be determined.

6.2 Applications *in vivo*

6.2.1 Imaging techniques

Radiography and computed tomography

Radiography and CT were used to assess tarsal fractures in Greyhounds. Radiography alone underestimated the severity of several injuries, whereas CT proved much more accurate and consistent for assessing the full extent of the injuries. Underestimating the severity of fracture has applications for practicing veterinary surgeons and welfare implications, where a decision to treat or euthanatise an animal has to be made based on the prognosis for recovery. While our findings show that CT should be used in conjunction with radiography for the most accurate diagnosis the substantial cost is likely to be a major factor limiting the use of CT.

Dual-energy x-ray absorptiometry

Bone mineral density (BMD) is the ratio of bone mineral content (BMC) to size. In humans and other animals, changes in BMC and BMD can be measured using dual-energy x-ray absorptiometry (DXA) (Grier *et al.* 1996; Lauten *et al.* 2000; Lauten *et al.* 2001; McClure *et al.* 2001; Zotti *et al.* 2004). The accuracy and precision of DXA in measuring BMC and BMD,

the minimal radiation exposure when compared to standard radiography and the opportunity for serial measurements in the same subject over time, provides excellent data for longitudinal studies in nutrition (Infante and Tormo 2000), growth and development (Zotti *et al.* 2004), disease progression and response to treatment (Eggelmeijer *et al.* 1996; Gonnelli *et al.* 2003) and effects of exercise (Bennell *et al.* 1997). DXA has been used in dogs to evaluate bone remodelling and healing (Markel *et al.* 1995), the effect of exercise on BMD (Puustjarvi *et al.* 1991), left-to-right asymmetries in BMD *in vivo* (Muir *et al.* 1995) and *ex vivo* (Emmerson *et al.* 2000), as well as the osteogenic effect of long-term cyclic training (Emmerson *et al.* 2000; Lipscomb *et al.* 2001).

DXA scanning of *ex vivo* Greyhound distal limb bones revealed almost all of the thoracic and some of the pelvic bones had left-to-right asymmetries in BMD (Chapter 3). DXA can potentially be used *in vivo* to periodically measure bone density in Greyhounds at the start of, and throughout, their racing career, which would allow the long term effects of racing on BMD to be determined. Accurate scanning of the carpal and tarsal bones would be difficult due to anatomical superimposition of the structures; however, the metacarpal and metatarsal bones are positioned side-by-side within the metacarpus/metatarsus (Evans and DeLahunta 1971; Miller *et al.* 1964) and, provided the limb was adequately positioned and stabilised, *in vivo* measurement of BMD would be possible. As small asymmetries in BMD may be difficult to determine *in vivo,* bones should be chosen that show relatively large asymmetries, such as the fifth metacarpal bone in the thoracic limbs (Emmerson *et al.* 2000; Lipscomb *et al.* 2001) and the second or third metatarsal bones in the pelvic limbs (Emmerson *et al.* 2000).

DXA could also be used to detect warning signs of fatigue fracture. Racing Greyhounds are prone to fatigue fracture of the central tarsal and adjacent tarsal bones (Boudrieau *et al.* 1984; Dee *et al.* 1976), metacarpal and metatarsal bones (Dee and Dee 1985; Gannon 1972)

and the acetabulum (Wendelburg *et al.* 1988). Valimaki *et al.* (2005) found that decreased BMC and BMD were a significant risk factor for fatigue fracture in military recruits: femoral neck and total hip BMC/BMD was significantly lower in military recruits that developed fatigue fractures of the metatarsals, tibia or calcaneus. Serial DXA scanning of the distal limb bones could be used to detect the warning signs of fatigue fracture, such as decreasing BMD and reversal of the usual asymmetric adaptive remodelling process. Training programmes could then be adapted to allow the dogs' time to repair the micro-damage that is believed to cause fatigue fracture.

The accurate determination of fracture healing is often not possible using the clinical assessments of manual manipulation and radiographic examination: manual manipulation may cause a loss of reduction and conventional radiographic examination may be inconclusive (Hammer *et al.* 1985). It can also be difficult to determine if there are any changes in callus density occurred between successive radiographs. In contrast, DXA provides an accurate, precise, and minimally invasive quantitative measure of BMD and can be used to monitor fracture healing as it allows changes in mineralization over time along the entire length of a fractured bone to be monitored (Cattermole *et al.* 1997). Therefore, DXA could also be used to monitor fracture healing to help determine the best time for a dog to return to training and racing.

6.2.2 Biochemical analysis of bone turnover

Biochemical analysis of bone extract was used to determine left-to-right asymmetries in bone turnover in Greyhound distal limb bones. We quantified levels of bone specific alkaline phosphatase (BALP), matrix metalloproteinases 2 and 9 (Chapter 3). While we used hydroxyproline levels to provide an estimation of collagen content, hydroxyproline can also be used as a marker of bone resorption when measured in urine. These markers, along with many others (such as osteocalcin, propeptides of type I collagen and telopeptides of type I

collagen), can also be determined in serum and urine (Allen *et al.* 2000a; Creemers *et al.* 1997; Jackson *et al.* 1996; Zucker *et al.* 1992), providing a non-invasive alternative to bone biopsy. Additionally, while imaging techniques such as radiography and DXA provide a snapshot of the skeletons' net bone balance at any given moment in time, serum and urinary assays quantify the formative and resorptive activities of bone cells in close to real time. The *ex vivo* analysis we carried out revealed asymmetries in the individual limb bones (Chapter 3), whereas quantification of these markers in serum or urine would represent the averaged global state of bone resorption and formation in the animals' skeleton. While lacking anatomical localisation, this could still be useful, although care would need to be taken in the choice of marker used for analysis. An ideal marker should be specific to the tissue of interest, in this case bone. Many of the markers used for the assessment of bone metabolism measure the levels of products associated with type I collagen synthesis or degradation (Allen 2003); these are not entirely bone-specific as type I collagen is present is many other tissues. In contrast, osteocalcin is synthesised only by osteoblasts and megakaryocytes (Thiede *et al.* 1994) and is therefore highly specific to bone. Repeated assessment of serum/urinary marker levels could be used to monitor overall bone metabolism in the Greyhound to help prevent fatigue fracture. This principle is used in human medicine: increased levels of bone turnover markers, in particular markers of bone resorption (e.g. osteocalcin), are associated with increased risk of vertebral and hip fractures in elderly women (Ivaska *et al.* 2010). It is also used in veterinary medicine: increased levels of bone turnover markers (osteocalcin and carboxyterminal cross-linked telopeptide of type I collagen) help identify Thoroughbred racehorses at risk of developing dorsal metacarpal disease (Jackson *et al.* 2005); a common source of lameness caused by high-strain cyclic fatigue leading to decreased bone stiffness which then results in periosteal new bone formation and fracture (Nunamaker 1996). If significant increases in

bone turnover are detected then the animals training regime could be adjusted to allow the bones time to heal thus preventing fracture.

Greyhounds also commonly sustain a range of muscle injuries (Molyneux 2005). Therefore, as well as markers of bone metabolism, markers of skeletal muscle damage would likely prove invaluable. Increased levels of serum creatine kinase is an indirect marker of muscle membrane permeability changes and generally indicatives muscle fibre injury (Friden *et al.* 1989). As with the markers of bone metabolism, repeated assessment of serum/urinary marker levels could be used to check for warning signs of muscle damage.

6.3 Potential future studies

Survey of non-catastrophic injuries in racing Greyhounds

There is a serious lack of data about the injuries sustained by racing Greyhounds in the United Kingdom (UK). Prole (1976) carried out a survey of injuries in Greyhounds racing at the London tracks. Since this time advances have been made in track design, which is one of the contributing factors to injury (Sicard *et al.* 1999). The injury data provided by this thesis relates only to injuries where a decision has been made not to treat and the dog has been euthanatized. Greyhounds also sustain a range of less severe injuries while racing. More up to date data regarding these less severe injuries is needed to form a complete picture of the nature and incidence of injuries sustained by Greyhounds racing in the UK today.

Development of a new classification system for the evaluation of CTB fractures in racing Greyhounds

The current CTB fracture classification system, created by Dee *et al.* (1976) was produced by evaluating radiographs of Greyhounds with fractured tarsi. We found that evaluation via

radiographs alone can underestimate the severity of CTB fractures; this underestimation may be exaggerated when the clinician evaluating the radiographs has less experience of dealing with the specific injuries that occur in racing Greyhounds. Evaluation using CT determined that all the Greyhounds used in the study had type V CTB fractures, whereas initial evaluation via radiography produced a wide range of classifications from type I to V. It seems likely that the radiographs used to develop the current classification system would have underestimated the severity of at least some of the CTB fractures. Therefore, there may be a smaller range of CTB fracture classification types and a greater preponderance of more severe injuries than previously thought. Further CT-based investigation of CTB fractures is required to define more accurately the types of injuries that are sustained. A redefinition of the classification system may then be possible.

In vivo monitoring of BMD and markers of bone and muscle damage

Long-term measurement of BMD and markers of bone turnover *in vivo* would allow us to monitor the response of bone to training from the beginning to the end of a racing career and help to predict the likelihood of fracture, allowing training regimes to be altered accordingly.

Analysis of the forces imposed on the distal limbs during racing

We showed left-to-right asymmetries and medial-to-lateral asymmetries in BMD across the Greyhound distal limbs. In humans, medial-to-lateral differences in BMD have been reported across the bones of the feet (Hastings *et al.* 2008; Sinacore *et al.* 2008), thought to result from the long duration of lateral loading during the stance phase of walking increasing bone formation and BMD within the lateral-side bones (Hastings *et al.* 2008). Greyhounds are thought to transfer their weight across to the left side of their limbs when they corner (Boemo 1998) placing higher stresses on those bones nearest to the inside of

the track and leading to the left-to-right asymmetries in BMD. Walter and Carrier (2007) analysed ground reaction forces applied by galloping dogs. The mediolateral ground forces exerted by the thoracic and pelvic limbs vary throughout the stance phase of gallop: the thoracic limbs had a longer duration of medially directed forces while the pelvic limbs were more variable (Walter and Carrier 2007). Their study, which did not record the mediolateral positions of the feet during gallop, involved running the dogs along a straight track and used a small number of dogs of various breeds. A more in depth analysis of the canine gallop, looking at the forces acting on the individual bones within each limb during straight line galloping and bend running has not been carried out. This analysis would be useful to determine how the bones are being loaded during the stance phase of gallop when the dogs race to see if it could explain the left-to-right and medial-to-lateral differences in BMD. Analysis of the forces acting on the Greyhound limbs could be carried out by using force plates to record the ground reaction forces as the dogs' race around the bends of the Greyhound track. Alternatively, DXA could be used to measure the BMD of the distal limb bones of Greyhounds that have never raced to determine if they have any asymmetries in BMD.

Quantification of micro-damage in bone

We determined that Greyhound CTBs have regional differences in their trabecular architecture across the bones from dorsal to plantar (Chapter 4) similar to the regional differences in trabecular architecture seen in carpal bones from treadmill trained (Firth *et al.* 1999) and race-trained Thoroughbred horses (Firth *et al.* 2000). Bone micro-damage is particularly prevalent in the dorsal and medial regions of the Greyhound CTB where trabecular bone has been extensively remodelled (Muir et al. 1999; Tomlin et al. 2000) and accumulation and coalescence of this micro-damage is believed to result in fracture of the CTB (Tomlin *et al.* 2000). As well as fatigue fracture of the CTB (Boudrieau *et al.* 1984; Dee

et al. 1976; Devas 1961) Greyhounds often sustain fatigue fractures of their metacarpal and metatarsal bones (Dee and Dee 1985; Gannon 1972). Fracture usually occurs at the approximate junction of the proximal and middle one third of the bones (Dee and Dee 1985). We determined that cortical thickness of Greyhound MC_5 bones is increased in the left limb bones compared to the right (Chapter 4) in the proximal half of the MC_5 diaphysis. Cortical bone at the mid-diaphysis region of MC_5 is heavily remodelled in Greyhounds, especially in the left limb (Johnson *et al.* 2001) and increased bone remodelling is stimulated by the formation of micro-damage (Burr 1993; Lee *et al.* 2002). Examination of the metacarpal/metatarsal diaphysis via scanning electron microscopy (SEM), similar to what has been done for Greyhound CTBs (Muir *et al.* 1999; Tomlin *et al.* 2000), could allow us to quantify the amount of micro-damage present and could determine if these bones also fail due to micro-damage accumulation and coalescence.

Mechanical testing of bone

We provided data regarding the physical and biochemical responses of bone to exercise. Destructive mechanical testing of Greyhound distal limb bones would help us to evaluate the mechanical consequences of these biochemical and physical changes. The fracture surfaces produced could then be examined using SEM to look for micro-damage and provide further information about how certain bones fracture.

Analysis of the effect of exercise on collagen

Type I collagen is the major component of the organic matrix of bone (Gelse *et al.* 2003; Viguet-Carrin *et al.* 2006) and is the major protein in tendon (Jozsa *et al.* 1989; Kirkendall and Garrett 1997). Changes in the material properties of tendon and bone due to exercise may reflect changes in collagen content, cross-linking, fibril diameter and orientation. Collagen fibre orientation can also provide information on how bones are loaded. Martin *et*

al. (1998) reported longitudinal fibres are found in regions of bone supporting tensile loads, while transverse fibres correspond to regions under compressive loading. Similarly, Riggs *et al.* (1993) showed that regions of the equine radius that are subjected to longitudinal tension contain a high proportion of longitudinal collagen fibres whereas regions subjected to longitudinal compression contain a high proportion of transverse collagen fibres. Analysis of collagen fibre distribution could provide insights into how bone and tendon adapt during high intensity cyclic training.

6.4 Concluding remarks

Racing Greyhounds sustain a number of musculoskeletal injuries. Several of these, notably fatigue fractures, are very similar to those seen in human athletes and military recruits (Armstrong *et al.* 2004; Beck *et al.* 2000; Brukner *et al.* 1996; Kowal 1980; Matheson *et al.* 1987). The most common distal limb injury, often leading to the dog being euthanatised, is fracture of the right tarsus.

Evidence of asymmetric adaptation in response to the pattern of stresses encountered during racing was seen in both the distal limb bones and the digital flexor tendons. The rail-side bones had significantly higher bone density and showed increased levels of markers of bone metabolism compared to contralateral bones, while the rail-side tendons were stronger, stiffer and returned more energy than those in the contralateral limb. There were also regional differences in the trabecular architecture of the Greyhound distal limb bones; seen as adaptive thickening of the trabeculae in the dorsal regions of the bone compared the plantar regions. In addition, we found evidence supporting the idea that characteristic fractures of the distal limb bones result from an imbalance in the bone resorption and formation processes.

Publications and proceedings arising from this PhD

Publications

Hercock, C.A., Young, I.S., McConnell, F., Guilliard, M., Hodson, D., & Innes, J.F., (2011) "Observer variation in the evaluation and classification of severe central tarsal bone fractures in racing Greyhounds", *Vet Comp Orthop Traumatol* Mar 3; 24(3) [Epub ahead of print].

Proceedings (presentations: peer reviewed abstracts)

Hercock, C.A., Innes, J.F., Hodson. D., & Young, I.S. "Built for flight or built to fight: the mechanical properties of digital flexor tendons from racing Greyhounds and Staffordshire Bull Terriers", *In: Abstracts of the Annual Main Meeting of the Society for Experimental Biology, 30th June - 3rd July 2010, Prague, Czech Republic. p.144-145.*

Hercock, C.A., Innes, J.F., Hodson. D., & Young, I.S. "Biochemical and physical markers of asymmetric adaptive remodelling in the central tarsal bones of racing Greyhounds", *In: British Small Animal Veterinary Association 53rd Annual Congress, 8th – 11th April 2010, Birmingham, England, Scientific Proceedings: Veterinary Programme, p.396-397*.

Hercock, C.A., Young, I.S., McConnell, F., Guilliard, M., Hodson, D., & Innes, J.F., "Comparison of radiography and computed tomography for evaluating central tarsal bone fractures in racing greyhounds", *In: British Small Animal Veterinary Association 52nd Annual Congress, 2nd – 5th April 2009, Birmingham, England, Scientific Proceedings: Veterinary Programme, p.448.*

Hercock, C.A., Innes, J.F., Hodson, D., & Young, I.S., "Adaptive remodelling of the distal thoracic limb bones of a canine athlete", *In: Abstracts of the Annual Main Meeting of the*

Society for Experimental Biology, 6th-10th July 2008, Marseille, France. Journal of Comparative Biochemistry and Physiology, Part A 150, p.S80.

Hercock, C.A., Innes, J.F., Piras, A., German, A.J., & Young, I.S., "Measurement of bone mineral densities in the distal thoracic limb bones of racing greyhounds", *In: British Small Animal Veterinary Association 51st Annual Congress, 3rd – 6th April 2008, Birmingham, England, Scientific Proceedings: Veterinary Programme, p.420-421.*

Proceedings (presentations: invited)

Hercock, C.A., Young, I.S., & Innes, J.F. "Bone and tendon adaptation in relation to athletic activity", *Presented at the Annual Meeting for the Society of Greyhound Vets, 20th March 2011, Kenilworth, England.*

Hercock, C.A., Young, I.S., Hodson. D., & Innes, J.F. "Adaptive remodelling in the distal limbs of a canine athlete", *Presented at the Annual Meeting for the Society of Greyhound Vets, 10th November 2009, Birmingham, England.*

Proceedings (posters: peer reviewed abstracts)

Hercock, C.A., Innes, J.F., Hodson. D., & Young, I.S. "μCT analysis of the trabecular structure of central tarsal bones from racing Greyhounds and Staffordshire Bull Terriers", *In: Abstracts of the Annual Main Meeting of the Society for Experimental Biology, 30th June - 3rd July 2010, Prague, Czech Republic. p.150.*

Hercock, C.A., Innes, J.F., Hodson. D., & Young, I.S. "Physical and biochemical evidence of asymmetric bone turnover in the distal limb bones of racing Greyhounds", *In: Abstracts of the Annual Main Meeting of the Society for Experimental Biology, 30th June - 3rd July 2010, Prague, Czech Republic. p.149-150.*

Proceedings (posters: other)

Hercock, C.A., Innes, J.F., Hodson. D., & Young, I.S. “Built to fight or built for flight: the mechanical properties of pelvic digital flexor tendons from racing Greyhounds and Staffordshire Bull Terriers”, *North West Biomechanics Meeting 2010*.

Appendices

Appendix I: Greyhound data for the dogs used in each chapter.

Greyhound	Gender	Age (years)	Weight (kg)	Number of Races Ran
Chapter 2				
1	Male	2.5	33.6	40
2	Male	2.1	30.5	13
3	Female	3.2	-	49
4	Female	2.6	-	17
5	Male	2.7	-	47
6	Male	3.1	-	54
7	Male	4.2	30.5	47
8	Male	2.3	31.8	19
9	Male	2.5	-	23
10	Female	4.6	-	83
11	Female	2.4	25.7	17
12	Male	3.1	27.1	89
13	Female	3.3	28.2	56
14	Male	2.6	32.9	6
Mean ± SD		3.0 ± 0.7	30.0 ± 2.8	40 ± 26
Chapter 3 DXA: Thoracic				
1	Male	2.5	33.6	40
2	Male	2.1	30.5	13
3	Female	3.2	-	49
4	Female	2.6	-	17
5	Male	2.7	-	47
6	Male	3.1	-	54
7	Male	3.3	-	62
8	Male	3.7	28.5	63
9	Female	3.3	28.0	53
10	Male	4.2	30.5	47
11	Male	2.3	31.8	19
12	Male	3.6	35.5	43

13	Male	3.0	-	49
14	Male	2.5	-	17
15	Male	2.5	-	23
16	Female	2.9	-	4
17	Female	4.6	-	83
18	Male	2.4	32.0	7
19	Female	2.7	26.5	51
20	Male	2.6	32.8	11
21	Male	2.8	35.0	10
Mean ± SD		3.0 ± 0.6	31.3 ± 2.9	36 ± 22
DXA: Intact Pelvic				
1	Male	5.8	32.0	94
2	Male	3.3	-	62
3	Male	3.7	28.5	63
4	Male	3.6	35.5	43
5	Male	3.0	-	49
6	Male	2.5	-	17
7	Female	2.9	-	4
8	Male	3.0	27.4	7
9	Female	2.7	26.5	51
10	Male	2.6	32.8	11
11	Male	3.7	33.3	84
12	Female	2.8	26.2	23
13	Male	2.6	28.4	11
14	Male	2.7	35.0	2
Mean ± SD		3.2 ± 0.9	30.6 ± 3.5	37 ± 31
DXA: Injured Pelvic				
1	Male	2.5	33.6	40
2	Male	2.1	30.5	13
3	Female	3.2	-	49
4	Female	2.6	-	17
5	Male	2.7	-	47
6	Male	3.1	-	54

7	Male	2.5	33.6	40
8	Male	4.2	30.5	47
9	Male	2.3	31.8	19
10	Male	2.5	-	23
11	Female	4.6	-	83
12	Female	2.7	25.7	17
13	Male	3.1	27.1	89
14	Female	3.3	28.2	56
15	Male	2.6	32.9	6
Mean ± SD		3.0 ± 0.7	29.8 ± 2.7	41 ± 25
Biochemistry				
1	Female	3.2	-	49
2	Male	5.8	32.0	94
3	Male	2.7	-	47
4	Male	3.1	-	54
5	Male	3.3	-	62
6	Male	3.7	28.5	63
7	Female	3.3	28.0	53
8	Male	3.0	-	49
9	Female	4.6	-	83
10	Female	2.7	26.5	51
11	Male	3.7	33.3	84
12	Male	3.1	27.1	89
13	Male	2.6	32.9	6
Mean ± SD		3.5 ± 0.8	29.1 ± 2.5	64 ± 17
Chapter 4 CTB: Low Raced				
1	Male	3.0	27.4	7
2	Male	2.7	35.0	10
3	Male	2.6	32.8	11
4	Male	2.5	-	17
5	Female	2.8	26.2	23
Mean ± SD		2.7 ± 0.7	30.3 ± 4.2	14 ± 6

CTB: High Raced				
1	Male	3.6	31.5	61
2	Female	4.4	26.2	45
3	Male	2.5	30.8	51
4	Female	3.8	29.4	53
5	Male	3.5	32.0	50
Mean ± SD		3.6 ± 0.7	30.0 ± 2.3	52 ± 6
MC_5				
1	Male	2.6	33.6	40
2	Male	3.6	35.5	43
3	Male	2.7	-	47
4	Male	4.2	30.5	47
5	Female	3.2	-	49
Mean ± SD		3.3 ± 0.7	33.2 ± 2.5	45 ± 4
Chapter 5				
Thoracic				
1	Female	25.7	2.5	18
2	Male	28.9	2.8	7
3	Male	32.1	3.1	38
4	Male	32.8	2.9	62
5	Male	32.6	2.9	13
6	Female	28.2	3.3	56
7	Female	27.6	2.9	54
8	Male	32.0	3.4	62
9	Male	32.0	2.2	2
Mean ± SD		30.2 ± 2.6	2.9 ± 0.4	35 ± 25
Pelvic				
1	Male	-	2.7	47
2	Male	30.5	4.2	47
3	Male	31.8	2.3	19
4	Male	33.3	3.7	84
5	Female	26.2	2.8	23
6	Male	28.4	2.6	11

7	Male	35.0	2.7	10
8	Female	25.7	2.7	17
9	Male	27.1	3.1	89
10	Female	28.2	3.3	56
11	Male	32.4	2.6	6
12	Male	27.0	3.1	46
13	Male	32.0	3.4	62
14	Male	32.0	2.1	5
15	Male	27.0	3.4	43
Mean ± SD		29.8 ± 3.0	3.0 ± 0.6	38 ± 27

Bibliography

Aaron, J.E., Makins, N.B. and Sagreiya, K. (1987) The microanatomy of trabecular bone loss in normal aging men and women. *Clin Orthop Relat Res*, 260-271.

Alexander, R.M. (1984) Elastic Energy Stores in Running Vertebrates. *American Zoologist* **24**, 85-94.

Alexander, R.M. (1988) *Elastic mechanisms in animal movement*, Cambridge University Press, Cambridge.

Alexander, R.M. (1991) Energy-saving mechanisms in walking and running. *Journal of Experimental Biology* **160**, 55-69.

Allen, L.C., Allen, M.J., Breur, G.J., Hoffmann, W.E. and Richardson, D.C. (2000a) A comparison of two techniques for the determination of serum bone-specific alkaline phosphatase activity in dogs. *Res Vet Sci* **68**, 231-235.

Allen, M.J. (2003) Biochemical markers of bone metabolism in animals: uses and limitations. *Vet Clin Pathol* **32**, 101-113.

Allen, M.J., Allen, L.C., Hoffmann, W.E., Richardson, D.C. and Breur, G.J. (2000b) Urinary markers of type I collagen degradation in the dog. *Res Vet Sci* **69**, 123-127.

Ameredes, B.T., Brechue, W.F., Andrew, G.M. and Stainsby, W.N. (1992) Force-Velocity Shifts with Repetitive Isometric and Isotonic Contractions of Canine Gastrocnemius Insitu. *Journal of Applied Physiology* **73**, 2105-2111.

Ammann, P., Rizzoli, R., Meyer, J.M. and Bonjour, J.P. (1996) Bone density and shape as determinants of bone strength in IGF-I and/or pamidronate-treated ovariectomized rats. *Osteoporos Int* **6**, 219-227.

An, Y.H. and Draughn, R.A. (2000) *Mechanical testing of bone and the bone-implant interface*, CRC Press, Boca Raton; London.

Armstrong, D.W., 3rd, Rue, J.P., Wilckens, J.H. and Frassica, F.J. (2004) Stress fracture injury in young military men and women. *Bone* **35**, 806-816.

Atkinson, P.J. (1967) Variation in trabecular structure of vertebrae with age. *Calcif Tissue Res* **1**, 24-32.

Balcerzak, M., Hamade, E., Zhang, L., Pikula, S., Azzar, G., Radisson, J., Bandorowicz-Pikula, J. and Buchet, R. (2003) The roles of annexins and alkaline phosphatase in mineralization process. *Acta Biochim Pol* **50**, 1019-1038.

Bassey, E.J. and Ramsdale, S.J. (1994) Increase in femoral bone density in young women following high-impact exercise. *Osteoporos Int* **4**, 72-75.

Bastien, G.J., Schepens, B., Willems, P.A. and Heglund, N.C. (2005) Energetics of load carrying in Nepalese porters. *Science* **308**, 1755.

Bateman, J.K. (1960) The Racing Greyhound. *Vet Rec* **72**, 5.

Bateman, J.K. (1964) Dropped thigh muscle in the racing greyhound. *Vet Rec* **76**, 201-202.

Baudinette, R.V. and Biewener, A.A. (1998) Young wallabies get a free ride. *Nature* **395**, 653-654.

Beck, T.J., Ruff, C.B., Shaffer, R.A., Betsinger, K., Trone, D.W. and Brodine, S.K. (2000) Stress fracture in military recruits: gender differences in muscle and bone susceptibility factors. *Bone* **27**, 437-444.

Bellenger, C.R., Johnson, K.A., Davis, P.E. and Ilkiw, J.E. (1981) Fixation of metacarpal and metatarsal fractures in greyhounds. *Aust Vet J* **57**, 205-211.

Bennell, K.L., Malcolm, S.A., Khan, K.M., Thomas, S.A., Reid, S.J., Brukner, P.D., Ebeling, P.R. and Wark, J.D. (1997) Bone mass and bone turnover in power athletes, endurance athletes, and controls: a 12-month longitudinal study. *Bone* **20**, 477-484.

Bennett, M.B., Ker, R.F., Dimery, N.J. and Alexander, R.M. (1986) Mechanical-Properties of Various Mammalian Tendons. *J Zool* **209**, 537-548.

Bentolila, V., Boyce, T.M., Fyhrie, D.P., Drumb, R., Skerry, T.M. and Schaffler, M.B. (1998) Intracortical remodeling in adult rat long bones after fatigue loading. *Bone* **23**, 275-281.

Besancon, M.F., Conzemius, M.G., Evans, R.B. and Ritter, M.J. (2004) Distribution of vertical forces in the pads of Greyhounds and Labrador Retrievers during walking. *Am J Vet Res* **65**, 1497-1501.

Biewener, A.A. (1998) Muscle-tendon stresses and elastic energy storage during locomotion in the horse. *Comparative Biochemistry and Physiology B-Biochemistry & Molecular Biology* **120**, 73-87.

Biewener, A.A. (2003) *Animal locomotion*, Oxford University Press, Oxford; New York.

Biewener, A.A. and Baudinette, R.V. (1995) In-Vivo Muscle Force and Elastic Energy-Storage during Steady-Speed Hopping of Tammar Wallabies (Macropus-Eugenii). *Journal of Experimental Biology* **198**, 1829-1841.

Biewener, A.A., Fazzalari, N.L., Konieczynski, D.D. and Baudinette, R.V. (1996) Adaptive changes in trabecular architecture in relation to functional strain patterns and disuse. *Bone* **19**, 1-8.

Biewener, A.A. and Roberts, T.J. (2000) Muscle and tendon contributions to force, work, and elastic energy savings: a comparative perspective. *Exerc Sport Sci Rev* **28**, 99-107.

Blake, G.M. and Fogelman, I. (2007) The role of DXA bone density scans in the diagnosis and treatment of osteoporosis. *Postgrad Med J* **83**, 509-517.

Boemo, C.M. (1998) Injuries of the metacarpus and metatarsus. In: *Canine sports medicine and surgery*, Eds: M.S. Bloomberg, J.F. Dee and R.A. Taylor, Saunders, Philadelphia; London. pp 150-165.

Boemo, C.M. and Eaton-Wells, R.D. (1995) Medial displacement of the tendon of origin of the biceps brachii muscle in 10 greyhounds. *J Small Anim Pract* **36**, 69-73.

Borah, B., Gross, G.J., Dufresne, T.E., Smith, T.S., Cockman, M.D., Chmielewski, P.A., Lundy, M.W., Hartke, J.R. and Sod, E.W. (2001) Three-dimensional microimaging (MRmicroI and microCT), finite element modeling, and rapid prototyping provide unique insights into bone architecture in osteoporosis. *Anat Rec* **265**, 101-110.

Boudrieau, R.J., Dee, J.F. and Dee, L.G. (1984) Central tarsal bone fractures in the racing Greyhound: a review of 114 cases. *J Am Vet Med Assoc* **184**, 1486-1491.

Brama, P.A., Bank, R.A., Tekoppele, J.M. and Van Weeren, P.R. (2001) Training affects the collagen framework of subchondral bone in foals. *Vet J* **162**, 24-32.

Branigan, C.A. (2003) *Adopting the racing greyhound*, 3rd ed. edn., Howell Book House, New York.

Brennan, P. and Silman, A. (1992) Statistical methods for assessing observer variability in clinical measures. *BMJ* **304**, 1491-1494.

Brown, J.P., Delmas, P.D., Malaval, L., Edouard, C., Chapuy, M.C. and Meunier, P.J. (1984) Serum bone Gla-protein: a specific marker for bone formation in postmenopausal osteoporosis. *Lancet* **1**, 1091-1093.

Brown, N.A.T., Kawcak, C.E., McIlwraith, C.W. and Pandy, M.G. (2003) Architectural properties of distal forelimb muscles in horses, Equus caballus. *Journal of Morphology* **258**, 106-114.

Brukner, P., Bradshaw, C., Khan, K.M., White, S. and Crossley, K. (1996) Stress fractures: a review of 180 cases. *Clin J Sport Med* **6**, 85-89.

Bryant, J.D., Bennett, M.B., Brust, J. and Alexander, R.M. (1987) Forces Exerted on the Ground by Galloping Dogs (Canis-Familiaris). *J Zool* **213**, 193-203.

Buchanan, C.I. and Marsh, R.L. (2001) Effects of long-term exercise on the biomechanical properties of the Achilles tendon of guinea fowl. *Journal of Applied Physiology* **90**, 164-171.

Buchanan, C.I. and Marsh, R.L. (2002) Effects of exercise on the biomechanical, biochemical and structural properties of tendons. *Comp Biochem Physiol A Mol Integr Physiol* **133**, 1101-1107.

Buchman, S.R., Sherick, D.G., Goulet, R.W. and Goldstein, S.A. (1998) Use of microcomputed tomography scanning as a new technique for the evaluation of membranous bone. *J Craniofac Surg* **9**, 48-54.

Buckwalter, J.A., Glimcher, M.J., Cooper, R.R. and Recker, R. (1996) Bone biology. I: Structure, blood supply, cells, matrix, and mineralization. *Instr Course Lect* **45**, 371-386.

Burr, D.B. (1993) Remodeling and the repair of fatigue damage. *Calcif Tissue Int* **53 Suppl 1**, S75-80; discussion S80-71.

Burr, D.B., Piotrowski, G. and Miller, G.J. (1981) Structural Strength of the Macaque Femur. *American Journal of Physical Anthropology* **54**, 305-319.

Burr, D.B., Ruff, C.B. and Johnson, C. (1989) Structural adaptations of the femur and humerus to arboreal and terrestrial environments in three species of macaque. *Am J Phys Anthropol* **79**, 357-367.

Butler, D.L., Goldstein, S.A. and Guilak, F. (2000) Functional tissue engineering: the role of biomechanics. *J Biomech Eng* **122**, 570-575.

Butler, D.L., Grood, E.S., Noyes, F.R. and Zernicke, R.F. (1978) Biomechanics of ligaments and tendons. *Exerc Sport Sci Rev* **6**, 125-181.

Byrt, T., Bishop, J. and Carlin, J.B. (1993) Bias, prevalence and kappa. *J Clin Epidemiol* **46**, 423-429.

Campbell, E.J., Cury, J.D., Shapiro, S.D., Goldberg, G.I. and Welgus, H.G. (1991) Neutral proteinases of human mononuclear phagocytes. Cellular differentiation markedly alters cell phenotype for serine proteinases, metalloproteinases, and tissue inhibitor of metalloproteinases. *J Immunol* **146**, 1286-1293.

Carlisle, C.H. and Reynolds, K.M. (1990) Radiographic anatomy of the tarsocrural joint of the dog. *J Small Anim Pract* **31**, 273-279.

Carrier, T.K., Estberg, L., Stover, S.M., Gardner, I.A., Johnson, B.J., Read, D.H. and Ardans, A.A. (1998) Association between long periods without high-speed workouts and risk of complete humeral or pelvic fracture in Thoroughbred racehorses: 54 cases (1991-1994). *Journal of the American Veterinary Medical Association* **212**, 1582-1587.

Carter, D.R. and Hayes, W.C. (1977) Compact bone fatigue damage: a microscopic examination. *Clin Orthop Relat Res*, 265-274.

Cattermole, H.C., Cook, J.E., Fordham, J.N., Muckle, D.S. and Cunningham, J.L. (1997) Bone mineral changes during tibial fracture healing. *Clin Orthop Relat Res*, 190-196.

Cavagna, G.A., Heglund, N.C. and Taylor, C.R. (1977) Mechanical work in terrestrial locomotion: two basic mechanisms for minimizing energy expenditure. *Am J Physiol* **233**, R243-261.

Clarke, B. (2008) Normal bone anatomy and physiology. *Clin J Am Soc Nephrol* **3 Suppl 3**, S131-139.

Cohen, J. (1960) A coefficient of agreement for nominal scales. *Educ Psychol Meas* **20**, 37-46.

Cohen, J. (1968) Weighted Kappa: nominal scale agreement with provision for scaled disagreement or partial credit. . *Psychol Bull* **70**, 213-220.

Colnot, C., Thompson, Z., Miclau, T., Werb, Z. and Helms, J.A. (2003) Altered fracture repair in the absence of MMP9. *Development* **130**, 4123-4133.

Compston, J.E., Mellish, R.W. and Garrahan, N.J. (1987) Age-related changes in iliac crest trabecular microanatomic bone structure in man. *Bone* **8**, 289-292.

Crabtree, N., Loveridge, N., Parker, M., Rushton, N., Power, J., Bell, K.L., Beck, T.J. and Reeve, J. (2001) Intracapsular hip fracture and the region-specific loss of cortical bone: analysis by peripheral quantitative computed tomography. *J Bone Miner Res* **16**, 1318-1328.

Creemers, L.B., Jansen, D.C., van Veen-Reurings, A., van den Bos, T. and Everts, V. (1997) Microassay for the assessment of low levels of hydroxyproline. *Biotechniques* **22**, 656-658.

Creighton, D.L., Morgan, A.L., Boardley, D. and Brolinson, P.G. (2001) Weight-bearing exercise and markers of bone turnover in female athletes. *J Appl Physiol* **90**, 565-570.

Crofton, P.M. (1982) Biochemistry of alkaline phosphatase isoenzymes. *Crit Rev Clin Lab Sci* **16**, 161-194.

Crook, T.C., Cruickshank, S.E., McGowan, C.M., Stubbs, N., Wakeling, J.M., Wilson, A.M. and Payne, R.C. (2008) Comparative anatomy and muscle architecture of selected hind limb muscles in the Quarter Horse and Arab. *J Anat* **212**, 144-152.

Dalen, N., Hellstrom, L.G. and Jacobson, B. (1976) Bone mineral content and mechanical strength of the femoral neck. *Acta Orthop Scand* **47**, 503-508.

Dalziel, H. (1955) *The Greyhound; its history, points, breeding, rearing, training and running*, 11th edn., Bazaar, Exchange & Mart: London.

Davis, P.E. (1967) Track injuries in racing greyhounds. *Aust Vet J* **43**, 180-190.

Davis, P.E. (1973) Toe and muscle injuries of the racing greyhound. *N Z Vet J* **21**, 133-146.

Dee, J.F., Dee, J. and Piermattei, D.L. (1976) Classification, management, and repair of central tarsal fractures in the racing greyhound. *J Am Anim Hosp Assoc* **12**, 398-405.

Dee, J.F. and Dee, L.G. (1985) Fractures and dislocations associated with racing greyhound. In: *Textbook of small animal orthopaedics*, Eds: C.D. Newton and D.M. Nunamaker, International Veterinary Information Service, Ithaca, New York.

Dee, J.F., Dee, L.G. and Eaton-Wells, R.D. (1990) Injuries of high performance dogs. In: *Canine orthopaedics*, 2nd edn., Ed: W.G. Whittick, Lea and Febiger, Philadelphia.

Dempster, D.W. (2000) The contribution of trabecular architecture to cancellous bone quality. *J Bone Miner Res* **15**, 20-23.

Devas, M.B. (1961) Compression stress fractures in man and the greyhound. *J Bone Joint Surg Br* **43-B**, 540-551.

Diamant, J., Keller, A., Baer, E., Litt, M. and Arridge, R.G. (1972) Collagen; ultrastructure and its relation to mechanical properties as a function of ageing. *Proc R Soc Lond B Biol Sci* **180**, 293-315.

Dimery, N.J., Alexander, R.M. and Ker, R.F. (1986) Elastic Extension of Leg Tendons in the Locomotion of Horses (Equus-Caballus). *J Zool* **210**, 415-425.

Drake, F.H., Dodds, R.A., James, I.E., Connor, J.R., Debouck, C., Richardson, S., Lee-Rykaczewski, E., Coleman, L., Rieman, D., Barthlow, R., Hastings, G. and Gowen, M. (1996) Cathepsin K, but not cathepsins B, L, or S, is abundantly expressed in human osteoclasts. *J Biol Chem* **271**, 12511-12516.

Dull, T.A. and Henneman, P.H. (1963) Urinary Hydroxyproline as an Index of Collagen Turnover in Bone. *New England Journal of Medicine* **268**, 132-&.

Eastoe, J.E. (1955) The amino acid composition of mammalian collagen and gelatin. *Biochem J* **61**, 589-600.

Eggelmeijer, F., Papapoulos, S.E., van Paassen, H.C., Dijkmans, B.A., Valkema, R., Westedt, M.L., Landman, J.O., Pauwels, E.K. and Breedveld, F.C. (1996) Increased bone mass with pamidronate treatment in rheumatoid arthritis. Results of a three-year randomized, double-blind trial. *Arthritis Rheum* **39**, 396-402.

Elliott, D.H. (1965) Structure and Function of Mammalian Tendon. *Biol Rev Camb Philos Soc* **40**, 392-421.

Emmerson, T.D., Lawes, T.J., Goodship, A.E., Rueux-Mason, C. and Muir, P. (2000) Dual-energy X-ray absorptiometry measurement of bone-mineral density in the distal aspect of the limbs in racing Greyhounds. *Am J Vet Res* **61**, 1214-1219.

Eriksen, E.F., Charles, P., Melsen, F., Mosekilde, L., Risteli, L. and Risteli, J. (1993) Serum markers of type I collagen formation and degradation in metabolic bone disease: correlation with bone histomorphometry. *J Bone Miner Res* **8**, 127-132.

Eriksen, E.F., Gundersen, H.J., Melsen, F. and Mosekilde, L. (1984) Reconstruction of the formative site in iliac trabecular bone in 20 normal individuals employing a kinetic model for matrix and mineral apposition. *Metab Bone Dis Relat Res* **5**, 243-252.

Eugenio, B.D. and Glass, M. (2004) The kappa statistic: a second look. *Comput Linguist* **30**, 95-101.

Evans, H.E. and DeLahunta, A. (1971) *Miller's guide to the dissection of the dog*, [New ed.] / [by] Howard E. Evans and Alexander deLahunta. edn., Saunders, Philadelphia; London.

Faulkner, K.G., Gluer, C.C., Majumdar, S., Lang, P., Engelke, K. and Genant, H.K. (1991) Noninvasive measurements of bone mass, structure, and strength: current methods and experimental techniques. *AJR Am J Roentgenol* **157**, 1229-1237.

Fawcett, D.W. and Bloom, W. (1994) *Bloom and Fawcett, a textbook of histology*, 12th ed / Don W. Fawcett. edn., Chapman & Hall, New York; London.

Fehling, P.C., Alekel, L., Clasey, J., Rector, A. and Stillman, R.J. (1995) A comparison of bone mineral densities among female athletes in impact loading and active loading sports. *Bone* **17**, 205-210.

Feinstein, A.R. and Cicchetti, D.V. (1990) High agreement but low kappa: I. The problems of two paradoxes. *J Clin Epidemiol* **43**, 543-549.

Feldkamp, L.A., Davis, L.C. and Kress, J.W. (1984) Practical Cone-Beam Algorithm. *J Opt Soc Am A* **1**, 612-619.

Feldkamp, L.A., Goldstein, S.A., Parfitt, A.M., Jesion, G. and Kleerekoper, M. (1989) The direct examination of three-dimensional bone architecture in vitro by computed tomography. *J Bone Miner Res* **4**, 3-11.

Firth, E.C., Delahunt, J., Wichtel, J.W., Birch, H.L. and Goodship, A.E. (1999) Galloping exercise induces regional changes in bone density within the third and radial carpal bones of Thoroughbred horses. *Equine Vet J* **31**, 111-115.

Firth, E.C., Rogers, C.W. and Jopson, N. (2000) Effects of racetrack exercise on third metacarpal and carpal bone of New Zealand thoroughbred horses. *J Musculoskelet Neuronal Interact* **1**, 145-147.

Fitch, R.B., Hathcock, J.T. and Montgomery, R.D. (1996) Radiographic and computed tomographic evaluation of the canine intercondylar fossa in normal stifles and after notchplasty in stable and unstable stifles. *Vet Radiol Ultrasound* **37**, 266-274.

Fleiss, J.L. (1971) Measuring nominal scale agreement among many raters. *Psychological Bulletin* **76**, 378-382.

Fleiss, J.L. (1981) *Statistical methods for rates and proportions*, 2nd ed. edn., Wiley, New York; Chichester.

Franke, S., Lehmann, G., Abendroth, K., Hein, G. and Stein, G. (1998) PICP as bone formation and NTx as bone resorption marker in patients with chronic renal failure. *Eur J Med Res* **3**, 81-88.

Friden, J., Sfakianos, P.N. and Hargens, A.R. (1989) Blood indices of muscle injury associated with eccentric muscle contractions. *J Orthop Res* **7**, 142-145.

Frost, H.M. (1966) Bone dynamics in metabolic bone disease. *J Bone Joint Surg Am* **48**, 1192-1203.

Frost, H.M. (1973) *Bone remodeling and its relationship to metabolic bone diseases*, Thomas, Springfield, IL.

Frost, H.M. (1987) Bone "mass" and the "mechanostat": a proposal. *Anat Rec* **219**, 1-9.

Frost, H.M. (1990a) Skeletal structural adaptations to mechanical usage (SATMU): 1. Redefining Wolff's law: the bone modeling problem. *Anat Rec* **226**, 403-413.

Frost, H.M. (1990b) Skeletal structural adaptations to mechanical usage (SATMU): 2. Redefining Wolff's law: the remodeling problem. *Anat Rec* **226**, 414-422.

Frost, H.M. (1992) Perspectives: bone's mechanical usage windows. *Bone Miner* **19**, 257-271.

Frost, H.M.e. (1964) *Bone biodynamics*, Little Brown, Boston.

Fujimura, R., Ashizawa, N., Watanabe, M., Mukai, N., Amagai, H., Fukubayashi, T., Hayashi, K., Tokuyama, K. and Suzuki, M. (1997) Effect of resistance exercise training on bone formation and resorption in young male subjects assessed by biomarkers of bone metabolism. *J Bone Miner Res* **12**, 656-662.

Gabriel, A., Jolly, S., Detilleux, J., Dessy-Doize, C., Collin, B. and Reginster, J.Y. (1998) Morphometric study of the equine navicular bone: variations with breeds and types of horse and influence of exercise. *J Anat* **193 (Pt 4)**, 535-549.

Galante, J., Rostoker, W. and Ray, R.D. (1970) Physical properties of trabecular bone. *Calcif Tissue Res* **5**, 236-246.

Gannon, J.R. (1972) Stress fractures in the greyhound. *Aust Vet J* **48**, 244-250.

Gans, C. (1982) Fiber architecture and muscle function. *Exerc Sport Sci Rev* **10**, 160-207.

Garbisa, S., Ballin, M., Daga-Gordini, D., Fastelli, G., Naturale, M., Negro, A., Semenzato, G. and Liotta, L.A. (1986) Transient expression of type IV collagenolytic metalloproteinase by human mononuclear phagocytes. *J Biol Chem* **261**, 2369-2375.

GBGB (2009) History of greyhound racing.

GBGB (2010) Rules of racing.

Gelse, K., Poschl, E. and Aigner, T. (2003) Collagens--structure, function, and biosynthesis. *Adv Drug Deliv Rev* **55**, 1531-1546.

Gertz, B.J., Clemens, J.D., Holland, S.D., Yuan, W. and Greenspan, S. (1998) Application of a new serum assay for type I collagen cross-linked N-telopeptides: assessment of diurnal changes in bone turnover with and without alendronate treatment. *Calcif Tissue Int* **63**, 102-106.

Gielen, I.M., De Rycke, L.M., van Bree, H.J. and Simoens, P.J. (2001) Computed tomography of the tarsal joint in clinically normal dogs. *Am J Vet Res* **62**, 1911-1915.

Gluer, C.C., Blake, G., Lu, Y., Blunt, B.A., Jergas, M. and Genant, H.K. (1995) Accurate assessment of precision errors: how to measure the reproducibility of bone densitometry techniques. *Osteoporos Int* **5**, 262-270.

Gomez, B., Jr., Ardakani, S., Ju, J., Jenkins, D., Cerelli, M.J., Daniloff, G.Y. and Kung, V.T. (1995) Monoclonal antibody assay for measuring bone-specific alkaline phosphatase activity in serum. *Clin Chem* **41**, 1560-1566.

Gonnelli, S., Cepollaro, C., Montagnani, A., Bruni, D., Caffarelli, C., Breschi, M., Gennari, L., Gennari, C. and Nuti, R. (2003) Alendronate treatment in men with primary osteoporosis: a three-year longitudinal study. *Calcif Tissue Int* **73**, 133-139.

Goody, P.C. (1997) *Dog anatomy : a pictorial approach to canine structure*, J. A. Allen, London.

Goring, R.L., Parker, R.B., Dee, L. and Eaton-Wells, R.D. (1984) Medial displacement of the tendon of origin of the biceps brachii muscle in the racing greyhound. *J Am Anim Hosp Assoc* **20**, 933-938.

Greene, P.R. (1987) Sprinting with banked turns. *J Biomech* **20**, 667-680.

Gregory, W.K. (1912) Notes on the principles of quadrupedal locomotion and on the mechanism of the limbs in hoofed animals. *Annals of the New York Academy of Sciences* **22**, 267-294.

Grier, S.J., Turner, A.S. and Alvis, M.R. (1996) The use of dual-energy x-ray absorptiometry in animals. *Invest Radiol* **31**, 50-62.

Grimston, S.K., Willows, N.D. and Hanley, D.A. (1993) Mechanical loading regime and its relationship to bone mineral density in children. *Med Sci Sports Exerc* **25**, 1203-1210.

Gross, G.J., Dufresne, T.E., Smith, T., Cockman, M.D., Chmielewski, P.A., Combs, K.S. and Borah, B. (1999) Bone architecture and image synthesis. *Morphologie* **83**, 21-24.

Grynpas, M.D., Alpert, B., Katz, I., Lieberman, I. and Pritzker, K.P. (1991) Subchondral bone in osteoarthritis. *Calcif Tissue Int* **49**, 20-26.

Guilliard, M.J. (1998) Enthesiopathy of the short radial collateral ligaments in racing greyhounds. *J Small Anim Pract* **39**, 227-230.

Guilliard, M.J. (2000) Fractures of the central tarsal bone in eight racing greyhounds. *Vet Rec* **147**, 512-515.

Guilliard, M.J. and Mayo, A.K. (2000a) Sprain of the short radial collateral ligament in a racing greyhound. *J Small Anim Pract* **41**, 169-171.

Guilliard, M.J. and Mayo, A.K. (2000b) Tears of the palmar superficial fascia in five racing greyhounds and a Labrador retriever. *J Small Anim Pract* **41**, 218-220.

Gundberg, C.M., Markowitz, M.E., Mizruchi, M. and Rosen, J.F. (1985) Osteocalcin in human serum: a circadian rhythm. *J Clin Endocrinol Metab* **60**, 736-739.

Guo, X.E. and Kim, C.H. (2002) Mechanical consequence of trabecular bone loss and its treatment: a three-dimensional model simulation. *Bone* **30**, 404-411.

Guy, C. and Ffytche, D. (2005) *An introduction to the principles of medical imaging*, Rev. ed. edn., Imperial College Press, London.

Guyomard, F. and Baron, R. (1974) Fluorescent Labeling Study of Remodeling of Rat Cribriform Plates during Physiological Drift. *J Dent Res* **53**, 736-736.

Gwet, K. (2001) Handbook of inter-rater reliability: How to estimate the level of agreement between two or multiple raters., STATAXIS Publishing Co, Gaithersburg, Maryland.

Gwet, K. (2002) Inter-rater reliability: dependence on trait prevalence and marginal homogeneity. *Statistical Methods For Inter-Rater Reliability Assessment* **2**, 1-9.

Gwet, K.L. (2008) Computing inter-rater reliability and its variance in the presence of high agreement. *Br J Math Stat Psychol* **61**, 29-48.

Haapasalo, H., Kannus, P., Sievanen, H., Heinonen, A., Oja, P. and Vuori, I. (1994) Long-term unilateral loading and bone mineral density and content in female squash players. *Calcif Tissue Int* **54**, 249-255.

Haapasalo, H., Kannus, P., Sievanen, H., Pasanen, M., Uusi-Rasi, K., Heinonen, A., Oja, P. and Vuori, I. (1998) Effect of long-term unilateral activity on bone mineral density of female junior tennis players. *J Bone Miner Res* **13**, 310-319.

Haapasalo, H., Sievanen, H., Kannus, P., Heinonen, A., Oja, P. and Vuori, I. (1996) Dimensions and estimated mechanical characteristics of the humerus after long-term tennis loading. *J Bone Miner Res* **11**, 864-872.

Hammer, R.R., Hammerby, S. and Lindholm, B. (1985) Accuracy of radiologic assessment of tibial shaft fracture union in humans. *Clin Orthop Relat Res*, 233-238.

Hansson, T., Roos, B. and Nachemson, A. (1980) The bone mineral content and ultimate compressive strength of lumbar vertebrae. *Spine (Phila Pa 1976)* **5**, 46-55.

Hastings, M.K., Gelber, J., Commean, P.K., Prior, F. and Sinacore, D.R. (2008) Bone mineral density of the tarsals and metatarsals with reloading. *Phys Ther* **88**, 766-779.

Hathcock, J.T. and Stickle, R.L. (1993) Principles and concepts of computed tomography. *Vet Clin North Am Small Anim Pract* **23**, 399-415.

Hattner, R., Epker, B.N. and Frost, H.M. (1965) Suggested sequential mode of control of changes in cell behaviour in adult bone remodelling. *Nature* **206**, 489-490.

Haut, R.C. (1983) Age-Dependent Influence of Strain Rate on the Tensile Failure of Rat-Tail Tendon. *Journal of Biomechanical Engineering-Transactions of the Asme* **105**, 296-299.

Heglund, N.C. and Taylor, C.R. (1988) Speed, stride frequency and energy cost per stride: how do they change with body size and gait? *J Exp Biol* **138**, 301-318.

Heglund, N.C., Taylor, C.R. and McMahon, T.A. (1974) Scaling stride frequency and gait to animal size: mice to horses. *Science* **186**, 1112-1113.

Heinonen, A., Oja, P., Kannus, P., Sievanen, H., Haapasalo, H., Manttari, A. and Vuori, I. (1995) Bone mineral density in female athletes representing sports with different loading characteristics of the skeleton. *Bone* **17**, 197-203.

Heinonen, A., Oja, P., Kannus, P., Sievanen, H., Manttari, A. and Vuori, I. (1993) Bone mineral density of female athletes in different sports. *Bone Miner* **23**, 1-14.

Heinonen, A., Sievanen, H., Kannus, P., Oja, P. and Vuori, I. (1996) Effects of unilateral strength training and detraining on bone mineral mass and estimated mechanical characteristics of the upper limb bones in young women. *J Bone Miner Res* **11**, 490-501.

Hercock, C., Young, I., Innes, J. and Hodson, D. (2008) Adaptive remodelling of the distal thoracic limb bones of a canine athlete. *Comp Biochem Phys A* **150**, S80-S80.

Herrick, W.C., Kingsbury, H.B. and Lou, D.Y.S. (1978) Study of Normal Range of Strain, Strain Rate, and Stiffness of Tendon. *Journal of Biomedical Materials Research* **12**, 877-894.

Hess, G.P., Cappiello, W.L., Poole, R.M. and Hunter, S.C. (1989) Prevention and treatment of overuse tendon injuries. *Sports Med* **8**, 371-384.

Heussen, C. and Dowdle, E.B. (1980) Electrophoretic analysis of plasminogen activators in polyacrylamide gels containing sodium dodecyl sulfate and copolymerized substrates. *Anal Biochem* **102**, 196-202.

Hickman, J. (1975) Greyhound injuries. *J Small Anim Pract* **16**, 455-460.

Hildebrand, M. and Goslow, G.E. (2001) *Analysis of vertebrate structure*, 5th ed. edn., Wiley, New York; Chichester.

Hildebrand, M. and Hildebrand, V. (1974) *Analysis of vertebrate structure*, Wiley, New York ; London.

Hill, A.V. (1938) The heat of shortening and the dynamic constants of muscle. *Proceedings of the Royal Society of London Series B-Biological Sciences* **126**, 136-195.

Hill, P.A., Buttle, D.J., Jones, S.J., Boyde, A., Murata, M., Reynolds, J.J. and Meikle, M.C. (1994a) Inhibition of bone resorption by selective inactivators of cysteine proteinases. *J Cell Biochem* **56**, 118-130.

Hill, P.A., Docherty, A.J., Bottomley, K.M., O'Connell, J.P., Morphy, J.R., Reynolds, J.J. and Meikle, M.C. (1995) Inhibition of bone resorption in vitro by selective inhibitors of gelatinase and collagenase. *Biochem J* **308 (Pt 1)**, 167-175.

Hill, P.A., Murphy, G., Docherty, A.J., Hembry, R.M., Millican, T.A., Reynolds, J.J. and Meikle, M.C. (1994b) The effects of selective inhibitors of matrix metalloproteinases (MMPs) on bone resorption and the identification of MMPs and TIMP-1 in isolated osteoclasts. *J Cell Sci* **107 (Pt 11)**, 3055-3064.

Hill, P.F., Chatterji, S., Chambers, D. and Keeling, J.D. (1996) Stress fracture of the pubic ramus in female recruits. *J Bone Joint Surg Br* **78**, 383-386.

Hinchliffe, J.R. and Johnson, D.R. (1980) *The development of the vertebrate limb: an approach through experiment, genetics and evolution*, Clarendon Press, Oxford.

Holy, X. and Zerath, E. (2000) Bone mass increases in less than 4 wk of voluntary exercising in growing rats. *Med Sci Sports Exerc* **32**, 1562-1569.

Huang, H., Zhang, J., Sun, K., Zhang, X. and Tian, S. (2011) Effects of repetitive multiple freeze-thaw cycles on the biomechanical properties of human flexor digitorum superficialis and flexor pollicis longus tendons. *Clin Biomech (Bristol, Avon)*.

Huddleston, A.L., Rockwell, D., Kulund, D.N. and Harrison, R.B. (1980) Bone mass in lifetime tennis athletes. *JAMA* **244**, 1107-1109.

Huiskes, R., Ruimerman, R., van Lenthe, G.H. and Janssen, J.D. (2000) Effects of mechanical forces on maintenance and adaptation of form in trabecular bone. *Nature* **405**, 704-706.

Infante, D. and Tormo, R. (2000) Risk of inadequate bone mineralization in diseases involving long-term suppression of dairy products. *J Pediatr Gastroenterol Nutr* **30**, 310-313.

Ivaska, K.K., Gerdhem, P., Vaananen, H.K., Akesson, K. and Obrant, K.J. (2010) Bone turnover markers and prediction of fracture: a prospective follow-up study of 1040 elderly women for a mean of 9 years. *J Bone Miner Res* **25**, 393-403.

Iwamoto, J. and Takeda, T. (2003) Stress fractures in athletes: review of 196 cases. *J Orthop Sci* **8**, 273-278.

Jackson, B., Eastell, R., Russell, R.G., Lanyon, L.E. and Price, J.S. (1996) Measurement of bone specific alkaline phosphatase in the horse: a comparison of two techniques. *Res Vet Sci* **61**, 160-164.

Jackson, B.F., Lonnell, C., Verheyen, K.L., Dyson, P., Pfeiffer, D.U. and Price, J.S. (2005) Biochemical markers of bone metabolism and risk of dorsal metacarpal disease in 2-year-old Thoroughbreds. *Equine Vet J* **37**, 87-91.

Janckila, A.J., Takahashi, K., Sun, S.Z. and Yam, L.T. (2001) Tartrate-resistant acid phosphatase isoform 5b as serum marker for osteoclastic activity. *Clin Chem* **47**, 74-80.

Jayasinghe, J.A., Jones, S.J. and Boyde, A. (1993) Scanning electron microscopy of human lumbar vertebral trabecular bone surfaces. *Virchows Arch A Pathol Anat Histopathol* **422**, 25-34.

Johnson, K.A. (1987) Accessory carpal bone fractures in the racing greyhound. Classification and pathology. *Vet Surg* **16**, 60-64.

Johnson, K.A., Dee, J.F. and Piermattei, D.L. (1989) Screw fixation of accessory carpal bone fractures in racing Greyhounds: 12 cases (1981-1986). *J Am Vet Med Assoc* **194**, 1618-1625.

Johnson, K.A., Muir, P., Nicoll, R.G. and Roush, J.K. (2000) Asymmetric adaptive modeling of central tarsal bones in racing greyhounds. *Bone* **27**, 257-263.

Johnson, K.A., Piermattei, D.L., Davis, P.E. and Bellenger, C.R. (1988) Characteristics of accessory carpal bone fractures in 50 racing greyhounds. *Veterinary and Comparative Orthopaedics and Traumatology* **2**, 104-107.

Johnson, K.A., Skinner, G.A. and Muir, P. (2001) Site-specific adaptive remodeling of Greyhound metacarpal cortical bone subjected to asymmetrical cyclic loading. *Am J Vet Res* **62**, 787-793.

Jones, H.H., Priest, J.D., Hayes, W.C., Tichenor, C.C. and Nagel, D.A. (1977) Humeral hypertrophy in response to exercise. *J Bone Joint Surg Am* **59**, 204-208.

Joo, Y.I., Sone, T., Fukunaga, M., Lim, S.G. and Onodera, S. (2003) Effects of endurance exercise on three-dimensional trabecular bone microarchitecture in young growing rats. *Bone* **33**, 485-493.

Jozsa, L., Lehto, M., Kvist, M., Balint, J.B. and Reffy, A. (1989) Alterations in dry mass content of collagen fibers in degenerative tendinopathy and tendon-rupture. *Matrix* **9**, 140-146.

Kannus, P. (2000) Structure of the tendon connective tissue. *Scand J Med Sci Sports* **10**, 312-320.

Kaptoge, S., Beck, T.J., Reeve, J., Stone, K.L., Hillier, T.A., Cauley, J.A. and Cummings, S.R. (2008) Prediction of incident hip fracture risk by femur geometry variables measured by hip structural analysis in the study of osteoporotic fractures. *J Bone Miner Res* **23**, 1892-1904.

Karlsson, R., Eden, S., Eriksson, L. and von Schoultz, B. (1992) Osteocalcin 24-hour profiles during normal pregnancy. *Gynecol Obstet Invest* **34**, 197-201.

Kastelic, J., Galeski, A. and Baer, E. (1978) The multicomposite structure of tendon. *Connect Tissue Res* **6**, 11-23.

Keene, D.R., Sakai, L.Y. and Burgeson, R.E. (1991) Human bone contains type III collagen, type VI collagen, and fibrillin: type III collagen is present on specific fibers that may mediate attachment of tendons, ligaments, and periosteum to calcified bone cortex. *J Histochem Cytochem* **39**, 59-69.

Kennel-Club (2000) Staffordshire bull terrier breed standard.

Kennel-Club (2009) Greyhound breed standard.

Ker, R.F. (1981) Dynamic tensile properties of the plantaris tendon of sheep (Ovis aries). *Journal of Experimental Biology* **93**, 283-302.

Ker, R.F., Alexander, R.M. and Bennett, M.B. (1988) Why Are Mammalian Tendons So Thick. *J Zool* **216**, 309-324.

Ker, R.F., Bennett, M.B., Bibby, S.R., Kester, R.C. and Alexander, R.M. (1987) The spring in the arch of the human foot. *Nature* **325**, 147-149.

Ker, R.F., Dimery, N.J. and Alexander, R.M. (1986) The Role of Tendon Elasticity in Hopping in a Wallaby (Macropus-Rufogriseus). *J Zool* **208**, 417-428.

Ker, R.F., Wang, X.T. and Pike, A.V. (2000) Fatigue quality of mammalian tendons. *Journal of Experimental Biology* **203**, 1317-1327.

Khan, K. (2001) *Physical activity and bone health*, Human Kinetics, Champaign, Ill; Leeds.

Kirkendall, D.T. and Garrett, W.E. (1997) Function and biomechanics of tendons. *Scand J Med Sci Sports* **7**, 62-66.

Kleerekoper, M., Villanueva, A.R., Stanciu, J., Rao, D.S. and Parfitt, A.M. (1985) The role of three-dimensional trabecular microstructure in the pathogenesis of vertebral compression fractures. *Calcif Tissue Int* **37**, 594-597.

Knott, L. and Bailey, A.J. (1998) Collagen cross-links in mineralizing tissues: a review of their chemistry, function, and clinical relevance. *Bone* **22**, 181-187.

Knuttgen, H.G. (1976) Development of muscular strength and endurance. In: *Neuromuscular mechanisms for therapeutic and conditioning exercise*, Ed: H.G. Knuttgen, University Park Press, Baltimore. pp 97-118.

Kowal, D.M. (1980) Nature and causes of injuries in women resulting from an endurance training program. *Am J Sports Med* **8**, 265-269.

Landis, J.R. and Koch, G.G. (1977) The measurement of observer agreement for categorical data. *Biometrics* **33**, 159-174.

Lane, N.E., Yao, W., Balooch, M., Nalla, R.K., Balooch, G., Habelitz, S., Kinney, J.H. and Bonewald, L.F. (2006) Glucocorticoid-treated mice have localized changes in trabecular bone material properties and osteocyte lacunar size that are not observed in placebo-treated or estrogen-deficient mice. *J Bone Miner Res* **21**, 466-476.

Lanyon, L.E. (1984) Functional strain as a determinant for bone remodeling. *Calcif Tissue Int* **36 Suppl 1**, S56-61.

Lanyon, L.E. (1992) Control of bone architecture by functional load bearing. *J Bone Miner Res* **7 Suppl 2**, S369-375.

Lanyon, L.E. (1996) Using functional loading to influence bone mass and architecture: objectives, mechanisms, and relationship with estrogen of the mechanically adaptive process in bone. *Bone* **18**, 37S-43S.

Lanyon, L.E. and Baggott, D.G. (1976) Mechanical function as an influence on the structure and form of bone. *J Bone Joint Surg Br* **58-B**, 436-443.

Lanyon, L.E. and Bourn, S. (1979) The influence of mechanical function on the development and remodeling of the tibia. An experimental study in sheep. *J Bone Joint Surg Am* **61**, 263-273.

Lauten, S.D., Cox, N.R., Baker, G.H., Painter, D.J., Morrison, N.E. and Baker, H.J. (2000) Body composition of growing and adult cats as measured by use of dual energy X-ray absorptiometry. *Comp Med* **50**, 175-183.

Lauten, S.D., Cox, N.R., Brawner, W.R., Jr. and Baker, H.J. (2001) Use of dual energy x-ray absorptiometry for noninvasive body composition measurements in clinically normal dogs. *Am J Vet Res* **62**, 1295-1301.

Lee, A.J., Hodges, S. and Eastell, R. (2000) Measurement of osteocalcin. *Ann Clin Biochem* **37 (Pt 4)**, 432-446.

Lee, D.V., Bertram, J.E. and Todhunter, R.J. (1999) Acceleration and balance in trotting dogs. *J Exp Biol* **202**, 3565-3573.

Lee, T.C., Staines, A. and Taylor, D. (2002) Bone adaptation to load: microdamage as a stimulus for bone remodelling. *J Anat* **201**, 437-446.

Legrand, E., Chappard, D., Pascaretti, C., Duquenne, M., Krebs, S., Rohmer, V., Basle, M.F. and Audran, M. (2000) Trabecular bone microarchitecture, bone mineral density, and vertebral fractures in male osteoporosis. *J Bone Miner Res* **15**, 13-19.

Lepage, O.M., Marcoux, M. and Tremblay, A. (1990) Serum osteocalcin or bone Gla-protein, a biochemical marker for bone metabolism in horses: differences in serum levels with age. *Can J Vet Res* **54**, 223-226.

Li, X.J., Jee, W.S., Li, Y.L. and Patterson-Buckendahl, P. (1990) Transient effects of subcutaneously administered prostaglandin E2 on cancellous and cortical bone in young adult dogs. *Bone* **11**, 353-364.

Lipscomb, V.J., Lawes, T.J., Goodship, A.E. and Muir, P. (2001) Asymmetric densitometric and mechanical adaptation of the left fifth metacarpal bone in racing greyhounds. *Vet Rec* **148**, 308-311.

Liu, Y., Liu, H., Wang, Y. and Wang, G. (2001) Half-scan cone-beam CT fluoroscopy with multiple x-ray sources. *Med Phys* **28**, 1466-1471.

Loitz, B.J., Zernicke, R.F., Vailas, A.C., Kody, M.H. and Meals, R.A. (1989) Effects of short-term immobilization versus continuous passive motion on the biomechanical and biochemical properties of the rabbit tendon. *Clin Orthop Relat Res*, 265-271.

Looker, A.C., Bauer, D.C., Chesnut, C.H., 3rd, Gundberg, C.M., Hochberg, M.C., Klee, G., Kleerekoper, M., Watts, N.B. and Bell, N.H. (2000) Clinical use of biochemical markers of bone remodeling: current status and future directions. *Osteoporos Int* **11**, 467-480.

Lozano-Calderon, S., Blazar, P., Zurakowski, D., Lee, S.G. and Ring, D. (2006) Diagnosis of scaphoid fracture displacement with radiography and computed tomography. *J Bone Joint Surg Am* **88**, 2695-2703.

Magnusson, P., Larsson, L., Magnusson, M., Davie, M.W. and Sharp, C.A. (1999) Isoforms of bone alkaline phosphatase: characterization and origin in human trabecular and cortical bone. *J Bone Miner Res* **14**, 1926-1933.

Maloiy, G.M., Heglund, N.C., Prager, L.M., Cavagna, G.A. and Taylor, C.R. (1986) Energetic cost of carrying loads: have African women discovered an economic way? *Nature* **319**, 668-669.

Markel, M.D., Bogdanske, J.J., Xiang, Z. and Klohnen, A. (1995) Atrophic nonunion can be predicted with dual energy x-ray absorptiometry in a canine ostectomy model. *J Orthop Res* **13**, 869-875.

Martin, B. (1995) Mathematical model for repair of fatigue damage and stress fracture in osteonal bone. *J Orthop Res* **13**, 309-316.

Martin, R.B. (1972) The effects of geometric feedback in the development of osteoporosis. *J Biomech* **5**, 447-455.

Martin, R.B. and Burr, D.B. (1989) *Structure, function, and adaptation of compact bone*, Raven Press, New York.

Martin, R.B., Burr, D.B. and Sharkey, N.A. (1998) *Skeletal tissue mechanics*, Springer, New York ; London.

Matheson, G.O., Clement, D.B., McKenzie, D.C., Taunton, J.E., Lloyd-Smith, D.R. and MacIntyre, J.G. (1987) Stress fractures in athletes. A study of 320 cases. *Am J Sports Med* **15**, 46-58.

Matrisian, L.M. (1992) The matrix-degrading metalloproteinases. *Bioessays* **14**, 455-463.

Maughan, R.J., Watson, J.S. and Weir, J. (1983) Strength and cross-sectional area of human skeletal muscle. *J Physiol* **338**, 37-49.

McBryde, A.M., Jr. (1975) Stress fractures in athletes. *J Sports Med* **3**, 212-217.

McCarthy, R.N. and Jeffcott, L.B. (1992) Effects of treadmill exercise on cortical bone in the third metacarpus of young horses. *Res Vet Sci* **52**, 28-37.

McClure, S.R., Glickman, L.T., Glickman, N.W. and Weaver, C.M. (2001) Evaluation of dual energy x-ray absorptiometry for in situ measurement of bone mineral density of equine metacarpi. *Am J Vet Res* **62**, 752-756.

Medler, S. (2002) Comparative trends in shortening velocity and force production in skeletal muscles. *Am J Physiol Regul Integr Comp Physiol* **283**, R368-378.

Meikle, M.C., Bord, S., Hembry, R.M., Compston, J., Croucher, P.I. and Reynolds, J.J. (1992) Human osteoblasts in culture synthesize collagenase and other matrix metalloproteinases in response to osteotropic hormones and cytokines. *J Cell Sci* **103 (Pt 4)**, 1093-1099.

Melkko, J., Kauppila, S., Niemi, S., Risteli, L., Haukipuro, K., Jukkola, A. and Risteli, J. (1996) Immunoassay for intact amino-terminal propeptide of human type I procollagen. *Clin Chem* **42**, 947-954.

Melkko, J., Niemi, S., Risteli, L. and Risteli, J. (1990) Radioimmunoassay of the carboxyterminal propeptide of human type I procollagen. *Clin Chem* **36**, 1328-1332.

Mendez, J. and Keys, A. (1960) Density and Composition of Mammalian Muscle. *Metabolism-Clinical and Experimental* **9**, 184-188.

Meyer-Sabellek, W., Sinha, P. and Kottgen, E. (1988) Alkaline phosphatase. Laboratory and clinical implications. *J Chromatogr* **429**, 419-444.

Milch, R.A., Rall, D.P. and Tobie, J.E. (1957) Bone localization of the tetracyclines. *J Natl Cancer Inst* **19**, 87-93.

Miller, M.E., Christensen, G.C. and Evans, H.E. (1964) *Anatomy of the dog*, 1st edn., Saunders, Philadelphia.

Minkin, C. (1982) Bone acid phosphatase: tartrate-resistant acid phosphatase as a marker of osteoclast function. *Calcif Tissue Int* **34**, 285-290.

Mohamadnia, A., Shahbazkia, H., Sharifi, S. and Shafaei, I. (2007) Bone-specific alkaline phosphatase as a good indicator of bone formation in sheepdogs. *Comparative Clinical Pathology* **16**, 265-270.

Molyneux, J. (2005) Vets on track: working as a greyhound vet. *In Practice* **27**, 277-279.

Mora, S., Prinster, C., Proverbio, M.C., Bellini, A., de Poli, S.C., Weber, G., Abbiati, G. and Chiumello, G. (1998) Urinary markers of bone turnover in healthy children and adolescents: age-related changes and effect of puberty. *Calcif Tissue Int* **63**, 369-374.

Morgan, J.W., Santschi, E.M., Zekas, L.J., Scollay-Ward, M.C., Markel, M.D., Radtke, C.L., Sample, S.J., Keuler, N.S. and Muir, P. (2006) Comparison of radiography and computed tomography to evaluate metacarpo/metatarsophalangeal joint

pathology of paired limbs of thoroughbred racehorses with severe condylar fracture. *Vet Surg* **35**, 611-617.

Mori, S. and Burr, D.B. (1993) Increased intracortical remodeling following fatigue damage. *Bone* **14**, 103-109.

Mosekilde, L. (1993) Vertebral structure and strength in vivo and in vitro. *Calcif Tissue Int* **53 Suppl 1**, S121-125; discussion S125-126.

Muir, P., Johnson, K.A. and Ruaux-Mason, C.P. (1999) In vivo matrix microdamage in a naturally occurring canine fatigue fracture. *Bone* **25**, 571-576.

Muir, P., Markel, M.D., Bogdanske, J.J. and Johnson, K.A. (1995) Dual-energy x-ray absorptiometry and force-plate analysis of gait in dogs with healed femora after leg-lengthening plate fixation. *Vet Surg* **24**, 15-24.

Nagase, H. (1997) Activation mechanisms of matrix metalloproteinases. *Biol Chem* **378**, 151-160.

Nagase, H. and Woessner, J.F., Jr. (1999) Matrix metalloproteinases. *J Biol Chem* **274**, 21491-21494.

Ness, M.G. (1993) Metatarsal III fractures in the racing greyhound. *Journal of Small Animal Practice* **34**, 85-89.

Newton, C.D. and Nunamaker, D.M. (1985) *Textbook of small animal orthopaedics*, Lippincott, Philadelphia, Pa.

Nigg, B.M., MacIntosh, B.R. and Mester, J. (2000) *Biomechanics and biology of movement*, Human Kinetics, Champaign.

Nishimoto, S.K., Chang, C.H., Gendler, E., Stryker, W.F. and Nimni, M.E. (1985) The effect of aging on bone formation in rats: biochemical and histological evidence for decreased bone formation capacity. *Calcif Tissue Int* **37**, 617-624.

Niyibizi, C. and Eyre, D.R. (1994) Structural characteristics of cross-linking sites in type V collagen of bone. Chain specificities and heterotypic links to type I collagen. *Eur J Biochem* **224**, 943-950.

Notomi, T., Lee, S.J., Okimoto, N., Okazaki, Y., Takamoto, T., Nakamura, T. and Suzuki, M. (2000) Effects of resistance exercise training on mass, strength, and turnover of bone in growing rats. *Eur J Appl Physiol* **82**, 268-274.

Notomi, T., Okimoto, N., Okazaki, Y., Tanaka, Y., Nakamura, T. and Suzuki, M. (2001) Effects of tower climbing exercise on bone mass, strength, and turnover in growing rats. *J Bone Miner Res* **16**, 166-174.

Nunamaker, D.M. (1996) Metacarpal stress fractures. In: *Equine Fracture Repair*, Ed: A.J. Nixon, W. B. Saunders Co., Philadelphia. pp 195-199.

Nunamaker, D.M., Butterweck, D.M. and Provost, M.T. (1989) Some geometric properties of the third metacarpal bone: a comparison between the thoroughbred and standardbred racehorse. *J Biomech* **22**, 129-134.

Nunamaker, D.M., Butterweck, D.M. and Provost, M.T. (1990) Fatigue fractures in thoroughbred racehorses: relationships with age, peak bone strain, and training. *J Orthop Res* **8**, 604-611.

O'Brien, M. (1997) Structure and metabolism of tendons. *Scand J Med Sci Sports* **7**, 55-61.

Orava, S., Puranen, J. and Ala-Ketola, L. (1978) Stress fractures caused by physical exercise. *Acta Orthop Scand* **49**, 19-27.

Ost, P.C., Dee, J.F., Dee, L.G. and Hohn, R.B. (1987) Fractures of the calcaneus in racing greyhounds. *Vet Surg* **16**, 53-59.

Parfitt, A.M. (1992) Implications of architecture for the pathogenesis and prevention of vertebral fracture. *Bone* **13 Suppl 2**, S41-47.

Parfitt, A.M. (1994) Osteonal and hemi-osteonal remodeling: the spatial and temporal framework for signal traffic in adult human bone. *J Cell Biochem* **55**, 273-286.

Parfitt, A.M. (2000) The mechanism of coupling: a role for the vasculature. *Bone* **26**, 319-323.

Parfitt, A.M., Mathews, C.H., Villanueva, A.R., Kleerekoper, M., Frame, B. and Rao, D.S. (1983) Relationships between surface, volume, and thickness of iliac trabecular bone in aging and in osteoporosis. Implications for the microanatomic and cellular mechanisms of bone loss. *J Clin Invest* **72**, 1396-1409.

Parker, H.G., Kim, L.V., Sutter, N.B., Carlson, S., Lorentzen, T.D., Malek, T.B., Johnson, G.S., DeFrance, H.B., Ostrander, E.A. and Kruglyak, L. (2004) Genetic structure of the purebred domestic dog. *Science* **304**, 1160-1164.

Pasi, B.M. and Carrier, D.R. (2003) Functional trade-offs in the limb muscles of dogs selected for running vs. fighting. *Journal of Evolutionary Biology* **16**, 324-332.

Payne, R.C., Crompton, R.H., Isler, K., Savage, R., Vereecke, E.E., Gunther, M.M., Thorpe, S.K.S. and D'Aout, K. (2006) Morphological analysis of the hindlimb in apes and humans. I. Muscle architecture. *Journal of Anatomy* **208**, 709-724.

Payne, R.C., Hutchinson, J.R., Robilliard, J.J., Smith, N.C. and Wilson, A.M. (2005) Functional specialisation of pelvic limb anatomy in horses (Equus caballus). *J Anat* **206**, 557-574.

Payne, R.C., Veenman, P. and Wilson, A.M. (2004) The role of the extrinsic thoracic limb muscles in equine locomotion. *J Anat* **205**, 479-490.

Peel, N. and Eastell, R. (1993) Measurement of bone mass and turnover. *Baillieres Clin Rheumatol* **7**, 479-498.

Phillips, I.R. (1979) A survey of bone fractures in the dog and cat. *J Small Anim Pract* **20**, 661-674.

Piras, A. (2005) Customized single hook plate for fractures of metacarpal/tarsal bones in racing greyhounds. *AO Dialogue* **18**, 31-33.

Pollock, C.M. and Shadwick, R.E. (1994) Allometry of muscle, tendon, and elastic energy storage capacity in mammals. *Am J Physiol* **266**, R1022-1031.

Poulter, D. (1991) Greyhound injuries. *Acupunt Med* **9**, 35-39.

Price, J.S., Jackson, B., Eastell, R., Wilson, A.M., Russell, R.G., Lanyon, L.E. and Goodship, A.E. (1995) The response of the skeleton to physical training: a biochemical study in horses. *Bone* **17**, 221-227.

Prole, J.H. (1976) A survey of racing injuries in the Greyhound. *J Small Anim Pract* **17**, 207-218.

Puustjarvi, K., Karjalainen, P., Nieminen, J., Arokoski, J., Parviainen, M., Helminen, H.J. and Soimakallio, S. (1992) Endurance training associated with slightly lowered serum

estradiol levels decreases mineral density of canine skeleton. *J Bone Miner Res* **7**, 619-624.

Puustjarvi, K., Karjalainen, P., Nieminen, J., Helminen, H.J., Soimakallio, S., Kivimaki, T. and Arokoski, J. (1991) Effects of long-term running on spinal mineral content in dogs. *Calcif Tissue Int* **49 Suppl**, S81-82.

Raeke, C. (2004) *The best finish : adopting a retired racing greyhound*, T.F.H., Neptune City, N.J. ; Havant. p 96 p.

Rahnama, N., Lees, A. and Bambaecichi, E. (2005) Comparison of muscle strength and flexibility between the preferred and non-preferred leg in English soccer players. *Ergonomics* **48**, 1568-1575.

Raisz, L.G. (1999) Physiology and pathophysiology of bone remodeling. *Clin Chem* **45**, 1353-1358.

Reeves, N.D., Maganaris, C.N. and Narici, M.V. (2003) Effect of strength training on human patella tendon mechanical properties of older individuals. *J Physiol* **548**, 971-981.

Rho, J.Y., Kuhn-Spearing, L. and Zioupos, P. (1998) Mechanical properties and the hierarchical structure of bone. *Medical Engineering & Physics* **20**, 92-102.

Riechert, K., Labs, K., Lindenhayn, K. and Sinha, P. (2001) Semiquantitative analysis of types I and III collagen from tendons and ligaments in a rabbit model. *J Orthop Sci* **6**, 68-74.

Riemersma, D.J. and Schamhardt, H.C. (1985) In vitro mechanical properties of equine tendons in relation to cross-sectional area and collagen content. *Res Vet Sci* **39**, 263-270.

Rifas, L., Fausto, A., Scott, M.J., Avioli, L.V. and Welgus, H.G. (1994) Expression of metalloproteinases and tissue inhibitors of metalloproteinases in human osteoblast-like cells: differentiation is associated with repression of metalloproteinase biosynthesis. *Endocrinology* **134**, 213-221.

Rifas, L., Halstead, L.R., Peck, W.A., Avioli, L.V. and Welgus, H.G. (1989) Human osteoblasts in vitro secrete tissue inhibitor of metalloproteinases and gelatinase but not interstitial collagenase as major cellular products. *J Clin Invest* **84**, 686-694.

Rigby, B.J., Hirai, N., Spikes, J.D. and Eyring, H. (1959) The Mechanical Properties of Rat Tail Tendon. *J Gen Physiol* **43**, 265-283.

Riggs, C.M., Lanyon, L.E. and Boyde, A. (1993) Functional associations between collagen fibre orientation and locomotor strain direction in cortical bone of the equine radius. *Anat Embryol (Berl)* **187**, 231-238.

Riley, G.P., Harrall, R.L., Constant, C.R., Chard, M.D., Cawston, T.E. and Hazleman, B.L. (1994) Tendon degeneration and chronic shoulder pain: changes in the collagen composition of the human rotator cuff tendons in rotator cuff tendinitis. *Ann Rheum Dis* **53**, 359-366.

Risteli, J., Elomaa, I., Niemi, S., Novamo, A. and Risteli, L. (1993) Radioimmunoassay for the pyridinoline cross-linked carboxy-terminal telopeptide of type I collagen: a new serum marker of bone collagen degradation. *Clin Chem* **39**, 635-640.

Risteli, L. and Risteli, J. (1993) Biochemical markers of bone metabolism. *Ann Med* **25**, 385-393.

Ritter, D.A., Nassar, P.N., Fife, M. and Carrier, D.R. (2001) Epaxial muscle function in trotting dogs. *Journal of Experimental Biology* **204**, 3053-3064.

Robins, S.P., Duncan, A., Wilson, N. and Evans, B.J. (1996) Standardization of pyridinium crosslinks, pyridinoline and deoxypyridinoline, for use as biochemical markers of collagen degradation. *Clin Chem* **42**, 1621-1626.

Robins, S.P., Woitge, H., Hesley, R., Ju, J., Seyedin, S. and Seibel, M.J. (1994) Direct, enzyme-linked immunoassay for urinary deoxypyridinoline as a specific marker for measuring bone resorption. *J Bone Miner Res* **9**, 1643-1649.

Rosenbrock, H., Seifert-Klauss, V., Kaspar, S., Busch, R. and Luppa, P.B. (2002) Changes of biochemical bone markers during the menopausal transition. *Clin Chem Lab Med* **40**, 143-151.

Rowe, R.W. (1985) The structure of rat tail tendon fascicles. *Connect Tissue Res* **14**, 21-30.

Rubin, C.T. and Lanyon, L.E. (1985) Regulation of bone mass by mechanical strain magnitude. *Calcif Tissue Int* **37**, 411-417.

Ruff, C.B. and Hayes, W.C. (1983) Cross-sectional geometry of Pecos Pueblo femora and tibiae--a biomechanical investigation: I. Method and general patterns of variation. *Am J Phys Anthropol* **60**, 359-381.

Sadeghi, H., Allard, P., Prince, F. and Labelle, H. (2000) Symmetry and limb dominance in able-bodied gait: a review. *Gait Posture* **12**, 34-45.

Sartoris, D.J. and Resnick, D. (1990) Current and innovative methods for noninvasive bone densitometry. *Radiol Clin North Am* **28**, 257-278.

Schaaf, O.R., Eaton-Wells, R. and Mitchell, R.A. (2009) Biceps brachii and brachialis tendon of insertion injuries in eleven racing greyhounds. *Vet Surg* **38**, 825-833.

Schaffler, M.B. and Burr, D.B. (1988) Stiffness of compact bone: effects of porosity and density. *J Biomech* **21**, 13-16.

Seeman, E. (2003) Reduced bone formation and increased bone resorption: rational targets for the treatment of osteoporosis. *Osteoporos Int* **14 Suppl 3**, S2-8.

Seibel, M.J. (2000) Molecular markers of bone turnover: biochemical, technical and analytical aspects. *Osteoporos Int* **11 Suppl 6**, S18-29.

Seibel, M.J. (2005) Biochemical markers of bone turnover: part I: biochemistry and variability. *Clin Biochem Rev* **26**, 97-122.

Seibel, M.J., Woitge, H.W., Pecherstorfer, M., Karmatschek, M., Horn, E., Ludwig, H., Armbruster, F.P. and Ziegler, R. (1996) Serum immunoreactive bone sialoprotein as a new marker of bone turnover in metabolic and malignant bone disease. *J Clin Endocrinol Metab* **81**, 3289-3294.

Seyedin, S.M., Kung, V.T., Daniloff, Y.N., Hesley, R.P., Gomez, B., Nielsen, L.A., Rosen, H.N. and Zuk, R.F. (1993) Immunoassay for urinary pyridinoline: the new marker of bone resorption. *J Bone Miner Res* **8**, 635-641.

Shadwick, R.E. (1990) Elastic energy storage in tendons: mechanical differences related to function and age. *Journal of Applied Physiology* **68**, 1033-1040.

Sicard, G.K., Short, K. and Manley, P.A. (1999) A survey of injuries at five greyhound racing tracks. *J Small Anim Pract* **40**, 428-432.

Silva, M.J. and Gibson, L.J. (1997) Modeling the mechanical behavior of vertebral trabecular bone: effects of age-related changes in microstructure. *Bone* **21**, 191-199.

Sinacore, D.R., Bohnert, K.L., Hastings, M.K. and Johnson, J.E. (2008) Mid foot kinetics characterize structural polymorphism in diabetic foot disease. *Clin Biomech (Bristol, Avon)* **23**, 653-661.

Smith, J. (2008) A brief history: the staffordshire bull terrier.

Sone, T., Imai, Y., Joo, Y.I., Onodera, S., Tomomitsu, T. and Fukunaga, M. (2006) Side-to-side differences in cortical bone mineral density of tibiae in young male athletes. *Bone* **38**, 708-713.

Stephens, P.R., Nunamaker, D.M. and Butterweck, D.M. (1989) Application of a Hall-effect transducer for measurement of tendon strains in horses. *Am J Vet Res* **50**, 1089-1095.

Sternlicht, M.D. and Werb, Z. (2001) How matrix metalloproteinases regulate cell behavior. *Annu Rev Cell Dev Biol* **17**, 463-516.

Tezuka, K., Nemoto, K., Tezuka, Y., Sato, T., Ikeda, Y., Kobori, M., Kawashima, H., Eguchi, H., Hakeda, Y. and Kumegawa, M. (1994) Identification of matrix metalloproteinase 9 in rabbit osteoclasts. *J Biol Chem* **269**, 15006-15009.

Thiede, M.A., Smock, S.L., Petersen, D.N., Grasser, W.A., Thompson, D.D. and Nishimoto, S.K. (1994) Presence of messenger ribonucleic acid encoding osteocalcin, a marker of bone turnover, in bone marrow megakaryocytes and peripheral blood platelets. *Endocrinology* **135**, 929-937.

Thorpe, S.K., Crompton, R.H., Gunther, M.M., Ker, R.F. and McNeill Alexander, R. (1999) Dimensions and moment arms of the hind- and forelimb muscles of common chimpanzees (Pan troglodytes). *Am J Phys Anthropol* **110**, 179-199.

Tidswell, H.K., Innes, J.F., Avery, N.C., Clegg, P.D., Barr, A.R., Vaughan-Thomas, A., Wakley, G. and Tarlton, J.F. (2008) High-intensity exercise induces structural, compositional and metabolic changes in cuboidal bones--findings from an equine athlete model. *Bone* **43**, 724-733.

Tietz, N.W., Rinker, A.D. and Shaw, L.M. (1983) IFCC methods for the measurement of catalytic concentration of enzymes Part 5. IFCC method for alkaline phosphatase (orthophosphoric-monoester phosphohydrolase, alkaline optimum, EC 3.1.3.1). *J Clin Chem Clin Biochem* **21**, 731-748.

Tomlin, J.L., Lawes, T.J., Blunn, G.W., Goodship, A.E. and Muir, P. (2000) Fractographic examination of racing greyhound central (navicular) tarsal bone failure surfaces using scanning electron microscopy. *Calcif Tissue Int* **67**, 260-266.

Turner, C.H. (2002) Biomechanics of bone: determinants of skeletal fragility and bone quality. *Osteoporos Int* **13**, 97-104.

Udenfriend, S. (1966) Formation of hydroxyproline in collagen. *Science* **152**, 1335-1340.

Uebelhart, D., Gineyts, E., Chapuy, M.C. and Delmas, P.D. (1990) Urinary excretion of pyridinium crosslinks: a new marker of bone resorption in metabolic bone disease. *Bone Miner* **8**, 87-96.

Ulrich, D., van Rietbergen, B., Laib, A. and Ruegsegger, P. (1999) The ability of three-dimensional structural indices to reflect mechanical aspects of trabecular bone. *Bone* **25**, 55-60.

Usherwood, J.R. and Wilson, A.M. (2005) Biomechanics: no force limit on greyhound sprint speed. *Nature* **438**, 753-754.

Vailas, A.C., Pedrini, V.A., Pedrini-Mille, A. and Holloszy, J.O. (1985) Patellar tendon matrix changes associated with aging and voluntary exercise. *J Appl Physiol* **58**, 1572-1576.

Valimaki, V.V., Alfthan, H., Lehmuskallio, E., Loyttyniemi, E., Sahi, T., Suominen, H. and Valimaki, M.J. (2005) Risk factors for clinical stress fractures in male military recruits: a prospective cohort study. *Bone* **37**, 267-273.

Vaughan, L.C. (1969) Gracilis muscle injury in greyhounds. *J Small Anim Pract* **10**, 363-375.

Vaughan, L.C. (1985) Disorders of the carpus in the dog. I. *Br Vet J* **141**, 332-341.

Verheyen, K., Price, J., Lanyon, L. and Wood, J. (2006) Exercise distance and speed affect the risk of fracture in racehorses. *Bone* **39**, 1322-1330.

Vignery, A. and Baron, R. (1980) Dynamic histomorphometry of alveolar bone remodeling in the adult rat. *Anat Rec* **196**, 191-200.

Viguet-Carrin, S., Garnero, P. and Delmas, P.D. (2006) The role of collagen in bone strength. *Osteoporos Int* **17**, 319-336.

Viidik, A. (1967) The effect of training on the tensile strength of isolated rabbit tendons. *Scand J Plast Reconstr Surg* **1**, 141-147.

Vilarta, R. and Vidal Bde, C. (1989) Anisotropic and biomechanical properties of tendons modified by exercise and denervation: aggregation and macromolecular order in collagen bundles. *Matrix* **9**, 55-61.

Vincent, J.F.V. (1992) *Biomechanics--materials*, IRL Press at Oxford University Press. pp xviii,247p.

Vu, T.H. and Werb, Z. (2000) Matrix metalloproteinases: effectors of development and normal physiology. *Genes Dev* **14**, 2123-2133.

Walter, R.M. and Carrier, D.R. (2007) Ground forces applied by galloping dogs. *Journal of Experimental Biology* **210**, 208-216.

Wang, H.K. and Cochrane, T. (2001) Mobility impairment, muscle imbalance, muscle weakness, scapular asymmetry and shoulder injury in elite volleyball athletes. *J Sports Med Phys Fitness* **41**, 403-410.

Wang, J.H. (2006) Mechanobiology of tendon. *J Biomech* **39**, 1563-1582.

Wang, K., Vishwanath, P., Eichler, G.S., Al-Sebaei, M.O., Edgar, C.M., Einhorn, T.A., Smith, T.F. and Gerstenfeld, L.C. (2006) Analysis of fracture healing by large-scale transcriptional profile identified temporal relationships between metalloproteinase and ADAMTS mRNA expression. *Matrix Biol* **25**, 271-281.

Wang, X.T. and Ker, R.F. (1995) Creep rupture of wallaby tail tendons. *Journal of Experimental Biology* **198**, 831-845.

Watts, N.B. (1999) Clinical utility of biochemical markers of bone remodeling. *Clin Chem* **45**, 1359-1368.

Weiner, S., Traub, W. and Wagner, H.D. (1999) Lamellar bone: structure-function relations. *J Struct Biol* **126**, 241-255.

Weiner, S. and Wagner, H.D. (1998) The material bone: Structure mechanical function relations. *Annual Review of Materials Science* **28**, 271-298.

Wells, J.B. (1965) Comparison of Mechanical Properties between Slow and Fast Mammalian Muscles. *Journal of Physiology-London* **178**, 252-&.

Wendelburg, K., Dee, J., Kaderly, R., Dee, L. and Eaton-Wells, R. (1988) Stress fractures of the acetabulum in 26 racing Greyhounds. *Vet Surg* **17**, 128-134.

Whitelock, R. (2001) Conditions of the carpus in the dog. *In Pract.* **23**, 2-13.

Williams, S.B., Payne, R.C. and Wilson, A.M. (2007a) Functional specialisation of the pelvic limb of the hare (Lepus europeus). *J Anat* **210**, 472-490.

Williams, S.B., Wilson, A.M., Daynes, J., Peckham, K. and Payne, R.C. (2008a) Functional anatomy and muscle moment arms of the thoracic limb of an elite sprinting athlete: the racing greyhound (Canis familiaris). *J Anat* **213**, 373-382.

Williams, S.B., Wilson, A.M. and Payne, R.C. (2007b) Functional specialisation of the thoracic limb of the hare (Lepus europeus). *J Anat* **210**, 491-505.

Williams, S.B., Wilson, A.M., Rhodes, L., Andrews, J. and Payne, R.C. (2008b) Functional anatomy and muscle moment arms of the pelvic limb of an elite sprinting athlete: the racing greyhound (Canis familiaris). *J Anat* **213**, 361-372.

Wishart, J.M., Need, A.G., Horowitz, M., Morris, H.A. and Nordin, B.E. (1995) Effect of age on bone density and bone turnover in men. *Clin Endocrinol (Oxf)* **42**, 141-146.

Woessner, J.F., Jr. (1991) Matrix metalloproteinases and their inhibitors in connective tissue remodeling. *FASEB J* **5**, 2145-2154.

Woittiez, R.D., Huijing, P.A. and Rozendal, R.H. (1983) Influence of muscle architecture on the length-force diagram of mammalian muscle. *Pflugers Arch* **399**, 275-279.

Wolff, J. (1986) *The law of bone remodelling*, Springer-Verlag, Berlin; New York.

Woo, S.L., Gomez, M.A., Amiel, D., Ritter, M.A., Gelberman, R.H. and Akeson, W.H. (1981a) The effects of exercise on the biomechanical and biochemical properties of swine digital flexor tendons. *J Biomech Eng* **103**, 51-56.

Woo, S.L., Gomez, M.A., Woo, Y.K. and Akeson, W.H. (1982) Mechanical properties of tendons and ligaments. II. The relationships of immobilization and exercise on tissue remodeling. *Biorheology* **19**, 397-408.

Woo, S.L., Kuei, S.C., Amiel, D., Gomez, M.A., Hayes, W.C., White, F.C. and Akeson, W.H. (1981b) The effect of prolonged physical training on the properties of long bone: a study of Wolff's Law. *J Bone Joint Surg Am* **63**, 780-787.

Woo, S.L., Ritter, M.A., Amiel, D., Sanders, T.M., Gomez, M.A., Kuei, S.C., Garfin, S.R. and Akeson, W.H. (1980) The biomechanical and biochemical properties of swine tendons--long term effects of exercise on the digital extensors. *Connect Tissue Res* **7**, 177-183.

Wu, J., Ishizaki, S., Kato, Y., Kuroda, Y. and Fukashiro, S. (1998) The side-to-side differences of bone mass at proximal femur in female rhythmic sports gymnasts. *J Bone Miner Res* **13**, 900-906.

Wucherpfennig, A.L., Li, Y.P., Stetler-Stevenson, W.G., Rosenberg, A.E. and Stashenko, P. (1994) Expression of 92 kD type IV collagenase/gelatinase B in human osteoclasts. *J Bone Miner Res* **9**, 549-556.

Yamamoto, N., Ohno, K., Hayashi, K., Kuriyama, H., Yasuda, K. and Kaneda, K. (1993) Effects of stress shielding on the mechanical properties of rabbit patellar tendon. *J Biomech Eng* **115**, 23-28.

Young, D.R., Richardson, D.W., Markel, M.D. and Nunamaker, D.M. (1991) Mechanical and morphometric analysis of the third carpal bone of Thoroughbreds. *Am J Vet Res* **52**, 402-409.

Zotti, A., Isola, M., Sturaro, E., Menegazzo, L., Piccinini, P. and Bernardini, D. (2004) Vertebral mineral density measured by dual-energy X-ray absorptiometry (DEXA) in a group of healthy Italian boxer dogs. *J Vet Med A Physiol Pathol Clin Med* **51**, 254-258.

Zucker, S., Lysik, R.M., Gurfinkel, M., Zarrabi, M.H., Stetler-Stevenson, W., Liotta, L.A., Birkedal-Hansen, H. and Mann, W. (1992) Immunoassay of type IV collagenase/gelatinase (MMP-2) in human plasma. *J Immunol Methods* **148**, 189-198.